PREPARATION AND PROPERTIES OF BIODEGRADABLE THERMOPLASTIC GRAFTED CASSAVA STARCH FILMS WITH DIFFERENT TYPES OF VINYL MONOMERS

CHAYAPA WEERAPOPRASIT

A THESIS SUBMITTED IN PARTIAL FULFILLMENT OF THE REQUIREMENT FOR THE DEGREE OF DOCTOR OF PHILOSOPHY IN APPLIED CHEMISTRY
DEPARTMENT OF CHEMISTRY FACULTY OF SCIENCE
KING MONGKUT'S INSTITUTE OF TECHNOLOGY LADKRABANG
2019

KMITL-2019-SC-D-010-043

PREPARATION AND PROPERTIES OF BIODEGRADABLE THERMOPLASTIC GRAFTED CASSAVA STARCH FILMS WITH DIFFERENT TYPES OF VINYL MONOMERS

CHAYAPA WEERAPOPRASIT

A THESIS SUBMITTED IN PARTIAL FULFILLMENT OF THE REQUIREMENT FOR THE DEGREE OF DOCTOR OF PHILOSOPHY IN APPLIED CHEMISTRY
DEPARTMENT OF CHEMISTRY FACULTY OF SCIENCE
KING MONGKUT'S INSTITUTE OF TECHNOLOGY LADKRABANG
2019

KMITL-2019-SC-D-010-043

This material is reserved for educational use only, not allowed for commercial use.
Forbidden to modify the content, and cite the document when use.

COPYRIGHT 2019
FACULTY OF SCIENCE
KING MONGKUT'S INSTITUTE OF TECHNOLOGY LADKRABANG

This material is reserved for educational use only, not allowed for commercial use.
Forbidden to modify the content, and cite the document when use.

Thesis Title	Preparation and properties of biodegradable thermoplastic grafted cassava starch films with different types of vinyl monomers
Student Name	Miss Chayapa Weerapoprasit
Student ID	57605004
Degree	Doctor of Philosophy (Applied Chemistry)
Department	Chemistry
Year	2019
Thesis Advisor	Assoc. Prof. Dr. Jutarat Prachayawarakorn

Abstract

Due to high brittleness, high water absorption affinity and low thermal stability of thermoplastic native starch (TPNS) film; in this work, cassava starch was grafted with different vinyl monomers including methacrylamide (MAM), methacrylic acid (MAA) and methyl methacrylate (MMA) at different percentages of grafting: 20, 40, 60 and 90 % in order to obtain thermoplastic grafted starch (TPGS) films, prepared by a compression molding technique. The results revealed that the graft copolymerization was successful, as evident from new characteristic IR peaks of amide (C=O stretching and N-H bending), carboxylic group and carboxylate group (C=O stretching) for different grafted starch (GS) and TPGS films as well as an increase in intrinsic viscosity, molecular weight and thermal property. The morphology of starch granules was changed with all types of vinyl monomers. All TPGS films showed the decrease in degree of crystallinity. With higher grafting percentages, the degree of crystallinity, degree of swelling, WVP and percentage of moisture uptake were reduced compared to TPGS films with low percentage of grafting. In addition, thermal property, strain at maximum load or flexibility and surface roughness of TPGS films increased with increasing percentage of grafting. The biodegrability of all TPGS film was also confirmed by a soil burial test. TPGS film grafted with MMA showed higher flexibility and hydrophobicity than those of TPGS films grafted with MAA and MAM. Between TPGS films grafted with MAA and MAM, TPGS film grafted with MAM presented a higher flexibility and lower hydrophilicity than those of TPGS film grafted with MAA. Moreover, the highest thermal degradation temperature was found in TPGS film grafted with MAA, followed by with MMA and MAM. Based on these results, TPGS-90MMA was regarded to be the best performance for a biodegradable

This material is reserved for educational use only, not allowed for commercial use.
Forbidden to modify the content, and cite the document when use.

packaging film because of its highest flexibility and lowest water absorption capacity.

Keywords : Biodegradable polymer, Grafted starch, Thermoplastic starch, Vinyl monomer

This material is reserved for educational use only, not allowed for commercial use.
Forbidden to modify the content, and cite the document when use.

Acknowledgement

The author would like to sincerely express gratefulness to her advisor, Associate. Prof. Dr. Jutarat Prachayawarakorn for giving invaluable guidance, useful advices, kind and constructive criticism as well as consistent inspiration and encouragement throughout this thesis work. In addition, I am grateful to the thesis committee, Associate. Prof. Dr. Supranee Kaewpirom, Associate. Prof. Dr. Somsak Woramongkolchai, Assistant. Prof. Dr. Panpailin Seeharaj and Assistant. Prof. Dr. Patchanee Charoenying, their invaluable comments. We greatly appreciate all teachers who have instilled invaluable knowledge while studying at the Faculty of Science, King Mongkut's Institute of Technology Ladkrabang. I am grateful for the financial support provide by KMITL Research Fund (KREF 046108). I also would like to thank KMITL research and innovation services proofreaders, Mr. Pratana Kangsadal and Associate. Prof. Dr. John Morris, for proofreading and editing the English in this thesis. I wish to acknowledge the supports from all staff members of the Industrial Chemistry and Polymer Technology Workshop. Finally, I would like to express deep thanks to our parents and numerous friends for their help and encouragement.

Chayapa Weerapoprasit

This material is reserved for educational use only, not allowed for commercial use.
Forbidden to modify the content, and cite the document when use.

Table of Contents

This material is reserved for educational use only, not allowed for commercial use.
Forbidden to modify the content, and cite the document when use.

Table of Contents (continued)

This material is reserved for educational use only, not allowed for commercial use.
Forbidden to modify the content, and cite the document when use.

Table of Contents (continued)

This material is reserved for educational use only, not allowed for commercial use.
Forbidden to modify the content, and cite the document when use.

List of Tables

This material is reserved for educational use only, not allowed for commercial use.
Forbidden to modify the content, and cite the document when use.

List of Tables (continued)

Table **Page**

This material is reserved for educational use only, not allowed for commercial use.
Forbidden to modify the content, and cite the document when use.

List of Figures

This material is reserved for educational use only, not allowed for commercial use.
Forbidden to modify the content, and cite the document when use.

List of Figures (continued)

This material is reserved for educational use only, not allowed for commercial use.
Forbidden to modify the content, and cite the document when use.

List of Figures (continued)

This material is reserved for educational use only, not allowed for commercial use.
Forbidden to modify the content, and cite the document when use.

List of Figures (continued)

This material is reserved for educational use only, not allowed for commercial use.
Forbidden to modify the content, and cite the document when use.

List of Figures (continued)

Figure **Page**

This material is reserved for educational use only, not allowed for commercial use.
Forbidden to modify the content, and cite the document when use.

Abbreviations/Symbols

NS	: Native starch
GS	: Grafted starch
TPNS	: Thermoplastic native starch
TPGS	: Thermoplastic grafted starch
MAM	: Methacrylamide
MAA	: Methacrylic acid
MMA	: Methyl methacrylate
PPS	: Potassium persulfate
FT-IR	: Fourier transform infrared spectroscopy
XRD	: X-ray diffraction
SEM	: Scanning electron microscopy
TGA	: Thermo gravimetric analysis
WVP	: Water vapor permeability
CL	: Caprolactone
AM	: Acrylamide
AA	: Acrylic acid
G	: Grafting

King Mongkut's Institute of Technology Ladkrabang

This material is reserved for educational use only, not allowed for commercial use.
Forbidden to modify the content, and cite the document when use.

Chapter 1
Introduction

1.1 Research Motivation

In recent years, disposal of non-biodegradable plastics is a growing and intractable environmental problem. On the other hand, biodegradable polymers can be effectively degraded by living microorganisms [1]. For this reason, researches and developments of biodegradable polymers that are based on agricultural raw materials have been greatly stimulated [2-3].

Starch is one of the most extensively produced biodegradable polymers. It is the major carbohydrate existing as granules in fruits and roots of many plants. Starch granules contain amylose and amylopectin that are useful as precursors for biodegradable plastic due to its natural abundance, renewability, low price and totally biodegradability and cassava is one of the most commonly grown starch sources in Thailand in many regions of the country, especially in the eastern and north-eastern regions. Annually, Thailand exports a large amount of cassava starch to many countries [4].

Thermoplastic native starch (TPNS) is one of the low cost biodegradable polymers that are used for many applications. By itself, TPNS is not actually thermoplastic. However, by mixing it with a plasticizer under high shear, pressure and temperature, the mixture can melt and flow-like a thermoplastic material. Nevertheless, TPNS still shows poor tensile and thermal stability as well as absorbs high moisture or water. Various attempts have been made to overcome the inherent drawbacks of TPNS by using chemical modification methods such as crosslinking, oxidation, acetylation, esterification, acid hydrolysis, graft copolymerization, etc. [5-7].

Among all these chemical modifications, graft-polymerization with a vinyl monomer has been a very fascinating field of research. It has been widely used to improve several desirable properties including flexibility, ion exchange capability, absorbency and thermal stability as well as to add new desirable functional groups into the starch structure. Starch graft copolymers are becoming increasingly important because of their various applications related to agriculture, industry and medical applications. Many researchers have reported improvements of some properties of native starch (NS) by grafting its backbone with various vinyl monomers such as caprolactone (CL), acrylamide (AM), acrylic acid (AA), methacrylamide (MAM), methacrylic acid (MAA) and methyl methacrylate (MMA) [8-9]. Each of these monomers adds to grafted starch (GS) a different functional group that alters its structure and physicochemical properties.

This material is reserved for educational use only, not allowed for commercial use.
Forbidden to modify the content, and cite the document when use.

Among them, MAM and MAA are particularly interesting because of its good hydrophilicity, high polarity, good thermal stability and low toxicity [10-11]. MMA also has low water solubility, low toxicity, good thermal stability and weatherability [12]. Therefore, they were investigated as promising grafting monomers in this study. These monomers have already been extensively used in commercial applications such as drug delivery, adsorbent of metal ions and dyes, wastewater treatment and plastic production [13]. Also, previous studies reported that a significant decrease in solubility and swelling property of GS was observed when GS was grafted with high content MAA, MAM or MMA monomers [14-16].

One useful technique for improving the properties and reducing the water uptake of TPNS film is using GS in TPS preparation. M.C. Li *et al.* (2012) reported that the use of GS with MMA for producing a biodegradable starch film by a casting technique improved the film's mechanical property and thermal stability. The morphology of the cast thermoplastic grafted starch film (TPGS) changed after the biodegradability test, confirming evidence of biodegradation [17]. TPGS cast film with CL was also prepared from banana starch. The result showed that crystallinity percentage and moisture absorption of cast TPGS films with CL were noticeably decreased [18]. Z. B. Cuevas-Carballo *et al.* (2017) mentioned that compressed TPGS sheet with CL from corn starch exhibited ability to degrade by enzymatic degradation [19]. The improvement in elongation and hydrophobicity of cast TPGS film from sago starch was observed, caused by grafting with CL [20]. Morphology of compressed TPGS film with butyl acrylate (BA)-co-MMA presented rougher surface than that of TPNS film. The decrease in degradation temperature and molecular weight of the starch were observed from biodegradable test due to enzymatic attack [21]. Most of the researches were focused on the effect of graft copolymerization to starch granules. However, there have been no reports on the influence of different percentages of grafting on physicochemical properties of different TPS films grafted with MAM, MAA and MMA monomers by a compression molding technique and comparison of several properties of different TPGS films prepared from these monomers.

Therefore, the aims of this research were to prepare TPGS films from different types of vinyl monomers i.e., MAM, MAA and MMA and to determine their physicochemical properties. The effects of grafting at different percentages (%G)—20%, 40%, 60% and 90%—on several properties of TPGS films were also evaluated and compared. Furthermore, the films were investigated by Fourier transform infrared spectroscopy (FT-IR), X-ray diffractometry (XRD) and fractured morphology, and their following properties were determined: degree of swelling, moisture uptake, water permeability, mechanical, thermal and biodegradable properties.

This material is reserved for educational use only, not allowed for commercial use.
Forbidden to modify the content, and cite the document when use.

1.2 Objectives of the study

1) To prepare and characterize MAM-, MAA- and MMA-grafted starch

2) To prepare and determine the various properties of differently prepared TPGS films.

1.3 Scope of the study

The scope of this study is limited to preparation of GS from several different types of vinyl monomers (MAM, MAA and MMA), investigation of effects of grafting at different percentages (20%, 40%, 60% and 90% G) on the properties of TPGS films and characterization of these films by Fourier-transform infrared spectroscopy (FT-IR), X-ray diffraction (XRD) and scanning electron microscopy (SEM) as well as investigation of several of their properties including degree of swelling, moisture uptake, water vapor permeability (WVP), mechanical, thermal and biodegradable properties.

1.4 Benefits of the study

1) Higher flexibility and lower water uptake affinity of TPGS film.

2) Improvement in several properties of TPNS film.

3) TPGS film can replace plastic for packaging application hence leading to a reduction of non-biodegradable plastic wastes.

This material is reserved for educational use only, not allowed for commercial use.
Forbidden to modify the content, and cite the document when use.

Chapter 2
Theory and Literature Reviews

2.1 Polymer and plastic

Plastic materials are classified into two major categories: thermosetting material and thermoplastic materials.

1. Thermoplastics contain linear or slightly branched polymers that soften at the glass temperature T_g (amorphous polymers) or melt at the melting temperature T_m (semi-crystalline polymers). They are usually processed at temperatures above these temperatures. The transformation solid melt is reversible. Cooling below T_g (amorphous) or T_m (semi-crystalline) delivers slabs, tubes, films and other formed articles. Raw materials for thermoplastics are usually polymers, sometimes oligomers, and rarely monomers.

2. Thermosets result from the chemical cross-linking of monomers or oligomers to tightly cross-linked polymers. These monomers and oligomers are sometimes called active resins or thermosetting resins if they are solid or semi-solid; oligomers are also known prepolymers. Thermosetting resins are simultaneously reacted and shaped. They cannot be remelted and reshaped without chemical degradation after the thermosetting operation. The transformation liquid or solid is irreversible [22].

2.1.1 Vinyl monomer

Most industrially used polymers are commonly synthesized from the monomers by polymerization. Such monomers must be at least bifunctional. They usually belong to one of the following three groups:

1. Monomers with two (or more) functional end groups, such as hydroxycarbooxylic acids HO-Z-COOH, amino acids H_2N-Z-COOH, diamines H_2N-Z-NH_2, tri amines $Y(NH_2)_3$, tetracarboxylic acids $X(COOH)_2$, dichlorides Cl-X-Cl. disodium sulfide Na_2S, etc., where Z denotes a bifunctional unit, Y denotes a trifunctional or tetrafunctional.

2. Monomers with multiple bonds, mostly with carbon-carbon double bonds C-C, less often with carbon-carbon triple bonds -C≡C-, carbon-nitrogen bonds -C-N-, or carbon-oxygen double bonds C=O. Examples are propylene CH_2=$CHCH_3$, 1,3-butadiene CH_2 CH-CH-CH_2, formaldehyde H_2C=O, and acetylene HC≡CH.

3. Cyclic monomers with heteroatoms in the ring. Examples are ethylene oxide, tetrahydrofuran, hexamethylcyclotrisiloxae or caprolactam [22]. The chemical structure of vinyl monomers is shown in Figure 2.1

This material is reserved for educational use only, not allowed for commercial use.
Forbidden to modify the content, and cite the document when use.

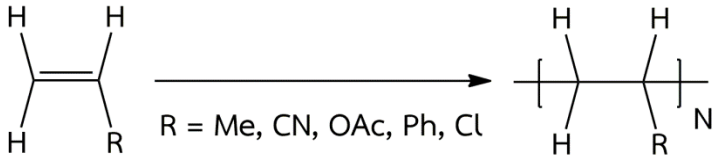

Figure 2.1 Chemical structure of vinyl monomers [22]

2.1.2 Homopolymer and copolymer

Homopolymer is derived from one species of the monomers such as polyethylene, polystyrene, polyacrylamide, poly(vinyl chloride), etc. Poly condensates originating from one single diacid-dialcohol system are also usually quoted as homopolymers. In this case, however, the repeat unit is constituted of two monomers (base units), while syntheses of copolymers require two or more species of monomers. They are referred to as copolymers. The term of the copolymer is sometimes used as a synonym for bipolymer, i.e., a copolymer derived from two species of monomers. The copolymers from three, four, five species of monomers are accordingly called terpolymers, quarterpolymers and quinterpolymers. An order term for copolymer is interpolymer. The copolymer is distinguished according to the sequence of the various monomeric units. They are subdivided into random, alternating, block and graft copolymer [22].

2.2 Degradable plastic

Degradable plastic is a material designing to overcome significant alteration in physicochemical properties, which result from bond scission in the polymer chain through irradiation, light, chemical reaction, microorganism attack and physical forces in the environment at a rate which is reasonably accelerated, when compare to a control, and which results in fragmentation or disintegration of the plastic. In both cases, the term polymer degradation involves deterioration in the functionality of polymer materials, which is usually called denaturation [19]. It is useful to categorize this broad field into 5 groups according to its various modes of initiation as follows:

2.2.1 Photodegradable plastic

It is a degradation plastic in which the degradation caused by irradiation with ultraviolet or the action of sunlight or visible light. The existence of chromophoric (light absorbing) group in the macromolecules of degradation plastic is a perquisite

This material is reserved for educational use only, not allowed for commercial use.
Forbidden to modify the content, and cite the document when use.

for the initiation of photochemical reaction. The resulting degradable processes may lead to severe property deterioration.

2.2.2 Oxidatively degradable plastic

It is a degradation plastic in which the degradation caused by the oxidation reaction, which results in a decrease in molecular weight and viscosity of polymers.

2.2.3 Mechanically degradable plastic

It is a degradation plastic in which the degradation caused by the influence of shear forces. This process in plastic materials primary causes bond raptures in the main-chains of the polymer. This method can be utilized for the mechano-chemical initiation of polymerization reactions with the synthesizing of block-copolymer.

2.2.4 Hydrolytically degradable plastic

It is a degradation plastic in which the degradation caused by the hydrolysis, which is induced under the influence of acid and water.

2.2.5 Biodegradable plastic

It is a plastic material that degrades under environmental conditions in a reasonable and demonstrable period of time, where the primary mechanism is the natural action of microorganisms such as bacteria, yeast, fungi and algae. Produced enzymes from microorganisms are capable of attacking with polymer backbone [23].

2.3 Biodegradable plastic

In general, the fully recyclable materials are completely biodegradable within a considerably short period of time. There is an enormous potential for the application of natural biopolymers as the packaging materials and coatings of the future generation. Biodegradable plastic is a degradable plastic, which can be produced from oil or biopolymers such as polysaccharides, proteins, lipids and their derivatives. The microbial attack of the biopolymer is a degradable process which is caused by the microorganisms (bacteria, fungi or algae) in order to obtain food. Under appropriate conditions, the growth of microorganisms will occur simultaneously with the decomposition of any biological species after the latter has decayed as shown in Figure 2.2. Also, soil burial tests have been employed rather frequently in order to check for polymer weight losses or molecular weight changes caused by microbial attack [23].

This material is reserved for educational use only, not allowed for commercial use.
Forbidden to modify the content, and cite the document when use.

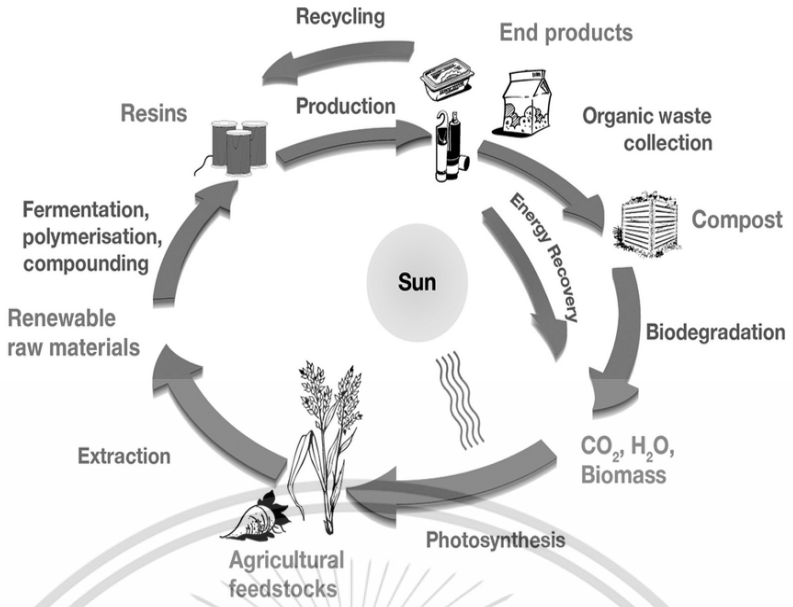

Figure 2.2 Life cycle of biodegradable plastic [24]

2.3.1 Mode of biodegradable of polymer

Generally, natural and synthetic polymers can be attacked by living organisms either chemically or mechanically. The chemical mode relates to the decomposition of polymers in the digestive tracts of highly organized living species, humans, for example, or to the attack of microorganisms. Commonly, enzymes are involved in the chemical mode of polymer degradation. Although a great number of microorganisms can produce a variety of enzymes, microorganisms usually specialize in the attack of only a single substrate and are, therefore, producing only one or a few enzymes. If the substrate is changed, the microorganisms start, after a few weeks or months, the production of new enzymes capable of attacking the new substrate. The capability of microorganisms to adapt to a new substrate is, of course, of great importance to the problem of the biodegradability of synthetic polymers. It is now generally accepted that a great number of microorganisms are capable of attacking synthetic polymers. At this point, it must be emphasized that generally synthetic polymers are biodegradable. The reason is not usually confronted with problems because the microbial attack of the synthetic polymer is simply and this class of material is in principle brand new to nature. Thus, it can be anticipated that the situation will become different after the microorganisms have adapted more generally to man-made polymers.

The mechanical mode of biodegradation of polymers relates to the attack by certain mammals (e.g. rodents) and insects. Regarding materials composed of natural polymers, wood and wool, for instance, the attack by animals is a serious problem. In a number of cases, the reasons for attacking the polymer include also the nutritional needs for the attacking mammal or insect (e.g. death-watch beetles and

This material is reserved for educational use only, not allowed for commercial use.
Forbidden to modify the content, and cite the document when use.

termites digest wood or moths eat wool). Synthetic polymers (e.g. polyethylene or polystyrene), on the other hand, are not attacked for reasons of nutrition. The attacking animal bites or chews articles made of synthetic polymers because the physical properties of the polymeric material are compatible with the natural needs of the animal. A typical example is the need of rodents for biting, which can cause serious problems, e.g. for plastic insulation of electrical cables placed in the ground [25].

2.3.2 Examples of biodegradable polymers

Biodegradable for short-lived goods must lead to degradation conducts that are ecologically safe. They are thus usually restricted to medical goods (e.g., surgical sutures) or agricultural materials (film, seed, coating, etc.). The energy content of plastics is of course wasted during biodegradation. The examples of biodegradation polymers are shown below;

- Poly(glycolide) (PGL): PGL is prepared by chain polymerization of the cyclic dimer of glycolic acid.
- Polylactic acid (PLA): PLA is prepared by chain polymerization of the cyclic dimer of lactic acid or by microbiological synthesis of lactic acid.
- Poly(ε-caprolactone) (PCL): PCL is prepared by chain polymerization of lactone of 6-hydroxy-hexanoic acid.
- Poly(3-hydroxybutyrate-co-hydroxyvalerate) (PHB-HV): PHB-HV is prepared from glucose by microbiological synthesis.
- Starch: starch is produced by extraction from all botanical plants [22].

2.4 Starch

Starch is one of the major components of cereal grains and storage organs including seeds, fruits, tubers and storage roots. Starch is commercially prepared from corn, potato, wheat, rice, cassava, banana, taro, sorghum, etc. The major plant sources of commercial starch in Thailand are rice and cassava. The starch obtains from these plant sources as a fine powder (granular starch). It occurs as very small water-insoluble granules, usually associated with proteins, fats and inorganic salts. The granules vary in shape and size ranging from about 2 to 150 μm in diameter depending on the plant sources [26].

This material is reserved for educational use only, not allowed for commercial use.
Forbidden to modify the content, and cite the document when use.

2.4.1 Molecular structure of starch

Starch is one of the most abundant polysaccharides consisting of glucose monosaccharide repeating units joined together by α-(1,4) and α-(1,6) glycosidic bonds and occurs in the form of granules with a density of approximately 1.5×10^{3} kg/cm^{3}. Starch is a carbohydrate as an empirical formula of $C_6H_{10}O_5$. In a granule form, starch is semi-crystalline structure, insoluble in cold water and swells slightly in water. Most common starch is made up of two different types of polysaccharides of different structures namely, amylose and amylopectin [26].

2.4.1.1 Amylose

Amylose is a linear structure of polysaccharide of α-D-glucopyranosyl units joined by α-D-(1,4)-glucosidic linkage and is typically semi–crystalline. The stable macroconformation of amylose is that of a helix. This helix forms inclusion complexes with iodine; the blue color of these complexes is due to the linear arrangement of iodine atoms in the channel provided by the helix. The degree of polymerization (D.P.) varies from about 250 to 4,000 anhydroglucose unit (AGU) per amylose molecule with molecular weight about 40,000 to 650,000. In general, amylose is crystalline part of the starch particle. Amylose can be separated from starch granules by dissolving the starch granule in water and removing the amylose as an insoluble complex with a polar organic solvent such as butanol in water. The relatively smaller amylose polymers are soluble in warm water and will crystallize from the solution when the temperature is lowered [26]. Figure 2.3 presents chemical structure of amylose.

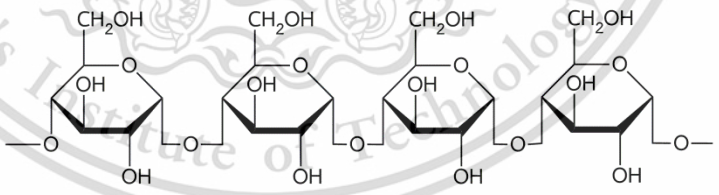

Figure 2.3 Chemical structure of amylose [26]

2.4.1.2 Amylopectin

Amylopectin is a branched structure of polysaccharide of α-D-glucopyranosyl units joined by α-D-(1,4) and α-D-(1,6) glucosidic linkages and is relatively non–crystalline. Amylopectin is a much larger polymer than amylose and the average molecular weight of amylopectin is around 10^{8} g/mol. Amylopectin contains 1 branching unit per 18-27 glucose units; the branching is via 1,6 position. It does not form a complex which giving deep blue coloration with iodine. The D.P. varies from

This material is reserved for educational use only, not allowed for commercial use.
Forbidden to modify the content, and cite the document when use.

12 to 50 AGU, yet the average D.P. is about 20 AGU. Moreover, most of the starch structure also has amylopectin more than amylose [26]. Figure 2.4 shows chemical structure of amylopectin.

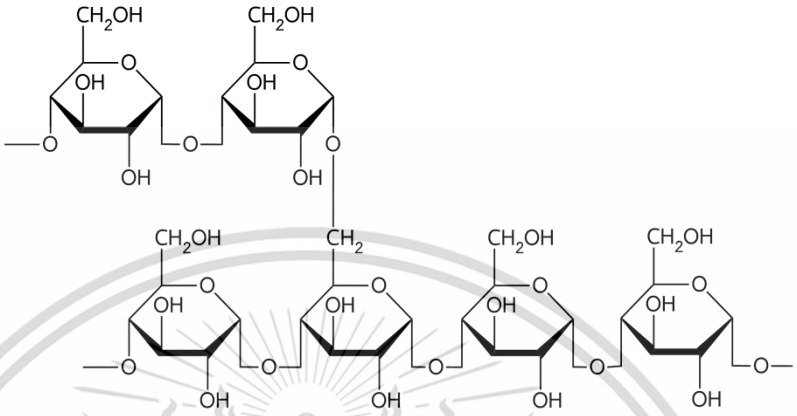

Figure 2.4 Chemical structure of amylopectin [26]

2.4.2 Starch granules

Starch occurs of the source evidence of a granular form, with the shape of the granule being characteristic of the starch. Analysis of granules with polarized light shows a layered structure in the granule, particularly for wheat, although many plants only exhibit the rings or lamellae after pretreatment from hydrolytic enzymes. The reason for these rings is the subject for some evidence to indicate that there may be some correlation layers and these rings. It has, however, been shown that starch granules have an arrangement thought to be the crystalline structure which can be seen as patterns when the granule is viewed between crossed polarizers. It has been concluded that starch molecules are arranged with their axes in a radial direction, caution must be exercised in interpretation. Which these results due to the present knowledge of helical and folded forms and the lack of detailed knowledge of the crystalline structure of starch, despite the application of X-ray diffraction and laser light-scattering techniques Isolation of the starch granule from the plant tissues can be achieved without degradation because they are insoluble in cold water, whereas many of the contaminants are soluble.

The starch granule can be separated into two distinctly different components using a variety of techniques, the most common large-scale method being precipitation of an insoluble complex. The starch granule is burst using, for example, ethanol (for industrial procedures) or dimethylsulphoxide (for laboratory procedures) and the resulting aqueous dispersion is treated with thymol or butanol

This material is reserved for educational use only, not allowed for commercial use.
Forbidden to modify the content, and cite the document when use.

with amylose to give an insoluble complex which is removed by centrifugation. The amylose is purified by redissolving in boiling water and recrystallization with butanol on cooling.

Morphology of starch granules shows a difference in sizes and shapes depending on the starch types. Starch granules in leaves are very small about 1 μm in diameter. Starch granules in storage organ are generally bigger than the ones in leaves. Granules of rice starch are polygonal in shape and mostly run about 3 to 8 μm in diameter. They tend to aggregate in clusters. Corn and maize starch have polygonal and some round granules which range from about 5 to 25 μm in diameter, with about a 15 μm average. Cassava starch granules usually have round shapes, which are truncated at one end. They average about 20 μm in diameter, but may range from 5 to 35 μm in diameter. Wheat starch has flat, round or elliptical granules, which tend to cluster in two size ranges from 2 to 10 μm [27]. The sizes and granular shapes of different starch granules are shown in Table 2.1 and Figure 2.5.

Table 2.1 The size and granular shape of different starch granules [27].

Source	Diameter (μm)		Granular shape
	Range	Mean	
Maize	5-25	14	Polyhedral and rounded
White potato	15-100	33	Large over
Sweet potato	15-55	25-50	Large over
Cassava	6-36	20	Round
Wheat	2-38	20-22	Discs
Rice	3-9	5	Discs

This material is reserved for educational use only, not allowed for commercial use.
Forbidden to modify the content, and cite the document when use.

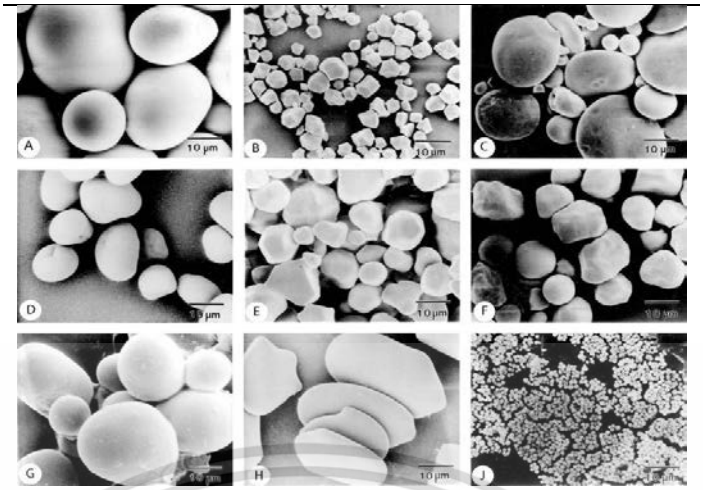

Figure 2.5 Scanning electron micrographs (SEM) of starch granules: (A) potato, (B) rice, (C) wheat, (D) mung bean, (E) maize, (F) waxy maize, (G) cassava, (H) shoti and (J) leaf starch [28].

2.4.3 Crystal structure of starch

Granules of starch consist of semi-crystalline and amorphous growth rings which form an onion-like structure. Starch granules show a lamellar structure which consists of stacks of nanometric subunits with a periodicity of 9-10 nm in starch granules. Amylose actually exists in the crystalline region of starch and amylopectin side chains fully form into amorphous non-crystalline region. The crystal structure of NS granules can be determined by X-ray diffraction (XRD) technique. Cereal starch, such as maize, exhibits an A-type crystal, while tuber and amylose-rich starch normally show a B-type crystal. C-type crystal will be shown when A-type and B-type crystals are coexisting in starch. During the gelatinization of starch, the V_h-type X-ray diffraction pattern is demonstrated after thermoplastic starch is prepared and processed, referring to the complex of amylose with fatty acids and monoglycerides [27]. X-ray diffraction patterns of starch are shown in Figure 2.6.

This material is reserved for educational use only, not allowed for commercial use.
Forbidden to modify the content, and cite the document when use.

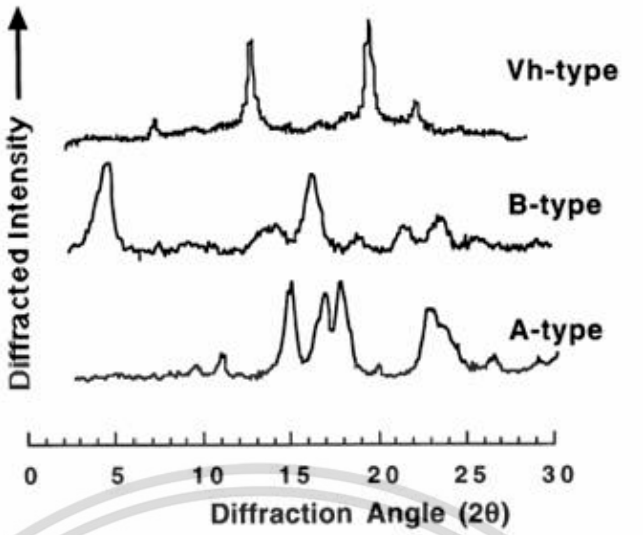

Figure 2.6 X-ray diffraction patterns of starch [29]

The degree of crystallinity refers to the percentage of the crystalline regions with respect to the total materials. The crystallinity of starch can be determined via XRD technique. Based on this concept, the diffraction pattern can be separated into crystal and amorphous parts, the areas relating to the contribution of crystalline and amorphous region are determined and compared, and then the crystallinity can be determined. However, according to the crystal-defect concept, the simple pattern separation method is questionable because a fraction of X-ray scattering from the crystalline region can diffuse and cause the change of the amorphous phase. Other techniques for investigating crystallinity of starch is to compare the experimental diagrams to several discrete crystalline diffraction peaks (100% crystallinity diagrams) and an amorphous diffraction peaks (100% amorphous diagram). Although different results based on different techniques is reported, a typical range of the crystallinity of starch granules is around 15-45%. The degree of crystallinity, gelatinization temperatures and amylose contents of various types of starch are given in Table 2.2 [27].

This material is reserved for educational use only, not allowed for commercial use.
Forbidden to modify the content, and cite the document when use.

Table 2.2 Degree of crystallinity, gelatinization temperature and amylose content of various types of starch [29]

Type of starch	Degree of crystallinity (%)	Gelatinization temperature (˚C)	Amylose content (%)
A-type			
Oat	33	60.7	23
Waxy rice	37	64.5	-
Rice	38	70.0	17
Corn	40	71.3	27
Corn starch	40	72.7	0
B-type			
Sago	26	70.5	28
Potato	28	67.3	22
Cassava	43	66.0	18
C-type			
Sweet potato	38	70.0	20
Mungbean	45	68.0	32

2.4.4 Starch gelatinization and retrogradation

Gelatinization process is a heating process which starch granule is broken and allows water to enter into crystalline structures to swell amylopectin and migrate amylose out of the granule to surrounding water. This process changes the viscosity of starch mixture to become a gel. When the temperature is cooled down, linear part of starch molecules such as amylose and amylopectin can retrograde and rearrange to form into the crystalline structure. Retrogradation ratio depends on amylose/amylopectin ratio in starch granules, temperature, a concentration of starch and the kind of starch. Amylose chain length with glucose residue 80-100 shows the best retrogradation, at least 8-10 glucose residues of amylose chain length can retrograde and a short chain length of amylopectin with glucose residues longer than 15 residues can retrograde. High amylose ratio can retrograde more than low amylose ratio. Interestingly, maize starch and wheat starch which contain high amylose content than cassava and waxy maize starch, thus, the degree of retrogradation shows in the order: maize or wheat starch>cassava starch>waxy maize starch, respectively.

This material is reserved for educational use only, not allowed for commercial use.
Forbidden to modify the content, and cite the document when use.

NS granules are insoluble in cold water. However, when the starch suspension is heated to a gelatinization temperature, the starch granules can swell by absorbing water. Water penetrates into the amorphous phases of the starch granules. The hydrogen bonds between starch molecules are disassociated. After the granules swell to many times, the starch granules are disrupted and disintegrated with continuous heating and stirring. After the starch granules are completely fragmented, a starch gelatinized solution is produced. Different types of starch have different gelatinization temperatures at a range of 55 to 80°C. The gelatinization process of starch can be monitored by a differential scanning calorimeter (DSC) measurement.

For some applications, starch pastes or solutions need to be prepared by following a certain cooking process. During the cooking process, starch slurries will experience a viscosity increase step and follow by a viscosity decrease step. The viscosity change of starch dispersion during cooking is normally monitored and characterized by using a Brabender Viscograph.

When cooked starch solutions are cooled, hydrogen bonds are formed between the hydrated amylose molecules and the chains wrap abound to form double helices, resulting in the formation of colloidal crystallites. This phenomenon is called retrogradation which is a non-reversible process. Many factors, such as starch concentration, molecular weight, degree of hydration, temperature, pH and salt concentration, may affect the rate of retrogradation. For diluted starch solutions, particulate precipitation can be observed. For solutions with high concentrations, a gel is normally formed [30]. The representations of gelatinization and retrogradation of starch are shown in Figures 2.7-2.8.

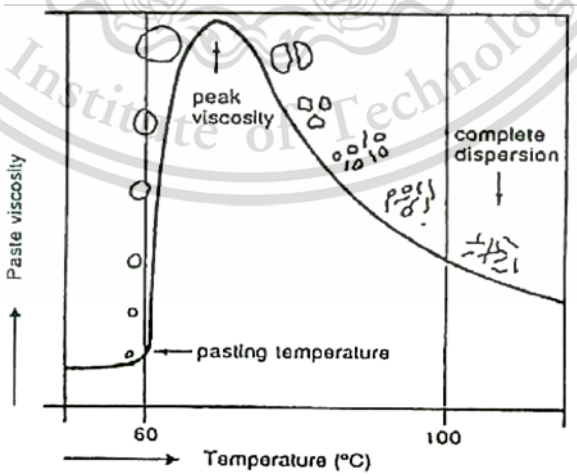

Figure 2.7 Gelatinization of starch [31]

This material is reserved for educational use only, not allowed for commercial use.
Forbidden to modify the content, and cite the document when use.

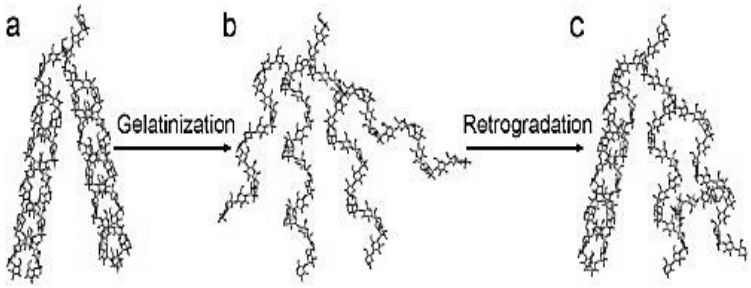

Figure 2.8 Retrogradation of starch [32]

2.4.5 Starch swelling

The granules owe their integrity and insolubility in cold water to intermolecular hydrogen bonds between segments of amylopectin branches. When the starch suspension is heated beyond a critical temperature, which varies with the starch type, the hydrogen bonds weaken and the granules imbibe water. As the process precedes, the viscosity increases dramatically and as the hydrogen bonds break the swollen granules rupture into molecular dispersions and aggregates, the viscosity decreases with the extent depending on the type of starch. During the initial stage of swelling before the swollen granules start rupturing, the cook develops a viscous-like texture, which is quite palatable from a food standpoint. However, it is in a very dilute state, which disappears quickly as the granules rupture and the sol develops elastic and cohesive texture. On cooling, dispersions of regular cereal starch will lose their clarity and form opaque gels. Starch such as cassava and potato tends to form cohesive and elastic sols under similar conditions [30].

2.4.6 Starch applications

Starch can be used to produce food and non-food products. Because of its cheap and being degradable product, so it can replace or be filled in non-degradable materials, both original and modified form. It has been extensively utilized in various applications such as paper, textile, binders, explosives, clothing, fuel and adhesive industry. It has been used in the food industry: as fermentation medium in the brewing industry, in sugar grinding, as a bulking agent in dry mixes, as a dusting agent, a molding medium in candy making, etc. In some food applications, a cooked starch is also used to thicken or provide texture to food system. Furthermore, in pharmaceutical industry, starch can be used as encapsulation, fillers and carrier materials. Currently, it is also used for preparation of biodegradable plastics [33].

2.4.7 Disadvantages of starch-based materials

The crystalline structure of starch is disrupted and molecules of water can interact with the hydroxyl groups in the starch backbone in heating process. These observations cause partially dissolve of starch granules. Thus, the hydrophilicity of starch results in the decrease of water resistance, which restricts the starch-based

This material is reserved for educational use only, not allowed for commercial use.
Forbidden to modify the content, and cite the document when use.

material development. Therefore, unmodified starch has serious limitations. Modified starch is developed to overcome one or more of the following shortcomings associated with NS [33].

2.5 Starch modification

The term "native starch" is defined as the product extracted from plant roots, seeds, fruits and tubers, which is called "starch". The physical properties of NS and the colloidal sols produced from NS on heating limit the usefulness of starch in many applications. Therefore, modified starch is developed to overcome one or more of these shortcomings and thus expands the usefulness of starch for a myriad of industrial applications. While in the broadest sense any product in which the chemical and physical properties of NS have been altered. The range of modifications will be limited to those in which the chemical and physical properties of NS are modified by molecular scission, molecular rearrangement, oxidation or introduction of substituent chemical group into the starch molecule [34].

Generally, the resulting products perform more effectively unmodified starch or impart unique properties. There are various types of modified starch such as bleached starch, converted starch, linked starch, mono-substituted starch and cross-linked starch. In addition, modifications of starch are classified into three major categories as follows:

1. Chemical modification

The aim of this modification is to change the chemical structure of starch by reacting starch with chemical reagents such as crosslinking agent, oxidizing agents, and bleaching agents. Hydroxyl groups of anhydrous glucose unit in starch are substituted with various functional groups such as ether, hydroxypropyl, aldehyde, carboxymethyl, carboxyl or carbonyl groups. The methods of chemical modification of starch normally include conversion, acid hydrolysis, grafting, oxidation, substitution, and crosslinking. The chemical modification of starch alters the available three hydroxyl groups at C-2, C-3 and C-6 positions [34].

2. Physical modification

NS can be mechanically modified by pre-gelatinization, particle size reduction and moisture adjustments using annealing technique and spray drying technique. Ball mill grinding, high pressure homo-gelatinization and extrusion are typical means used for reducing starch particle sizes. For some specific applications, such as fat substitutes and filler in plastic films, a smaller granule size is required [34].

This material is reserved for educational use only, not allowed for commercial use.
Forbidden to modify the content, and cite the document when use.

3. Enzymatic modification

Starch modified with amylase enzyme produces derivative with good adhesion property. The enzymatic modification involves the exposure of starch suspension to a number of enzymes primarily including hydrolyzing enzymes that tend to produce highly functional derivatives. The modified method is hydrolysis of partial starch granules to form starch containing low molecular weight called maltodextrin or dextrin. This modified starch is extensively utilized for food and pharmaceutical industries. It is widely utilized as a colorant in coating of food [34]. The properties and applications of different types of modified starch are given in Table 2.3.

Table 2.3 Properties and applications of different types of modified starch [35]

Type of modification	Property	Use
1. Physical	- soluble cold water - low gelatinization temperature	- snack extrusion at low temperature
2. Biological	- low viscosity at a high temperature	- instant fruit - pie filling - beggary - candy
3.Chemical		
3.1Derivatization	- low retrogradation -low pasting temperature	- freeze/thaw stability - UHT custards
3.2 Hydrolysis	- high paste and viscosity - high water- holding capacity	- frozen pizza and topping - candy
3.3 Oxidation	- low viscosity - higher binder - low pasting temperature	- chocolate - tablet binder - sauces
3.4 Cross-linking	- decrease retrogradation of amylose - clarity pasting - increase distribution of solid - lower retrogradation and swelling	- pie filling - pudding cheese and sauces

This material is reserved for educational use only, not allowed for commercial use.
Forbidden to modify the content, and cite the document when use.

2.6 Graft copolymerization of starch

Graft copolymerization is a substantial chemical modification procedure to improve several properties of NS granules. GS is induced by free radical copolymerization with unsaturated vinyl monomers and an initiator. Many studies have been investigated the degree of grafting by using various amounts of starch, initiator, monomers and different grafting techniques. In addition to the α-D-1,4 and α-D-1,6-glycosidic linkage in starch, the hydroxyl groups on both the primary and secondary carbon atoms offer the opportunity for chemical modification, incorporating near and useful properties. Graft copolymers have been prepared using starch as a backbone. Grafting onto starch often superimposes the physical and chemical characteristics of the copolymer. There are two steps for the graft copolymerization of starch as follows [36]:

1. The side chain polymer can be reacted directly with an initiator to the starch chain.

2. The starch structure has active sites such as free radicals or ions formed upon it. These can be used to polymerize a vinyl monomer to generate the graft copolymer. Figure 2.9 shows schematic structure of starch graft copolymer.

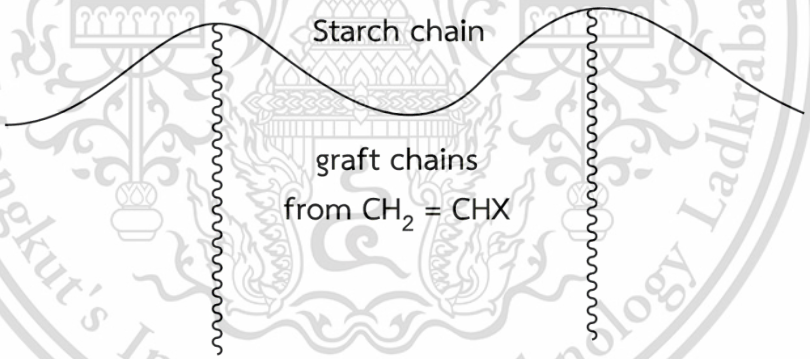

Figure 2.9 Schematic structure of starch graft copolymer [37]

2.6.1 Free radical copolymerization

Free radical polymerizations of graft copolymer are initiated by radicals and propagated by macroradicals. These radicals exhibit an unpaired electron. They are historically called radicals in order to distinguish them from "bound" radicals (nowadays called substituents or ligands (IUPAC)). Initiating radicals are rarely formed by monomers themselves but rather thermal, start electrochemically or photochemically from deliberately added initiators. Three steps of free radical polymerization are considered in a chain polymerization process as follows:

This material is reserved for educational use only, not allowed for commercial use.
Forbidden to modify the content, and cite the document when use.

1. Initiation: this reaction results in formation of an active site on a monomer molecule. In the reaction, an initiator radical (I*) adds a monomer molecule (R) and becomes a monomer radical (R*), which adds further monomer molecules.

2. Propagation: chain growth (or propagation) comprises a large number of steps. Each of them implies the addition of a monomer molecule to an active site. This can occur by opening of the double bond or by ring opening. As a result, the monomer is incorporated into the chain and the site is restored at chain end. Growth steps are required to build an n-mer (polymer constituted of n base units).

3. Termination step: termination involves the destruction of the site whereby the growth of the chain is stopped; growing macroradicals (IR_nR) may react with their own kind or with initiator radicals which terminates both the individual polymer chain and the kinetic chain. These termination reactions limit the total of active centers in polymerizations radicals. Two can bump together and stick, their unshared electron combining to form a single bond between them (combination).

Depending on polymerization conditions, the same monomer may deliver polymers that differ in constitution (degree of branching), configuration (tacticity), molar mass, molar mass distribution, and, subsequently, in properties. Free radical polymerization is the most important class of industrial polymerizations since many different monomers can be polymerized free-radically and the reaction can be easily controlled by additives, the reaction temperature and the state of matter [22, 37]. The schematic reaction of free radical copolymerization is presented in Figure 2.10.

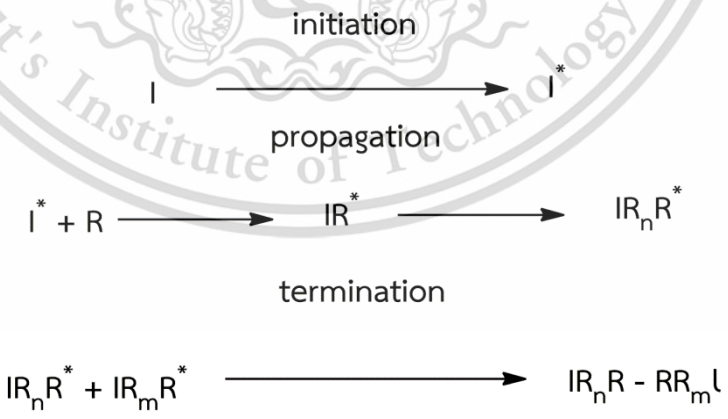

Figure 2.10 The schematic reaction of free radical copolymerization [37]

This material is reserved for educational use only, not allowed for commercial use.
Forbidden to modify the content, and cite the document when use.

2.6.2 Initiators for graft copolymerization

The initiator is a substance that generates radical by homolytic scission when it is heated or may initiate free radical polymerization under certain conditions. An effective initiator is a molecule that is subjected to heat, electromagnetic or chemical reaction, will readily undergo homolytic fission into radical of rather a reactivity than the monomers radical. These radical must also be stable long enough for reacting with a monomer and creating an active centre.

The free radical initiators can be classified for several groups as follows:

1. Persulfate such as potassium persulfate (PPS) or ammonium persulfate (APS)
2. Peroxide such as benzoyl peroxide (BPO) or dibenzoyl peroxide (DBPO)
3. Peresters like *t*-butyl-benzoate
4. Aliphatic azo compounds such as azobisisobutyronitrile (AIBN).

When the rate of initiation is considered, the rate of decomposition of initiator decomposition is highly temperature dependent. A consequence is that each initiator presents different domains of temperature than fits well for initiation; the rate of formation of primary radicals is too slow at a lower temperature, while the rate of initiator decomposes too high at high temperature [22].

2.6.3 Factors affected grafting percentage (%G)

The factors affected grafting percentage for the synthesis of graft copolymer include:

1.Temperature: this factor increases the mobility of monomer molecules.

2. Initiator: this factor increases the number of free radical sites on the starch.

3. Concentration of monomer: this factor increases the reaction of monomers on grafting sites.

4.Time: this factor increases the effect of monomer and concentration initiator in the reaction on grafting sites [38].

2.6.4 Applications of grafted copolymer

The starch graft copolymer is one type of chemical modified starch. The graft products are water soluble and useful as thickeners, absorbents, sizing agents, adhesives, flocculants for dye removal and wastewater treatment agents. The graft products are water-insoluble and potentially useful as resins and plastics [39].

This material is reserved for educational use only, not allowed for commercial use.
Forbidden to modify the content, and cite the document when use.

2.7 Cassava starch

2.7.1 Source of cassava starch

Cassava or Manioc or Yuca are the common names of a plant with starch and the scientific name is *Manihot Esculenta Crantz*. Cassava originates in Brazil. It becomes one of the most important starch crops in tropical regions (Asia, Africa and part of Latin America), especially in Africa which produces more than half of the world output. Cassava is a common raw material in starch production [40].

2.7.2 Preparation of cassava starch

Cassava starch is prepared for consumption by pouring it slowly into a pot of boiling water over a fire and stirring it on the fire until it forms a brownish and viscous paste. The paste is allowed to cool and harden.

2.7.3 Properties of cassava starch

Cassava starch presents a white appearance in the dry state. When some cereal starch is compared, amylose content of cassava starch has been shown less variation ranging from 17-24%, and other significant features found for cassava starch was its low contents of lipid (0.1%), protein/nitrogen (around 0.01%), and phosphorous (0.001-0.008%). The gelatinization temperature range is 58-70˚C. Viscosity and clarity of cooked cassava starch are its most important characteristics. Viscosity development in a dilute slurry as recorded in the Brabender-Visco-graph is a means of determining the gelatinization temperature, the rate of viscosity development, the maximum viscosity and the viscosity loss after the peak. In unmodified cassava starch, these factors are influenced by variety and age of the roots at harvest time as well as the climate, soil, fertility and rainfall during the growing period [40].

2.7.4 Applications of cassava starch

A long-term and wide use of cassava starch in food manufacturing, especially baby food, has been attributed to the physical properties of its paste (clarity and stability) and bland flavor contribution. Another food application of cassava starch reliant upon its flavor absence and fast melt away (due to the low retrogradation tendency) is in pudding products. Furthermore, cassava has been used as a lubricant in oil and in the textile industry and as a substrate for the production of dextrins, which are used in glues [40]. General properties of cassava starch are shown in Table 2.4.

This material is reserved for educational use only, not allowed for commercial use.
Forbidden to modify the content, and cite the document when use.

Table 2.4 General properties of cassava starch [40]

Property	Quantity
Chemical composition (% w/w of dry starch)	
Protein	0.1
Fats	0.1
Ash	0.2
Phosphorus	0.01
Moisture	13.0
Size of granule (pm)	3-34
Cold paste clarity (%)	40-50
Whiteness (Kett)	81.0-96.0
Amylose (%)	17-23
Size of amylose (DPn)	2000-4600
Solubility at 85°C (%)	22-42
Swell of power at 85°C (%)	40-62
Gelatinization temperature (°C)	59-70

2.8 Thermoplastic starch (TPS)

An important property of starch is its semi-crystallinity. In order to make a thermoplastic starch (TPS) product by conventional processing technique, it is important to disturb the starch granule and soften in part of the crystalline structure. TPS is biodegradable plastic based on starch and plasticizer. The semi-crystalline starch granules are disrupted by thermal and mechanical processing under heat, high pressure and shear force in order to produce TPS material. The properties of TPS are dependent on the type and amount of plasticizers. TPS can be prepared via conventional processing techniques such as injection, extrusion, blow and compression molding, etc. Common plasticizers of TPS are water and glycerol. Although thermoplastic materials can be processed via conventional processing, they often have high viscosity and poor melt properties in comparison with synthetic polymers and often lead to brittle and water sensitive products [41-42].

This material is reserved for educational use only, not allowed for commercial use.
Forbidden to modify the content, and cite the document when use.

2.9 Methacrylamide monomer

Methacrylamide (MAM) is a functional monomer with three functional groups—vinyl, methyl, and amide—in one molecule. MAM is soluble in water, ethylene, glycol and mixture of acetone and water. It is utilized as a modifier for acrylic emulsion, fiber treatment agent, resin and in latex production. It is a chemical monomer utilized in the synthesis of various types of polymers, copolymers, and acrylic resins. It is produced for the use as an industrial chemical to produce many products based on the polymer. It is utilized as a raw material in the production of chemicals for industrial application such as textile, leather, fur, bulk, large scale chemicals, fine chemicals, formulations, building, construction work, electricity, steam, gas, water supply and sewage treatment. In addition, it is a precursor of methyl methacrylate (MMA) monomer. It is also used in applications involving flocculation or to increase the viscosity of aqueous systems. Flocculation is the major use for MAM monomer, which includes clarification of water used in industrial processes (e.g. as a pretreatment or boiled water). In sewage treatment, MAM increases the removal of solids in the primary settlings step, improves clarification of the discharged water, aids in sludge thickening, improves clarity in the supernatant for digestors and increases water removal during sludge dewatering [43]. The chemical structure, properties and material data safety sheet (MSDS) of MAM are displayed in Figure 2.11 and Tables 2.5-2.6.

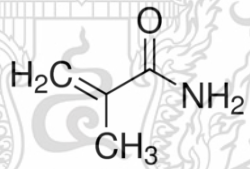

Figure 2.11 Chemical structure of MAM [43]

This material is reserved for educational use only, not allowed for commercial use.
Forbidden to modify the content, and cite the document when use.

Table 2.5 Properties of MAM [43]

Property	Detail
Molecular Formula	C_4H_7NO
Appearance	White solid powder or colorless liquid
Molecular weight	86.11 g/mol
Density	1.10-1.12 g/cm^3
Melting point	106.0-109.0°C
Boiling point	215.0°C
Water solubility	Soluble, 160.0 g/L
Viscosity (25°C)	0.69 centipoise

Table 2.6 MSDS of MAM [44]

Data	Detail
IUPAC name	2-Methyl-2-propenamide
Chemical name	Methacrylamide
CAS No.	79-39-0
RTECS code	SC353674
NFPA number	 -NFPA health hazard: 1 - Materials that cause irritation upon exposure, but only minor injury is sustained even if no medical treatment is provided. -NFPA fire hazard: 1 - Materials that must be strongly heated before ignition will occur. -NFPA reactivity: 0 - Materials that are stable even under exposure to fire.

This material is reserved for educational use only, not allowed for commercial use.
Forbidden to modify the content, and cite the document when use.

2.10 Methacrylic acid monomer

Methacrylic acid, also called MAA, is an organic compound. It is an α-, β-unsaturated monocarboxylic acid that is acrylic acid in which the hydrogen is substituted by a methyl group (Figure 2.12 and Tables 2.7-2.8). It is derived from an acrylic acid monomer. It is a conjugate acid of a methacrylate. This chemical compound is white solid powder or colorless and viscous liquid of carboxylic acid. It is easily soluble in water, dimethylformamide, dioxane and 2-ethoxyethanol. MAA is manufactured on a large scale as a precursor to its esters, especially methyl methacrylate (MMA). MAA occurs naturally in small amounts in the oil. In the most common method, acetone and cyanide react to produce acetone cyanohydrin, which is converted to methacrylamide sulfate and produced sulfuric acid.

MAA is most generally utilized for vinyl ester resins using in a wide range of composite applications. This monomer is commonly added to adhesives. It is most likely to be present to different extents in the majority of adhesive resins, due to the hydrolysis of the ester group in other monomers. MAA is highly versatile material in that the acid and ester side groups can partake in a variety of reactions to produce a very large number of polymerizable monomers. For one particularly interesting approach, two MAA groupings can primarily link together because there are two double bonds in the molecule. In these cases, it is possible to polymerize via each of these double bonds separately and will generate a cross-linked network structure. An advantage of MAA in this market is their weather ability, low burning rate, low smoke emission and ease of removal of stains and burn marks. The most important of MAA monomer are the uses as adhesives, thickeners, coating, flocculants, dispersants, fluidizers, in cosmetics, pharmaceuticals, ion exchange processes, etc. In addition, it is important warp sizes in adhesives, dispersants and textile processing [45].

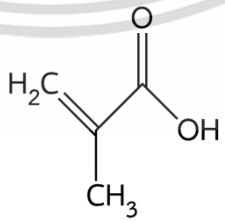

Figure 2.12 Chemical structure of MAA [45]

This material is reserved for educational use only, not allowed for commercial use.
Forbidden to modify the content, and cite the document when use.

Table 2.7 Properties of MAA [45]

Property	Detail
Molecular Formula	$C_4H_6O_2$
Appearance	White solid powder or colorless liquid
Molecular weight	83.06 g/mol
Density	1.01 g/cm^3
Melting point	14.0-15.0°C
Boiling point	161.0°C
Water solubility	Soluble, 200.0 g/L
Viscosity (25°C)	0.65 centipoise

Table 2.8 MSDS of MAA [44]

Data	Detail
IUPAC name	2-methylpropenoic acid
Chemical name	Methacrylic acid
CAS No.	79-41-4
RTECS code	OZ2975000
NFPA number	 -NFPA health hazard: 2 - Materials that can cause incapacitation or residual injury, during intense or continued exposure, unless prompt medical treatment is provided. -NFPA fire hazard: 1 - Materials that must be strongly heated before ignition will occur. -NFPA reactivity: 0 - Materials that are stable even under exposure to fire.

This material is reserved for educational use only, not allowed for commercial use.
Forbidden to modify the content, and cite the document when use.

2.11 Methyl methacrylate monomer

Methyl methacrylate (MMA) is an organic compound with the formula of $CH_2=C(CH_3)COOCH_3$. This chemical compound is white solid powder or colorless liquid. The methyl ester of methacrylic acid (MAA) is a monomer, which is commonly used to produce the poly(methyl methacrylate) (PMMA). MMA monomer is produced by several procedures, the principal one being the acetone cyanohydrin (ACH) method. ACH is produced by condensation of acetone and hydrogen cyanide. The cyanohydrin is hydrolyzed in the presence of sulfuric acid to a sulfate ester of the methacrylamide (MAM). Methanolysis of this ester produces ammonium bisulfate and MMA.

MMA is one of the most attractive monomers used in the wide range of plastic applications. MMA has numerous applications in different technical fields and in domestic uses. MMA is a raw material for the manufacture of other methacrylates. These derivatives include ethyl methacrylate (EMA), butyl methacrylate (BMA) and 2-ethyl hexyl methacrylate (2-EHMA). It is also utilized for the synthesis of the copolymer methyl methacrylate-butadiene-styrene (MBS), using as a modifier for PVC plastic material. It is used as organic glass for windows for transportation vehicles, as molding powder for technical items and consumer goods, medical and laboratory equipment, dentures, films, etc. Biaxial stretching improves both mechanical properties and surface smoothness of MMA film [46]. The chemical structure, properties and MSDS of MMA are given in Figure 2.13 and Tables 2.9-2.10.

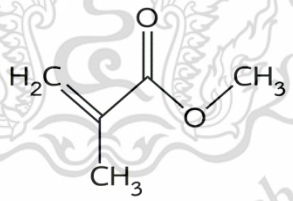

Figure 2.13 Chemical structure of MMA [46]

This material is reserved for educational use only, not allowed for commercial use.
Forbidden to modify the content, and cite the document when use.

Table 2.9 Properties of MMA [46]

Property	Detail
Molecular Formula	$C_5H_8O_2$
Appearance	White solid powder or colorless liquid
Molecular weight	100.12 g/mol
Density	0.94 g/cm^3
Melting point	-48.0°C
Boiling point	101.0°C
Water solubility	Soluble (1.5 g/L)
Viscosity (25°C)	0.87 centipoise

Table 2.10 MSDS of MMA [44]

Data	Detail
IUPAC name	methyl 2-methylpropenoate
Chemical name	Methyl methacrylate
CAS No.	80-62-6
RTECS code	OZ5250000
NFPA number	 -NFPA health hazard: 1 - Materials that cause irritation upon exposure, but only minor injury is sustained even if no medical treatment is provided. -NFPA fire hazard: 1 - Materials that must be strongly heated before ignition will occur. -NFPA reactivity: 0 - Materials that are stable even under exposure to fire.

This material is reserved for educational use only, not allowed for commercial use.
Forbidden to modify the content, and cite the document when use.

2.12 Potassium persulfate

Potassium persulfate (PPS) is the inorganic compound with the chemical formula of $K_2S_2O_8$. it is a white solid that is easily soluble in cold water, but moderately soluble in warm water. This inorganic salt is a powerful oxidant and has been widely utilized to initiate polymerizations. PPS can be produced by electrolysis of a cold solution potassium bisulfate in sulfuric acid.

$$2\ KHSO_4 \longrightarrow K_2S_2O_8 + H_2$$

It can also be produced by adding potassium bisulfate ($KHSO_4$) into a solution of ammonium peroxydisulfate salt $(NH_4)_2S_2O_8$. It can be produced by chemical oxidation of potassium sulfate using fluorine [47]. The chemical structure, properties and MSDS of PPS are illustrated in Figure 2.14 and Tables 2.11-2.12.

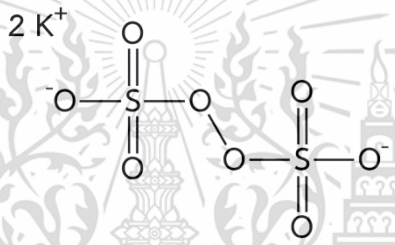

Figure 2.14 Chemical structure of PPS [47]

The wide applications of PPS are shown below:

1. PPS is utilized to initiate free radical polymerization of various polymers such as styrene-butadiene rubber (SBR) and polytetrafluoroethylene (PTFE) and other materials. Chemical reaction of initiation polymerization with PPS is illustrated in Figure 2.15.

2. It is utilized as an oxidizing agent, for instance in the persulfate oxidation of phenols.

3. It is utilized as a bleaching agent and a lightener in hair.

4. Such brief and non-continuous use is normally hazard-free. It is also utilized as an improving agent for flour that is used to combine with flour in order to increase the speed of dough rising and to improve the strength and workability of the dough during cooking [48].

This material is reserved for educational use only, not allowed for commercial use.
Forbidden to modify the content, and cite the document when use.

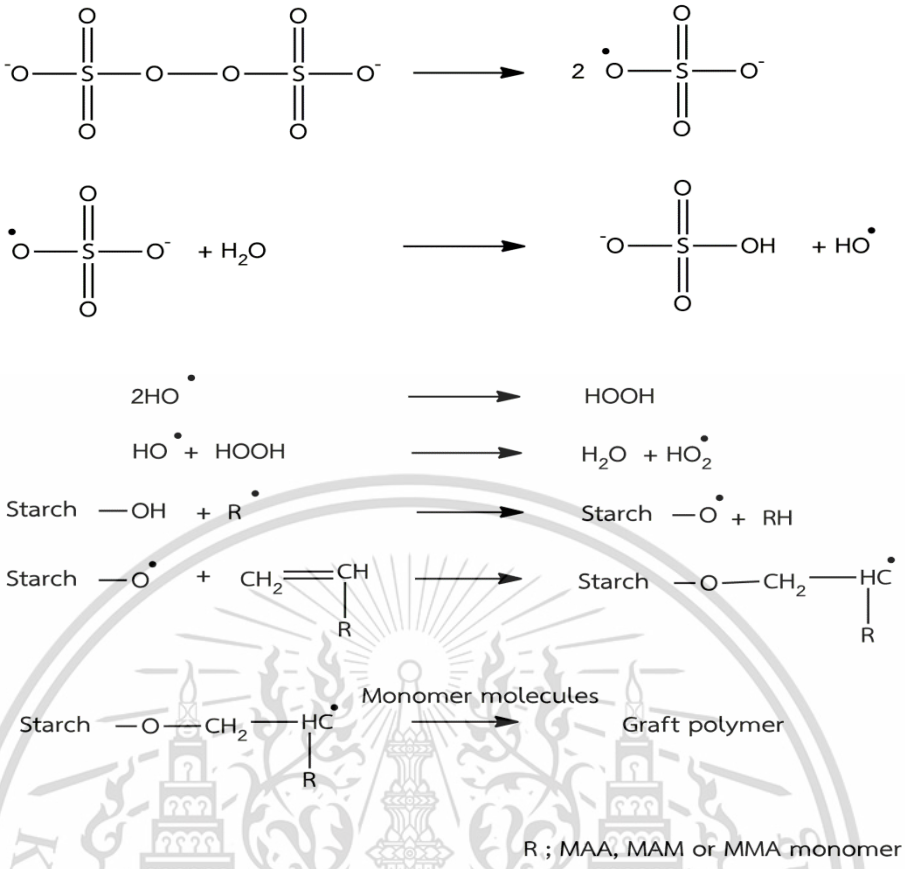

Figure 2.15 Chemical reaction of initiation polymerization by PPS [48]

Table 2.11 Properties of PPS [47]

Property	Detail
Molecular Formula	$K_2S_2O_8$
Appearance	White solid powder
Molecular weight	270.32 g/mol
Density	2.48 g/cm^3
Melting point	100.0°C
Boiling point	170.0°C
Water solubility	Soluble

This material is reserved for educational use only, not allowed for commercial use.
Forbidden to modify the content, and cite the document when use.

Table 2.12 MSDS of PPS [44]

Data	Detail
IUPAC name	dipotassium peroxodisulphate, potassium persulphate
Chemical name	Potassium persulfate
CAS No.	7727-21-1
RTECS code	SE0400000
NFPA number	 -NFPA health hazard: 1 - Materials that cause irritation upon exposure, but only minor injury is sustained even if no medical treatment is provided. -NFPA fire hazard: 1 - Materials that must be strongly heated before ignition will occur. -NFPA reactivity: 0 - Materials that are stable even under exposure to fire.

2.13 Plasticizer

The plasticizer is an additive, used to enhance the extensibility, flexibility or plasticity of the plastic. This mechanism of plasticizer is to reduce the inter-chain bonding strength and allows the chain segments greater mobility resulting in improved flexibility and decreased stress at maximum or rigidity of the plastic. Usually, a plasticizer is chosen for its solubility in the polymer, since a soluble plasticizer can penetrate the polymer more easily than a non-soluble one. Most liquid plasticizers are low molecular weight organic materials with a glass transition temperature (T_g) around -148°C to -48°C. There are two main groups of plasticizers: internal and external plasticizers [49]:

1.External plasticizer: the plasticizer is a discrete material that is added to the polymer but for the most part never chemically combined with it.

2.Internal plasticizer: the original polymer can be modified chemically, or a related polymer can be synthesized that will have more flexibility or better low-temperature properties. The development of the desired properties in the

This material is reserved for educational use only, not allowed for commercial use.
Forbidden to modify the content, and cite the document when use.

polymer itself is called internal plasticization. The final product is usually an internally plasticized resin that comes close to the desired properties but still requires an external plasticizer in small amounts to achieve the best performance [49].

Glycerol (Figure 2.16 and Tables 2.13-2.14) is one of the most effective internal plasticizers in polymer or plastic film application. It also called glycerin. It is a basic polyol compound. It is a colorless, odorless, sweet-tasting and non-toxic viscous liquid. The main chain of the glycerol is found in all lipids (triglycerides). The glycerol has been extensively utilized in pharmaceutical formulations and food industry as a sweetener, emulsifier and humectant. Glycerol contains three hydroxyl groups which are an important factor for its solubility in water and hydrophilicity. For applications of glycerol, it is utilized in foods, pharmaceuticals, cosmetic products, industrial chemicals, etc. [50].

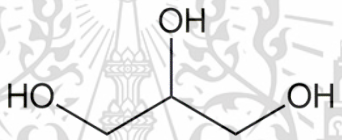

Figure 2.16 Chemical structure of the glycerol [50]

Table 2.13 Properties of the glycerol [51]

Property	Detail
Appearance	Colorless and Odorless liquid
Molecular weight	34.02 g/mol
Density	1.26 g/cm^3
Melting point	17.9°C
Boiling point	290.0°C
Water solubility	Soluble
Viscosity	17.0 centipoise

This material is reserved for educational use only, not allowed for commercial use.
Forbidden to modify the content, and cite the document when use.

Table 2.14 MSDS of glycerol [44]

Data	Detail
IUPAC name	Propane-1,2,3-Triol
Chemical name	Glycerol, Glycerin
CAS No.	56-81-5
RTECS code	MA 8050000
NFPA number	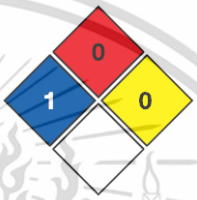 NFPA health hazard: 1 - Materials that cause irritation upon exposure, but only minor injury is sustained even if no medical treatment is provided. NFPA fire hazard: 0 - Materials that will not burn. NFPA reactivity: 0 - Materials that are stable even under exposure to fire.

2.14 Literature Reviews

M. Celik (2006) prepared GS from MAM by using benzoyl peroxide as an initiator. In this study, different percentages of grafting were investigated by varying the contents of initiator, monomer and starch including temperatures. It was found that the optimum concentration of MAM monomer that produced the highest graft yield (66%G) was 0.2-0.3 molar. The graft yield was also observed to increase with the monomer concentration and temperature. No optimum value of temperature was found. GS was characterized by FT-IR, TGA, XRD, water uptake, moisture retainment and SEM. It was found that the additional peaks at 1666 cm^{-1} and 1620 cm^{-1} arisen from C=O and N-H stretching of amide group were observed in FT-IR spectrum, confirming the success in grafting with MAM monomer onto cassava starch. TGA thermograms showed that the thermal stability of the starch increased with the percentage of grafting. The degree of crystallinity, water uptake and moisture retainment values of GS noticeably decreased with high percentage of grafting (%G).

This material is reserved for educational use only, not allowed for commercial use.
Forbidden to modify the content, and cite the document when use.

SEM micrographs exhibited that the original granules of starch disappeared after graft copolymerization [14].

A. Umar *et al.* (2016) investigated the preparation of NS from sweet potato starch grafted with MAM monomer by using an ammonium persulfate initiator and characterized it. The effect of reaction conditions on graft copolymerization was examined. The highest percentage grafting (%G) of MAM-grafted starch in this study was 351.60% G, which was carried out under the experimental conditions of 1:1 of starch: MAM weight ratio, 0.4 g of ammonium persulfate (APS) and a reaction temperature of 90°C. FT-IR study revealed new MAM peaks at 1662 cm^{-1} and 1602 cm^{-1} assigned to C=O stretching and N-H bending of MAM-grafted starch, respectively. It was observed that the grafted copolymerization was able to improve the thermal stability of NS. The thermal degradation temperature of MAM-grafted starch was at around 430°C, while that of NS was about 320°C [10].

S. Velickovic *et al.* (2012) investigated the synthesis of MAA-graft starch by free radical polymerization under various conditions including different amounts of PPS initiator (0.00075–0.0025 mol), different concentrations of MAA monomer (0.775–1.452 mol/mL), different amounts of amine activator (0.001–0.005 mol), different temperatures (55–75°C) and different reaction times (30–270 min). The obtained percentages of grafting (%G) of MAA-grafted starch under various conditions were examined. MAA-grafted starch was tested by FT-IR spectroscopy and SEM technique. The optimum grafting yield (40.92% G) was obtained at 0.001 mol PPS initiator, 0.775 mol/mL MAA monomer, 10 g starch and 70°C. The accomplishment of grafting was confirmed by FT-IR spectroscopy: a peak on 1730 cm^{-1} arisen from C=O stretching of acrylic group was observed. The morphology of MAA-grafted starch showed a changed starch granular structure and the attachment of MAA monomer onto starch granules [51].

Kh.M. Mostafa (1995) studied grafting of MAA onto NS from maize starch by using $KMnO_4$/citric acid as initiator. The effects of variations in reaction time, temperature, a concentration of $KMnO_4$/citric acid and the initial amount of starch on the degree of grafting of GS with MAA were investigated. It was found that a higher percentage of grafting was obtained with more extended reaction time. The maximum grafting degree (144% G) was attained at a polymerization temperature of 50°C, a reaction time of 3 h, 4 g of starch, 0.825 molar of $KMnO_4$ and 0.8 g of citric acid. It was obvious that the molecular weight and specific viscosity increased with increasing percentage of grafting; whereas, the percentage solubility decreased from 76 to 55% which could be explained by new strong hydrogen bonding between two MAA groups [52].

This material is reserved for educational use only, not allowed for commercial use.
Forbidden to modify the content, and cite the document when use.

D. Pathania and R. Sharma (2012) studied grafted copolymerization of MAA monomer onto potato starch achieved by using chromic acid as an initiator. Various reaction conditions (temperature as well as initiator and monomer concentrations) were optimized in order to obtain the highest of percentage grafting, which was 87.5% G at 60°C and initiator and monomer concentrations of 0.02 and 0.81 mol/cm^3, respectively. The thermal and swelling properties, water uptake and morphology of MMA-grafted starch were investigated; FT-IR and XRD analysis of MAA-grafted starch were also conducted. An additional peak at 1720 cm^{-1} arisen from C=O stretching of acrylic group was observed in the FT-IR spectrum, confirming the grafting of MAA monomer onto potato starch. With the increasing grafting percentage, the water uptake, swelling capacity and degree of crystallinity of GS grafted with MAA tended to decrease. In addition, thermal properties of GS improved considerably by grafting with MAA [15].

M. Celik and M. Sacak (2002) investigated the synthesis and characterization of MMA-grafted starch. The graft copolymerization onto starch was achieved by using azobisisobutyronitrile (AIBN) as an initiator. The graft copolymerization was performed within a temperature range of 65–95°C and the influences of the initiator, monomer concentration and starch content on the percentage of grafting were also examined. MMA-grafted starch was then characterized by FT-IR, SEM and TGA techniques. The data indicated that the highest graft yield (38% G) was achieved by using the ratio of starch to monomer at 1:1. The optimum conditions for temperature and monomer concentration were not observed in this study. A rise in the percentage of grafting was observed when the monomer concentration and temperature were increased. SEM micrographs showed that no starch granules existed after graft copolymerization and MMA monomer particles were attached to the surface of the starch. Besides, the thermal stability of the starch was clearly improved after grafting with MMA [16].

V. Pimpam and P. Thothong (2006) studied the optimization of reaction conditions of the synthesis of MMA-grafted cassava starch, which included the reaction time as well as the amounts of benzoyl peroxide (BPO), starch and MMA monomer. These parameters influenced the grafting percentage of MMA-grafted starch. The optimum conditions with the maximum percentage of grafting (95% G) were found to be the following: 5 g of starch and MMA monomer, 0.1 g of BPO and a reaction time of 3 h. The successful preparation of MMA-grafted starch was confirmed initially by function group analysis by FT-IR. An additional absorption peak of C=O stretching was observed at 1730 cm^{-1}, related to the carbonyl group of MMA group. Graft copolymerization was also confirmed by SEM analysis. The morphology of MMA-grafted starch showed a change in starch granular structure [53].

This material is reserved for educational use only, not allowed for commercial use.
Forbidden to modify the content, and cite the document when use.

M.C. Li *et al.* (2012) prepared MMA-grafted corn starch film by casting technique by using DMSO as a solvent and without plasticizer. MMA-grafted corn starch was carried out at 40˚C for 3 h by using ceric ammonium nitrate as an initiator. Percentage of grafting (%G) of 30.6%, 44.9%, 68.7%, 89.2%, and 110.4% were obtained from reacting with different CS/MMA weight ratio of 7/3, 6/4, 5/5, 4/6, and 3/7, respectively. The morphology and function groups of grafted CS were examined. Its thermal properties were examined by TGA and differential scanning calorimetry (DSC), while its biodegradability was examined by an amylase treatment of MMA-grafted starch. The structure of MMA-grafted starch was confirmed by an FT-IR analysis where a new absorption peak was observed at 1726 cm^{-1} attributable to C=O stretching of MMA. MMA-grafted starch showed good biodegradability after amylase treatment. The thermal properties of CS were improved after graft copolymerization with MMA and the decomposition temperature of starch was increased with the increasing percentage of grafting [17].

R. H. Aurelio *et al.* (2018) studied the physicochemical, mechanical and biodegradable properties of CL-grafted starch films from banana starch. The CL-grafted starch cast film with 80% G was prepared by a casting technique using 30 wt% of glycerol plasticizer. The SEM images of the films showed CL particles distributed evenly on the CL-grafted starch. The results of the XRD study and the determined mechanical property indicated that the crystalline phase of the films decreased to 46% and percentage of elongation increased up to 50% after grafting. CL-grafted starch film presented faster biodegradability than ungrafted starch film. The thermal degradation temperature and moisture absorption capacity of the films were declined by more than 15˚C and 6.5%, respectively. In addition, the incorporation of CL monomers into the starch structure caused a drop in water vapor permeation value of GS cast films [18].

Z. B. Cuevas-Carballo *et al.* (2017) reported several properties and biodegradability of TPGS sheet grafted with CL by using different amounts of a mixture of glycerol and sorbitol (25 and 35 wt% of dry starch) plasticizer. The sample sheet was blended in a mixer for 10 min at 150˚C at a rotor speed of 40 rpm and shaped by a compression molding method at 150˚C. The grafted corn starch was prepared by using N-methylimidazole (NMI) as a catalyst. The effects of the amounts of starch, CL monomer and catalyst on the degree of CL grafting were investigated. The highest grafting percentage (76% G) was achieved with a starch/monomer ratio of 50/50 and 35 wt% of plasticizer. The successful grafting of CL onto the starch granules was confirmed by the presence of carbonyl groups in the FT-IR spectra and the increase in diameter of GS granules observed in the SEM images. The low hardness and high flexibility of TPNS and TPGS prepared with 35 wt% of the mixture

This material is reserved for educational use only, not allowed for commercial use.

Forbidden to modify the content, and cite the document when use.

of sorbitol and glycerol resembled those of a plastic material. The use of CL-grafted starch instead of NS caused a significant increase in the extensibility of TPGS. On the other hand, TPNS was completely biodegraded while TPGS prepared with CL was only partially biodegraded after enzymatic degradation [19].

S. Sekar *et al.* (2015) prepared NS sheets and MMA-grafted starch sheets from sago starch using 15 wt% of ethylene glycol as a plasticizer by a casting technique and compared their physicochemical and mechanical properties. MMA-grafted starch was produced by a free radical graft copolymerization process at 80°C with 2 wt% of potassium persulfate (PPS) as an initiator. The successful synthesis of MMA-grafted starch was confirmed by FT-IR analysis. MMA-grafted starch sheets showed a lower tearing strength and tensile strength than those of non-grafted NS sheets but higher elongation at break. Grafting with MMA also improved the hydrophobicity of NS sheets. From the results, it was concluded that this material could be used as a biodegradable wound dressing [20].

G. Canché-Escamilla *et al.* (2011) investigated the physicochemical properties and biodegradability of TPGS sheets from corn starch grafted with butyl acrylate (BA)-co-MMA monomers. The maximum grafting percentage (75% G) was achieved at 30°C with 0.1 M ceric ammonium nitrate as an initiator. TPNS and TPGS sheets were prepared by mixing NS or GS with 30 wt% of a mixture of water and glycerol plasticizer in an internal mixer with a rotor speed of 40 rpm at 170°C and then molded by a compression molding technique at 170°C. TPGS sheet exhibited a rougher surface than that of a TPNS sheet. TPGS sheets prepared with BA-co-MMA showed low tensile strength and high flexibility as determined by dynamic mechanical analysis (DMA). The biodegradability of TPNS and TPGS sheets was investigated by a technique related to the growth of *Aspergillus* niger-fungus on these sheets. The biodegradability of TPGS sheet can also be examined by the decrease of degradation temperature and molecular weight of the starch due to enzymatic attack [21].

In brief, most reports focused on the effect of grafted copolymerization with MAM, MAA and MMA monomers to starch granules. However, the effect of grafting percentage on physicochemical of TPGS films with these monomers has never been reported and will be examined thoroughly in this present study.

This material is reserved for educational use only, not allowed for commercial use.
Forbidden to modify the content, and cite the document when use.

Chapter 3
Research methodology

3.1 Materials

1. Cassava starch; from Chaopraya Phuchrai 1999 Co., Ltd., Thailand

Table 3.1 The compositions of cassava starch

Component	Weight percentage (%)
Amylose	16.4±3
Amylopectin	83.6±2
Lipid	0.25±0.1
Protein	6.50-7.50
Humidity	<13
Ash	0.23±0.1
Size	<160 μm
pH	6-7

Remark : Data of the manufacturer

2. Methacrylamide monomer; analysis grade from Carlo Erba Co., Ltd., France
3. Methacrylic acid monomer; analysis grade from Italmar Co., Ltd., Thailand
4. Methyl methacrylate monomer; analysis grade from Chemipan Co., Ltd., Thailand
5. Potassium persulfate; analysis grade from Merck Co., Ltd., Germany
6. Methanol; analysis grade from Merck Co., Ltd., Germany
7. Distilled water
8. Acetone; analysis grade from Lab-scan Asia Co., Ltd., Thailand
9. Glycerol; commercial grade from Lab System Co., Ltd., Thailand
10. Magnesium stearate; trading grade from Union Chemical 1986 Co, Ltd., Thailand
11. Dimethyl sulfoxide (DMSO); analysis grade from Carlo Erba Co., Ltd., France

This material is reserved for educational use only, not allowed for commercial use.
Forbidden to modify the content, and cite the document when use.

3.2 Devices and Instruments

1. Three-neck round bottom flask; 500 and 1000 ml
2. Beaker; 250, 500, 1000 and 200 ml
3. Heating mantle; MQ 1000 ml from FALC Co., Ltd., Italy
4. Hot plate stirrer; CMAG HS7 5000 from IKA Co., Ltd., Thailand
5. Mechanical stirrer; RW 20 D from IKA Co., Ltd., Thailand
6. Analytical balance; MS204TS/00 from Mettler Toledo Co., Ltd., Thailand
7. Hot air oven; UF110 from Memmert Co., Ltd., U.S.A.
8. Blender; EM 44A from Sharp Co., Ltd, Thailand.
9. Vacuum filter; A35 from Eyela Co., Ltd, U.S.A
10. Granulator; ZM100 from Retsch Co., Ltd., Germany
11. Internal mixer; MX500-D75L90 from Chareon Co., Ltd., Thailand
12. Compression molding; LP-20 from Labtech Engineering Co., Ltd., Thailand
13. Capillary viscometer; from Thomas Scientific Co., Ltd., U.S.A
14. Universal testing machine; LR 5 K from Lloyd Instrument Co., Ltd., UK
15. Fourier transform infrared spectrophotometer (FT-IR); SPECTRUM GX from Perkin Elmer Co., Ltd. U.S.A.
16. Scanning Electron Microscopy (SEM); JSM-5410 from Jeol Co., Ltd., Japan.
17. X-ray diffractometer (XRD); D8 Advance from Bruker Co., Ltd., U.S.A.
18. Thermogravimetric analyzer (TGA); Pyris 1 from Perkin Elmer Co., Ltd, U.S.A.

This material is reserved for educational use only, not allowed for commercial use.
Forbidden to modify the content, and cite the document when use.

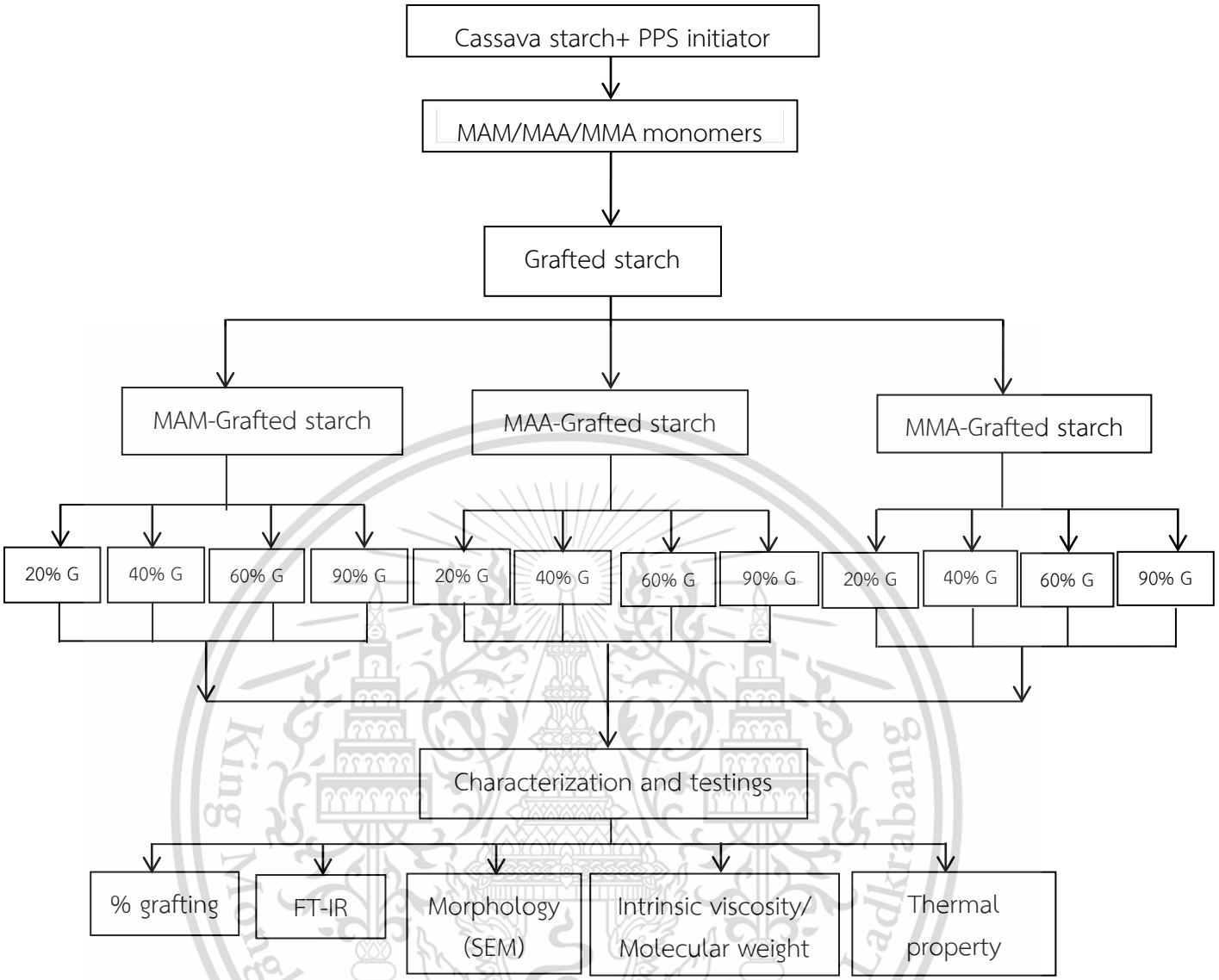

Figure 3.1 Flowchart of preparation of different types of GS

This material is reserved for educational use only, not allowed for commercial use.
Forbidden to modify the content, and cite the document when use.

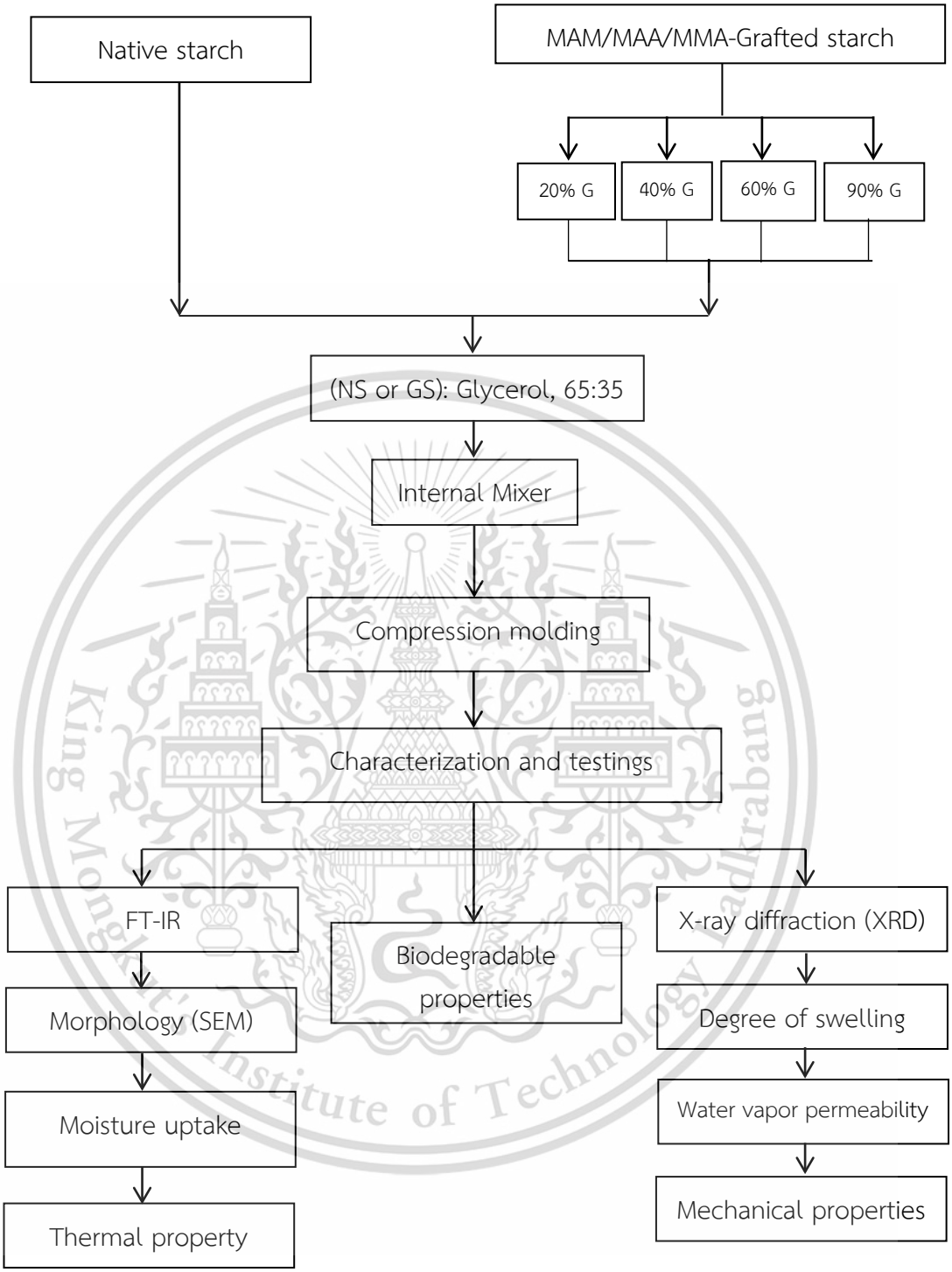

Figure 3.2 Flowchart of preparation of different TPGS films

This material is reserved for educational use only, not allowed for commercial use.
Forbidden to modify the content, and cite the document when use.

3.3 Method

In this study, flowcharts of preparation of different types of GS and different TPGS films are given in Figures 3.1-3.2.

3.3.1 Preparation of various grafted starch (GS)

1. Firstly, 25 g cassava starch was suspended in 500 mL of distilled water in a 1,000 mL three-neck round bottom flask.

2. The starch suspension was stirred with a mechanical stirrer at a rotor speed of 300 rpm and then, heated and maintained at 80±5°C for 30 min under nitrogen atmosphere and formed a gel-like slurry.

3. Then, 0.5 g (2 wt% of dry starch) of PPS initiator was added to the slurry; the slurry was stirred for 10 min to disperse the initiator thoroughly.

4. 25 g MAM, MAA or MMA monomer (starch to monomer ratio, 1:1) was, then, added to the slurry.

5. The gelatinized starch-monomer mixture was continuously stirred in the three-neck round bottom flask at 300 rpm under a controlled temperature of 80±5°C and nitrogen atmosphere for the different reaction times, i.e., 1, 2, 3, 4, 5 and 6 h, then the flask was closed tightly with a piece of aluminium foil and a piece of paraffin film.

6. After 1, 2, 3, 4, 5 or 6 h of reaction time, the resulting GS was precipitated with excess methanol and isolated by filtration.

7. The substance on the top of the filter was extracted thoroughly with warm water to remove MAM or MAA homopolymer or with acetone to remove MMA homopolymer.

8. GS was dried in a hot air-oven (Memmert, Germany) at 50°C for 24 h until its weight became constant, then it was ground into powder (granular size = 0.08 mm) with a granulator (Retsch, Germany).

9. Finally, GS was weighed in order to find out the percentage of grafting (%G). GS products with 20, 40, 60 and 90% G were used to produce TPGS films.

3.3.2 Preparation of TPNS film and various TPGS films

1. The ingredients were weighed according to the formulas shown in Table 3.2.

2. Either NS or GS was pre-mixed with glycerol, as a plasticizer, in a polyethylene bag and kept overnight.

3. The mixture was, then, blended and heated thoroughly in an internal mixer at 150°C at a speed of 40 rpm for 5 min.

This material is reserved for educational use only, not allowed for commercial use.
Forbidden to modify the content, and cite the document when use.

4. The material was then compressed to a 0.3 mm thickness using a spacer from a commercial teflon sheet (PTFE) with a compression molding machine at 150°C for 5 min and a pressure of 1700 psi and then left to cool down in the machine for 5 min.

Table 3.2 The compositions of TPNS and different TPGS films

Sample	Native starch (g)	MAM-/MAA-/MMA-grafted starch (g)				Glycerol (g)
		20% G	40% G	60% G	90% G	
TPNS	65	-	-	-	-	35
TPGS-20MAM	-	65	-	-	-	35
TPGS-40MAM	-	-	65	-	-	35
TPGS-60MAM	-	-	-	65	-	35
TPGS-90MAM	-	-	-	-	65	35
TPGS-20MAA	-	65	-	-	-	35
TPGS-40MAA	-	-	65	-	-	35
TPGS-60MAA	-	-	-	65	-	35
TPGS-90MAA	-	-	-	-	65	35
TPGS-20MMA	-	65	-	-	-	35
TPGS-40MMA	-	-	65	-	-	35
TPGS-60MMA	-	-	-	65	-	35
TPGS-90MMA	-	-	-	-	65	35

This material is reserved for educational use only, not allowed for commercial use.
Forbidden to modify the content, and cite the document when use.

3.4 Characterization

3.4.1 Percentage of grafting

Percentage of grafting was determined by the following equation:

$$\text{Percentage of grafting } (\%) = \frac{W_s}{W_i} \times 100 \qquad \text{Equation 1}$$

where W_s is the weight of GS and W_i is the initial weight of starch [14, 16].

3.4.2 Average molecular weight

The method of intrinsic viscosity was used to determine the average molecular weight (MW) of a sample. The test was carried out at 25.0±0.1˚C with an Ubbelohde Viscometer. The starch was dissolved in dimethyl sulfoxide (DMSO) solvent. The average molecular weight of starch was determined based on intrinsic viscosity measurements. Intrinsic viscosity was determined according to an equation of Mark-Houwink:

$$[\eta] = KM^a, \qquad \text{Equation 2}$$

where $[\eta]$ is intrinsic viscosity; K and a are constants equal to 8.5×10^{-3} mL/g and 0.76, respectively; and M is the average molecular weight [54].

3.4.3 Fourier-transform infrared spectroscopy (FT-IR)

Samples were characterized by FT-IR spectroscopy with a Spectrum 2000 GX spectrometer (Perkin Elmer, U.S.A.) and potassium bromide (KBr) disk technique. KBr powder and dried powder sample were fully ground, mixed and pressed into pellets. The spectra of the samples were taken in the wavelength range of 4000–400 cm^{-1}. Ten scans at a resolution of 4 cm^{-1} were run. The ratio of characteristic peak height was calculated by the ratio of peak height of interested peak to peak height of referenced peak of 859 cm^{-1}, that peak presented constant intensity peak.

3.4.4 X-ray diffraction technique (XRD)

An XRD diffraction pattern of the film was recorded with a D8 Advance X-ray diffractometer (Bruker, Madison, U.S.A.) and CuK_α radiation. A sample was scanned over an angular range of 2θ from 5˚ to 60˚ (2θ, θ is the Bragg angle) at a scan rate of 1˚/min. The percentage crystallinity of the sample was quantitatively estimated by following equation:

$$\text{Crystallinity } (\%) = \frac{A_c}{A_c + A_a} \times 100 \qquad \text{Equation 3}$$

This material is reserved for educational use only, not allowed for commercial use.
Forbidden to modify the content, and cite the document when use.

where A_c and A_a refer to the area of crystalline peak diffraction and the total area of the X-ray diffractogram, respectively.

3.4.5 Scanning electron microscopy (SEM)

The cross-section morphology of the films was observed in images taken by a scanning electron microscope (LEO 1450 VP). The films were cryofractured by liquid nitrogen immersion before testing then a thin layer of gold was sputter-coated on the sample surface to improve electrical conductivity. Samples were examined at a magnification of 4000X and 15 kV accelerating voltage.

3.4.6 Moisture uptake

The percentage of moisture uptake was examined by an ASTM D-570 standard method. The samples were firstly dried at 105˚C for 2 h to determine their initial dry weight and then they were placed in a closed container at 100% RH and room temperature with a cup of distilled water. The wet weights of the samples were measured daily until there was no change in weight. The average weight of a sample was calculated from three measurements. The percentage of moisture uptake is given by the following equation:

$$\text{Moisture uptake (\%)} = \frac{W_2 - W_1}{W_1} \times 100 \qquad \text{Equation 4}$$

where W_2 is the weight of the sample after immersion and W_1 is the weight of the sample before immersion.

3.4.7 Degree of swelling

The degree of swelling for the samples was examined. A sample (20×20 mm^2) was firstly dried at 105˚C for 2 h and weighed (W_1). The dried film was, then, immersed in distilled water at room temperature for 24 h. The weight of the wet film (W_2) was measured after removal of water from the surface with blotting paper. Three specimens were measured for each of the testing. Percentage of swelling was determined as follows:

$$\text{Swelling (\%)} = \frac{W_2 - W_1}{W_1} \times 100 \qquad \text{Equation 5}$$

where W_1 and W_2 were the weight of the sample before and after immersion, respectively.

This material is reserved for educational use only, not allowed for commercial use.
Forbidden to modify the content, and cite the document when use.

3.4.8 Water vapor permeability (WVP)

WVP was determined by an ASTM E-96 standard gravimetric method. A test cup containing the dry silica gel was sealed with a film sample. The cup was initially placed in the humidity chamber at 75±5% RH and 25±2°C together with a sodium chloride saturated solution for 1 day. The weight of the silica gel (used according to the standard ASTM E-96 method) was measured daily for a period of 7 days. Each sample was weighed three times and the average value was used to determine its WVP value. The WVP was estimated by the following equation:

$$WVP = \frac{W \times X}{t \times A \times \Delta P} \qquad \text{Equation 6}$$

where W is the weight of silica gel (g); t is the time (days); X is the thickness of the film sample (mm); A is the exposed area of the film (32.15 cm^2); and ΔP is the difference in partial vapor pressures at the top and bottom sides of the film (KPa) [55].

3.4.9 Mechanical properties

Mechanical properties were examined according to ASTM D-882. A film was cut into 15×100 mm^2 strips. Before testing, the strips were equilibrated in closed containers by using a saturated solution of ammonium nitrate in a closed vessel at 25±1°C and 60±5% RH for 24 h. The measurements were made with a Universal Testing Machine (Lloyd Instrument, LR 5K, West Sussex, UK). The test speed was 50 mm/min with a cell load of 100 N and a gauge length of 50 mm. The value of each mechanical property was reported as an average of ten independently tested specimens.

Stress at maximum load was calculated from the following equation:

$$\text{Stress at maximum load (MPa)} = F/A \qquad \text{Equation 7}$$

where F is force applied (N) and A is average area of a sample (mm^2)

$$\text{Strain at maximum load (\%)} = [(L-L_0)/L_0] \times 100 \qquad \text{Equation 8}$$

where L is final length (mm) and L_0 is initial length (mm)

$$\text{Young's modulus} = \frac{F/A}{(L-L_0)/L_0} \qquad \text{Equation 9}$$

This material is reserved for educational use only, not allowed for commercial use.
Forbidden to modify the content, and cite the document when use.

3.4.10 Thermogravimetric analysis (TGA)

The thermal property of the samples was characterized by a thermogravimetric analyzer (Pyris TGA HT, Perkin Elmer, U.S.A.). A 10-12 mg mass of sample was placed on an aluminum pan and undergone the measurement in the temperature range of 50 to 600˚C at a heating rate of 10°C/min under nitrogen atmosphere.

3.4.11 Biodegradability

The biodegradability of the film samples was estimated from the changes in mechanical properties of the samples after a soil buried test. The film samples were buried under approximately 10 cm of soil in a closed container. The temperature and pH of the soil were controlled at 25±2˚C and 7±1, respectively. The soil moisture was maintained at approximately 5-10% by weight. The test was carried out over periods of 5 and 10 days. At predetermined intervals, ten samples were thoroughly removed from the soil and tested of their mechanical properties.

King Mongkut's Institute of Technology Ladkrabang

This material is reserved for educational use only, not allowed for commercial use.
Forbidden to modify the content, and cite the document when use.

Chapter 4
Main results and discussion

This present study focused on the effects of graft copolymerization with different types of vinyl monomers on the properties of thermoplastic grafted starch (TPGS) films. The vinyl monomers included methacrylamide (MAM), methacrylic acid (MAA) and methyl methacrylate (MMA) with tested grafting percentages as 20, 40, 60 and 90%. Characterization techniques included Fourier transform infrared spectroscopy (FT-IR), X-ray diffractometry (XRD) and scanning electron microscopy (SEM). The degree of swelling, moisture uptake and water vapor permeability (WVP) as well as several mechanical and thermal properties were determined. Biodegradable properties of the films were also investigated by a soil burial test. Abbreviations and symbols of the terms used in this study are shown in Table 4.1.

Table 4.1 Abbreviations and symbols

No.	Abbreviation	Meaning
1	NS	Native cassava starch
2	GS-20MAM	Cassava starch grafted by methacrylamide with 20% grafting
3	GS-40MAM	Cassava starch grafted by methacrylamide with 40% grafting
4	GS-60MAM	Cassava starch grafted by methacrylamide with 60% grafting
5	GS-90MAM	Cassava starch grafted by methacrylamide with 90% grafting
6	GS-20MAA	Cassava starch grafted by methacrylic acid with 20% grafting
7	GS-40MAA	Cassava starch grafted by methacrylic acid with 40% grafting
8	GS-60MAA	Cassava starch grafted by methacrylic acid with 60% grafting
9	GS-90MAA	Cassava starch grafted by methacrylic acid with 90% grafting
10	GS-20MMA	Cassava starch grafted by methyl methacrylate with 20% grafting
11	GS-40MMA	Cassava starch grafted by methyl methacrylate with 40% grafting
12	GS-60MMA	Cassava starch grafted by methyl methacrylate with 60% grafting
13	GS-90MMA	Cassava starch grafted by methyl methacrylate with 90% grafting
14	TPNS	Thermoplastic native cassava starch
15	TPGS-20MAM	Thermoplastic grafted cassava starch by methacrylamide with 20% grafting

This material is reserved for educational use only. Not allowed for commercial use.
Forbidden to modify the content, and cite the document when use.

No.	Abbreviation	Meaning
16	TPGS-40MAM	Thermoplastic grafted cassava starch by methacrylamide with 40% grafting
17	TPGS-60MAM	Thermoplastic grafted cassava starch by methacrylamide with 60% grafting
18	TPGS-90MAM	Thermoplastic grafted cassava starch by methacrylamide with 90% grafting
19	TPGS-20MAA	Thermoplastic grafted cassava starch by methacrylic acid with 20% grafting
20	TPGS-40MAA	Thermoplastic grafted cassava starch by methacrylic acid with 40% grafting
21	TPGS-60MAA	Thermoplastic grafted cassava starch by methacrylic acid with 60% grafting
22	TPGS-90MAA	Thermoplastic grafted cassava starch by methacrylic acid with 90% grafting
23	TPGS-20MMA	Thermoplastic grafted cassava starch by methyl methacrylate with 20% grafting
24	TPGS-40MMA	Thermoplastic grafted cassava starch by methyl methacrylate with 40% grafting
25	TPGS-60MMA	Thermoplastic grafted cassava starch by methyl methacrylate with 60% grafting
26	TPGS-90MMA	Thermoplastic grafted cassava starch by methyl methacrylate with 90% grafting

4.1 Properties of differently grafted starch (GS)

4.1.1 Schematic reactions of different GS

The proposed schematic reactions and possible chemical structures of different GS are presented in Figures 4.1-4.3.

A reaction involving free radicals is the most widely cited mechanism of a grafting process. The principal reaction responsible for formation of graft copolymers involves radical transfer to the polymer. This type of reaction is considered most likely to occur in a growing polymer chain. The following mechanism is proposed for graft copolymerization of vinyl monomers with a potassium persulphate (PPS) initiator. To produce primary radicals, PPS undergoes a thermal dissociation as follows:

This material is reserved for educational use only, not allowed for commercial use.
Forbidden to modify the content, and cite the document when use.

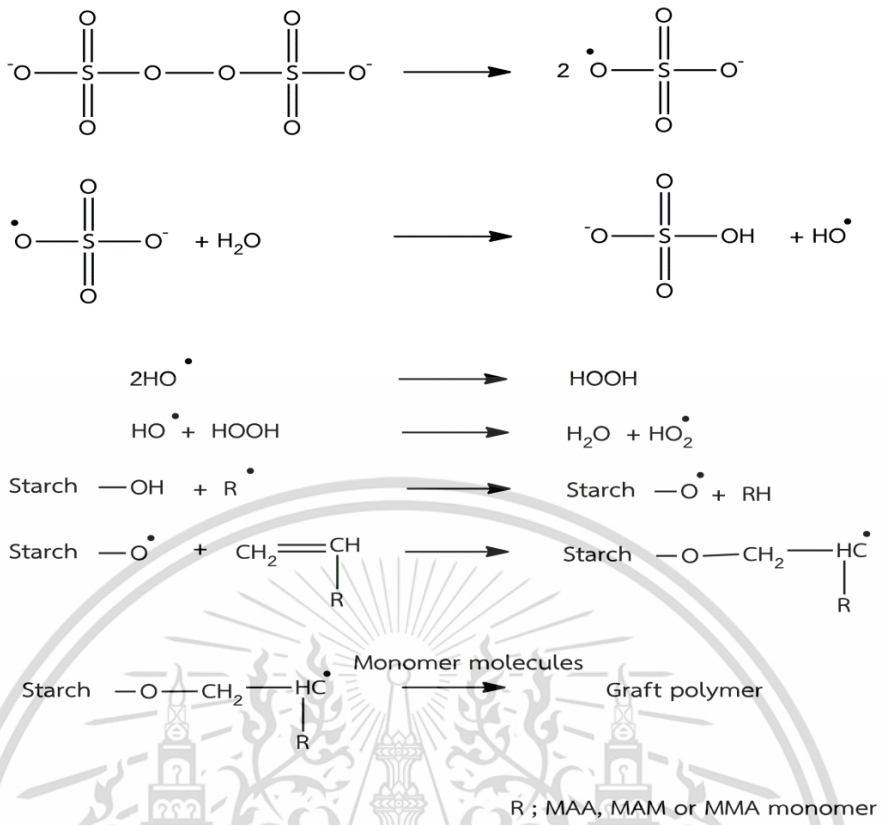

Figure 4.1 Possible mechanism of initiation reaction with PPS as an initiator [48]

PPS can further dissociate into persulphate radicals and oxygen. The persulphate radicals formed can either initiate the grafting onto starch backbones via hydrogen abstraction (hydrogen atom transfer) or homopolymerization of monomer via free radical addition to carbon-carbon starch bonds. Then, the propagation reaction occurs and generated the growing grafted starch chains. After termination of the reaction by combination, the final product obtained from graft copolymerization was the grafted starch (GS) as shown in Figure 4.2. Chemical structures of GS grafted with different types of vinyl monomers are presented in Figure 4.3.

This material is reserved for educational use only, not allowed for commercial use.
Forbidden to modify the content, and cite the document when use.

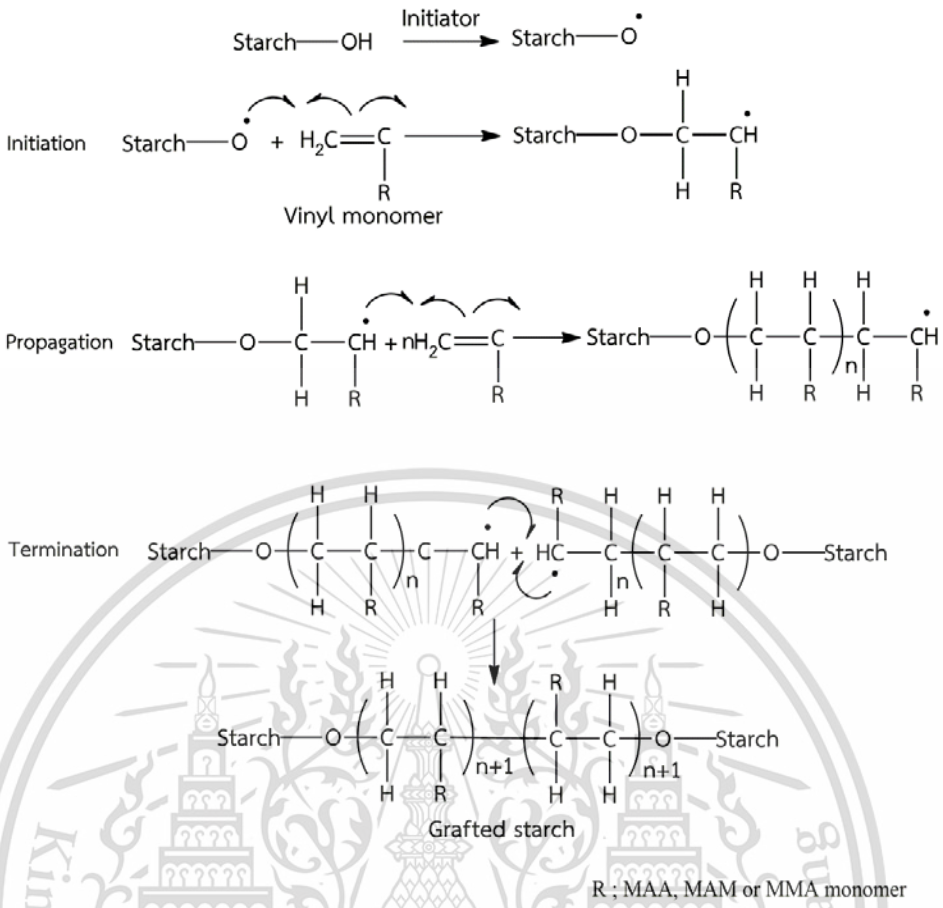

Figure 4.2 Possible mechanism for graft copolymerization of starch with PPS as an initiator [36]

This material is reserved for educational use only, not allowed for commercial use.
Forbidden to modify the content, and cite the document when use.

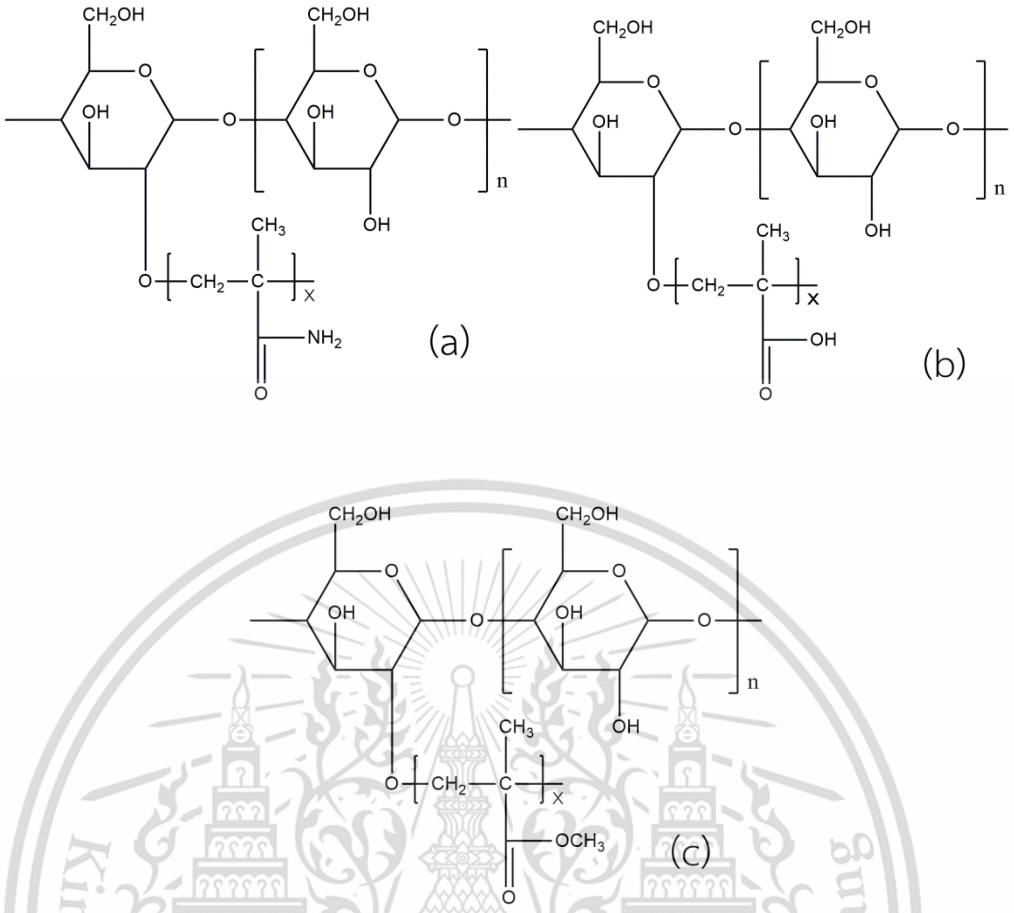

Figure 4.3 Chemical structures of GS grafted with different types of vinyl monomers: (a) MAM-grafted starch (b) MAA-grafted starch and (c) MMA-grafted starch

4.1.2 Effect of reaction time on grafting percentage (% G)

Table 4.2 Grafting percentages of various GS grafted by MAM, MAA and MMA monomers using diverse reaction times

Reaction time (h)	MAM	MAA	MMA
	%G	%G	%G
1	20.3±2.1	19.3±1.9	21.3±1.2
2	38.9±1.8	40.3±2.3	39.5±2.2
3	48.3±2.4	58.1±1.8	45.0±1.5
4	59.7±2.0	90.5±1.5	60.9±1.2
5	90.9±1.6	87.0±2.0	81.6±1.4
6	83.0±1.8	65.7±1.6	90.1±2.3

This material is reserved for educational use only, not allowed for commercial use.
Forbidden to modify the content, and cite the document when use.

Table 4.2 depicts the influence of reaction time on grafting percentage (% G) of different GS samples. With increasing reaction time from 1 to 6 hours, % G clearly increased, with maximum value of approximately 90±2%. Optimal graft yields of GS with MMA, MAM and MAA (90±2% G) were observed at reaction times of 6 h, 5 h and 4 h, respectively. Different types of vinyl monomers affected a difference in percentages of grafting at various reaction times, possibly because of differences in reactivity ratios of starch to monomer and in viscosities of different vinyl monomers at the same concentration (as shown in table 2.5, 2.7 and 2.9). Reactivity ratios of starch to monomer of different vinyl monomers are ranked as follows: MAA>MAM>MMA. This result was because MAA monomer showed the most electron deficient group. On the contrary, the least electron deficient group was found in MMA monomer, leading to slower rate of graft copolymerization [36]. Also, the maximum and minimum viscosity were found in MMA and MAA monomers [45-46]. In general, the monomers with lower viscosity can more easily react with hydroxyl groups of starch backbones as compared to that of higher viscosity, leading to a faster rate of graft copolymerization reaction [36]. Our findings revealed that a more complete grafting process occurred with longer reaction time. Increase in graft yield with time was related to increase in the number of grafting sites on starch chains in the initial stage of polymerization [53]. However, a decrease of %G occurred at reaction times of 4 h for MAA-grafted starch and 5 h for MAM-grafted starch since both monomer and initiator were depleted and the number of available active backbone grafting sites decreased [53]. GS at different percentages of 20%, 40%, 60% and 90% were prepared and their physiochemical and mechanical properties were measured.

4.1.3 Fourier-transform infrared spectroscopy (FT-IR)

Generally, FT-IR is used to investigate and identify functional groups of materials. Table 4.3 summarizes peak assignments of the characteristic bands of FT-IR spectra of various GS grafted by MAM, MAA and MMA monomers with different grafting percentages.

This material is reserved for educational use only, not allowed for commercial use.
Forbidden to modify the content, and cite the document when use.

Table 4.3 Peak assignments of characteristic bands of FT-IR spectra of NS and different GS samples [56]

Wave number (cm^{-1})	Assigned vibration mode
3600 – 3200	O-H stretching
3000 – 2800	Alkane C-H stretching
1750 – 1730	Carbonyl Ester C=O stretching
1730 – 1710	Carbonyl Carboxylic C=O stretching
1670 – 1650	Carbonyl Amide C=O stretching
1650 – 1630	Bounded water
1620 – 1590	N-H bending
1485 – 1420	O-H bending
1300 – 1100	C-O-C stretching
1200 – 1000	C-O-H bending
900 – 940	C-H out-of-plane bending
800 – 860	C-H out-of-plane bending
735 – 770	C-H out-of-plane bending

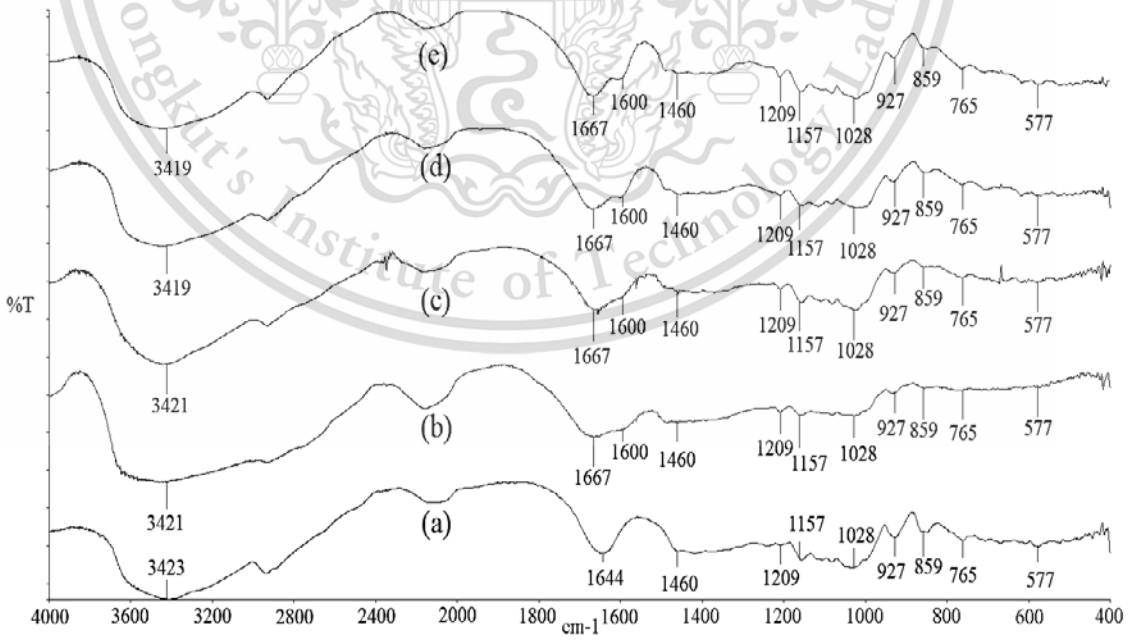

Figure 4.4 FT-IR spectra of NS and various MAM-grafted starch with different grafting percentages **(a)** NS **(b)** GS-20MAM **(c)** GS-40MAM **(d)** GS-60MAM and **(e)** GS-90MAM

This material is reserved for educational use only, not allowed for commercial use.
Forbidden to modify the content, and cite the document when use.

Table 4.4 Characteristic peak heights and ratios of characteristic peak height of NS and various MAM-grafted starch with different grafting percentages

Sample	Peak height			Ratio of peak height	
	1667 cm^{-1}	1600 cm^{-1}	859 cm^{-1}	1667 cm^{-1}/ 859 cm^{-1}	1600 cm^{-1} /859 cm^{-1}
GS-20MAM	32.84	25.42	21.05	1.56	1.21
GS-40MAM	39.93	28.46	21.24	1.88	1.34
GS-60MAM	42.87	30.88	21.65	1.98	1.56
GS-90MAM	47.47	35.39	21.58	2.20	1.64

Remark: ratio of peak height = peak height of interested peak/peak height of referenced peak of 859 cm^{-1}

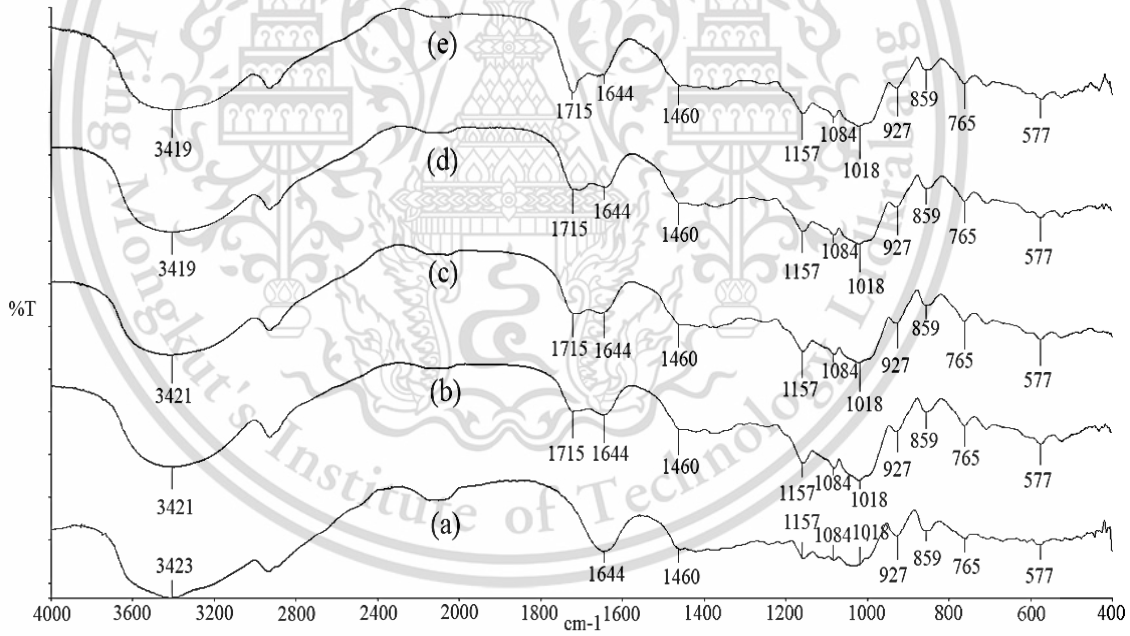

Figure 4.5 FT-IR spectra of NS and various MAA-grafted starch with different grafting percentages (a) NS (b) GS-20MAA (c) GS-40MAA (d) GS-60MAA and (e) GS-90MAA

This material is reserved for educational use only, not allowed for commercial use.
Forbidden to modify the content, and cite the document when use.

Table 4.5 Characteristic peak heights and ratios of characteristic peak height of NS and various MAA-grafted starch with different grafting percentages

Sample	Peak height		Ratio of peak height
	1715 cm^{-1}	859 cm^{-1}	1715 cm^{-1}/859 cm^{-1}
GS-20MAA	32.48	21.09	1.54
GS-40MAA	37.42	20.23	1.85
GS-60MAA	40.58	20.67	1.97
GS-90MAA	44.37	20.45	2.17

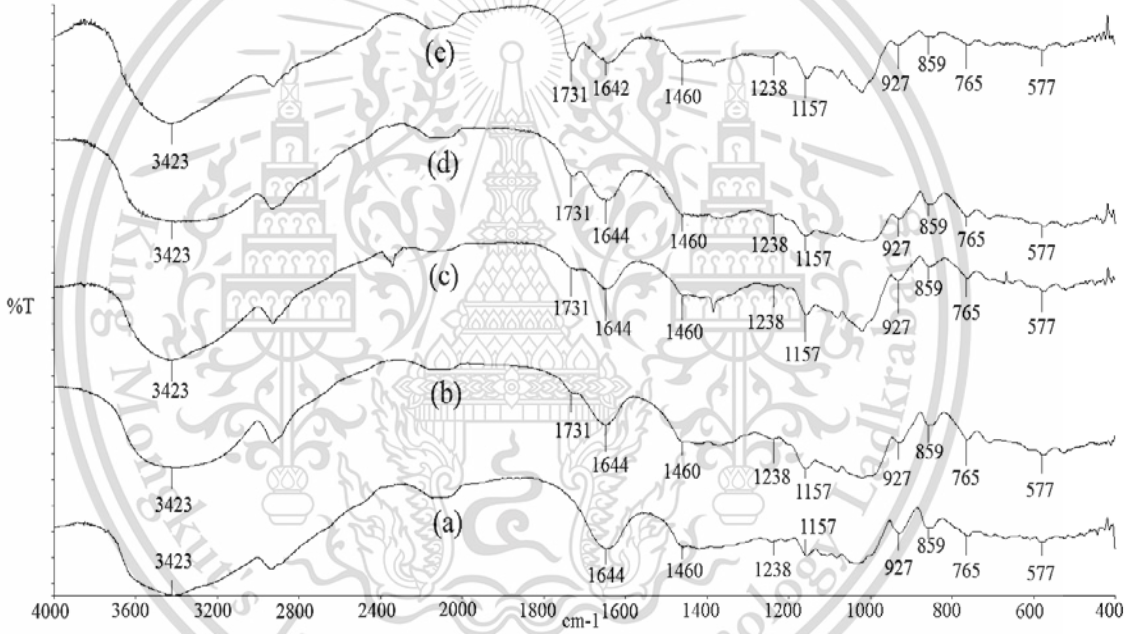

Figure 4.6 FT-IR spectra of NS and various MMA-grafted starch with different grafting percentages (a) NS (b) GS-20MMA (c) GS-40MMA (d) GS-60MMA and (e) GS-90MMA

This material is reserved for educational use only, not allowed for commercial use.
Forbidden to modify the content, and cite the document when use.

Table 4.6 Characteristic peak height and ratio of characteristic peak height of NS and MMA-grafted starch with different grafting percentages

Sample	Peak height		Ratio of peak height
	1731 cm^{-1}	859 cm^{-1}	1731 cm^{-1}/859 cm^{-1}
GS-20MMA	32.17	20.23	1.59
GS-40MMA	37.76	19.98	1.89
GS-60MMA	40.64	20.02	2.03
GS-90MMA	44.35	19.89	2.23

FT-IR technique was used to detect the functional groups of grafted starch. GS with low and high grafting percentages were evaluated and compared by FT-IR analysis together with NS. The FT-IR spectra of NS and various GS grafted by MAM, MAA and MMA monomers with different grafting percentages are shown in Figures 4.4-4.6 and Tables 4.4-4.6. In the infrared spectrum of NS (Figures 4.4-4.6(a)), the wide band observed in the range of 3400-3500 cm^{-1} was attributed to the O-H stretching of starch structure and its broadness was explained by formation of inter and intramolecular hydrogen bonds via various hydroxyl groups of the starch. The band at 2800-3000 cm^{-1} was attributed to asymmetric stretching of C-H. The fingerprint region from 1600 to 1650 cm^{-1} was dominated by vibration of bound water and an additional band at 1460 cm^{-1} corresponded to O-H bending. A peak of C-O-C stretching was presented at 1000-1300 cm^{-1}, while the peak observed in the range of 1100-1200 cm^{-1} was dominated by C-O-H bending [56-57].

FT-IR spectra of MAM-grafted starch showed that all characteristic absorption peaks of cassava starch were still present. In Figure 4.4, additional peaks at 1667 cm^{-1} (C=O stretching) and 1600 cm^{-1} (N-H bending) were characteristic of amide groups ($-CONH_2$) in the grafted MAM monomer [10, 14]. The most important peak at 1715 cm^{-1} for MAA-grafted starch in Figure 4.5 was attributed to C=O stretching of carboxyl groups (-COOH) [15]. Peaks of C=O stretching of carboxylate groups ($-COOCH_3$) at 1731 cm^{-1} were observed that was the indicator of successful grafting of MMA-grafted starch as presented in Figure 4.6 [16-17]. This observation indicated that the grafting with these vinyl monomers was obviously successful.

Characteristic peak heights and ratios at two different wavenumbers for MAM, MAA and MMA grafted starch with different grafting percentages are shown in Tables 4.4-4.6. As high content MAM, MAA and MMA monomers were grafted onto cassava starch, the intensity of distinguishing absorption peaks of C=O stretching and N-H

This material is reserved for educational use only, not allowed for commercial use.
Forbidden to modify the content, and cite the document when use.

bending of amide groups for MAM-grafted starch at 1667 cm^{-1} and 1600 cm^{-1} (Figure 4.4 and Table 4.4), C=O stretching of carboxyl groups for MAA-grafted starch at 1715 cm^{-1} (Figure 4.5 and Table 4.5) and C=O stretching of carboxylate groups at 1731 cm^{-1} of MMA-grafted starch (Figure 4.6 and Table 4.6) increased with increasing grafting percentage, indicating incremental formation of starch grafted chains [15-17].

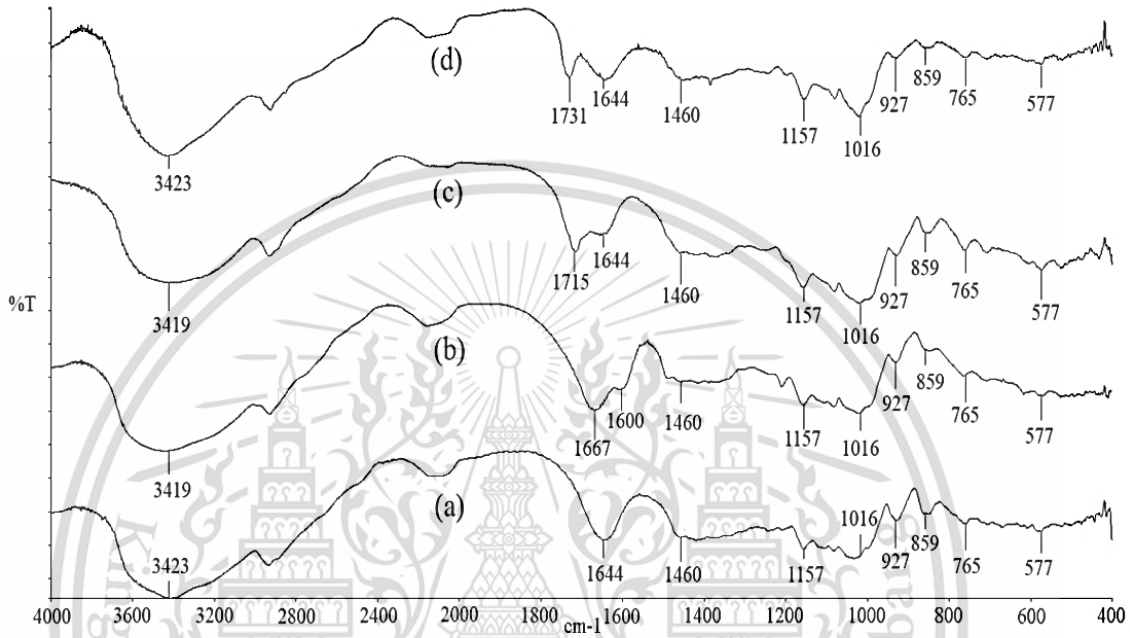

Figure 4.7 FT-IR spectra of NS and various GS grafted with different types of vinyl monomers at 90**%** G **(a)** NS **(b)** GS-90MAM **(c)** GS-90MAA and **(d)** GS-90MMA

A comparison of FT-IR spectra between NS and various GS grafted with different types of vinyl monomers at 90**%** G is presented in Figure 4.7. All GS structures were based on polysaccharide, which resulted in similar peaks of FT-IR spectra compared to NS. Figure 4.7 depicting FT-IR spectra of various GS grafted with different types of vinyl monomers represented a difference in characteristic peaks (Figures 4.7(b)-(d)). This result was related to functional groups of different types of vinyl monomer. New characteristic peaks of GS-90MAM appeared at wavenumbers 1667 and 1600 cm^{-1} which related to C=O stretching and N-H bending of amide groups (Figure 4.7(b)) [14]. For GS-90MAA, an additional peak was observed at 1715 cm^{-1} attributed to C=O stretching of carboxyl groups (Figure 4.7(c)) [15]. Regarding FT-IR of MMA-grafted starch (Figure 4.7(d)), a new absorbent peak at 1731 cm^{-1} was attributed to C=O stretching of carboxylate groups [16]. These results confirmed the success of graft copolymerization for all types of vinyl monomer onto cassava starch chains.

This material is reserved for educational use only, not allowed for commercial use.
Forbidden to modify the content, and cite the document when use.

4.1.4 Morphology of starch granules

SEM was used to identify the morphology of NS and various GS grafted by MAM, MAA and MMA monomers with different grafting percentages. SEM micrographs at 4000X magnification of NS and various types of GS are shown in Figures 4.8-4.10.

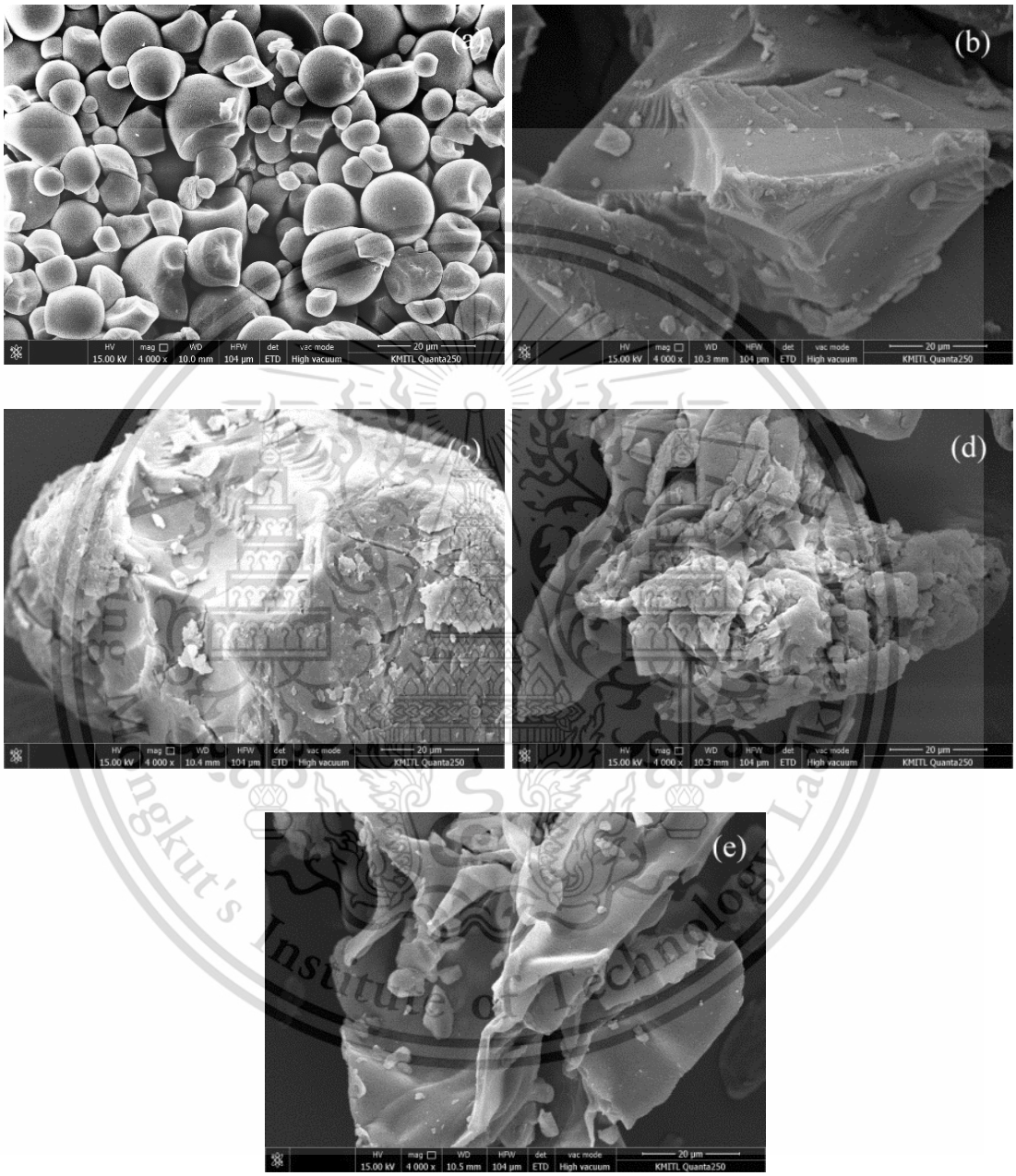

Figure 4.8 Fractured morphology at 4000X magnification of NS and various MAM-grafted starch with different grafting percentages **(a)** NS **(b)** GS-20MAM **(c)** GS-40MAM **(d)** GS-60MAM and **(e)** GS-90MAM

This material is reserved for educational use only, not allowed for commercial use.
Forbidden to modify the content, and cite the document when use.

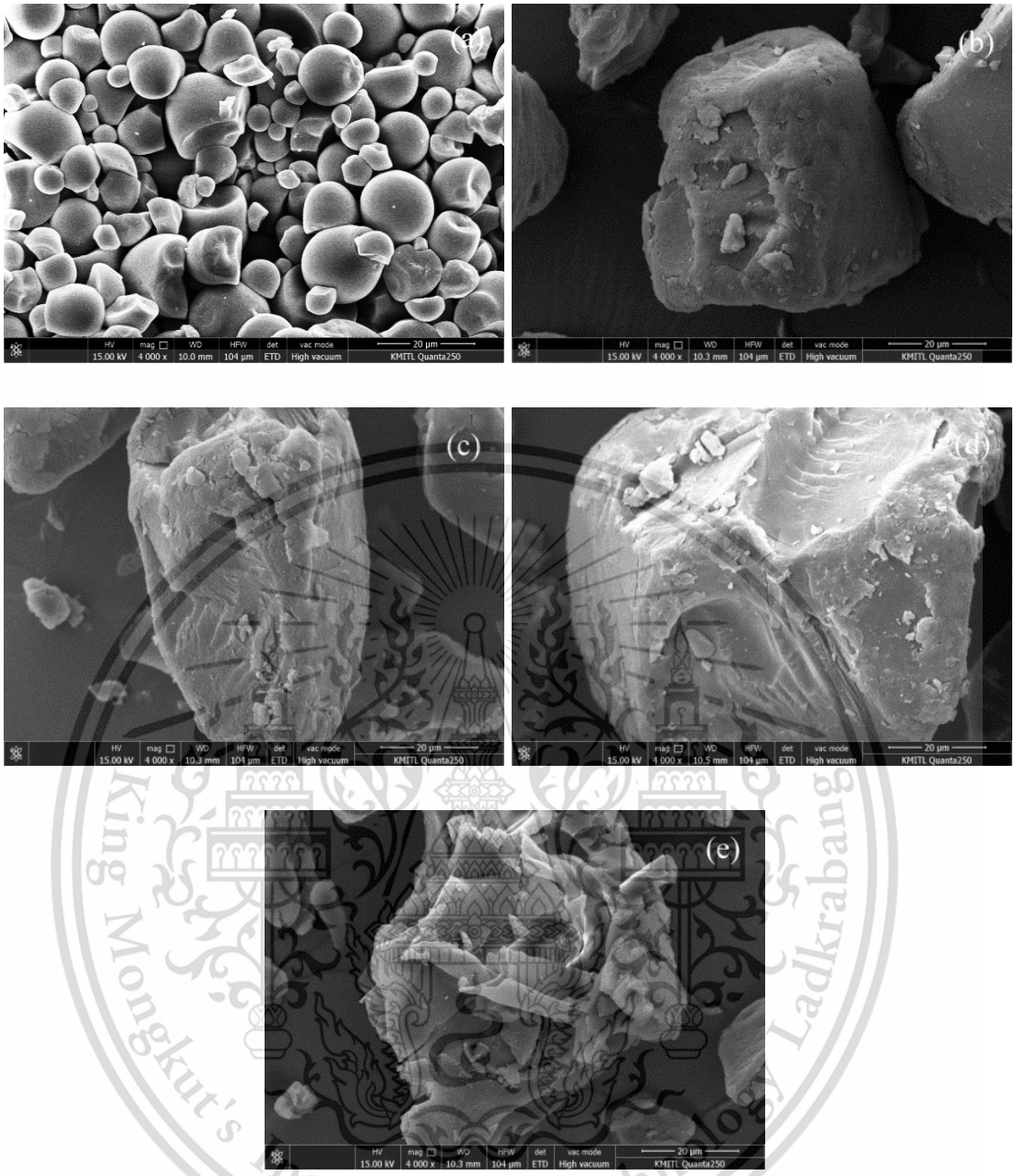

Figure 4.9 Fractured morphology at 4000X magnification of NS and various MAA-grafted starch with different grafting percentages **(a)** NS **(b)** GS-20MAA **(c)** GS-40MAA **(d)** GS-60MAA and **(e)** GS-90MAA

This material is reserved for educational use only, not allowed for commercial use.
Forbidden to modify the content, and cite the document when use.

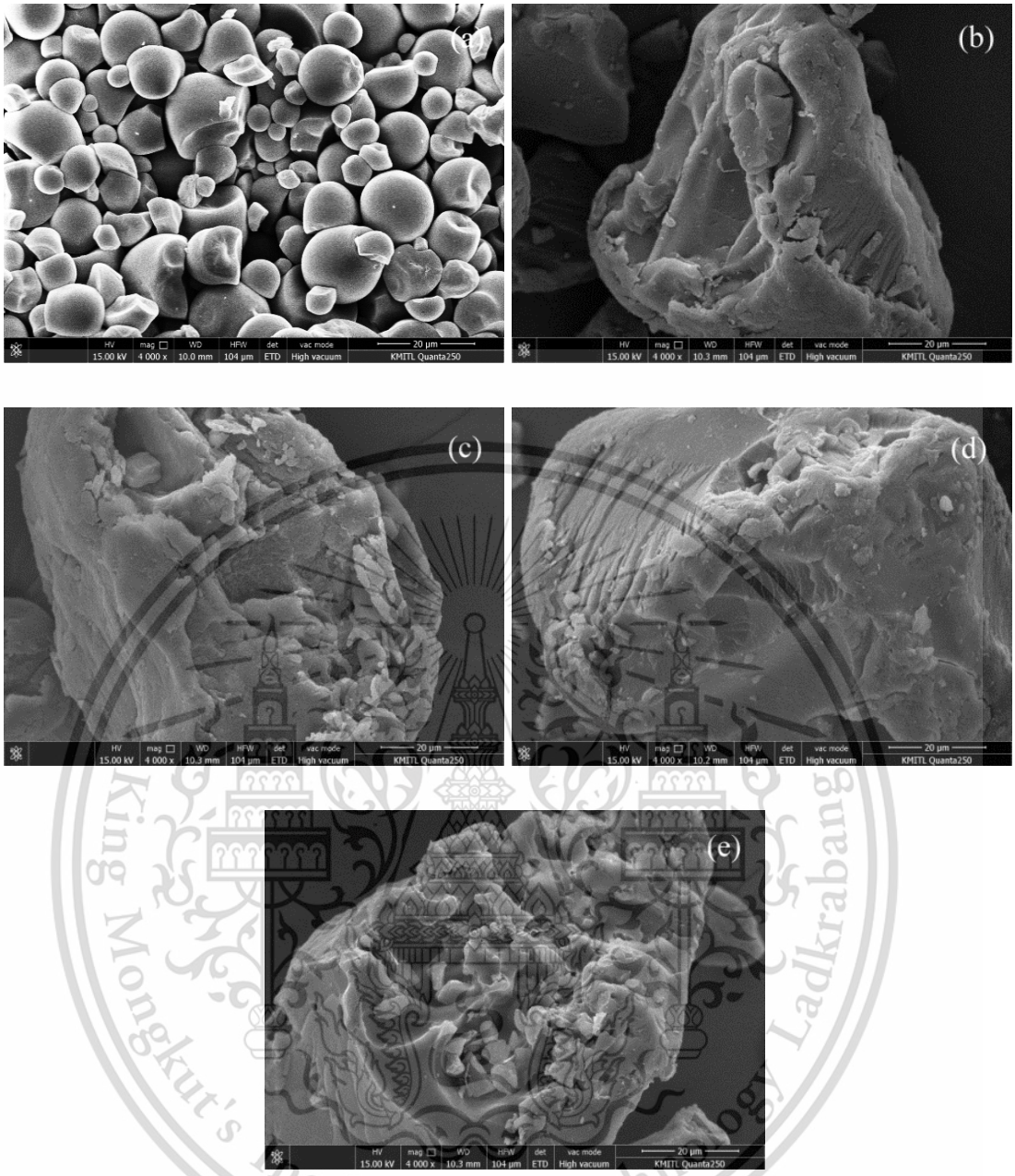

Figure 4.10 Fractured morphology at 4000X magnification of NS and various MMA-grafted starch with different grafting percentages (a) NS (b) GS-20MMA (c) GS-40MMA (d) GS-60MMA and (e) GS-90MMA

From Figures 4.8-4.10, SEM micrographs at 4000X magnification of NS (Figures 4.8-4.10(a)) showed almost all starch granules with regular oval shape. Figures 4.8-4.10((b)-(e)) showed all GS samples exhibiting different morphologies. The granular starch structure was completely destroyed as the starch was grafted with vinyl monomers. In addition, morphologies of all GS samples exhibited plates (panels), increase in average granular size and rougher surface **[**15-17**].** For all GS samples, as percentage of grafting increased, their surfaces became rougher with increasing MAM,

This material is reserved for educational use only, not allowed for commercial use.
Forbidden to modify the content, and cite the document when use.

MAA or MMA monomers. Shapes of the starch granules were irregular due to the disruption by the grafting process and the formation of grafted branch chains. These results implied that surface roughness was positively related to percentage of grafting for all GS samples.

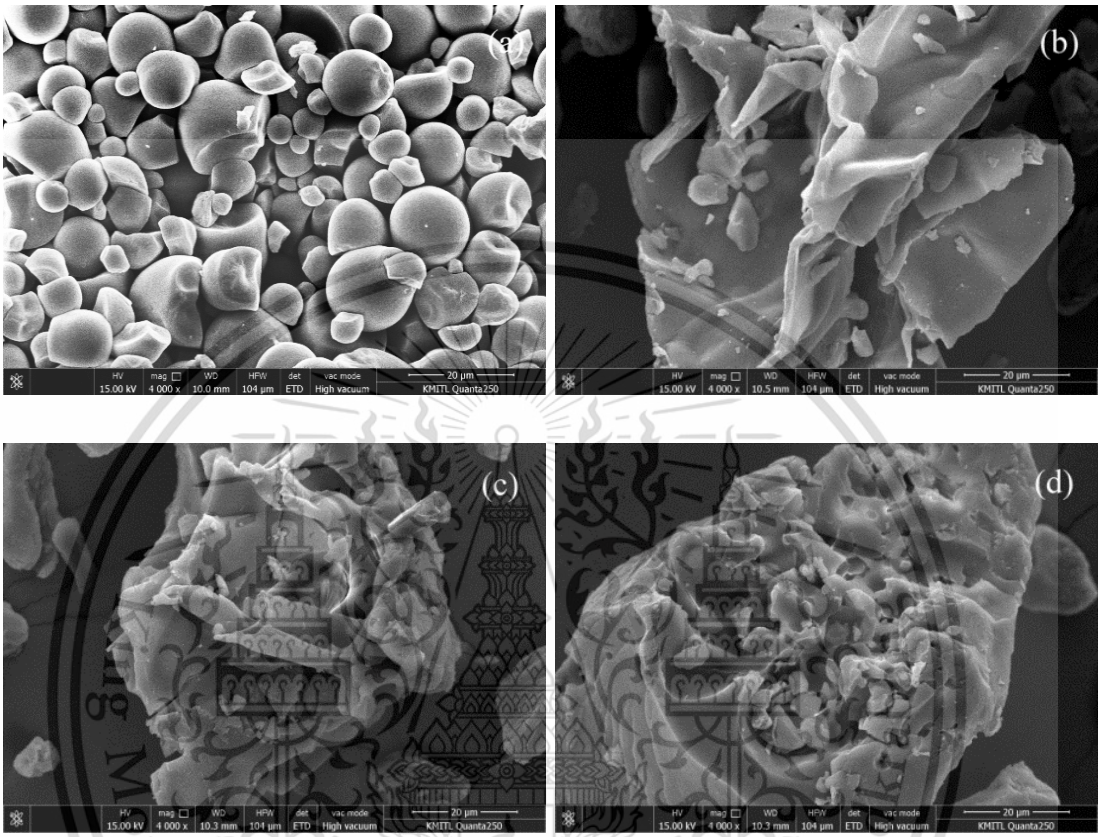

Figure 4.11 Fractured morphology at 4000X magnification of NS and various GS grafted with different types of vinyl monomers at 90**%** G **(**a**)** NS **(**b**)** GS**-**90MAM **(**c**)** GS**-**90MAA and **(**d**)** GS**-**90MMA

Compared to the morphology of NS sample **(**Figure 4.11**(**a**)).** The morphologies of all GS samples **(**Figure 4.11**(**b**)-(**d**))** were clearly different that exhibited a substantial changed starch granular structure and rough surface because of the disruption of granular starch structure and the formation of grafted branch structure by grafted copolymerization**.** On the other hand, morphologies of GS with different types of vinyl monomers at 90**%** G were similar; their surfaces were all rougher than NS granules**.**

This material is reserved for educational use only, not allowed for commercial use.
Forbidden to modify the content, and cite the document when use.

4.1.5 Intrinsic viscosity and average molecular weight (MW) of NS and various types of GS

Intrinsic viscosity and average molecular weight were examined using the Mark-Houwink equation. Effects of graft copolymerization on intrinsic viscosity and average molecular weight of various types of GS grafted by MAM, MAA and MMA monomers with different grafting percentages are shown in Table 4.7.

Table 4.7 Intrinsic viscosity and MW of NS and various GS grafted by MAM, MAA and MMA monomers with different grafting percentages

Sample	Intrinsic viscosity (mL/g)	MW (g/mol)
NS	245.1±0.1	$(73.8\pm0.5)\times10^4$
GS-20MAM	351.8±0.1	$(118.8\pm0.2)\times10^4$
GS-40MAM	491.2±0.4	$(184.3\pm0.2)\times10^4$
GS-60MAM	570.8±0.5	$(224.6\pm0.3)\times10^4$
GS-90MAM	623.2±0.6	$(252.1\pm0.4)\times10^4$
GS-20MAA	323.5±0.4	$(108.5\pm0.2)\times10^4$
GS-40MAA	445.3±0.7	$(162.0\pm0.6)\times10^4$
GS-60MAA	520.3±0.4	$(198.8\pm0.7)\times10^4$
GS-90MAA	590.9±0.5	$(235.1\pm0.5)\times10^4$
GS-20MMA	380.5±0.8	$(131.7\pm0.4)\times10^4$
GS-40MMA	534.1±0.3	$(205.8\pm0.3)\times10^4$
GS-60MMA	613.5±0.2	$(246.9\pm0.5)\times10^4$
GS-90MMA	660.2±0.4	$(272.3\pm0.6)\times10^4$

Intrinsic viscosity and MW of NS and various GS grafted by MAM, MAA and MMA monomers with different grafting percentages are shown in Table 4.7. All GS samples exhibited higher intrinsic viscosity and MW than NS, when MAM, MAA and MMA monomers were grafted onto NS. This result suggested that the graft copolymerization caused accumulation of grafted monomer molecules into starch chains, leading to higher viscosity and MW of all types of GS [17]. As higher percentages of monomer were additionally grafted onto NS, intrinsic viscosity and MW increased because side chains of the graft copolymers lengthened [17]. Comparatively, intrinsic viscosity and MW of the various types of GS samples were ranked as follows: MMA>MAM>MAA. On the basis of graft copolymerization, this ranking was attributed to MW and viscosity of the different grafted monomers, i.e.,

This material is reserved for educational use only, not allowed for commercial use.
Forbidden to modify the content, and cite the document when use.

MMA and MAA monomers provided the longest and shortest grafted side chains, respectively. These results also indicated that graft copolymerization occurred.

4.1.6 Thermal properties

Thermal properties as decomposition temperature of NS and various GS grafted by MAM, MAA and MMA monomers with different grafting percentages were investigated by thermal gravimetric analysis (TGA) technique in the range of 50-600°C under nitrogen atmosphere at a heating rate of 10°C/min. The decomposition temperature of a substance is the temperature at which it chemically decomposes. TGA and DTG thermograms of NS and different GS samples are shown in Figures 4.12-4.15 and decomposition temperatures from these thermograms are tabulated in Tables 4.8 and 4.9.

King Mongkut's Institute of Technology Ladkrabang

This material is reserved for educational use only, not allowed for commercial use.
Forbidden to modify the content, and cite the document when use.

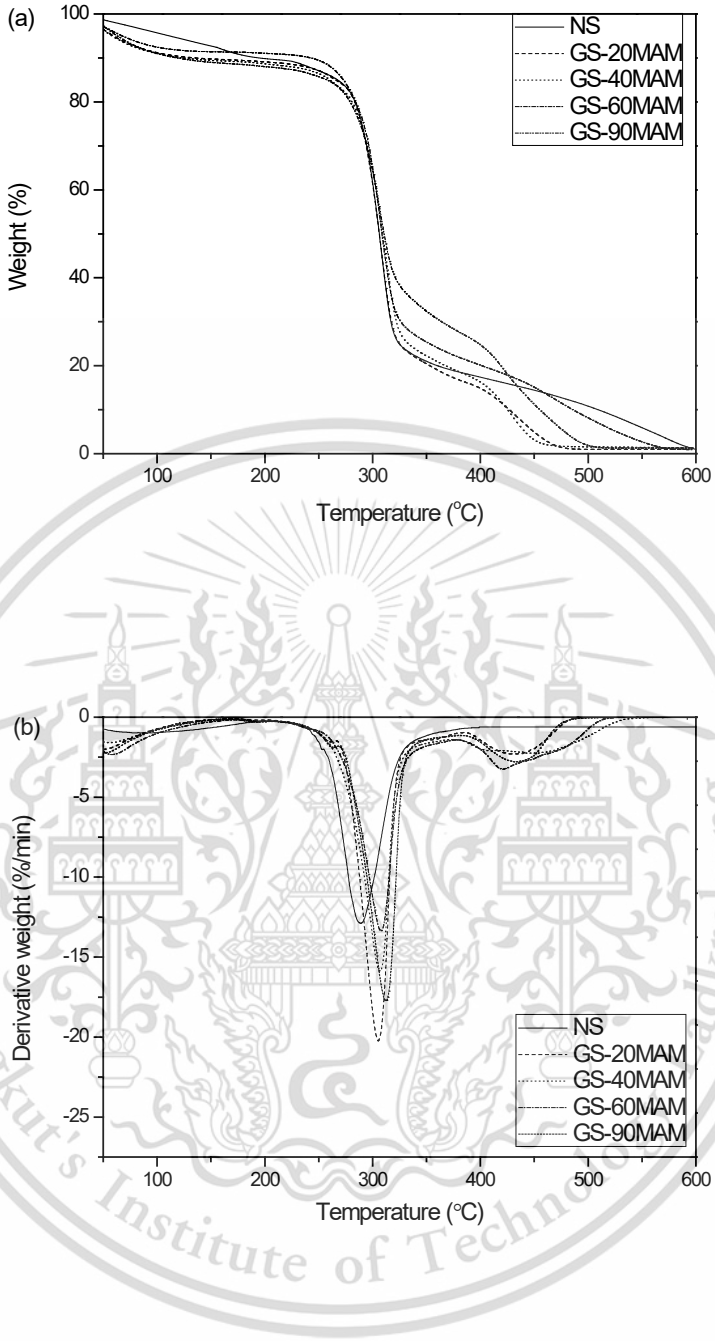

Figure 4.12 (a) TGA and (b) DTG thermograms of NS and various MAM-grafted starch with different grafting percentages

This material is reserved for educational use only, not allowed for commercial use.
Forbidden to modify the content, and cite the document when use.

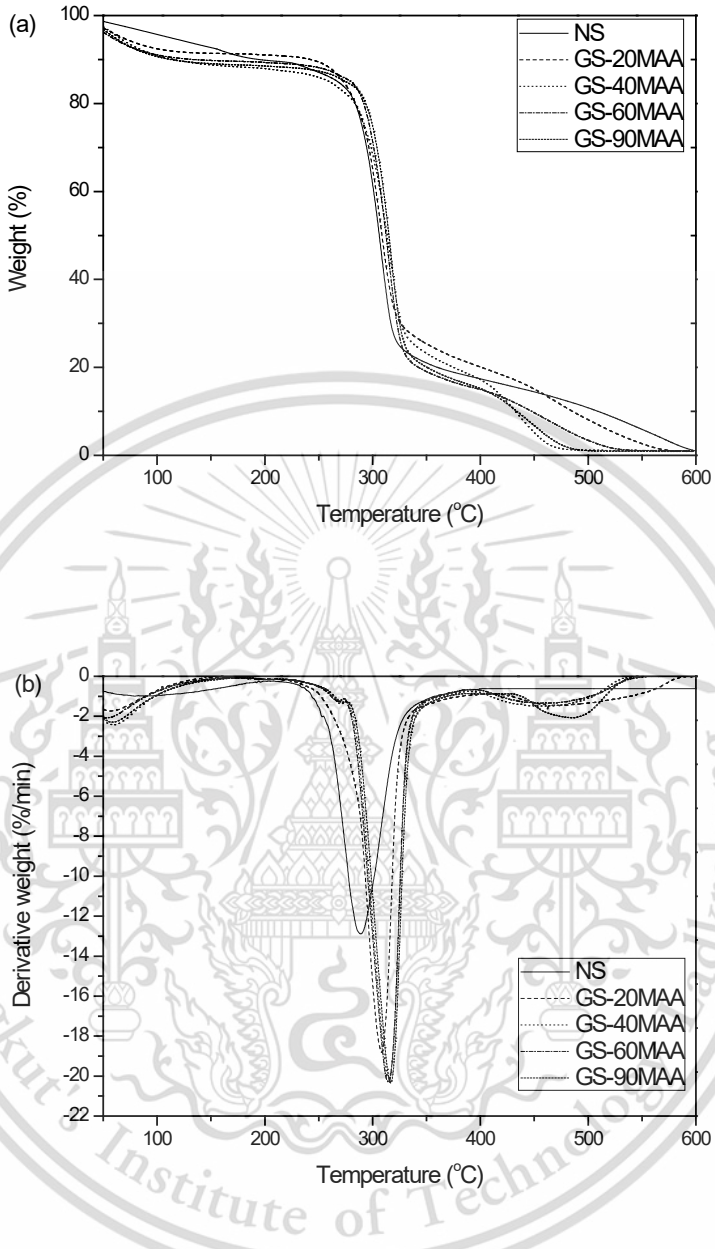

Figure 4.13 (a) TGA and (b) DTG thermograms of NS and various MAA-grafted starch with different grafting percentages

This material is reserved for educational use only, not allowed for commercial use.
Forbidden to modify the content, and cite the document when use.

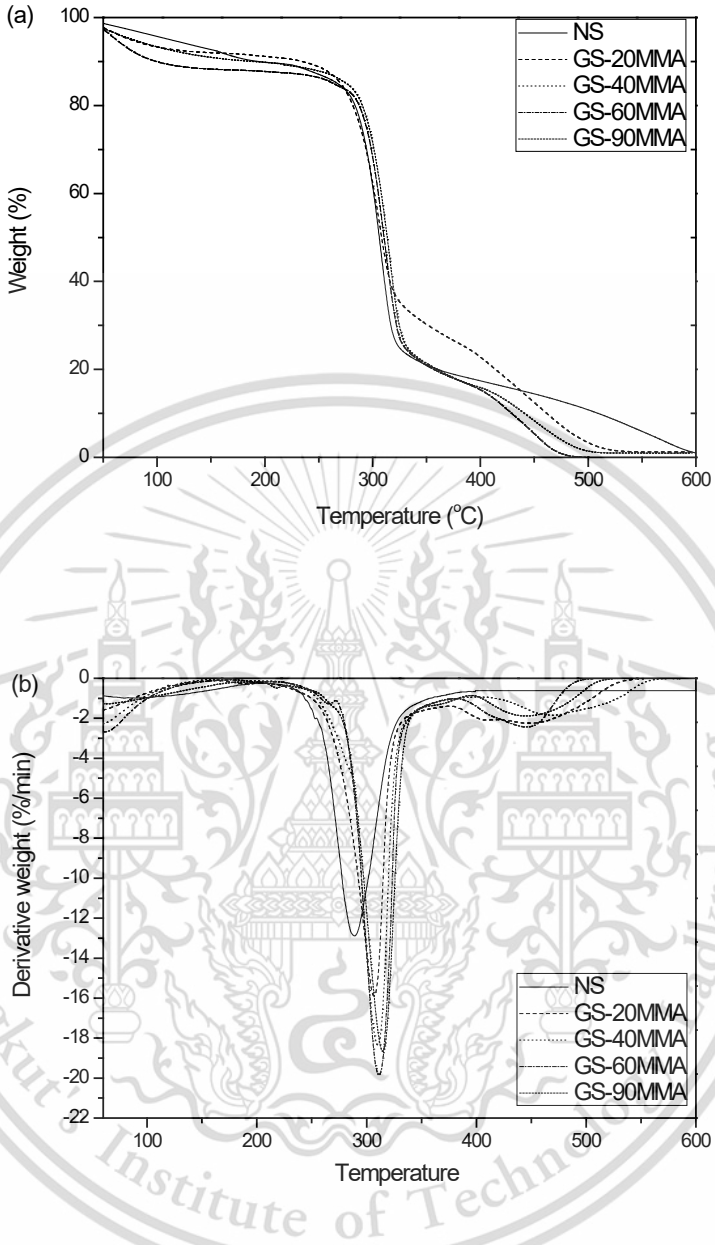

Figure 4.14 (a) TGA and (b) DTG thermograms of NS and various MMA-grafted starch with different grafting percentages

This material is reserved for educational use only, not allowed for commercial use.
Forbidden to modify the content, and cite the document when use.

Table 4.8 Decomposition temperatures of NS and various GS grafted by MAM, MAA and MMA monomers with different percentages

Sample	Decomposition temperature (°C)	
	Step 1 (Starch)	Step 2 (Monomer)
NS	299.0	-
GS-20MAM	302.4	418.5
GS-40MAM	306.9	432.5
GS-60MAM	307.1	421.0
GS-90MAM	312.4	426.3
GS-20MAA	308.0	473.8
GS-40MAA	314.1	484.8
GS-60MAA	314.7	489.3
GS-90MAA	316.9	477.0
GS-20MMA	306.9	447.5
GS-40MMA	310.2	458.8
GS-60MMA	311.1	445.8
GS-90MMA	314.1	444.8

Figures 4.12-4.14 display TGA and DTG thermograms of NS and various GS grafted by MAM, MAA and MMA monomers. The thermal decomposition temperatures (T_d) of NS and various GS samples are tabulated in Table 4.8. The TGA thermogram of NS exhibited one main step of degradation. The initial step was observed in the ranges of 299-320℃ were attributed to starch decomposition. On the other hand, the TGA thermogram of GS samples showed two degradation steps. The main degradation step from 299-320°C was attributed to decomposition of the starch. The new second stage from 410-500°C was attributed to decomposition of each type of monomer and these results confirmed the success of graft copolymerization [13-17]. For the first step, decomposition temperatures of all types of GS samples were noticeably higher than NS sample indicating that GS samples exhibited higher thermal stability than NS because of the presence of MAM, MAA or MMA grafted chains that dramatically changed the molecular structure. These observations indicated that grafting increased thermal properties of NS structure [15].

When grafting was increased from 20 to 90% G, the degradation temperatures of the main transition step of all types of GS samples showed an increasing trend because graft copolymerization with vinyl monomers enhanced the thermal

This material is reserved for educational use only, not allowed for commercial use.
Forbidden to modify the content, and cite the document when use.

properties and stability of the starch chains [14-15]. This result concurred with improved thermal properties of GS from corn, potato and cassava starch grafted with MAM, MAA and MMA monomers [13-16].

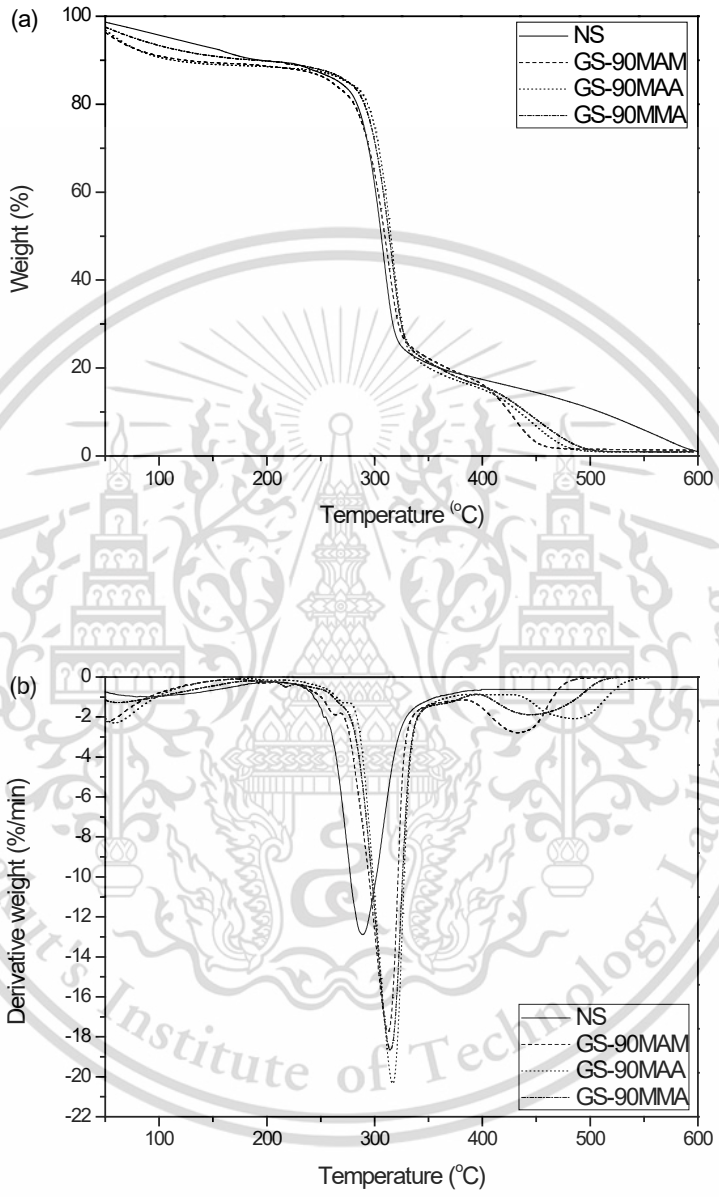

Figure 4.15 **(a)** TGA and **(b)** DTG thermograms of NS and various GS grafted with different types of vinyl monomers at 90**%** G

This material is reserved for educational use only, not allowed for commercial use.
Forbidden to modify the content, and cite the document when use.

Table 4.9 Degradation temperatures of NS and various GS grafted with different types of vinyl monomers at 90% G

Sample	Decomposition temperature (°C)	
	Step 1 (Starch)	Step 2 (Monomer)
NS	299.0	-
GS-90MAM	312.4	426.3
GS-90MAA	316.9	477.0
GS-90MMA	314.1	444.8

Figure 4.15 presents TGA and DTG thermograms of NS and GS grafted with different types of vinyl monomers at 90% G. The degradation temperatures of NS and GS grafted with different types of vinyl monomers at 90% G are shown in Table 4.9. The starch degradation temperatures of all types of GS samples increased compared to NS due to the formation of grafted chains that drastically changed and improved the stabilization of the starch structure [18-19]. When comparing the degradation temperatures in the first transition of GS grafted with different types of vinyl monomers, the degradation temperatures of GS samples are ranked as follows: MAA-grafted starch>MMA-grafted starch>MAM-grafted starch. As expected, different types of vinyl monomers exhibited different degradation temperatures; MAA monomers presented the highest degradation temperature of 470-500°C, followed by MMA monomers at 440-470°C and the lowest degradation temperature of MAM monomers in the range of 420-440°C. This result agreed well with their decomposition temperatures of MAM, MAA and MMA monomers reported by earlier studies [13-17].

4.2 Characterization of different TPGS films

4.2.1 FT-IR study

An FT-IR technique was used to detect the presence of functional groups of TPGS films. The FT-IR spectra of TPNS film and various TPGS films grafted by MAM, MAA and MMA monomers with different grafting percentages are displayed in Figures 4.16-4.19. Peak heights and ratios of the heights of characteristic peaks of different TPGS films are tabulated in Tables 4.10-4.12

This material is reserved for educational use only, not allowed for commercial use.
Forbidden to modify the content, and cite the document when use.

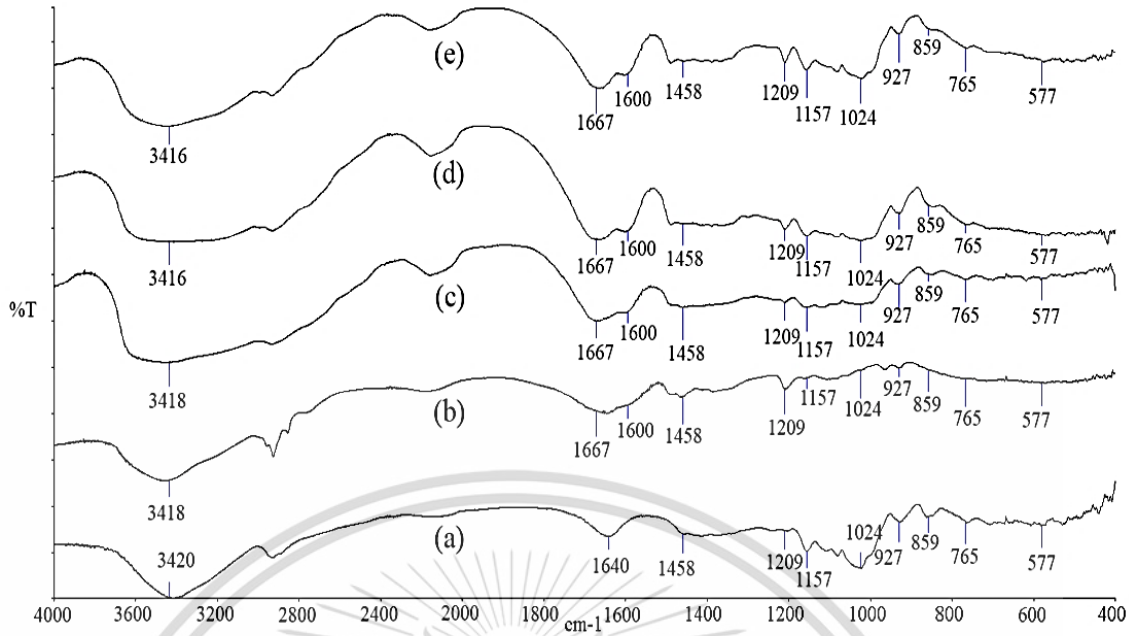

Figure 4.16 FT-IR spectra of TPNS film and various TPGS films by MAM with different grafting percentages (a) TPNS (b) TPGS-20MAM (c) TPGS-40MAM (d) TPGS-60MAM and (e) TPGS-90MAM

Table 4.10 Characteristic peak heights and ratios of characteristic peak height of TPNS film and various TPGS films by MAM with different grafting percentages

Sample	Peak height			Ratio of peak height	
	1667 cm^{-1}	1600 cm^{-1}	859 cm^{-1}	1667 cm^{-1} / 859 cm^{-1}	1600 cm^{-1} / 859 cm^{-1}
TPGS-20MAM	24.26	18.05	20.05	1.21	0.98
TPGS-40MAM	26.22	22.25	19.87	1.32	1.12
TPGS-60MAM	30.12	23.72	19.56	1.54	1.21
TPGS-90MAM	35.12	25.61	19.43	1.78	1.32

Remark: ratio of peak height = peak height of interested peak/peak height of referenced peak of 859 cm^{-1}

This material is reserved for educational use only, not allowed for commercial use.
Forbidden to modify the content, and cite the document when use.

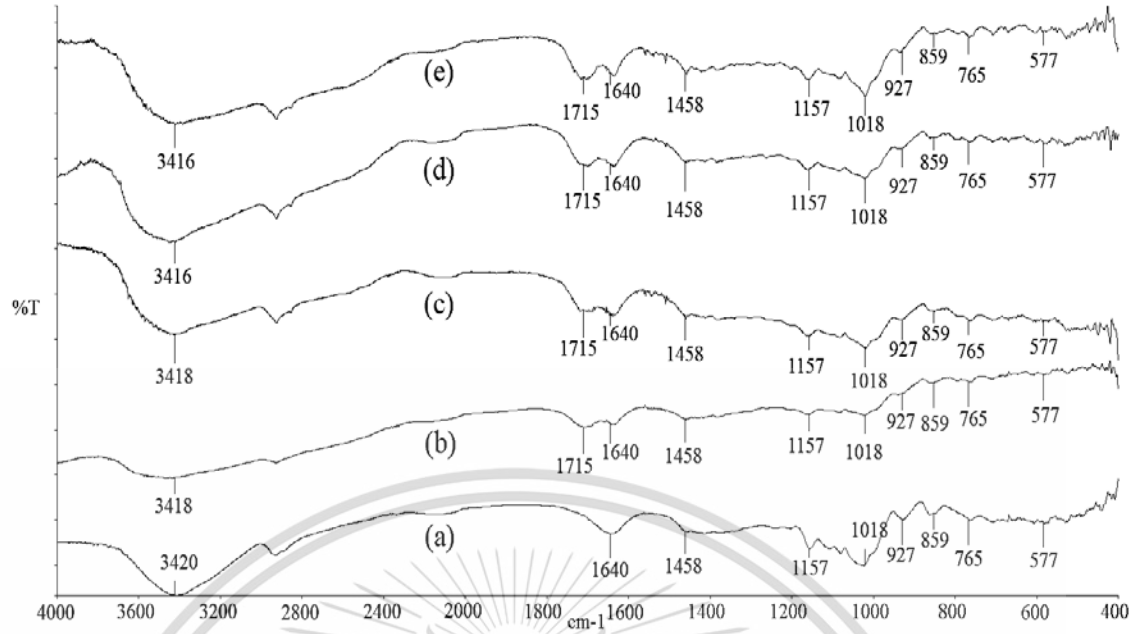

Figure 4.17 FT-IR spectra of TPNS film and various TPGS films by MAA with different grafting percentages (a) TPNS (b) TPGS-20MAA (c) TPGS-40MAA (d) TPGS-60MAA and (e) TPGS-90MAA

Table 4.11 Characteristic peak heights and ratios of characteristic peak height of TPNS film and various TPGS films by MAA with different grafting percentages

Sample	Peak height		Ratio of peak height
	1715 cm^{-1}	859 cm^{-1}	1715 cm^{-1}/859 cm^{-1}
TPGS-20MAA	25.31	20.24	1.25
TPGS-40MAA	26.90	19.78	1.36
TPGS-60MAA	30.90	19.56	1.58
TPGS-90MAA	34.42	19.67	1.75

This material is reserved for educational use only, not allowed for commercial use.
Forbidden to modify the content, and cite the document when use.

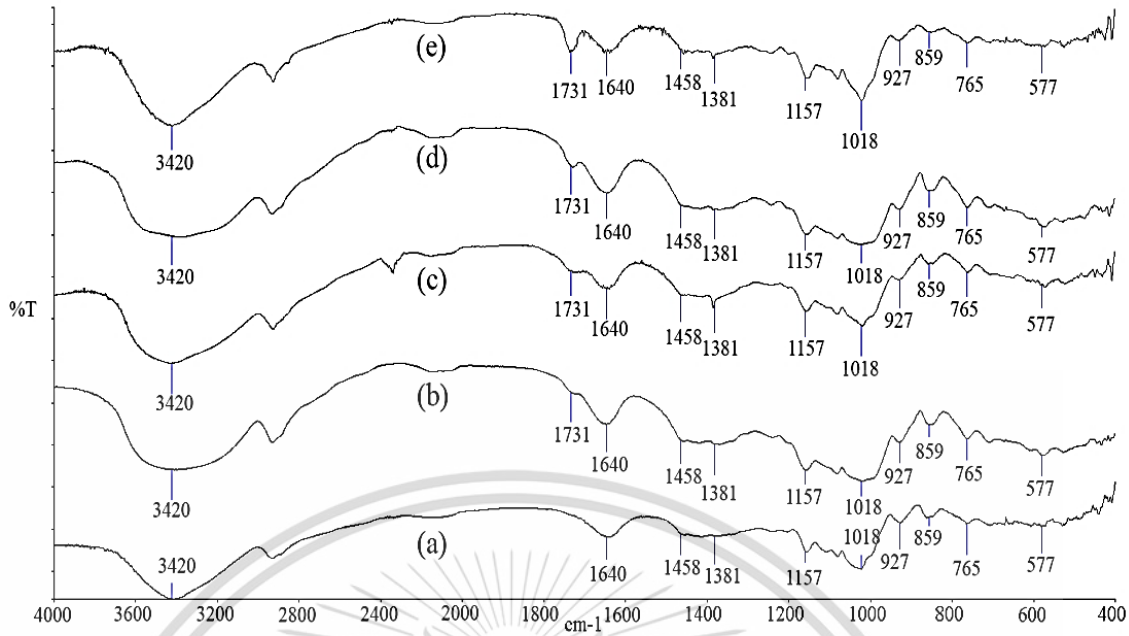

Figure 4.18 FT-IR spectra of TPNS film and various TPGS films by MMA with different grafting percentages (a) TPNS (b) TPGS-20MMA (c) TPGS-40MMA (d) TPGS-60MMA and (e) TPGS-90MMA

Table 4.12 Characteristic peak heights and ratios of characteristic peak height of TPNS film and various TPGS films by MMA with different grafting percentages

Sample	Peak height		Ratio of peak height
	1731 cm^{-1}	859 cm^{-1}	1731 cm^{-1} / 859 cm^{-1}
TPGS-20MMA	24.66	20.05	1.23
TPGS-40MMA	27.69	20.21	1.37
TPGS-60MMA	32.92	20.32	1.62
TPGS-90MMA	37.54	19.87	1.94

FT-IR was used to investigate the change in starch molecules before and after graft copolymerization. FT-IR spectra of TPNS film and various TPGS films grafted by MAM, MAA and MMA monomers with different grafting percentages are displayed in Figures 4.16-4.18. All starch films showed similar peaks in their FT-IR spectrum attributable to the characteristics of the polysaccharide structure. The broad absorption band ranging from 3500-3300 cm^{-1} was attributed to O-H stretching. The wavenumber at 2800-3000 cm^{-1} was ascribed to C–H asymmetric stretching. The absorption band at 1641-1646 cm^{-1} indicated vibration of bound water. An additional

This material is reserved for educational use only, not allowed for commercial use.
Forbidden to modify the content, and cite the document when use.

band in the range of 1450-1475 cm^{-1} was attributed to O-H bending. Peaks at 1070-1275 cm^{-1} and 1000-1200 cm^{-1} were attributed to C–O–C stretching and C–O–H bending, respectively [56-57].

FT-IR spectra of all TPGS films with MAM (Figures 4.16(b)-(e)) exhibited two new characteristic peaks at 1667 cm^{-1} and 1600 cm^{-1}, associated with C=O stretching and N-H bending of amide groups, respectively. For all TPGS films with MAA (Figures 4.17(b)-(e)), FT-IR spectra showed a characteristic peak at 1715 cm^{-1}, corresponding to C=O stretching vibration of carboxylic groups. In Figure 4.18(b)-(e), a characteristic peak of MMA for C=O stretching vibration of carboxylate groups was observed at 1731 cm^{-1}. As expected, these characteristic peaks confirmed successful grafting of these monomers onto the cassava starch molecules of TPGS films by replacing hydroxyl groups in the polysaccharide chains [13-16].

When TPGS films were grafted with higher percentages of each type of vinyl monomers, peak intensity of the characteristic functional groups increased (Tables 4.10-4.12). The characteristic peak for TPGS film with MAM was attributed to C=O stretching at 1667 cm^{-1} together with N-H bending at 1600 cm^{-1} (Figure 4.16). The characteristic peak for TPGS film with MAA was assigned to C=O stretching at 1715 cm^{-1} (Figure 4.17) and the characteristic peak for TPGS film with MMA was the C=O stretching peak at 1731 cm^{-1} (Figure 4.18). Also, the increasing intensities of the characteristic peaks clearly confirmed successful grafting of GS.

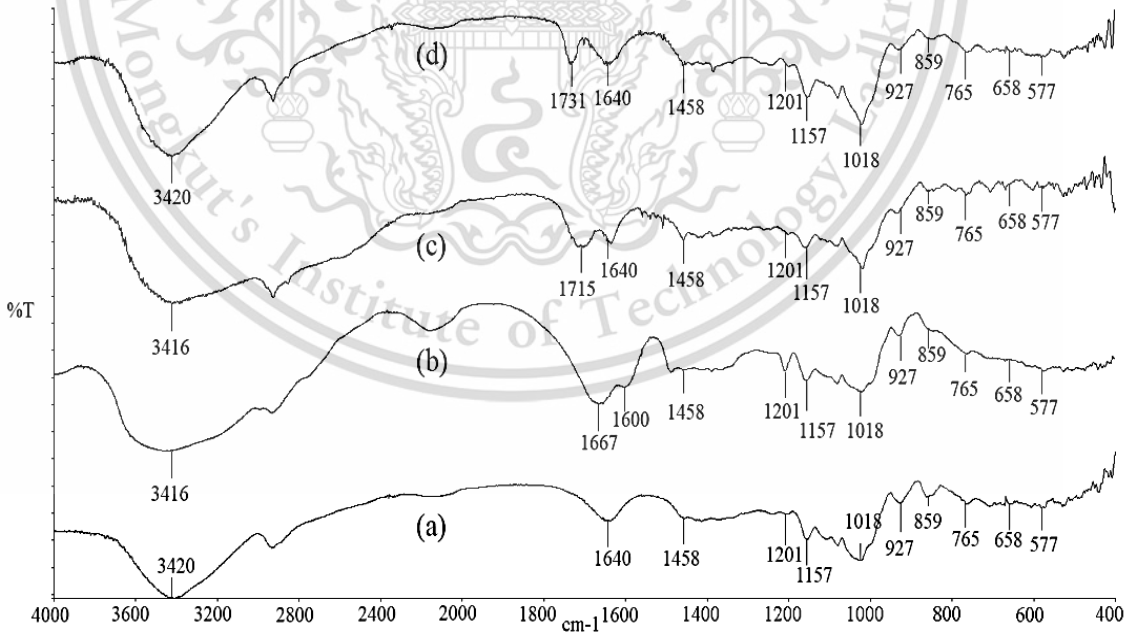

Figure 4.19 FT-IR spectra of TPNS film and vaarious TPGS films grafted with different types of vinyl monomers at 90% G (a) TPNS (b) TPGS-90MAM (c) TPGS-90MAA and (d) TPGS-90MMA

This material is reserved for educational use only, not allowed for commercial use.
Forbidden to modify the content, and cite the document when use.

Figure 4.19 shows FT-IR spectra of TPNS film and various TPGS films grafted with different types of vinyl monomers at 90% G. The result showed that FT-IR peak positions of all types of TPGS films were similar to TPNS film since they still consisted of the same polysaccharide chemical structures. Nevertheless, various TPGS films grafted with different types of vinyl monomers showed different additional characteristic peaks based on the specific functional groups of each type of grafted vinyl monomer. TPGS-90MAM showed additional peaks at 1667 cm^{-1} and 1600 cm^{-1} corresponding to C=O stretching and N-H bending vibrations in amide characteristics [14]. The FT-IR spectrum of TPGS-90MAA presented the most important peak at 1715 cm^{-1} which originated from C=O stretching of carboxylic groups [15]. In addition, the appearance in a new absorption peak of C=O stretching of carboxylate groups appeared in TPGS-90MMA at 1731 cm^{-1} [16]. Interestingly, these new characteristic peaks of different TPGS films grafted with various vinyl monomers also confirmed the success of graft copolymerization with MAA, MAM and MMA monomers onto cassava starch backbones [13-16].

4.2.2 XRD study

An XRD technique was used to produce X-ray diffraction patterns and analyze the degree of crystallinity of TPNS film and various TPGS films grafted by MAM, MAA and MMA monomers with different grafting percentages at an angular range of 2θ from 5° to 60° and a scan rate of 1°/min. The obtained XRD patterns and degrees of crystallinity of TPNS film and different TPGS films are shown in Figures 4.20-4.23 and Tables 4.13-4.14.

This material is reserved for educational use only, not allowed for commercial use.
Forbidden to modify the content, and cite the document when use.

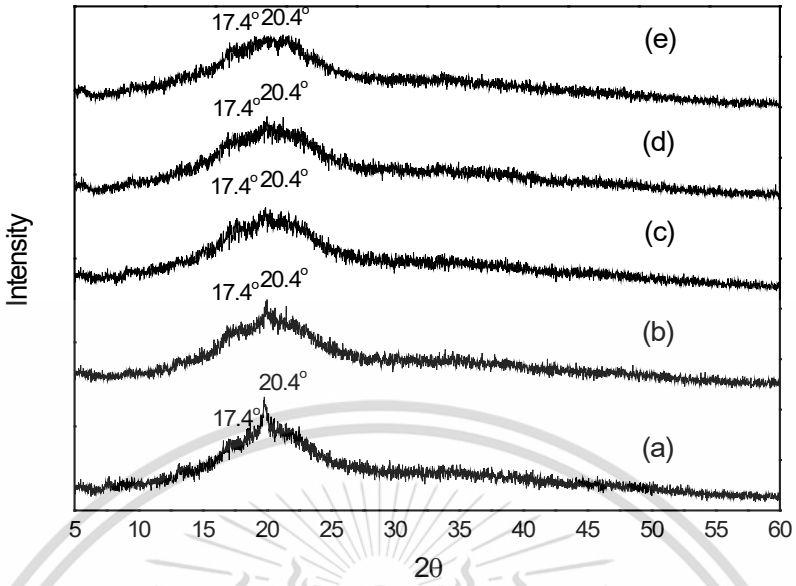

Figure 4.20 X-ray diffractograms of TPNS film and various TPGS films for MAM with different grafting percentages (a) TPNS (b) TPGS-20MAM (c) TPGS-40MAM (d) TPGS-60MAM and (e) TPGS-90MAM

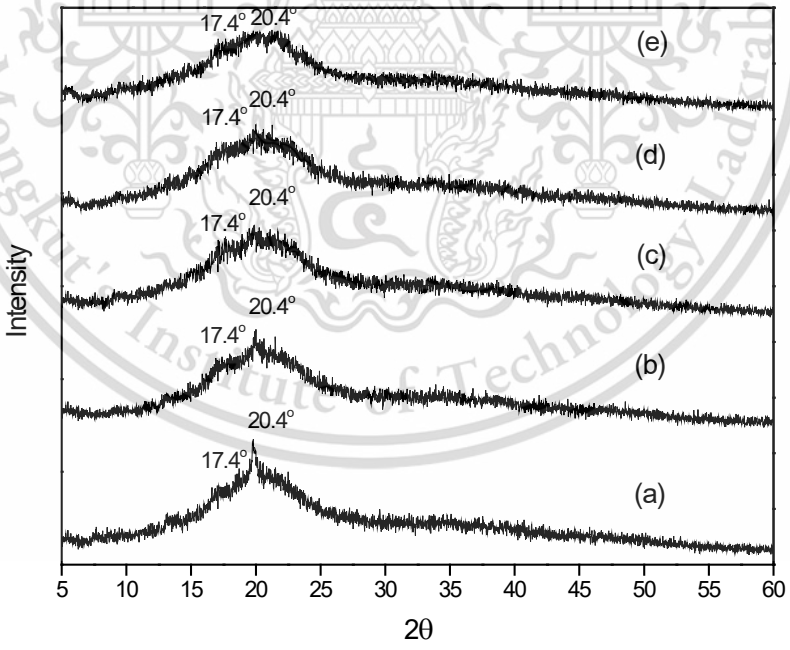

Figure 4.21 X-ray diffractograms of TPNS film and various TPGS films for MAA with different percentages grafting (a) TPNS (b) TPGS-20MAA (c) TPGS-40MAA (d) TPGS-60MAA and (e) TPGS-90MAA

This material is reserved for educational use only, not allowed for commercial use.
Forbidden to modify the content, and cite the document when use.

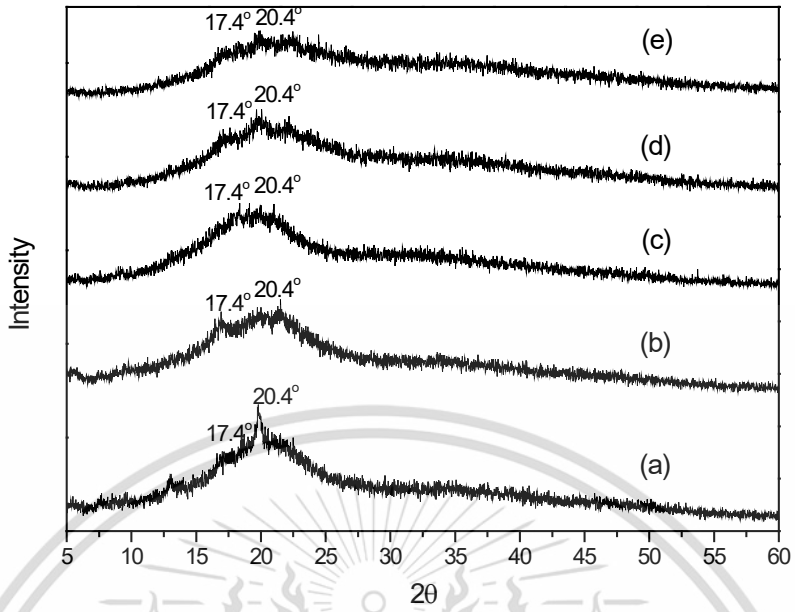

Figure 4.22 X-ray diffractograms of TPNS film and various TPGS films for MMA with different grafting percentages (a) TPNS (b) TPGS-20MMA (c) TPGS-40MMA (d) TPGS-60MMA and (e) TPGS-90MMA

Table 4.13 Degrees of crystallinity of TPNS film and various TPGS films grafted by MAM, MAA and MMA monomers with different grafting percentages

Sample	Degree of crystallinity (%)
TPNS	49.8±0.02
TPGS-20MAM	43.6±0.03
TPGS-40MAM	42.7±0.03
TPGS-60MAM	40.5±0.04
TPGS-90MAM	39.0±0.08
TPGS-20MAA	45.2±0.03
TPGS-40MAA	44.2±0.02
TPGS-60MAA	43.5±0.04
TPGS-90MAA	42.1±0.10
TPGS-20MMA	40.8±0.02
TPGS-40MMA	39.1±0.08
TPGS-60MMA	38.3±0.05
TPGS-90MMA	37.3±0.02

This material is reserved for educational use only, not allowed for commercial use.
Forbidden to modify the content, and cite the document when use.

XRD diffractograms of TPNS film and various TPGS films grafted by MAM, MAA and MMA monomers with different grafting percentages and degrees of crystallinity are shown in Figures 4.20-4.22 and Table 4.13, respectively. TPNS film and all TPGS films showed similar V_h-type X-ray diffraction patterns with diffraction peaks (2θ) at 17.4° and 20.4°[19]. Glycerol and water molecules penetrated into starch granules, replacing starch inter- and intra-molecular hydrogen bonds between the starch chains and destruction of starch granules under high pressure and shear force in preparation for TPNS and TPGS processing. In addition, the results showed that all TPGS films grafted with MAM, MAA or MMA monomers showed a reduction in the degree of crystallinity compared to TPNS film. This result can be explained because graft copolymerization of these monomers onto the cassava starch backbone formed grafted branches and increased free volume between the starch chains. As a result, starch molecules of TPGS films could not be re-crystallised because the grafted monomer replaced their hydroxyl groups [15].

Furthermore, with increasing grafting percentage, a decreasing trend of degree of crystallinity of all TPGS films was observed due to the effect of graft polymerization onto the starch chains. In general, graft copolymerization disrupts inter- and intra-molecular hydrogen bonding between hydroxyl groups of starch chains and prevents formation of crystal structure. The decrease in degree of crystallinity agreed well with observations in another study of syntheses of GS from potato starch grafted with MAA [15].

This material is reserved for educational use only, not allowed for commercial use.
Forbidden to modify the content, and cite the document when use.

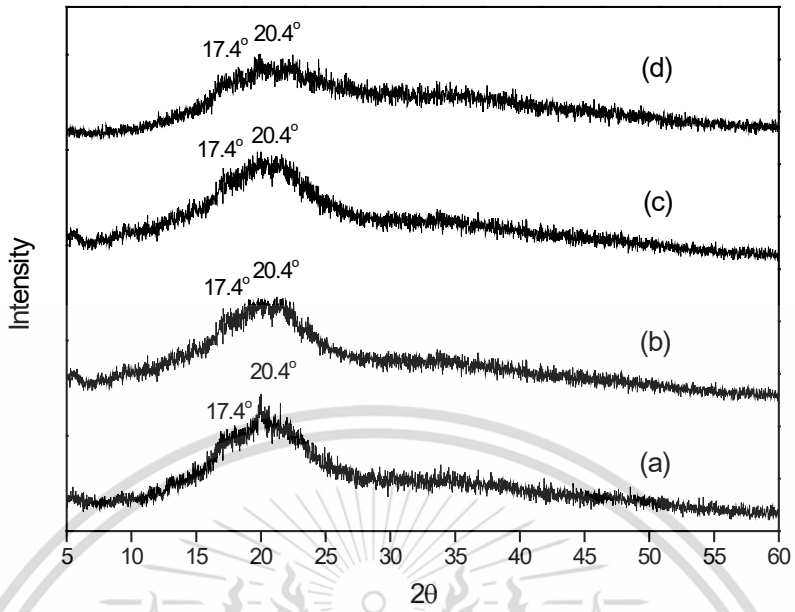

Figure 4.23 X-ray diffractograms of TPNS film and various TPGS films grafted with different types of vinyl monomers at 90% G (a) TPNS (b) TPGS-90MAM (c) TPGS-90MAA and (d) TPGS-90MMA

Table 4.14 Degrees of crystallinity of TPNS film and various TPGS films grafted with different types of vinyl monomers at 90% G

Sample	Degree of crystallinity (%)
TPNS	49.8±0.02
TPGS-90MAM	39.1±0.08
TPGS-90MAA	42.1±0.10
TPGS-90MMA	37.3±0.02

As shown in Figure 4.23 and Table 4.14, degree of crystallinity of TPGS films grafted with all types of vinyl monomers decreased compared to TPNS film. This result can be explained because the grafted monomers formed branches at the C-2, C-3 and C-6 positions of hydroxyl groups of the starch backbones which increased free volume between the starch chains that prevented the formation of crystal structure of starch [15].

Among the various TPGS films grafted with various types of vinyl monomers, TPGS-90MMA showed the lowest degree of crystallinity. This could be because the

This material is reserved for educational use only, not allowed for commercial use.
Forbidden to modify the content, and cite the document when use.

longest alkyl chain of the MMA group compared to MAA and MAM groups (Figure 4.3) resulted in an increase in free volume between starch backbones. As a result, the longest length of the alkyl chains of MMA resulted in the lowest degree of crystallinity of TPGS grafted films. Conversely, the highest degree of crystallinity was found in TPGS-90MAA due to its shortest alkyl chain length. These results implied that the length of the alkyl chain of the grafting monomer strongly affected degree of crystallinity of TPGS films.

4.2.3 Morphology of TPGS films

The SEM technique was used to investigate the morphology of TPNS film and various types of TPGS films. SEM micrographs of TPNS and various TPGS films grafted by MAM, MAA and MMA monomers with different grafting percentages at a magnification of 4000X are shown in Figures 4.24-4.27.

King Mongkut's Institute of Technology Ladkrabang

This material is reserved for educational use only, not allowed for commercial use.
Forbidden to modify the content, and cite the document when use.

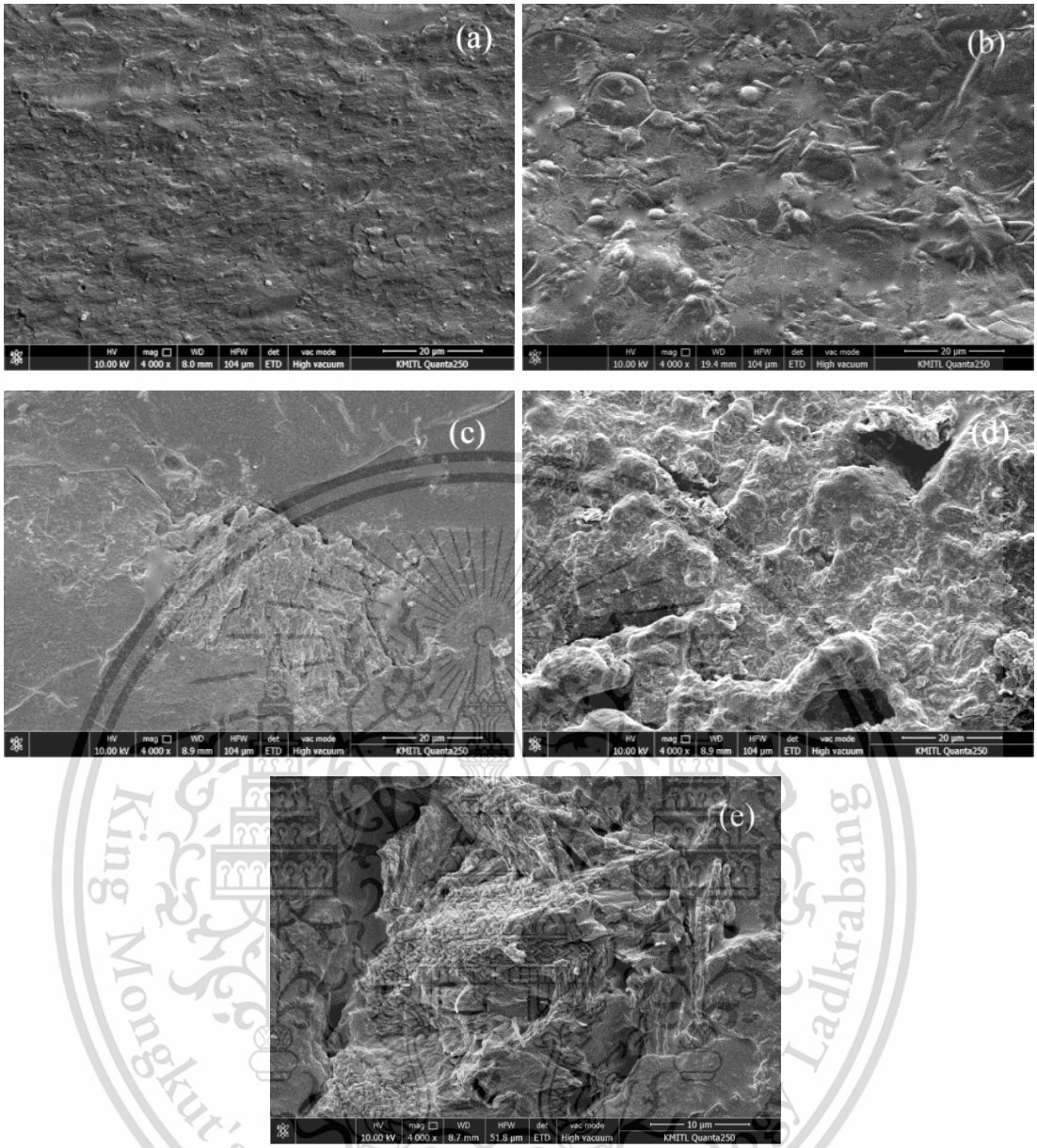

Figure 4.24 SEM micrographs at 4000X magnification of TPNS film and various TPGS films by MAM with different grafting percentages (a) TPNS (b) TPGS-20MAM (c) TPGS-40MAM (d) TPGS-60MAM and (e) TPGS-90MAM

This material is reserved for educational use only, not allowed for commercial use.
Forbidden to modify the content, and cite the document when use.

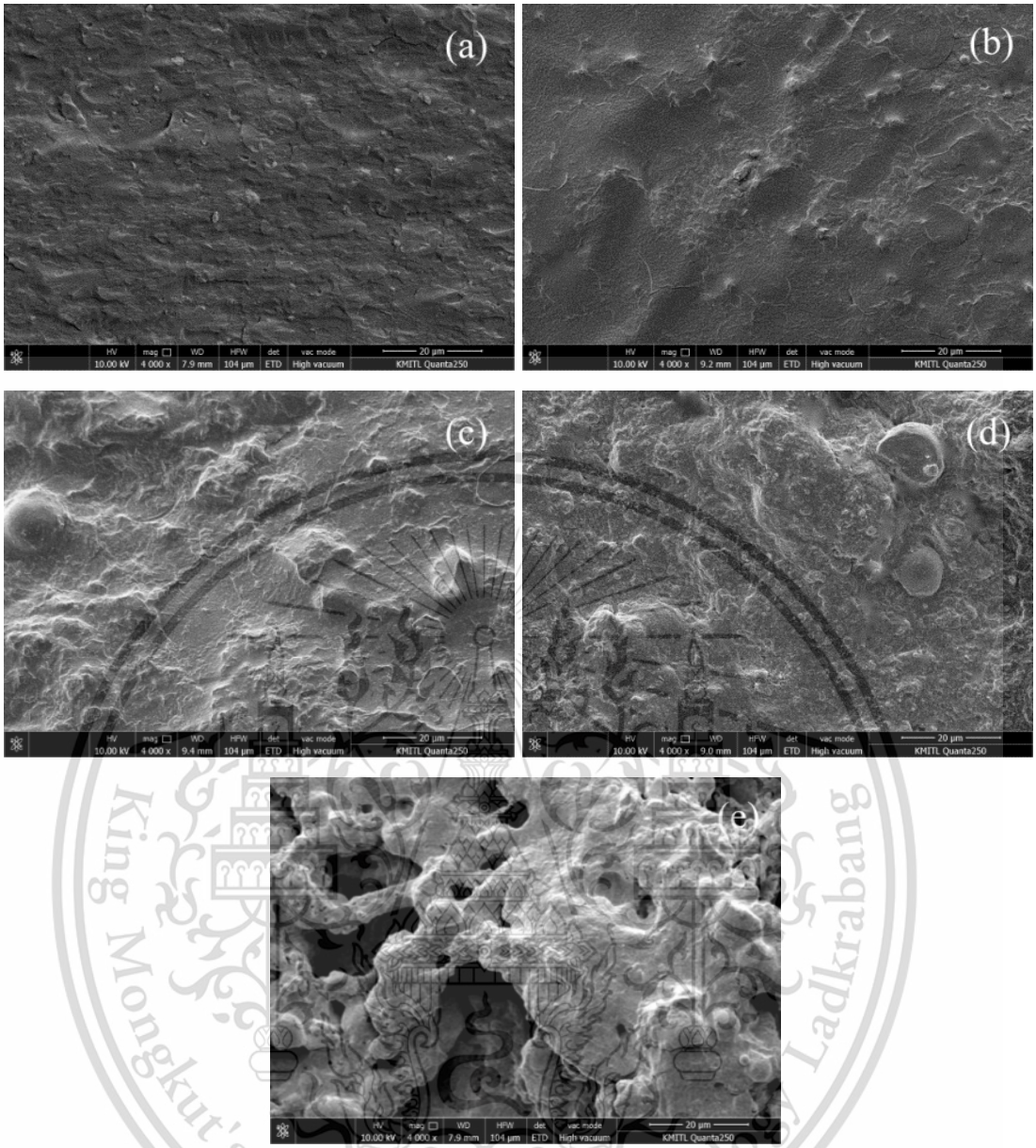

Figure 4.25 SEM micrographs at 4000X magnification of TPNS film and various TPGS films by MAA with different grafting percentages (a) TPNS (b) TPGS-20MAA (c) TPGS-40MAA (d) TPGS-60MAA and (e) TPGS-90MAA

This material is reserved for educational use only, not allowed for commercial use.
Forbidden to modify the content, and cite the document when use.

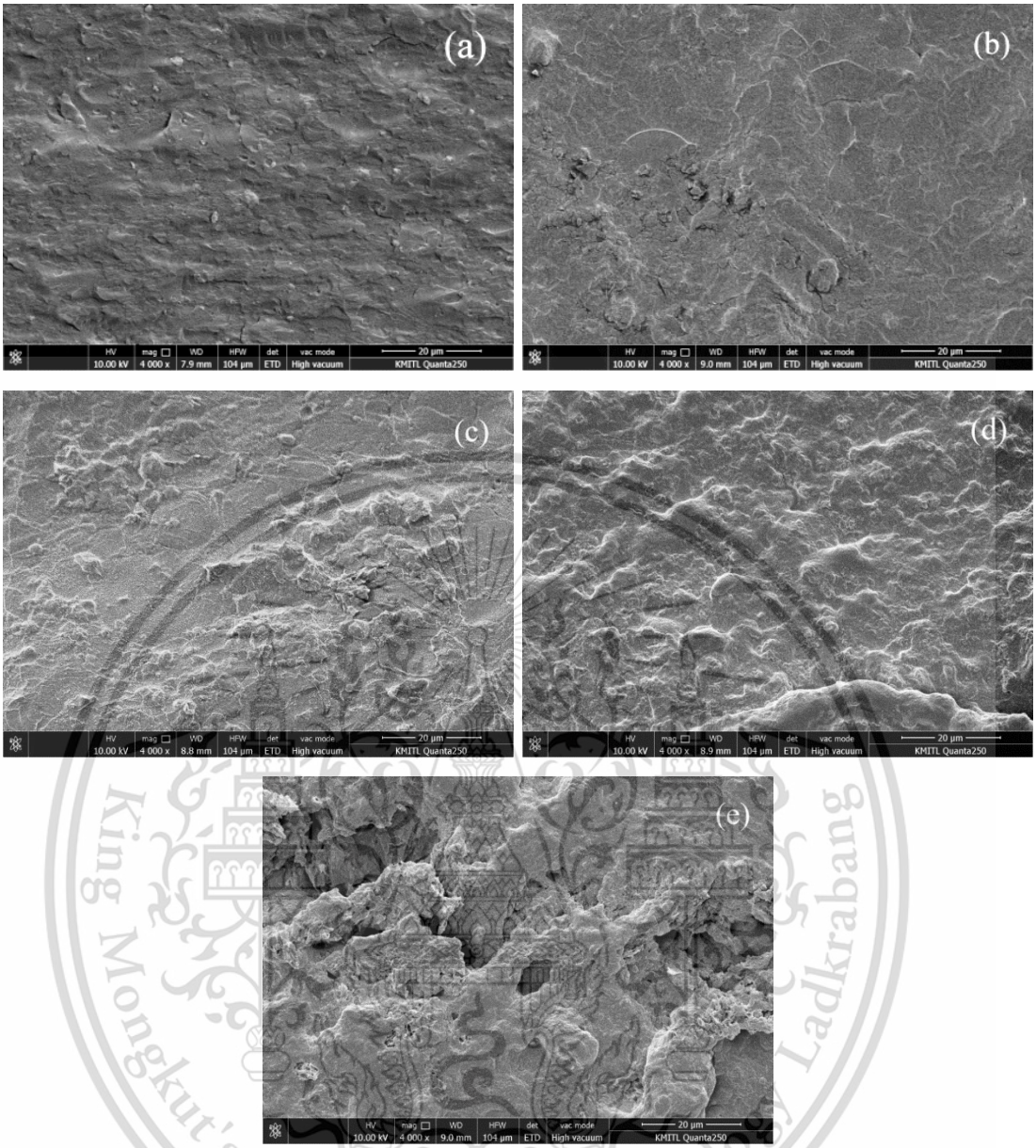

Figure 4.26 SEM micrographs at 4000X magnification of TPNS film and various TPGS films by MMA with different grafting percentages (a) TPNS (b) TPGS-20MMA (c) TPGS-40MMA (d) TPGS-60MMA and (e) TPGS-90MMA

SEM micrographs at magnification 4000X of TPNS film and various TPGS films grafted by MAM, MAA and MMA monomers with different grafting percentages are presented in Figures 4.24-4.26. Figures 4.24-4.26(a) show a smooth surface of TPNS film, whereas all TPGS films (Figures 4.24-4.26((b)-(e)) show different morphology as rough surfaces. The rough fracture surface was probably caused by the loss of hydrogen bonds and crystal phase destruction of starch structures and the formation

This material is reserved for educational use only, not allowed for commercial use.
Forbidden to modify the content, and cite the document when use.

of graft branch chains when grafted with monomers [17-18]. This observation indicated successful grafting with all types of vinyl monomers.

Furthermore, increasing grafting percentage of all TPGS films caused rougher surfaces. Rough morphologies of all TPGS films positively correlated with intrinsic viscosity and MW results and also concurred with findings of cast corn starch film grafted with CL and MMA [17-18].

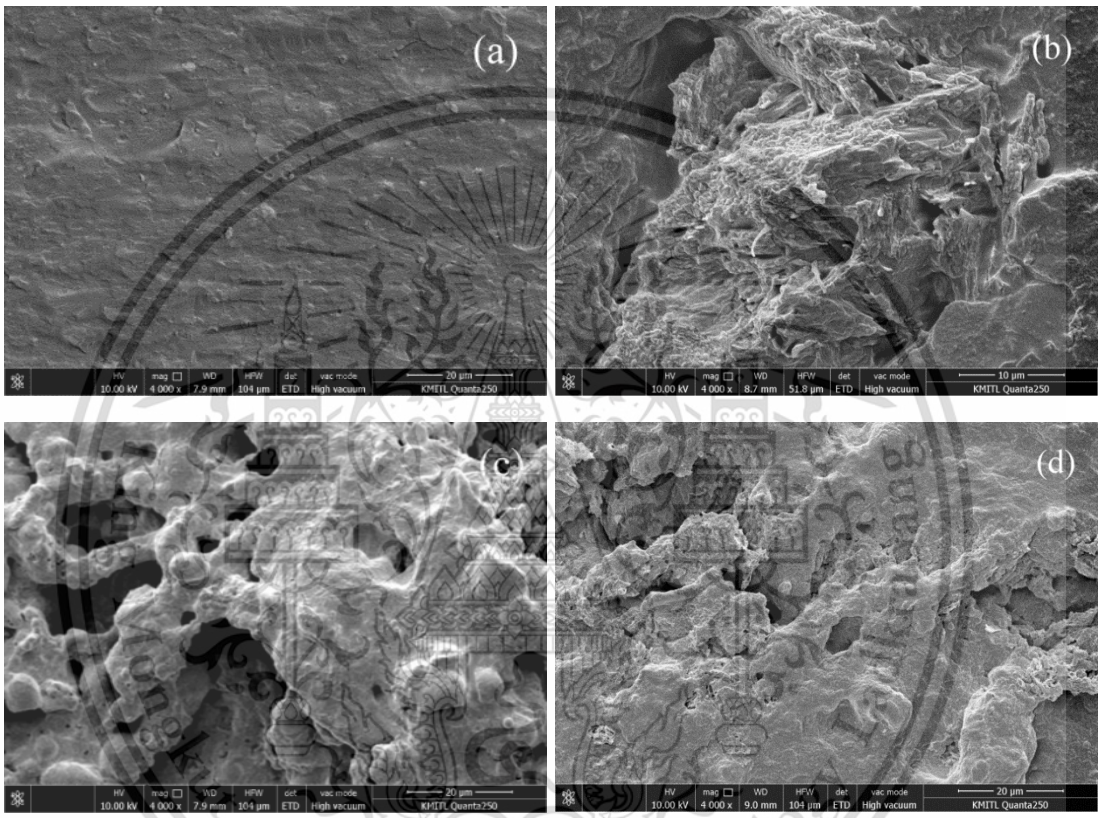

Figure 4.27 SEM micrographs at 4000X magnification of TPNS film and various TPGS films grafted with different types of vinyl monomers at 90% G (a) TPNS (b) TPGS-90MAM (c) TPGS-90MAA and (d) TPGS-90MMA

Figure 4.27 displays SEM micrographs as fractured surfaces at 4000X magnification of TPNS film and various TPGS films grafted with different types of vinyl monomers at 90% G. All TPGS films showed substantial differences in morphology from TPNS film with rougher surfaces. Morphologies of various TPGS films grafted with different types of vinyl monomers were rougher than TPNS film and presented no significant difference in morphology as compared to other TPGS films.

This material is reserved for educational use only, not allowed for commercial use.
Forbidden to modify the content, and cite the document when use.

4.2.4 Swelling behavior

Water absorbency of different TPGS films was characterized in terms of swelling capacity after immersion in distilled water for 1-6 h and 72 h. Swelling behavior is a diffusion phenomenon driven by the affinity of starch molecules to the surrounding fluid molecules. Correlations between swelling behavior and grafting percentage of TPNS film and various TPGS films grafted by MAM, MAA and MMA monomers with different grafting percentages are shown in Figures 4.28-4.31.

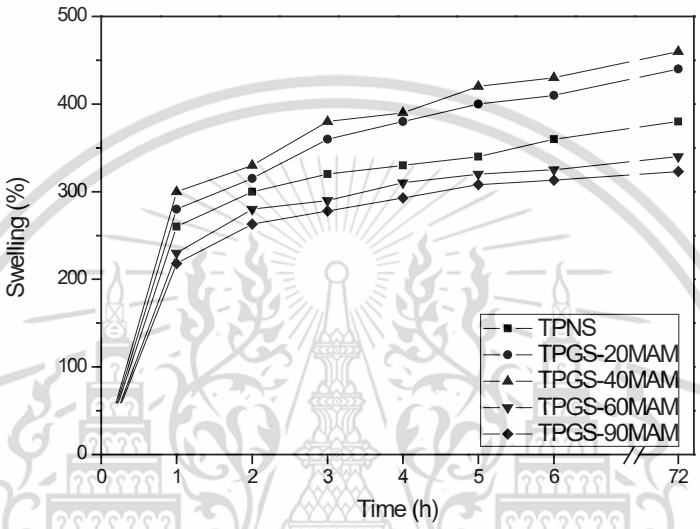

Figure 4.28 Degrees of swelling at 100% RH versus immersion time of TPNS film and various TPGS films by MAM with different percentages of grafting

This material is reserved for educational use only, not allowed for commercial use.
Forbidden to modify the content, and cite the document when use.

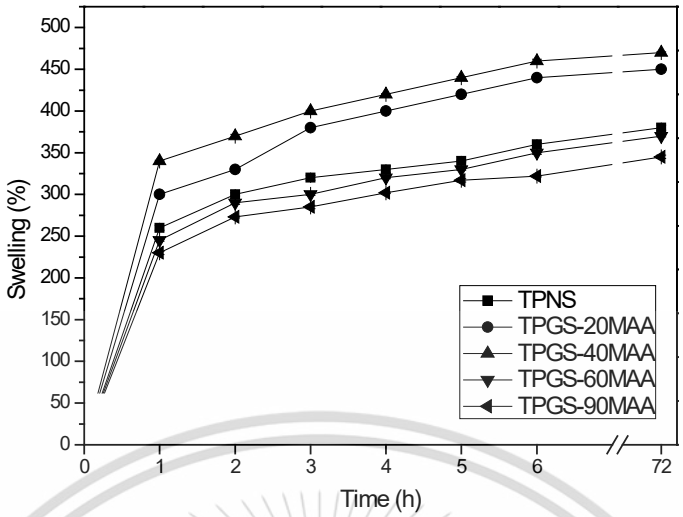

Figure 4.29 Degree of swelling at 100% RH versus immersion time of TPNS film and various TPGS films by MAA with different grafting percentages

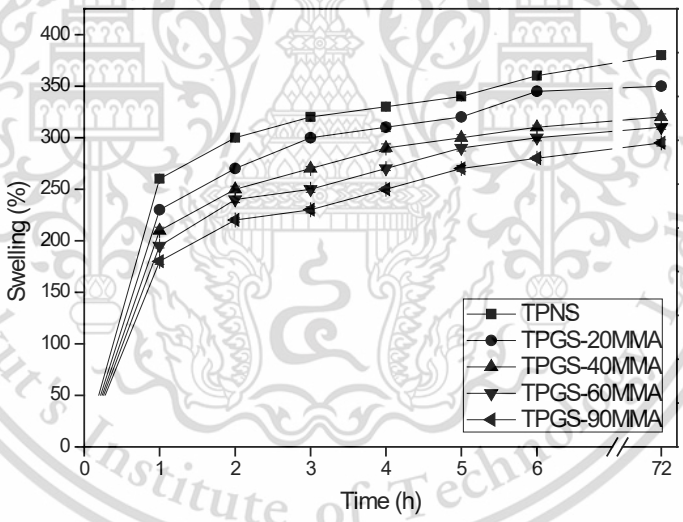

Figure 4.30 Degree of swelling at 100% RH versus immersion time of TPNS film and various TPGS films by MMA with different grafting percentages

Effects of graft copolymerization on degree of swelling at 100% RH of various TPGS films are displayed in Figures 4.28-4.30. Degree of swelling of TPGS films grafted with MAM or MAA (Figures 4.28-4.29) increased with grafting at 20 and 40%. This result was attributed to the hydrophilic nature of MAM and MAA functional groups. However, TPGS films grafted with MAM or MAA monomers at 60 and 90% G showed a declining trend of degree of swelling because high grafting percentage caused a

This material is reserved for educational use only, not allowed for commercial use.
Forbidden to modify the content, and cite the document when use.

decrease in available hydrophilic hydroxyl groups and concurrent with the formation of hydrogen bonding between the methacrylic groups or methacrylamide groups. The increase in hydrophicility at low grafting percentage and a subsequent decrease in hydrophicility at higher grafting percentage were also reported in earlier studies of GS grafted with MAA and MAM monomers [14-15].

On the other hand, for TPGS film grafted with MMA, a decrease in degree of swelling of TPGS films with MMA was observed for all grafting percentages (20-90% G). This result was attributed to the grafting of less polar MMA groups onto the starch chains, leading to lower hydrophilicity of TPGS films. Furthermore, degree of swelling of TPGS films grafted with MMA decreased with increasing grafting percentage since less polar MMA groups were introduced into the starch backbones, resulting in fewer available hydrophilic hydroxyl groups [20].

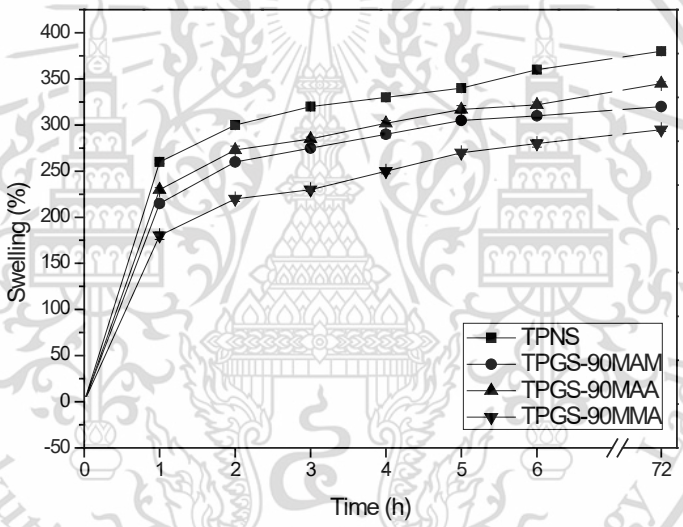

Figure 4.31 Degree of swelling at 100% RH versus immersion time of TPNS film and various TPGS films grafted with different types of vinyl monomers at 90% G

The degrees of swelling of TPNS film and various TPGS films with different types of vinyl monomers were compared as shown in Figure 4.31. It should be noted that all TPGS films grafted with the highest percentage of grafting (90% G) showed lower degrees of swelling value than that of TPNS film, suggesting that a graft copolymerization with MAM, MAA or MMA monomers at high percentage of grafting could improve hydrophobicity of TPNS film. This was because the decrease in hydrophilicity by declining of free hydroxyl groups and the high grafting process could restrict the water absorption capacity in starch matrix [14-15, 20].

This material is reserved for educational use only, not allowed for commercial use.
Forbidden to modify the content, and cite the document when use.

A comparison in TPGS films with different types of vinyl monomers at 90% G, TPGS-90MMA exhibited lower degree of swelling than those of TPGS film. This might be because the grafting with less polar MMA groups onto starch backbone, leading to lower degree of swelling of TPGS film. In addition, when degree of swelling between TPGS-90MAM and TPGS-90MAA was compared, it was found that TPGS-90MAM presented lower degree of swelling than TPGS-90MAA. This result was probably due to MAM groups presented lower polarity than MAA groups [47, 58], causing lower hydrophilicity of TPGS film. Overall results showed that the lowest percentage of swelling was found in TPGS-90MMA; while, the highest percentage of swelling was obtained from TPGS-40MAA.

4.2.5 Moisture uptake

Percentage of moisture uptake was examined using the ASTM D-570 standard method. Effects of graft copolymerization on moisture uptake properties of various TPGS films grafted by MAM, MAA and MMA monomers with different grafting percentages are shown in Figures 4.32-4.35.

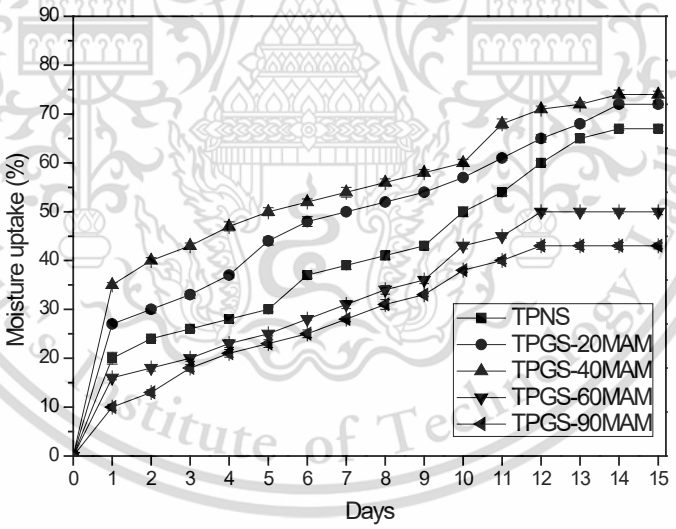

Figure 4.32 Percentage of moisture uptake at 100% RH versus immersion time for TPNS film and various TPGS films by MAM with different grafting percentages

This material is reserved for educational use only, not allowed for commercial use.
Forbidden to modify the content, and cite the document when use.

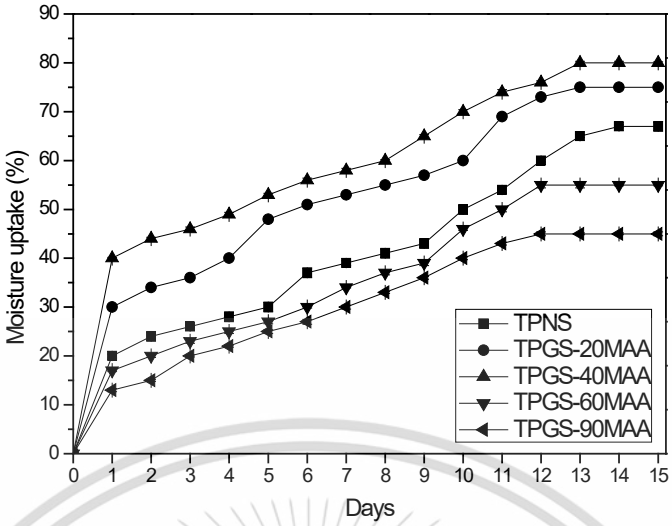

Figure 4.33 Percentage of moisture uptake at 100% RH versus immersion time of TPNS film and various TPGS films by MAA with different grafting percentages

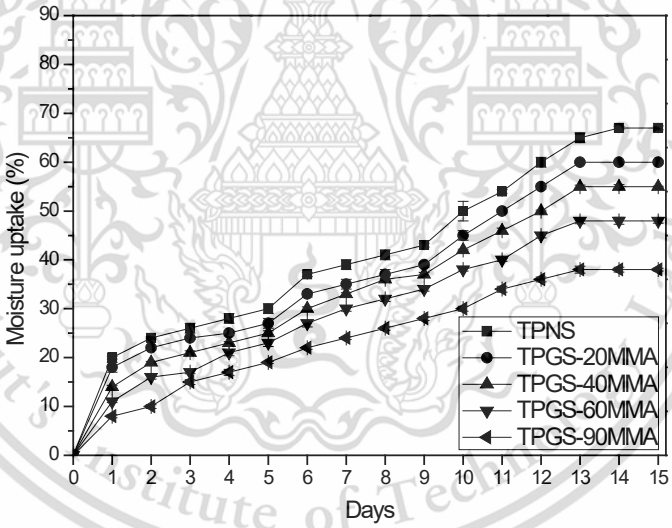

Figure 4.34 Percentage of moisture uptake at 100% RH versus immersion time of TPNS film and various TPGS films by MMA with different grafting percentages

Results in Figures 4.32-4.34 showed that moisture uptake percentages between TPNS film and different TPGS films grafted with various types of vinyl monomer were markedly different. Figures 4.32 and 4.33 revealed that percentages of moisture uptake of TPGS films with MAM and MAA at 20 and 40% G were considerably higher than TPNS film because greater polarity of MAM and MAA hydrophilic groups could absorb more water molecules. Nevertheless, a decreasing trend of percentage of

This material is reserved for educational use only, not allowed for commercial use.
Forbidden to modify the content, and cite the document when use.

moisture uptake was observed for TPGS films with MAM and MAA at 60 and 90**%** G**.** This was attributed to the formation of hydrogen bonding between the methacrylamide groups or methacrylic groups, resulting in restricted water absorption**.** A similar trend of decreasing moisture uptake with increasing grafting percentage was also reported for MAA and MAM grafted starch at high grafting percentage by other researchers **[**14**-**15**].**

All TPGS films with MMA illustrated lower percentages of moisture uptake than TPNS film and percentage of moisture uptake noticeably decreased with increasing grafting percentage**.** This result was attributed to the presence of less polar MMA groups in starch chains via the grafting process and concurred with moisture uptake properties of MMA**-**grafted starch from sago starch for previous study **[**20**].** In addition, moisture uptake results closely matched the degree of swelling results **(**Section 4.2.4**).**

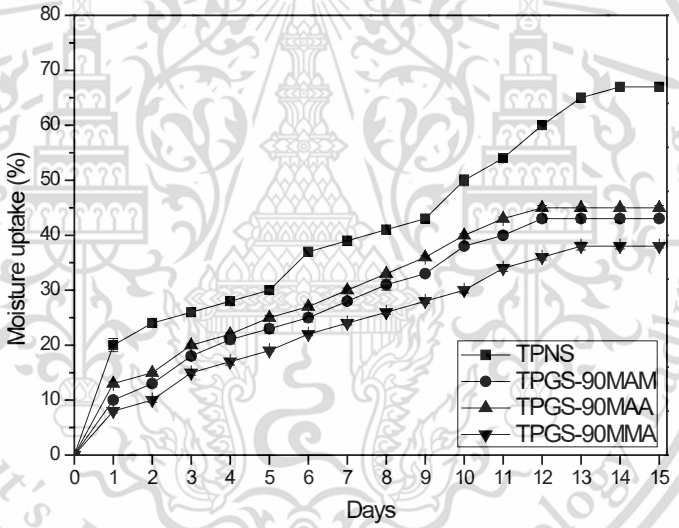

Figure 4.35 Percentages of moisture uptake at 100% RH versus time of TPNS film and various TPGS films grafted with various monomers at 90% G

Effects of various types of grafted vinyl monomers on percentage of moisture uptake are presented in Figure 4.35**.** TPNS film showed the highest percentage of moisture uptake followed by TPGS**-**90MAA and TPGS**-**90MAM together with the lowest percentage of moisture uptake were found in TPGS**-**90MMA**.** The highest moisture absorption capacity of TPNS reflected its high hydrophilic property, while graft copolymerization with all vinyl monomers at high percentage blocked water molecule absorption of TPGS films**.** In addition, lower percentage of moisture uptake

This material is reserved for educational use only, not allowed for commercial use.
Forbidden to modify the content, and cite the document when use.

of TPGS-90MMA arose from grafting with less polar groups that consequently reduced moisture uptake capacity [20]. TPGS-90MAM presented lower percentage of moisture uptake than TPGS-90MAA caused by higher natural hydrophilic acrylic groups than acrylamide groups [59]. Maximum and minimum percentages of moisture uptake were observed in TPGS-40MAA and TPGS-90MMA, respectively.

4.2.6 Water vapor permeability (WVP)

WVP of TPNS film and different TPGS films were performed by a gravimetric method following ASTM E-96 at 25±2°C and 75% RH. Effects of graft copolymerization on WVP of various TPGS films grafted by MAM, MAA and MMA monomers with different grafting percentages are presented in Tables 4.15-4.16.

Table 4.15 WVP values of TPNS film and various TPGS films grafted by MAM, MAA and MMA monomers with different grafting percentages

Sample	WVP ($g.mm/m^2.day.kPa$)
TPNS	20.1±0.02
TPGS-20MAM	23.7±0.03
TPGS-40MAM	24.5±0.04
TPGS-60MAM	18.2±0.03
TPGS-90MAM	16.3±0.08
TPGS-20MAA	25.7±0.02
TPGS-40MAA	26.5±0.03
TPGS-60MAA	19.2±0.02
TPGS-90MAA	17.3±0.05
TPGS-20MMA	16.3±0.03
TPGS-40MMA	15.2±0.06
TPGS-60MMA	13.8±0.05
TPGS-90MMA	12.3±0.07

WVP values of TPNS film and various TPGS films grafted by MAM, MAA and MMA monomers with different grafting percentages are shown in Table 4.15. Compared to TPNS film, WVP values of TPGS films with MAM and MAA at 20 and 40% grafting tended to be higher. This could be due to grafting more MAM or MAA hydrophilic

This material is reserved for educational use only, not allowed for commercial use.
Forbidden to modify the content, and cite the document when use.

groups onto starch chains [14-15]. However, further increase in grafting percentage (60 and 90% G) of TPGS films with both MAM and MAA decreased water vapor capacity, thereby lowering their WVP values. This observation was explained by the formation of hydrogen bonds at high degrees of the starch grafting process by MAM and MAA monomers which restricted and blocked water vapor permeability within the starch matrix [14-15].

However, WVP values of TPGS films with MMA were lower than for TPNS film. Additionally, WVP values of TPGS films with MMA decreased with increasing grafting percentage. This observation confirmed less polarity of the MMA monomer, leading to a lower WVP value. A similar result was observed by S. Sakar *et al*. (2015) who prepared GS from sago starch with MMA monomer [20]. The WVP results also related to degree of swelling values and moisture uptake results of all types of TPGS films (Figures 4.28-4.30 and Figures 4.32-4.34)

Table 4.16 WVP values of TPNS film and various TPGS films grafted with different types of vinyl monomers at 90% G

Sample	WVP ($g.mm/m^2.day.kPa$)
TPNS	20.1±0.02
TPGS-90MAM	16.3±0.08
TPGS-90MAA	17.3±0.05
TPGS-90MMA	12.3±0.15

WVP values of TPNS and different TPGS films grafted with various types of vinyl monomer at 90% G are shown in Table 4.16. Graft copolymerization of MAM, MAA and MMA onto cassava starch backbones at high grafting percentages resulted in the decrease in WVP of TPGS films. This observation was attributed to a decrease in the hydrophilic hydroxyl groups of starch chains and replacement of starch molecule hydroxyl groups by MMA groups and formation of hydrogen bonding between MAM or MAA groups via high amounts of grafting by MAM and MAA monomers.

WVP values of different TPGS films were ranked highest to lowest as TPGS-90MAA>TPGS-90MAM>TPGS-90MMA. The lowest WVP value was found in TPGS-90MMA, which was caused by the lowest polarity or grafting with substituted less polar groups onto starch chains. In addition, WVP value of TPGS-90MAA was higher than TPGS-90MAM. This was because the MAA group presented higher polarity than the MAM group [58-59], resulting in the highest WVP value among TPGS films.

This material is reserved for educational use only, not allowed for commercial use.
Forbidden to modify the content, and cite the document when use.

Overall, TPGS-90MMA displayed the lowest WVP value together with the highest WVP value was found in TPGS-40MAA.

4.2.7 Mechanical properties

Mechanical properties of different TPGS films grafted by various monomer with different percentages were investigated following ASTM D-882 using a Universal testing machine (UTM) at 60% RH and 25±1˚C. In addition, stress, strain at maximum load and Young's modulus of TPNS film and various TPGS films grafted by MAM, MAA and MMA monomers with different grafting percentages are presented in Figures 4.36-4.39.

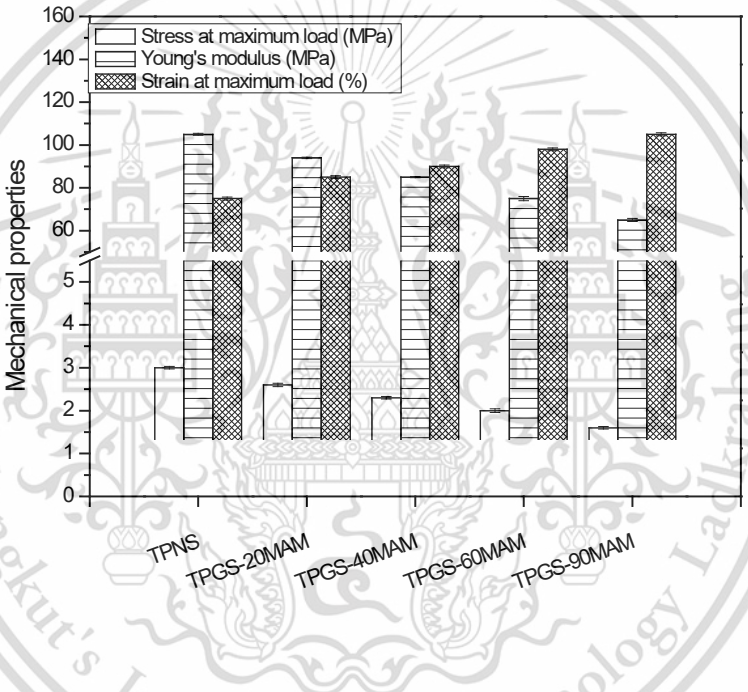

Figure 4.36 Mechanical properties of TPNS film and various TPGS films by MAM with different grafting percentages (a) stress at maximum load (b) Young' s modulus and (c) strain at maximum load

This material is reserved for educational use only, not allowed for commercial use.
Forbidden to modify the content, and cite the document when use.

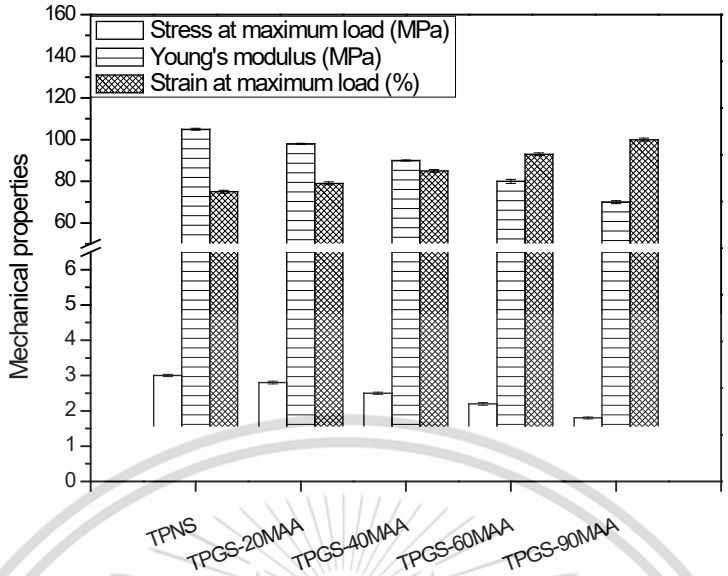

Figure 4.37 Mechanical properties of TPNS film and various TPGS films by MAA with different grafting percentages (a) stress at maximum load (b) Young' s modulus and (c) strain at maximum load

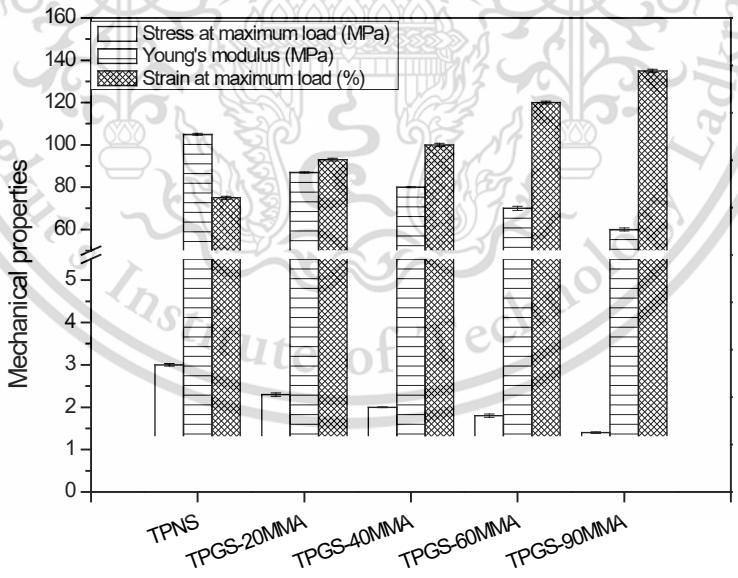

Figure 4.38 Mechanical properties of TPNS film and various TPGS films by MMA with different grafting percentages (a) stress at maximum load (b) Young' s modulus and (c) strain at maximum load

This material is reserved for educational use only, not allowed for commercial use.
Forbidden to modify the content, and cite the document when use.

Effects of graft copolymerization influenced the tensile properties of different TPGS films as shown in Figures 4.36-4.38. Use of all types of GS to produce TPGS films led to a more flexible structure that has been claimed to provide higher strain at maximum load. On the contrary, stress at maximum load and Young's modulus of all TPGS films were lower than TPNS film. A decrease in strength was due to graft copolymerization which destroyed molecular packing of the crystalline phase and hydrogen bonding between starch chains and increased free volume of starch molecules by the formation of graft chains, leading to increased flexibility of starch chains. This result correlated with the degree of crystallinity of different TPGS films (Section 4.2.2). Similar results of a decrease in strength and an increase in flexibility were observed in an earlier study of TPGS films from corn starch grafted with CL [18].

When graft yield was increased from 20 to 90% grafting, the percentage of strain at maximum load was noticeably increased; while, stress at maximum load and Young's modulus were decreased. These observations were because increased grafting caused greater destruction in hydrogen bonding between starch chains together with increasing their mobility by the formation of long alkyl grafted branch chains [18]. Mechanical properties of different TPGS films were also correlated to the degree of crystallinity (Section 4.2.2).

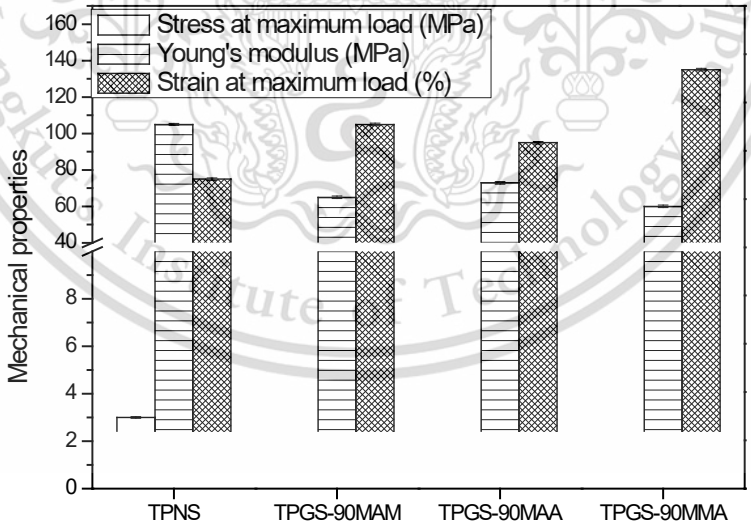

Figure 4.39 Mechanical properties of TPNS film and various TPGS films grafted with different types of vinyl monomers at 90% G (a) stress at maximum load (b) Young's modulus and (c) strain at maximum load

This material is reserved for educational use only, not allowed for commercial use.
Forbidden to modify the content, and cite the document when use.

Figure 4.39 shows that graft copolymerization with all types of vinyl monomers onto cassava starch backbones led to a substantial increase in flexibility as observed from the strain at maximum load value, together with a decline in tensile strength and Young's modulus of all TPGS films. This result occurred since the incorporation of grafted monomers was associated with increased flexibility of the starch chain and a decreasing tendency of hydrogen bonding by grafting with these monomers [18].

When mechanical properties of various TPGS films with different types of vinyl monomers at 90% G were compared, TPGS-90MMA exhibited the highest strain at maximum load together with the lowest tensile strength and Young's modulus because MMA monomers presented longer alkyl chain than MAA and MAM monomers, resulting in a decrease in molecular packaging and lowest of degree of crystallinity, thereby increasing the flexibility of TPGS films. Conversely, TPGS-90MAA showed lower strain at maximum load, but higher stress and Young's modulus at maximum load than TPGS-90MMA and TPGS-90MAM. This result was also attributed to the shorter length of alkyl chains of MAA, leading to a higher degree of crystallinity compared with TPGS films (Table 4.13). Overall, maximum flexibility was obtained from TPGS-90MMA; while, minimum flexibility was found in TPNS film.

4.2.8 Biodegradable properties

To evaluate the degradation of biodegradable modified starch films in a realistic environment a soil burial experiment was carried out. TPNS and various TPGS films were buried in the soil for 5 and 10 days to determine changes in mechanical properties such as tensile strength, maximum strain and Young's modulus. The results are displayed in Figures 4.40-4.43 and Tables 4.17-4.18.

This material is reserved for educational use only, not allowed for commercial use.
Forbidden to modify the content, and cite the document when use.

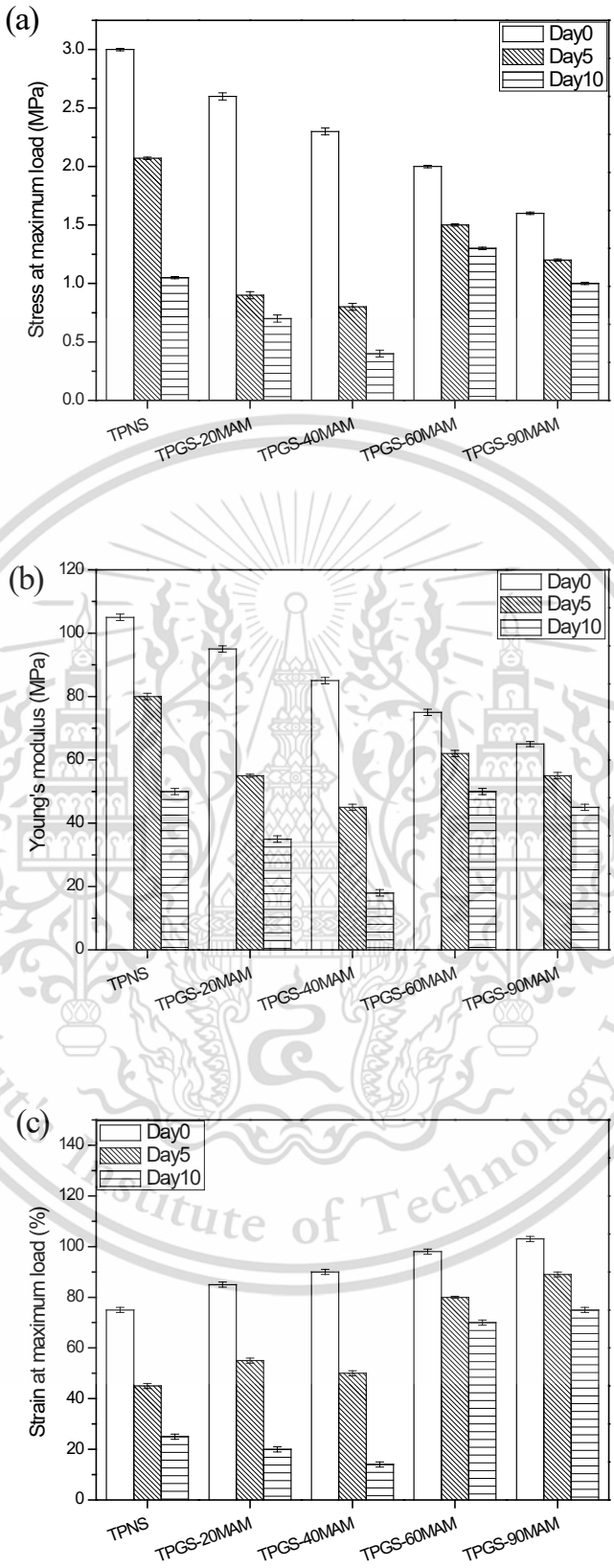

Figure 4.40 Mechanical properties after biodegradation by a soil burial test of TPNS film and various TPGS films by MAM with different grafting percentages **(a)** stress at maximum load **(b)** Young' s modulus and **(c)** strain at maximum load

This material is reserved for educational use only, not allowed for commercial use.
Forbidden to modify the content, and cite the document when use.

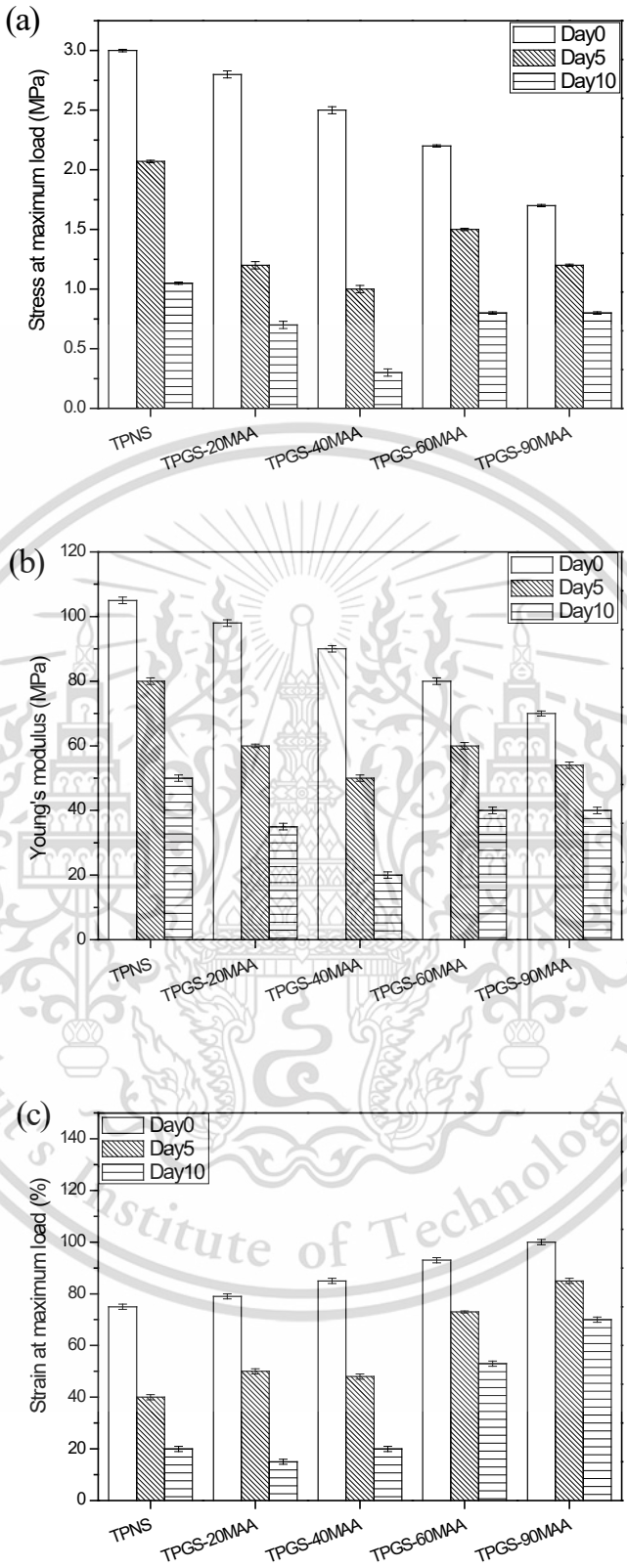

Figure 4.41 Mechanical properties after biodegradation by a soil burial test of TPNS film and various TPGS films by MAA with different grafting percentages (a) stress at maximum load (b) Young' s modulus and (c) strain at maximum load

This material is reserved for educational use only, not allowed for commercial use.
Forbidden to modify the content, and cite the document when use.

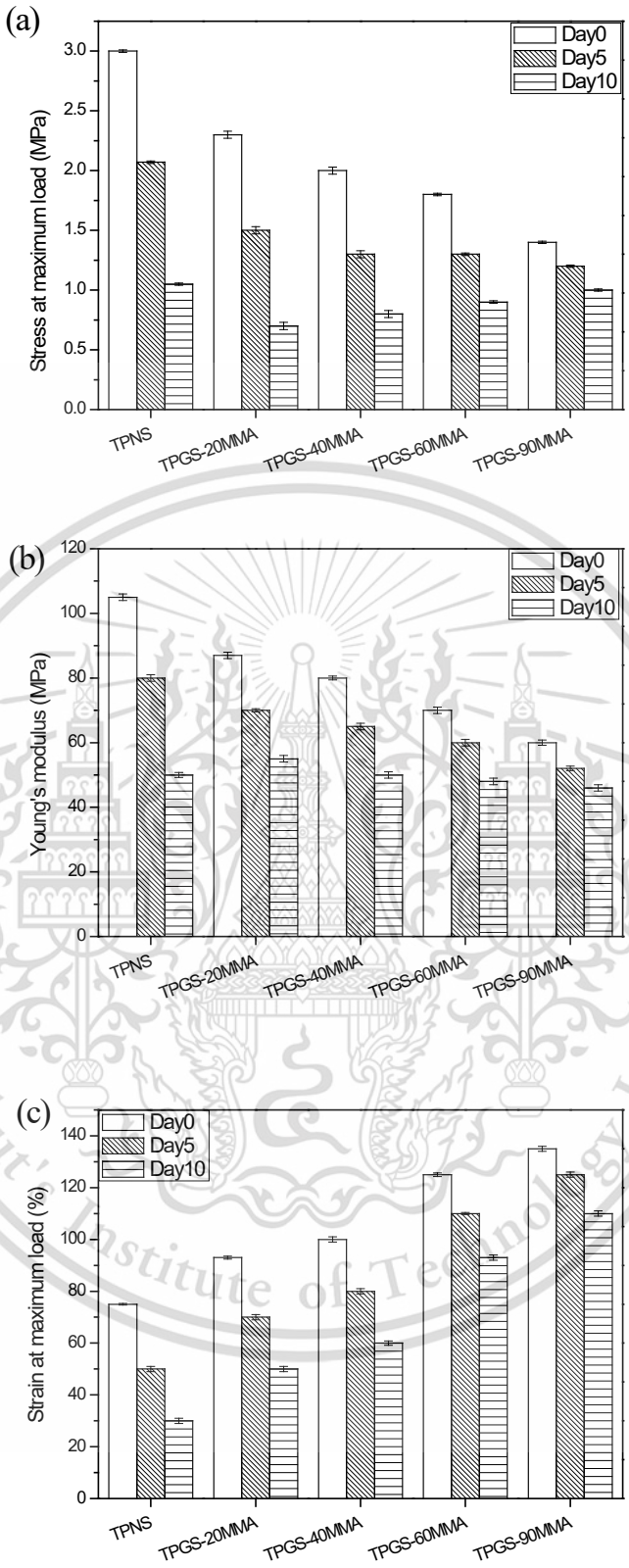

Figure 4.42 Mechanical properties after biodegradation by a soil burial test of TPNS film and various TPGS films by MMA with different grafting percentages (a) stress at maximum load (b) Young' s modulus and (c) strain at maximum load

This material is reserved for educational use only, not allowed for commercial use.
Forbidden to modify the content, and cite the document when use.

Table 4.17 Percentage reduction of mechanical properties of TPNS film and various TPGS films grafted by MAM, MAA and MMA monomers with different grafting percentages after 5 and 10 days of biodegradation in soil

Sample	Percentage of a reduction in mechanical properties for 5 days (%)			Percentage of a reduction in mechanical properties for 10 days (%)		
	Stress at maximum load	Young's modulus	Strain at maximum load	Stress at maximum load	Young's modulus	Strain at maximum load
TPNS	31.0	23.8	40.0	65.0	52.3	66.6
TPGS-20MAM	46.1	40.0	41.1	73.0	63.1	72.9
TPGS-40MAM	52.2	45.9	46.6	78.2	78.8	72.2
TPGS-60MAM	25.0	20.0	20.4	35.0	33.3	28.5
TPGS-90MAM	18.7	15.4	17.5	37.0	30.7	27.1
TPGS-20MAA	57.1	41.8	43.0	75.0	64.2	75.9
TPGS-40MAA	60.0	47.8	47.0	80.0	77.7	76.4
TPGS-60MAA	31.8	22.5	21.5	54.5	46.2	38.7
TPGS-90MAA	23.5	21.4	19.0	47.0	42.8	30.0
TPGS-20MMA	30.7	19.5	24.7	56.6	36.7	46.2
TPGS-40MMA	28.6	18.7	20.0	50.0	33.7	40.0
TPGS-60MMA	22.2	14.3	12.1	44.4	31.4	25.6
TPGS-90MMA	14.3	13.3	7.4	42.8	23.3	18.5

Biodegradable properties of TPNS film and different TPGS films were performed by testing mechanical properties after soil burial testing for 5 and 10 days. Results in Figures 4.40-4.42 and Table 4.17 exhibited the decrease in mechanical properties as stress at maximum load, Young's modulus and strain at maximum load after biodegradation following soil burial. This observation confirmed that TPNS film and all TPGS films showed the ability to degrade. The drop in tensile properties after samples were buried in soil was due to hydrolysis of the starch chains by absorption of water molecules by the sample and attack from microorganisms [18-19].

Regarding biodegradable properties of various TPGS films, the result revealed that TPGS films with MAM and MAA at 20 and 40 %G showed higher biodegradability due to their higher hydrophilicity; while, TPGS films grafted with MAM and MAA at 60 and 90 %G as well as all TPGS films with MMA presented lower biodegradability than TPNS film resulting from lower moisture uptake and hydrophilicity. Biodegradable properties were also correlated with results of moisture uptake, degree of swelling

This material is reserved for educational use only, not allowed for commercial use.
Forbidden to modify the content, and cite the document when use.

and WVP (Figures 4.28-4.35 and Tables 4.15-4.16). Biodegradation of starch grafted film was also reported on cast TPGS films with MMA and CL. The result showed that the cast TPGS film with MMA and CL could biodegrade by a soil burial test [17, 19].

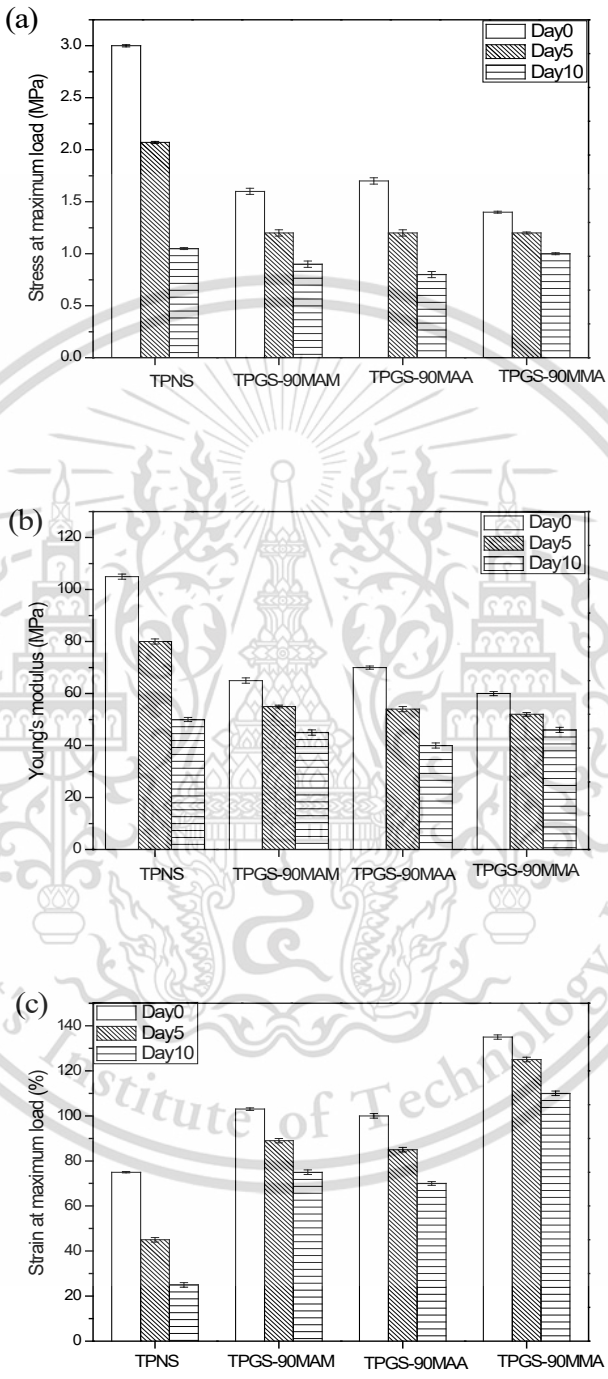

Figure 4.43 Mechanical properties after biodegradation by a soil burial test of TPNS film and various TPGS films grafted with different types of vinyl monomers at 90% G(a) stress at maximum load (b) Young' s modulus and (c) strain at maximum load

This material is reserved for educational use only, not allowed for commercial use.
Forbidden to modify the content, and cite the document when use.

Table 4.18 Percentage reduction of mechanical properties of TPNS film and various TPGS films grafted with different types of vinyl monomers at 90% G after 5 and 10 days of biodegradation in soil

Sample	Percentage of a reduction in mechanical properties for 5 days (%)			Percentage of a reduction in mechanical properties for 10 days (%)		
	Stress at maximum load	Young's modulus	Strain at maximum load	Stress at maximum load	Young's modulus	Strain at maximum load
TPNS	31.0	23.8	40.0	65.0	52.3	66.6
TPGS-90MAM	18.7	15.3	17.4	37.0	30.7	27.1
TPGS-90MAA	23.5	21.4	19.0	47.0	42.8	30.0
TPGS-90MMA	14.3	13.3	7.4	42.8	23.3	18.5

Figure 4.43 and Table 4.18 depict the mechanical properties after soil burial test of TPNS film and TPGS films grafted with various vinyl monomers at 90% G. Results showed a lower change in mechanical properties after biodegradation for all types of TPGS films due to their lower hydrophilic properties. This result implied that hydrophilicity highly affected the biodegradable properties of different TPGS films [18-19]. When biodegradable properties were compared among TPGS films, TPGS-90MAA showed more rapid biodegradation than the other TPGS films caused by higher hydrophilicity that was observed from swelling, WVP and moisture uptake (Figures 4.31, 4.35 and Table 4.16). On the other hand, TPGS-90MMA showed lower biodegradability than those of starch films grafted with MAM and MAA due to its lower hydrophilicity.

4.2.9 Thermal property

The TGA technique was employed to analyze the thermal properties of TPNS film and different TPGS films in the temperature range 50-600°C with heating rate of 10°C/min under nitrogen atmosphere. Degradation temperature was detected at maximum thermal decomposition. TGA and DTG thermograms of TPNS film and various TPGS films grafted by MAM, MAA and MMA monomers with different grafting percentages are displayed in Figures 4.44-4.47 and degradation temperatures are tabulated in Tables 4.19-4.20.

This material is reserved for educational use only, not allowed for commercial use.
Forbidden to modify the content, and cite the document when use.

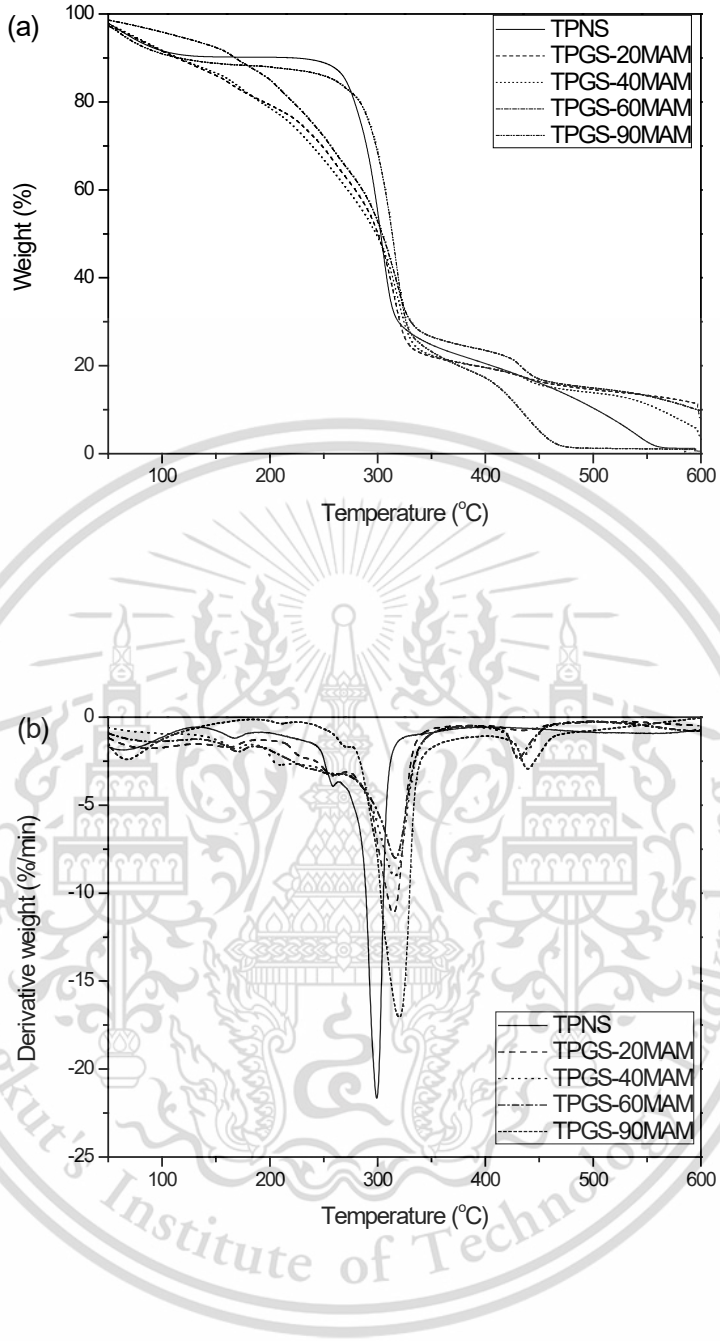

Figure 4.44 **(a)** TGA and **(b)** DTG thermograms of TPNS film and various TPGS films by MAM with different grafting percentages

This material is reserved for educational use only, not allowed for commercial use.
Forbidden to modify the content, and cite the document when use.

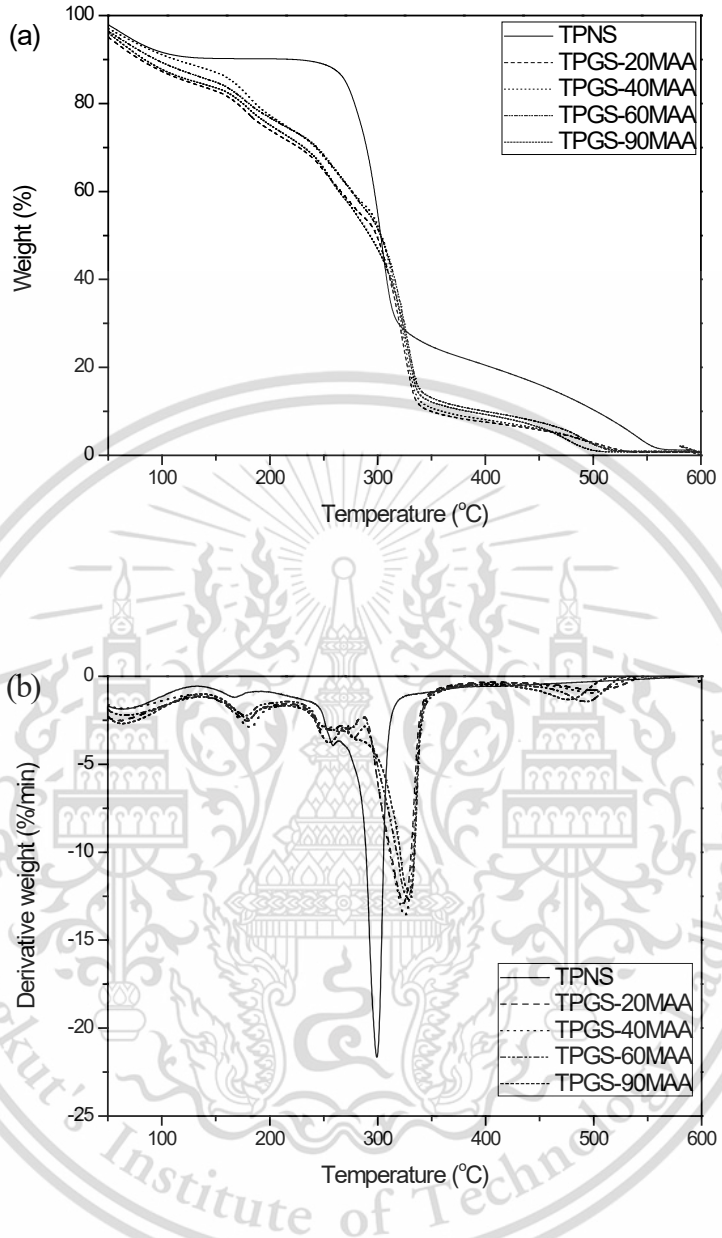

Figure 4.45 (a) TGA and (b) DTG thermograms of TPNS film and various TPGS films by MAA with different grafting percentages

This material is reserved for educational use only, not allowed for commercial use.
Forbidden to modify the content, and cite the document when use.

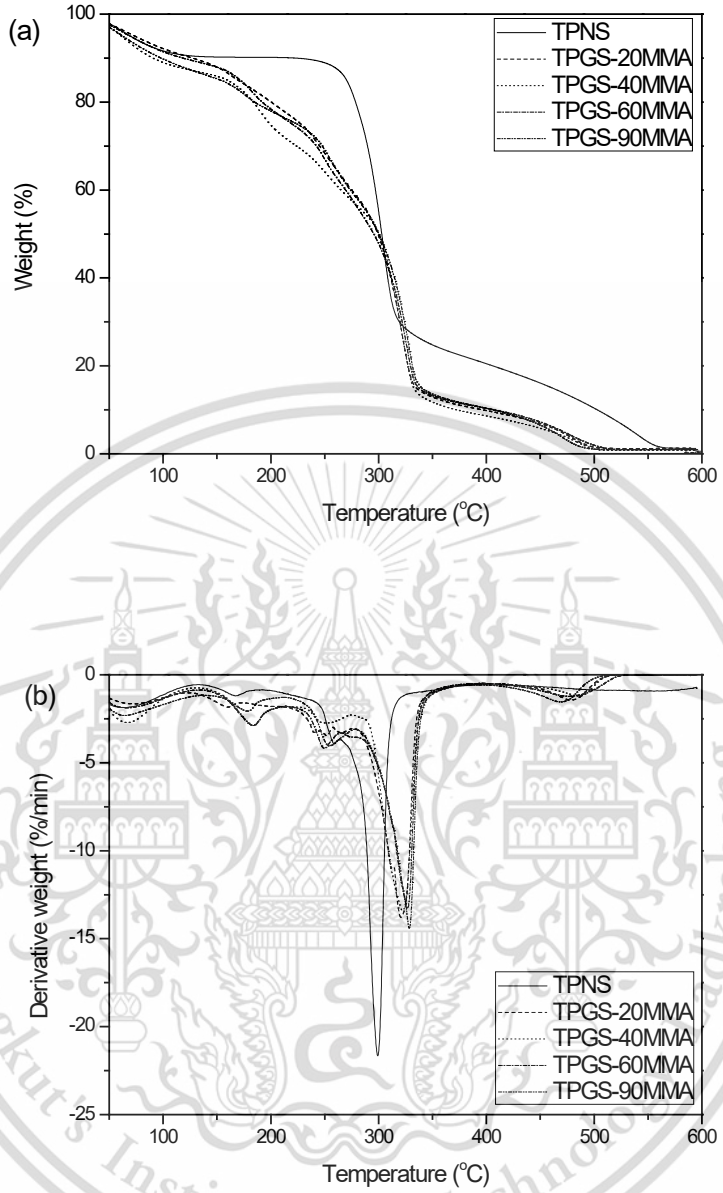

Figure 4.46 (a) TGA and (b) DTG thermograms of TPNS film and various TPGS films by MMA with different grafting percentages

This material is reserved for educational use only, not allowed for commercial use.
Forbidden to modify the content, and cite the document when use.

Table 4.19 Degradation temperatures of TPNS film and various TPGS films grafted by MAM, MAA and MMA monomers with different grafting percentages

Sample	Degradation temperature (˚C)			
	Step 1 (Glycerol)	Step 2 (Degraded starch)	Step 3 (Starch)	Step 4 (Monomer)
TPNS	167.7	258.4	299.3	-
TPGS-20MAM	161.8	260.5	314.4	433.9
TPGS-40MAM	195.8	265.5	314.7	435.8
TPGS-60MAM	167.7	258.6	316.1	432.6
TPGS-90MAM	204.7	269.5	317.4	433.0
TPGS-20MAA	179.2	256.6	323.4	500.2
TPGS-40MAA	181.4	265.6	325.1	497.3
TPGS-60MAA	178.1	267.4	329.0	492.2
TPGS-90MAA	180.5	249.3	330.7	489.3
TPGS-20MMA	159.5	251.6	320.8	478.3
TPGS-40MMA	191.5	251.0	322.2	474.9
TPGS-60MMA	183.7	249.3	326.7	475.4
TPGS-90MMA	177.9	254.4	328.1	468.2

Thermal properties of TPNS film and various TPGS films grafted by MAM, MAA and MMA monomers with different grafting percentages are shown in Figures 4.44-4.46 and Table 4.19. TPNS film exhibited 3 stages of thermal decomposition, while thermal transition of all TPGS films showed 4 stages of thermal degradation. The first stage at around 160-200˚C corresponded to the loss of glycerol plasticizer [19]. The second decomposition temperature at 245-270˚C corresponded to the degradation of starch molecules. The main third stage from 299 to 330˚C was attributed to decomposition of the starch, while the fourth stage from 430-500˚C was attributed to decomposition of grafted monomers, indicating a change in the structure of starch chains due to the grafting with vinyl monomers [19-20]. This observation confirmed the successful preparation of TPGS films. All TPGS films presented higher degradation temperatures in the third stage than TPNS film which implied that the grafting process improved thermal stability. Moreover, thermal degradation temperatures of starch proportionally increased with the increasing grafting percentage (20 to 90% G), indicating that increase in thermal degradation temperatures was caused by a rise in the amount of grafted monomers onto starch chains.

This material is reserved for educational use only, not allowed for commercial use.
Forbidden to modify the content, and cite the document when use.

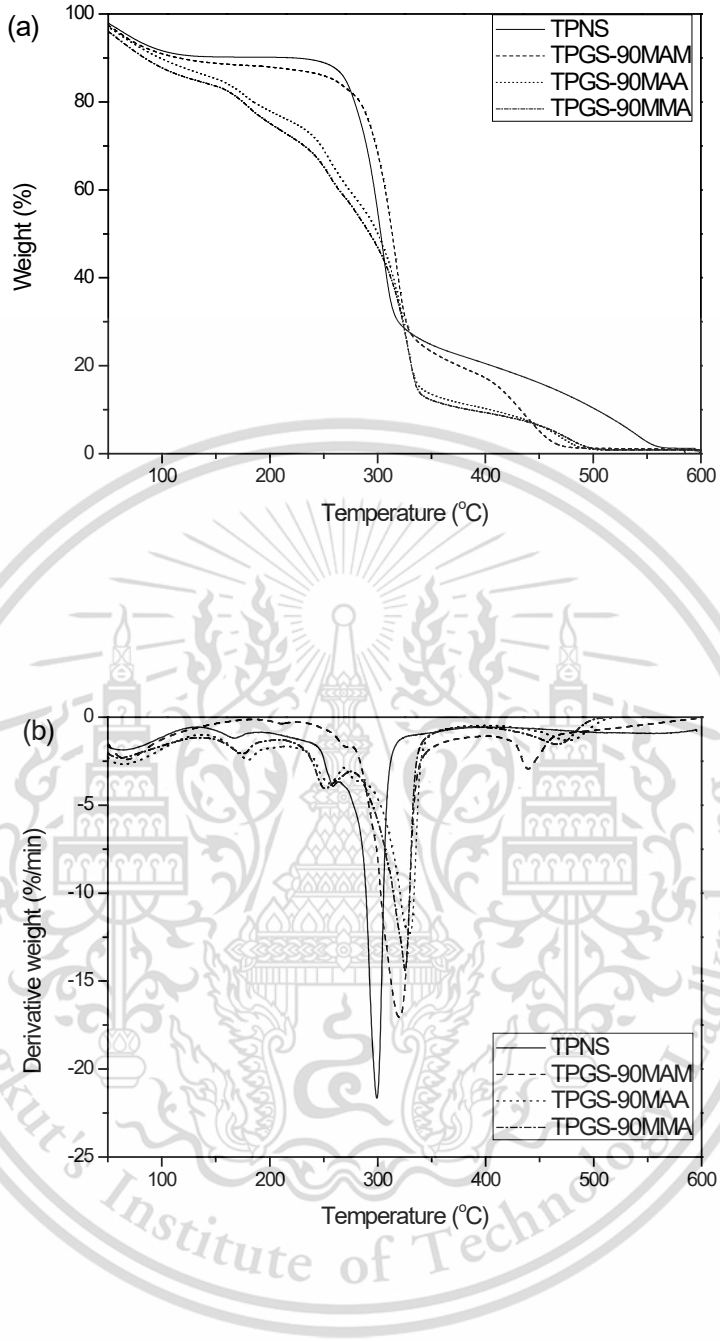

Figure 4.47 (a) TGA and (b) DTG thermograms of TPNS film and various TPGS films grafted with different types of vinyl monomers at 90% G

This material is reserved for educational use only, not allowed for commercial use.
Forbidden to modify the content, and cite the document when use.

Table 4.20 Degradation temperatures of TPNS film and various TPGS films grafted with different types of vinyl monomers at 90% G

Sample	Degradation temperature (˚C)			
	Step 1 (Glycerol)	Step 2 (Degraded starch)	Step 3 (Starch)	Step 4 (Monomer)
TPNS	167.7	258.4	299.3	-
TPGS-90MAM	204.7	269.5	317.4	433.0
TPGS-90MAA	180.5	249.3	330.7	489.3
TPGS-90MMA	177.9	254.4	328.1	468.2

In Figure 4.47 and Table 4.20, all TPGS films with high percentage of grafting showed higher thermal degradation temperatures than TPNS film. Graft copolymerization with MAA, MAM or MMA monomers improved thermal properties of TPNS film and the various TPGS films presented greater heat resistance. The third thermal degradation temperatures of various types of TPGS films are ranked as follows: TPGS-90MAA>TPGS-90MMA>TPGS-90MAM. This ranking was attributed to degradation temperatures of different types of vinyl monomers, i.e., MAA and MAM monomers provided the highest degradation temperature of 470-500°C and the lowest degradation temperature of 420-435 ˚C, respectively [13-17]. TPGS-90MAA recorded the highest thermal degradation temperature, while TPNS film showed the lowest thermal degradation temperature.

This material is reserved for educational use only, not allowed for commercial use.
Forbidden to modify the content, and cite the document when use.

Chapter 5

Conclusions and suggestions

5.1 Conclusions

Effects of graft copolymerization with different types of vinyl monomers including MAM, MAA and MMA at grafting percentages of 20, 40, 60 and 90**%** on several properties of differently GS and TPGS films were investigated. After characterization and testing, conclusions are presented as follows:

5.1.1 Properties of differently GS

5.1.1.1 Percentage of grafting proportionally increased with increasing reaction times. Highest grafting percentage was recorded at 90±2**%.** Optimum reaction synthesis time of MAA-grafted starch was 4 h, MAM-grafted starch was 5 h and MMA grafted starch was 6 h.

5.1.1.2 The success of different GS syntheses was confirmed by new characteristic FT-IR peaks. For MAM-grafted starch, additional peaks of C=O stretching and N-H stretching were characteristic of amide groups (-$CONH_2$). The important peak for MAA-grafted starch was attributed to C=O stretching of carboxyl groups (-COOH), while peak of C=O stretching of carboxylate groups (-$COCH_3$) was presented in MMA-grafted starch. As grafting percentages increased, intensities of their characteristic peaks also clearly increased.

5.1.1.3 Morphology results showed that starch granule shapes were irregular from disruption caused by the grafting process. As the percentage of grafting increased, all GS surfaces became rougher with increasing MAM, MAA and MMA contents.

5.1.1.4 Intrinsic viscosity and MW of differently GS increased with the increasing of grafting percentage. GS with MMA showed the highest intrinsic viscosity and MW, followed by GS with MAM and MAA.

5.1.1.5 As grafting percentages increased, thermal decomposition temperatures of starch were clearly increased. GS with MAA exhibited the highest thermal property, followed by GS with MMA and MAM. Moreover, GS-90MAA showed the maximum degradation temperatures.

5.1.2 Properties of different TPGS films

5.1.2.1 From the FT-IR study, TPGS films with MAM showed additional peaks corresponding to C=O stretching and N-H bending vibrations in amide characteristics. The FT-IR spectrum of TPGS films with MAA presented the most

This material is reserved for educational use only, not allowed for commercial use.
Forbidden to modify the content, and cite the document when use.

important peak of C=O stretching of carboxylic groups. In addition, a new peak of C=O stretching of carboxylate groups appeared in TPGS films with MMA.

5.1.2.2 Degrees of crystallinity of all TPGS films were decreased compared to TPNS film and degree of crystallinity was clearly decreased with the increasing grafting percentages. TPGS films with MMA showed the lowest degree of crystallinity among various TPGS films. TPGS films with MAM presented lower degree of crystallinity than TPGS films with MAA.

5.1.2.3 Morphologies of TPGS films showed different morphology as rough surface, while TPNS film showed a smooth fractured surface. As grafting percentage increased, all TPGS films showed rougher surfaces.

5.1.2.4 Degree of swelling of TPGS films grafted with MAM or MAA increased with grafting at 20 and 40**%**. However, TPGS films grafted with MAM or MAA monomers at 60 and 90**%** showed a declining trend. A decrease in degree of swelling of all TPGS films with MMA was clearly observed. The lowest percentage of swelling was found in TPGS-90MMA, while the highest was observed for TPGS-40MAA.

5.1.2.5 Percentages of moisture uptake of TPGS films with MAM and MAA at 20 and 40**%** G were higher than TPNS film; nevertheless, a decreasing trend of moisture uptake was presented for TPGS films with MAM and MAA at 60 and 90**%** G. All TPGS films with MMA exhibited lower percentages of moisture uptake than TPNS film. TPGS-40MAA showed the highest percentage of moisture uptake. The lowest percentage of moisture uptake was found in TPGS-90MMA.

5.1.2.6 WVP values of TPGS films with MAM and MAA at 20 and 40**%** G were higher compared to TPNS film. However, further increase in grafting percentage (60 and 90**%** G) of TPGS films with MAM and MAA showed a decrease in water vapor capacity. In addition, WVP values of TPGS films with MAM were lower than TPGS films with MAA. WVP values of TPGS films with MMA decreased with increasing grafting percentage and showed lower WVP values than TPNS film, TPGS films with MAM and MAA. The minimum WVP value recorded in TPGS-90MMA.

5.1.2.7 Mechanical properties of TPGS film in terms of strain at maximum load or extensibility were clearly enhanced by grafting with all vinyl monomers, but stress at maximum load and Young's modulus was reduced with the increasing grafting percentage. TPGS films with MMA showed the highest strain at maximum load, followed by TPGS films with MAM and MAA. In the present study, TPGS-90MMA exhibited the highest strain at maximum load together with the lowest stress at maximum load and Young's modulus.

5.1.2.8 The results showed that TPNS and all TPGS films showed biodegradability. TPGS films with MAM and MAA at 20 and 40**%** G degraded faster than TPNS film; while, TPGS films grafted with MAM and MAA at 60**%** and 90**%** G

This material is reserved for educational use only, not allowed for commercial use.
Forbidden to modify the content, and cite the document when use.

together with all TPGS films with MMA degraded at a slower rate as compared to TPNS film. In addition, TPGS-40MAA exhibited the quickest biodegradation.

5.1.2.9 Thermal property of TPGS films was improved by grafting with all types of vinyl monomers. TPGS films with MAA showed the greatest improvement in thermal property, followed by TPGS films with MMA and MAM. In addition, TPGS-90MAA illustrated the highest degradation temperatures among TPGS films.

5.1.2.10 Starch modification by graft copolymerization with MAM, MAA and MMA monomers could improve hydrophobicity, flexibility and thermal property of all TPGS films.

5.1.2.11 The best performance of biodegradable starch films was observed in TPGS-90MMA, which exhibited good elongation, high thermal stability together with the lowest hydrophilicity.

5.2 Suggestions

This research investigated improvements in the physicochemical properties of TPNS films by graft copolymerization using different types of vinyl monomers such as MAM, MAA and MMA monomers with different grafting percentages. Prepared TPGS films can be improved and developed as follows:

5.2.1 Further graft copolymerization at longer reaction times such as 7 or 8 hr can be considered to find out the grafting percentage and various properties of MMA-grafted starch such as thermal property.

5.2.2 Blending with fibers such as kapok and cotton fibers, which can increase tensile strength of TPGS films.

5.2.3 Dual modification with various types of GS such as grafted starch-crosslinking can improve the tensile strength of TPGS films.

5.2.4 Blending various types of GS such as blending CL-grafted starch with MMA-grafted starch may improve toughness, which can be considered for further wide-ranging applications of TPGS film.

This material is reserved for educational use only, not allowed for commercial use.
Forbidden to modify the content, and cite the document when use.

References

[1] Potts, I.E. Clrndinning, R.A. Ackart, W.B. and Neigisch, W.D. 1973. **Polymer and Ecological Problem.** New York : Plenum press.

[2] Kwpp, L.R. and jewel, W.J. 1992. "Biodegradability of Modified Plastic Films in Controlled Biological Environment." *Environmental Science and Technology*. 26(1) : 193-198.

[3] Janssen, L. and Moscicki, L. 2009. **Thermoplastic Starch: A Green Material for Various Industries**. New York : John Wiley and Sons.

[4] Bemiller, J.N. and Whistler, R.L. 2009. **Starch: Chemistry and Technology**. Amsterdam : Elsevier Academic Press.

[5] Rutenberg, M. and Solarek, D. 1984. "Starch Derivatives: Production and Uses." 324–328. in Whistler, R.L. Bemiller, J.N. and Paschell, E.F. **Starch: Chemistry and Technology**. Amsterdam : Elsevier Academic Press.

[6] Wu, M. Wang, J. Ge, Q. Yu, H. and Xiong, Y.L. 2018. "Rheology and Microstructure of Myofibrillar Protein–Starch Composite Gels: Comparison of Native and Modified Starches." *International Journal of Biological Macromolecules*. 118 : 988-996.

[7] Tomasik, P. and Schilling, C.H. 2004. **Advances in Carbohydrate Chemistry and Biochemistry**. Amsterdam : Elsevier Academic Press.

[8] Athawale, V.D. and Lele, V. 2000. "Thermal Studies on Granular Maize Starch and its Graft Copolymers with Vinyl Monomers." *Starch-Stärke*. 52(6-7) : 205–213.

[9] Trimnell, D. Stout, E.I. Doane, W.M. and Russell, C.R. 1977. "Graft Copolymers from Thiolated Starch and Vinyl Monomers." *Journal of Applied Polymer Science*. 21(3) : 655-663.

[10] Umar, A. Sanagi, M.M. Salisu, A. Ibrahim, W.A.W. Karim, K.J.A. and Keyon, A.S.A. 2016. "Preparation and Characterization of Starch Grafted with Methacrylamide Using Ammonium Persulphate Initiator." *Materials Letters*. 185 : 173–176.

[11] Bauer, W. 2002. "Methacrylic Acid and Derivatives" in **Ullmann's Encyclopedia of Industrial Chemistry**. Weinheim : Wiley-VCH.

This material is reserved for educational use only, not allowed for commercial use.
Forbidden to modify the content, and cite the document when use.

[12] Timothy, K. Jensen, J. and Mary, E. 2002. "Cardiovascular Effects of Poly(Methyl Methacrylate) Use in Percutaneous Vertebroplasty." *American Journal of Neuroradiology*. 23(4) : 601–604.

[13] Jyothi, A. N. 2010. "Starch Graft Copolymers: Novel Applications in Industry." *Composite Interfaces*. 17(2-3) : 165–174.

[14] Celik, M. 2006. "Preparation and Characterization of Starch-g-Polymethacrylamide Copolymers." *Journal of Polymer Research*. 13(5) : 427–432.

[15] Pathania, D. and Sharma, R. 2012. "Synthesis and Characterization of Graft Copolymers of Methacrylic Acid onto Gelatinized Potato Starch Using Chromic Acid Initiator in Presence of Air." *Advanced Material Letter*. 3 : 136-142.

[16] Celik, M. and Sacak, M. 2002. "Synthesis and Characterization of Starch-Poly(Methyl Methacrylate) Graft Copolymers." *Journal of Applied Polymer Science*. 86(1) : 53-57.

[17] Li, M.C. Lee, J.K. and Cho, U.R. 2012. "Synthesis, Characterization, and Enzymatic Degradation of Starch-Grafted Poly(Methyl Methacrylate) Copolymer Films." *Journal of Applied Polymer Science*. 125(1) : 405–414.

[18] Aurelio, R.H. Alejandro, A.S. José, L.M.M. Gerardo, G.G.G, Héctor, H.M. Eduardo, B. and Acevedo, C.C. 2018. "Clusters of Starch-g-PCL and Their Effect on The Physicochemical Properties of Films." *Starch-Starke*. 70(1-2) : 1700135

[19] Cuevas-Carballo, Z.B. Duarte-Aranda, S. and Canché-Escamilla, G. 2017. "Properties and Biodegradability of Thermoplastic Starch Obtained from Granular Starches Grafted with Polycaprolactone." *International Journal of Polymer Science*. 2017 : 3975692.

[20] Sakar, S. Ojha, K.M. Sankar, S. and Sastry, T.P. 2015. "Preparation and Partial Characterization of Sago Starch Based Graft Co-Polymers." *International Journal of Pharmacognosy and Phytochemical Research.* 4(2) : 385-395.

[21] Canché-Escamilla, G. Canché-Canché, M. Duarte-Aranda, S. Cáceres-Farfán, M. and Borges-Argáez, R. 2011. "Mechanical Properties and Biodegradation of Thermoplastic Starches Obtained from Grafted Starches with Acrylics." *Carbohydrate Polymers.* 86 : 1501– 1508.

This material is reserved for educational use only, not allowed for commercial use.
Forbidden to modify the content, and cite the document when use.

[22] Elias, H. G. 1997. **An Introduction to Polymer Science.** Weinheim **:** VCH publishing.

[23] Whistler, R.L. and Paschall, E.F. 1984. **Starch Chemistry and Technology**. 2nd ed. New York : Elsevier Academic Press.

[24] Anne, A. 2011. "An Overview of Degradable and Biodegradable Polyolefins." *Progress in Polymer Science*. 36(8) : 1015–1049.

[25] Song, J. H. and Coles, R. 2011. "Bioplastics." in Coles, R. and Kirwan, R. **Food and Beverage Packaging Technology**. 2nd ed. Hoboken : Blackwell Publishing.

[26] Brautlecht, C.A. 1953**. Starch Its Sources, Production and Uses.** New York : Reinhold Publishing.

[27] Cogan, T.M. 1992. "Starch." 2418-2421. in Hui, Y.H. **Encyclopedia of Food Science and Technology**. New York : John Wiley and Sons.

[28] Jane, J. L. Kasemsuwan, T. Leas, S. Zobel, H. and Robyt, J. F. 1994. "Anthology of Starch Granule Morphology by Scanning Electron Microscopy." *Starch-Stärke*. 46(4) : 121-129.

[29] Buleon, A. Colonna, P. Planchot, V. and Ball, S. 1998. "Starch Granules: Structure and Biosynthesis." *International Journal of Biological Macromolecules*. 23 : 85–112.

[30] Swinkles, J.J.M. 1985. "Source of Starch, Its Chemistry and Physics." 1-45. in Beynum, G.M.A. and Roles, J.A. **Starch Conversion Technology**. New York : Marcel Dekker.

[31] Schirmer, M. Jekle, M. and Becker, T. 2015. "Starch Gelatinization and Its Complexity for Analysis." *Starch-Starke*. 67(1-2) : 30-41.

[32] Xu, J. Fan, X. Ning, Y. Wang, P. Jin, Z. Lu, H. Xu, B. and Xu, X. 2013. "Effect of Spring Dextrin on Retrogradation of Wheat and Corn Starch Gels." *Food Hydrocolloids*. 33(2) : 361-367.

[33] Ayoub, A.S. and Rizvi, S.S.H. 2009. "An Overview on The Technology of Cross-linking of Starch for Nonfood Applications."*Journal of Plastic Film and Sheeting*. 25(1) : 25-45.

[34] Wurzburg, O.B. 1986. **Modified Starches: Properties and Uses**. Boca Raton : CRC Press.

This material is reserved for educational use only, not allowed for commercial use.
Forbidden to modify the content, and cite the document when use.

[35] Kearsley, M.W. and Dziedzic, S.Z. 1995. **Handbook of Starch Hydrolysis Products and their derivatives.** New York : Springer.

[36] Odian, G. 1983**. Principle of Polymerization**. 2nd ed. New York : McGraw-Hill.

[37] Kumar, D. Pandey, J. Raj, V. and Kumar, P. 2017. "A Review on The Modification of Polysaccharide Through Graft Copolymerization for Various Potential Applications." *The Open Medicinal Chemistry Journal*. 11 : 109-126.

[38] Carenza, M. 1992. "Recent Achievements in The Use of Radiation Polymerization and Grafting for Biomedical Applications." *International Journal of Radiation Applications and Instrumentation. Part C. Radiation Physics and Chemistry*. 39 : 485-493.

[39] Dretfuss, P. and Quirk. R.P. Graft Copolymers. 551-579. In Mark, H.F. **Encyclopedia of polymer science and engineering**. New York : John Wiley and Sons.

[40] Macrae, R. Robinson, R.K. and Sadler, M.J. 1993. "Cassava." 734-742. in **Encyclopedia of Food Science, Food Technology and Nutrition. Vol. 1**. New York : Acadamic Press Harcout Brace Jovanovich Publisher.

[41] Jarowenko, W. 1970. "Starch." 819-820. in Mark H.F. and Gayford, N.G. **Encyclopedia of Polymer Science and Technology**. New York : John Wiley and Sons.

[42] Stagner, J. Alves, V.D. Narayan, R. and Beleia, A. 2011. "Thermoplasticization of High Amylose Starch by Chemical Modification Using Reactive Extrusion." *Journal of Polymer and The Environment*. 19 : 589–597.

[43] Clayton, G.D. and Clayton, F.E. 1981. **Patty's Industrial Hygiene and Toxicology; Vol 2A**. 3rd ed. New York : John Wiley and Sons.

[44] Search by Catalog Number: [Online].

Available : http://www.labchem.com/tools/msds/index.php?all=true

[45] Mahboub, M.J.D. Dubois, J.L. Cavani, F. Rostamizadeh, M. and Patience, G.S. 2018. "Catalysis for The Synthesis of Methacrylic Acid and Methyl Methacrylate." *Chemical Society Reviews.* 20 : 7703-7738.

[46] Koichi, N. 2001. "New Developments in The Production of Methyl Methacrylate." *Applied Catalysis A: General.* 221 : 367–377.

This material is reserved for educational use only, not allowed for commercial use.
Forbidden to modify the content, and cite the document when use.

[47] Georg, B. 1963. **Handbook of Preparative Inorganic Chemistry**. 2nd ed. Amsterdam : Elsevier Academic Press.

[48] Chen, Q. Yu, H. Wang, L. Abdin, Z. Chen, Y. Wang, J. Zhou, W. Yang, X. Khan, R. U. Zhang, H. and Chen, X. 2015. "Recent Progress in Chemical Modification of Starch and Its Applications." *RSC Advances*. 5 : 67459–67474.

[49] Doolittle, A. K. 1954. **The Technology of Solvents and Plasticizers**. New York : John Wiley and Sons.

[50] Long, W.S. 1917. "The Composition of Commercial Fruit Extracts". *Transactions of The Kansas Academy of Science.* 28 : 157-161.

[51] Nikolic, V. Velickovic, S. and Popovic, A. 2012. "Amine Activators Influence on Grafting Reaction Between Methacrylic Acid and Starch." *Carbohydrate Polymers*. 88 : 1407–1413.

[52] Mostafa, Kh.M. 1995. "Graft Polymerization of Methacrylic Acid on Starch and Hydrolyzed Starches." *Polymer degradation and stability*. 50(2) : 184-194.

[53] Pimpan, V. and Thothong, P. 2006. "Synthesis of Cassava Starch-g-Poly(methyl methacrylate) Copolymers with Benzoyl Peroxide as An Initiator." *Journal of Applied Polymer Science*. 101(6) : 4083–4089.

[54] Sherma, J. 2008. "Principles of Gel Permeation Chromatography". *Journal of AOAC International*. 91(4) : 113A-118A.

[55] Gutierrez, T.J. Tapia, M.S. Perez, E. and Fama, L. 2015. "Structural and Mechanical Properties of Edible Films Made from Native and Modified Cush-Cush Yam and Cassava Starch." *Food Hydrocolloids*. 45 : 211-217.

[56] Bower, D.I. and Maddams, W.F. 1996**. The Vibrational Spectroscopy of Polymers**, 2nd ed. Cambridge : Cambridge University Press.

[57] Pal, S. Mal, D. and Singh, R. P. 2005. "Cationic Starch: An Effective Flocculating Agent." *Carbohydrate Polymers.* 59 : 417–423.

[58] Chowdhury, P.R. and Kale, K.M. 1970. "The Adiabatic Compressibility of Poly(Acrylic acid) And Polyacrylamide in Aqueous Solution." *Journal of Applied Polymer Science.*14 : 2937-2946.

[59] Athawale, V.D. and Rathi, S.C. 1997. "Role and Relevance of Polarity and Solubility of Vinyl Monomers in Graft Polymerization onto Starch." *Reactive and Functional Polymers.* 34 : 11-17.

This material is reserved for educational use only, not allowed for commercial use.
Forbidden to modify the content, and cite the document when use.

Appendices

This material is reserved for educational use only, not allowed for commercial use.
Forbidden to modify the content, and cite the document when use.

Appendix A

FT-IR study

FT-IR spectra of NS, various GS, TPNS film and various TPGS films

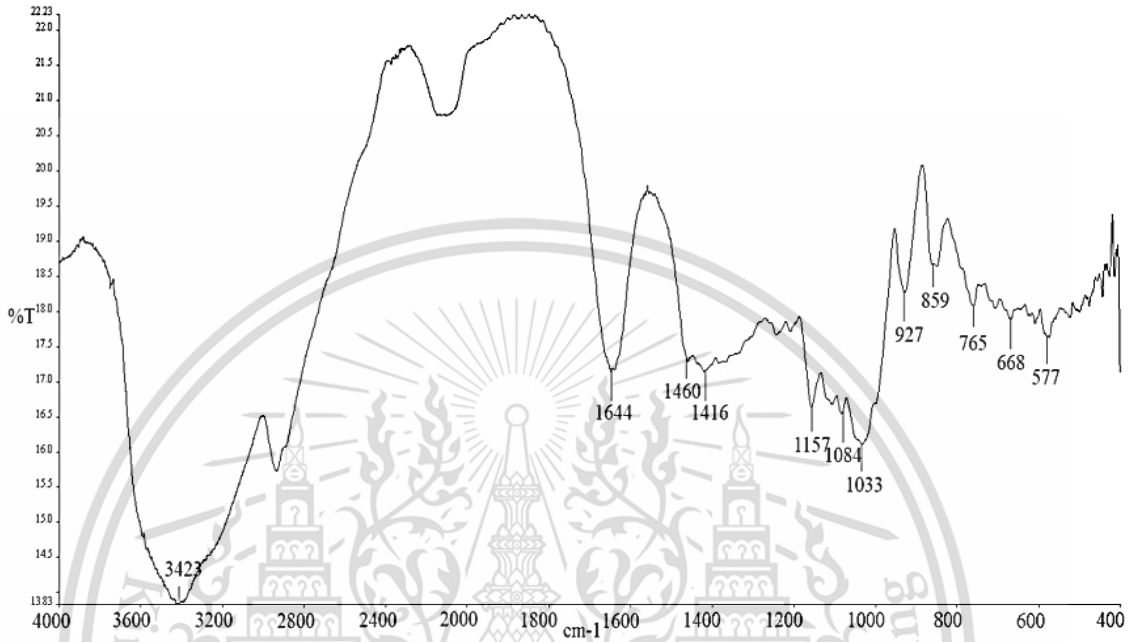

Figure A-1 FT-IR spectrum of NS

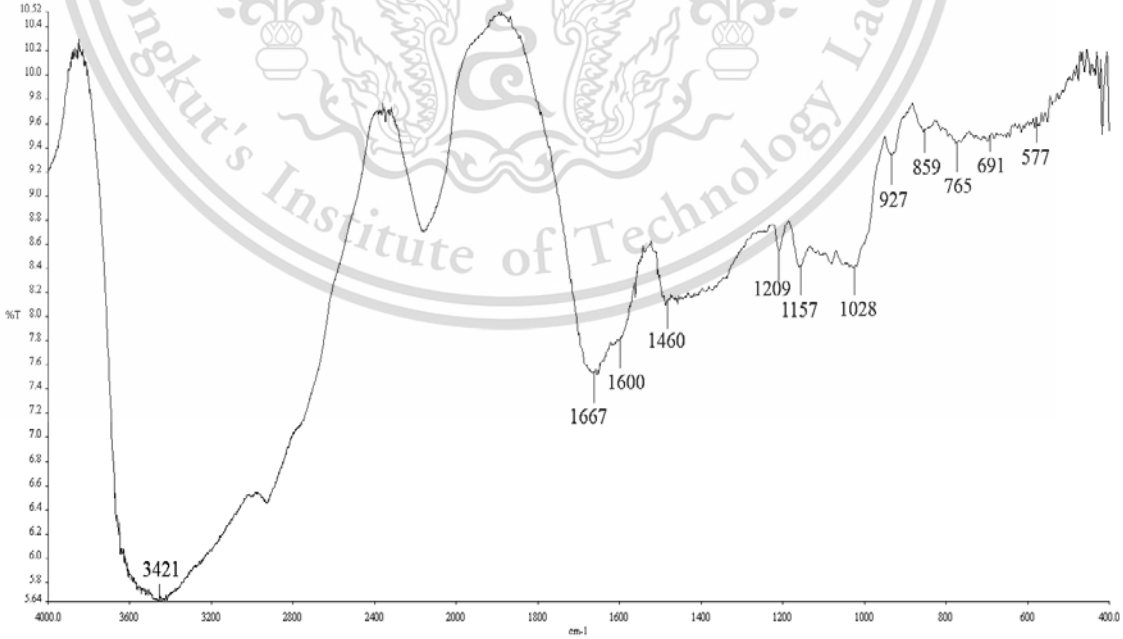

Figure A-2 FT-IR spectrum of GS-20MAM

This material is reserved for educational use only, not allowed for commercial use.
Forbidden to modify the content, and cite the document when use.

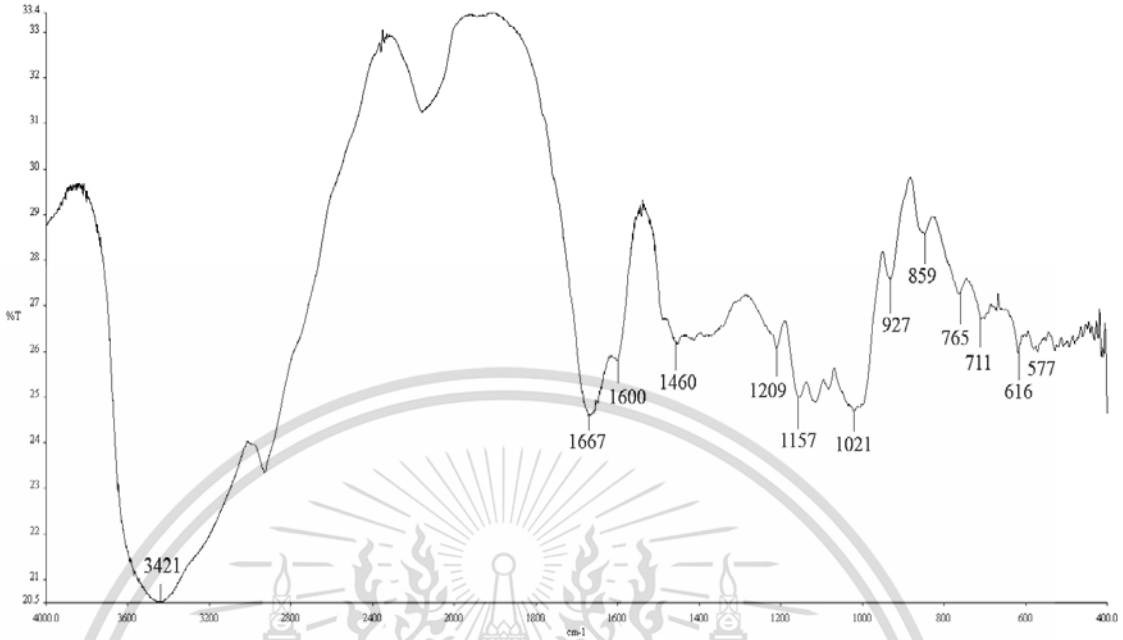

Figure A-3 FT-IR spectrum of GS-40MAM

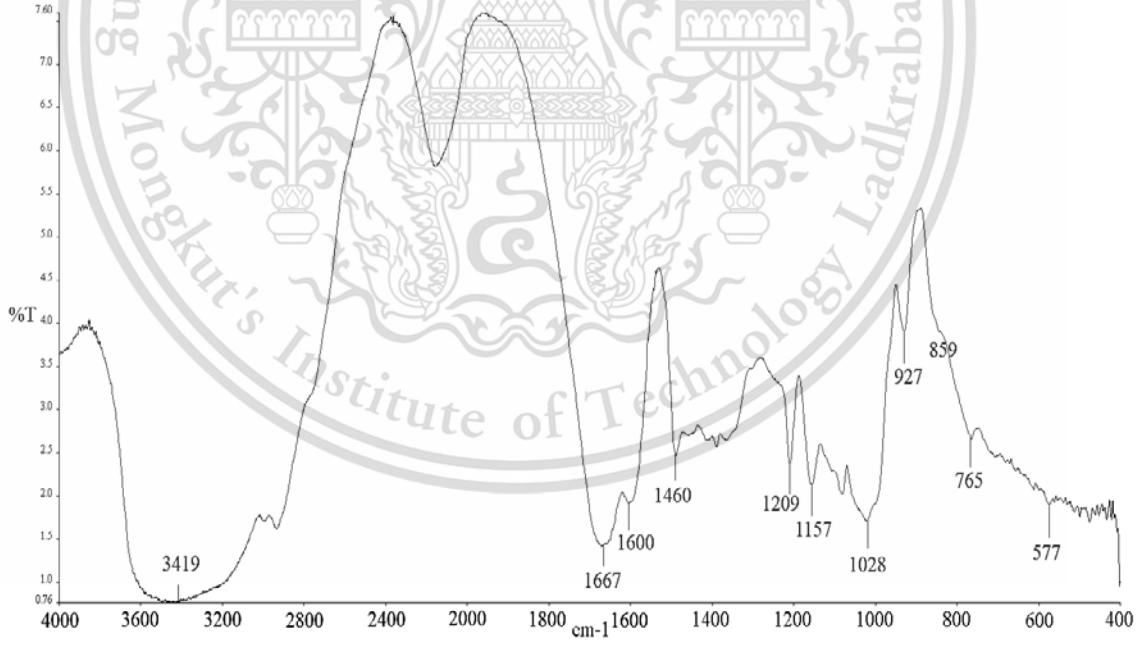

Figure A-4 FT-IR spectrum of GS-60MAM

This material is reserved for educational use only, not allowed for commercial use.
Forbidden to modify the content, and cite the document when use.

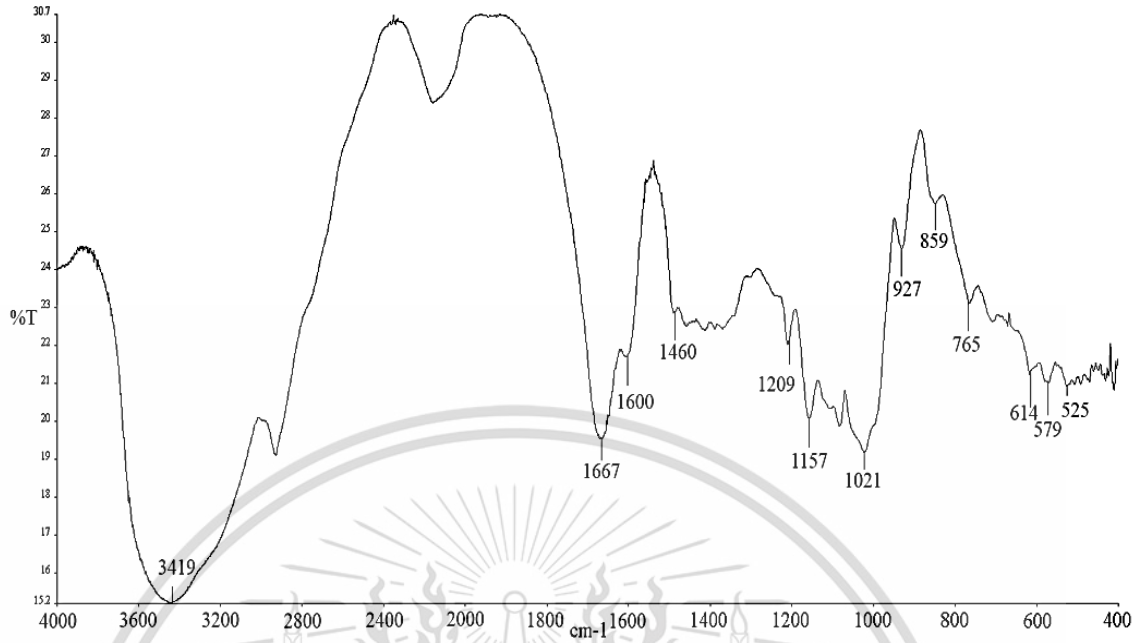

Figure A-5 FT-IR spectrum of GS-90MAM

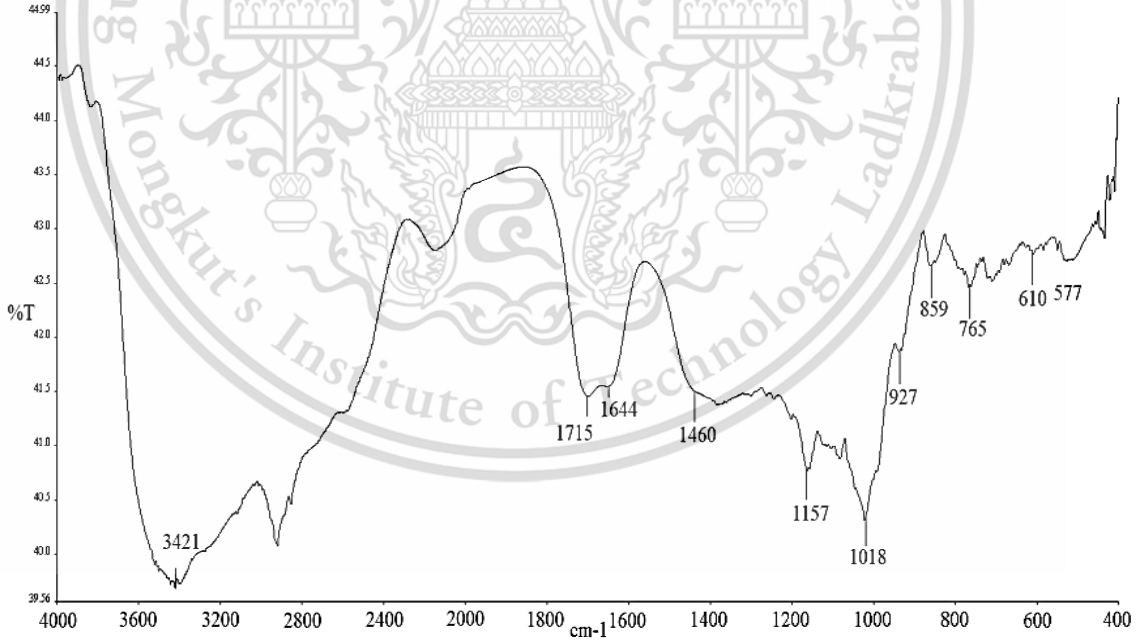

Figure A-6 FT-IR spectrum of GS-20MAA

This material is reserved for educational use only, not allowed for commercial use.
Forbidden to modify the content, and cite the document when use.

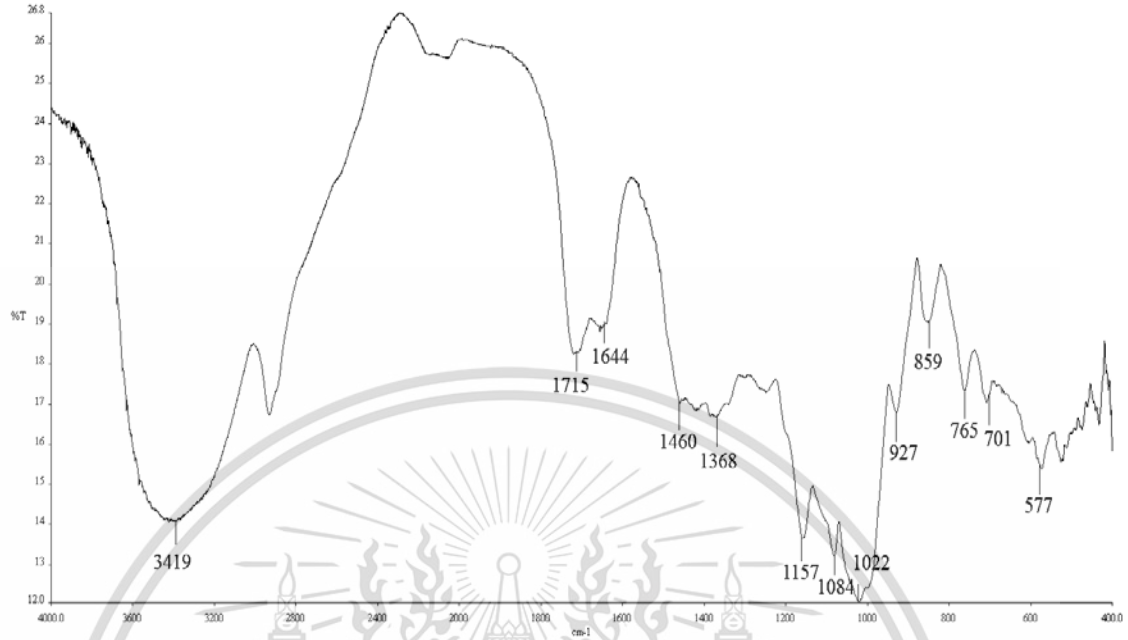

Figure A-7 FT-IR spectrum of GS-40MAA

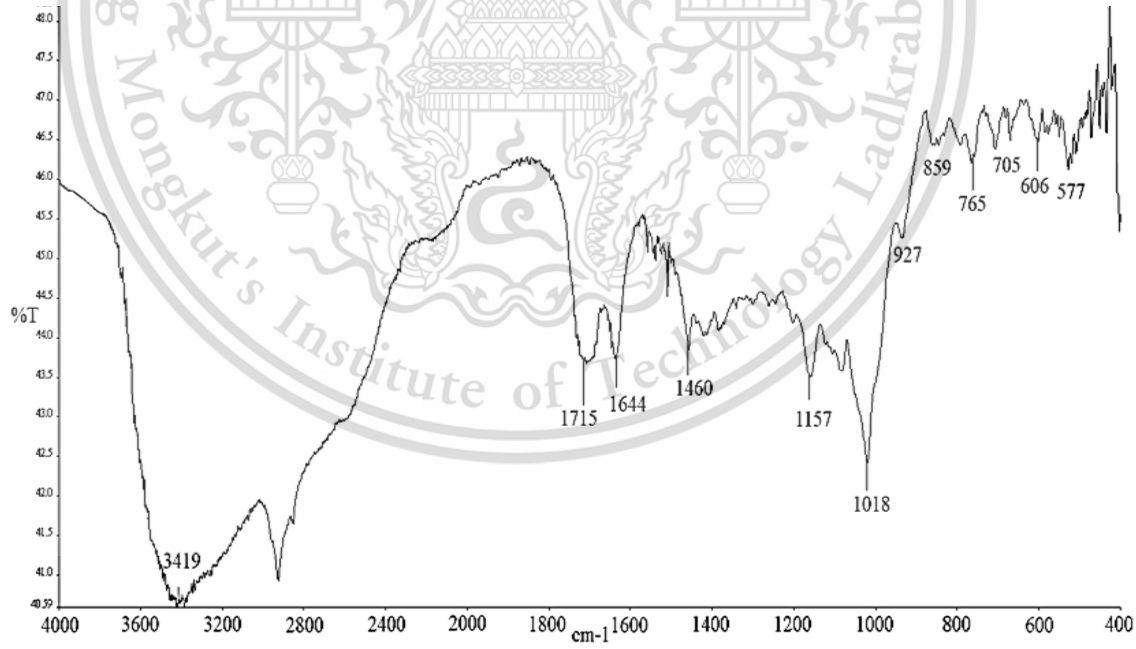

Figure A-8 FT-IR spectrum of GS-60MAA

This material is reserved for educational use only, not allowed for commercial use.
Forbidden to modify the content, and cite the document when use.

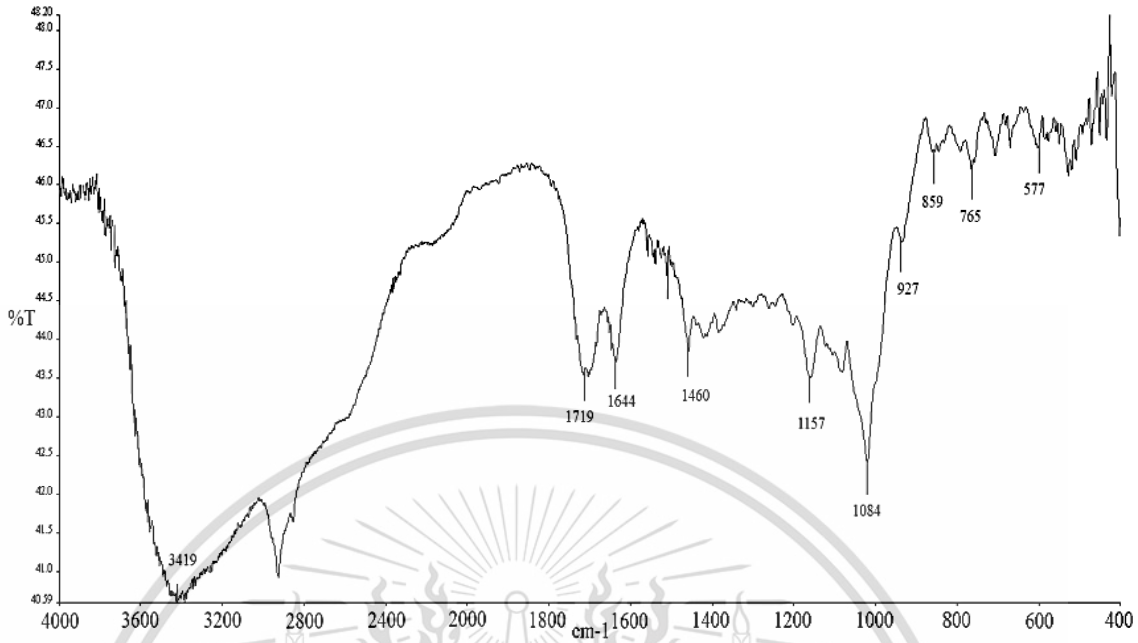

Figure A-9 FT-IR spectrum of GS-90MAA

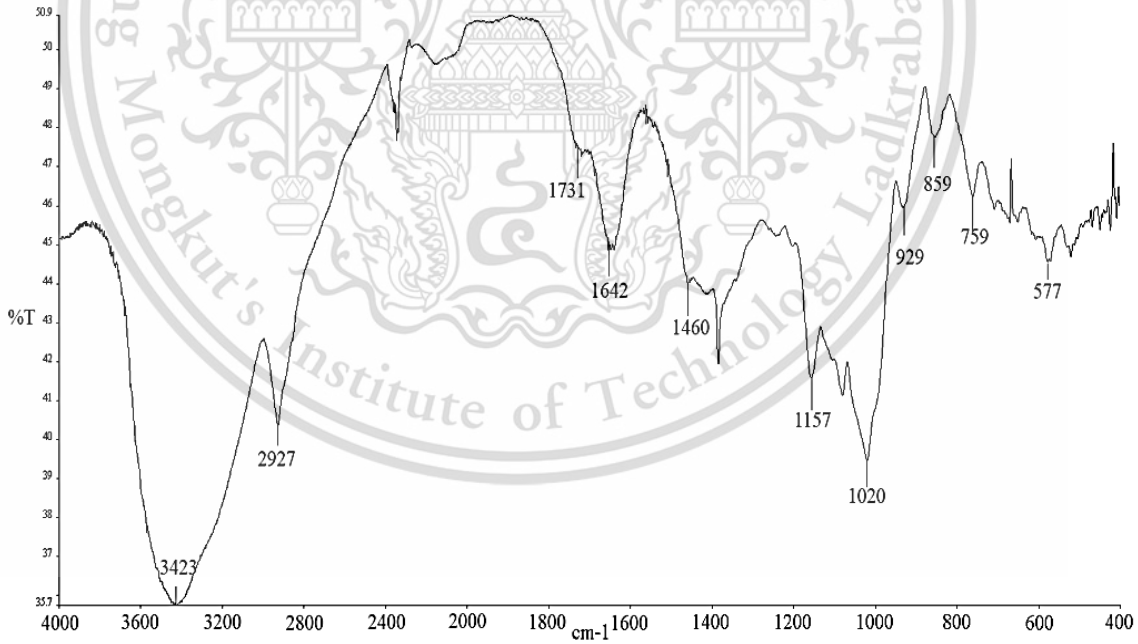

Figure A-10 FT-IR spectrum of GS-20MMA

This material is reserved for educational use only, not allowed for commercial use.
Forbidden to modify the content, and cite the document when use.

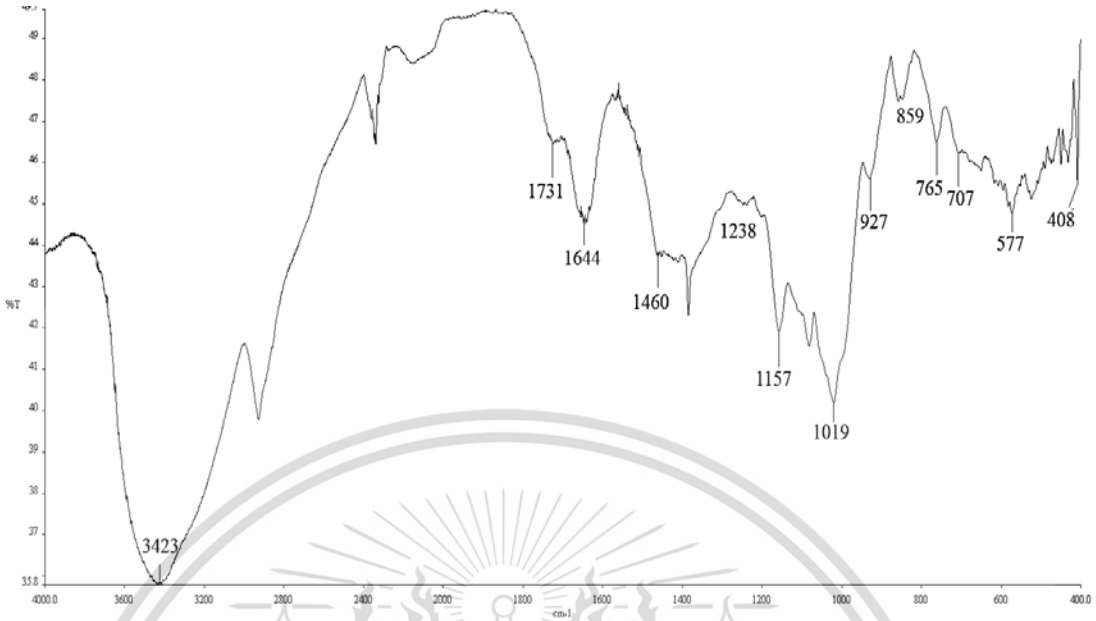

Figure A-11 FT-IR spectrum of GS-40MMA

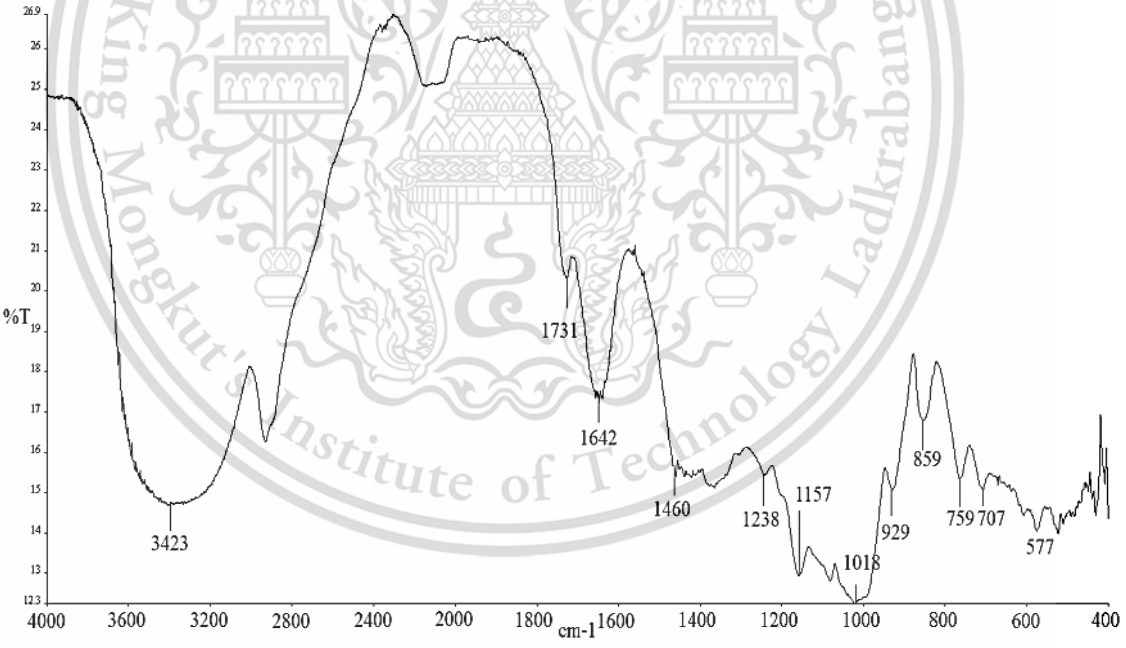

Figure A-12 FT-IR spectrum of GS-60MMA

This material is reserved for educational use only, not allowed for commercial use.
Forbidden to modify the content, and cite the document when use.

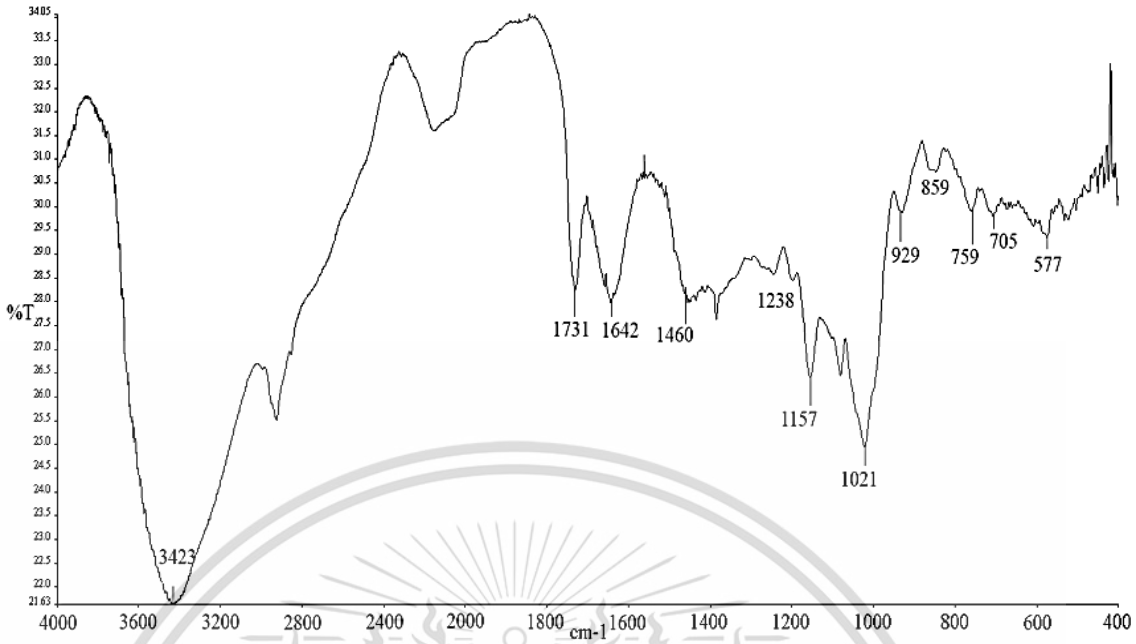

Figure A-13 FT-IR spectrum of GS-90MMA

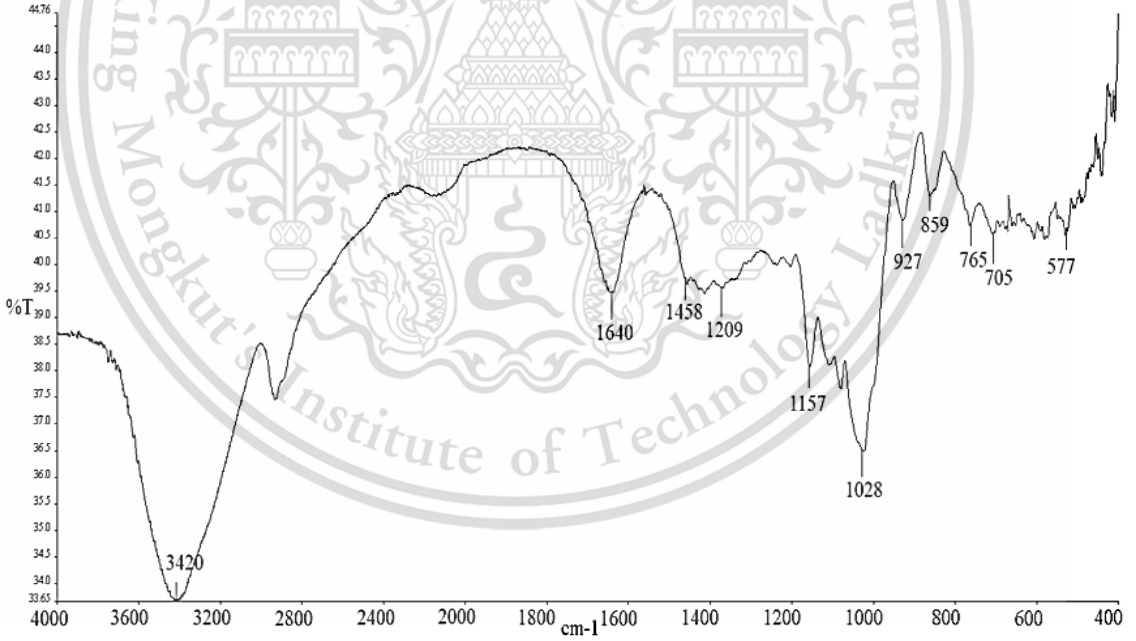

Figure A-14 FT-IR spectrum of TPNS

This material is reserved for educational use only, not allowed for commercial use.
Forbidden to modify the content, and cite the document when use.

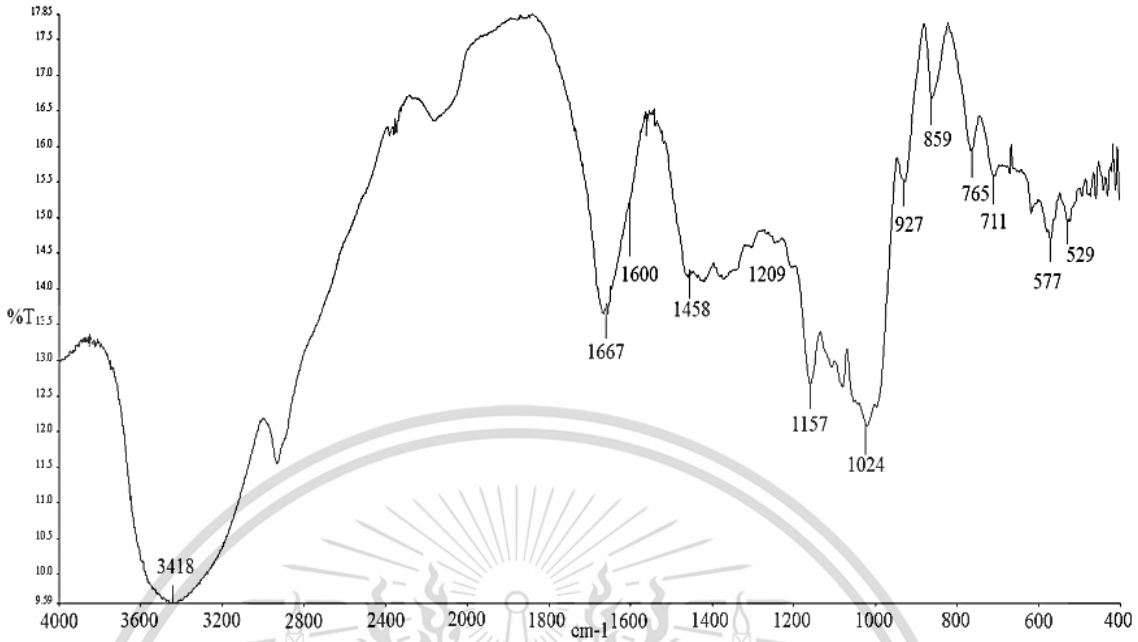

Figure A-15 FT-IR spectrum of TPGS-20MAM

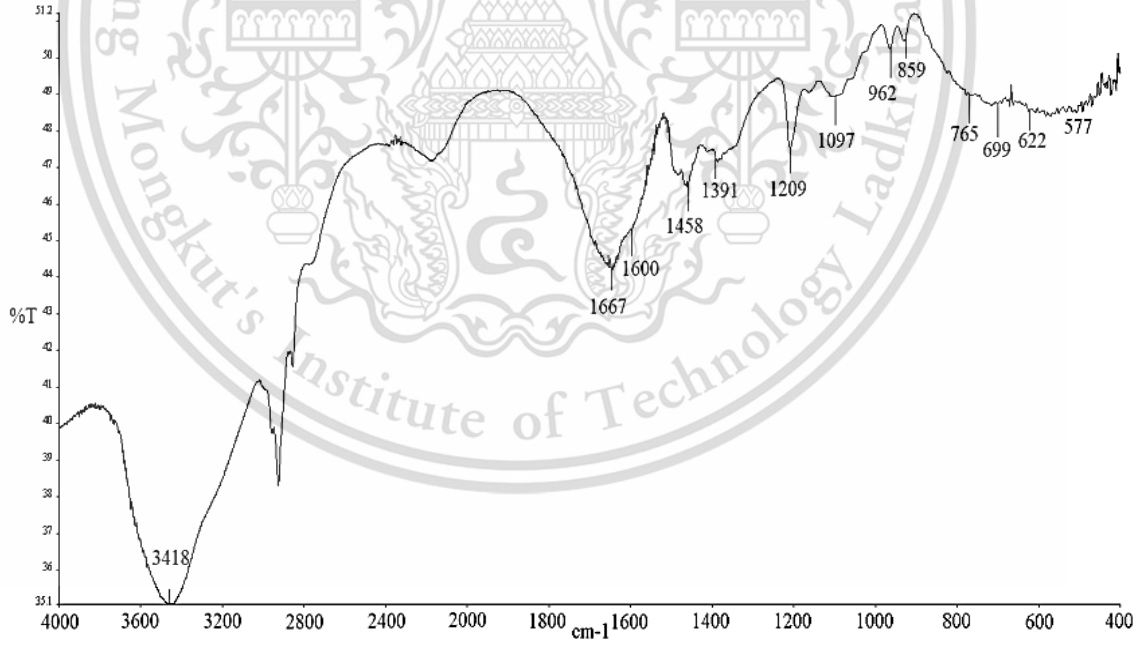

Figure A-16 FT-IR spectrum of TPGS-40MAM

This material is reserved for educational use only, not allowed for commercial use.
Forbidden to modify the content, and cite the document when use.

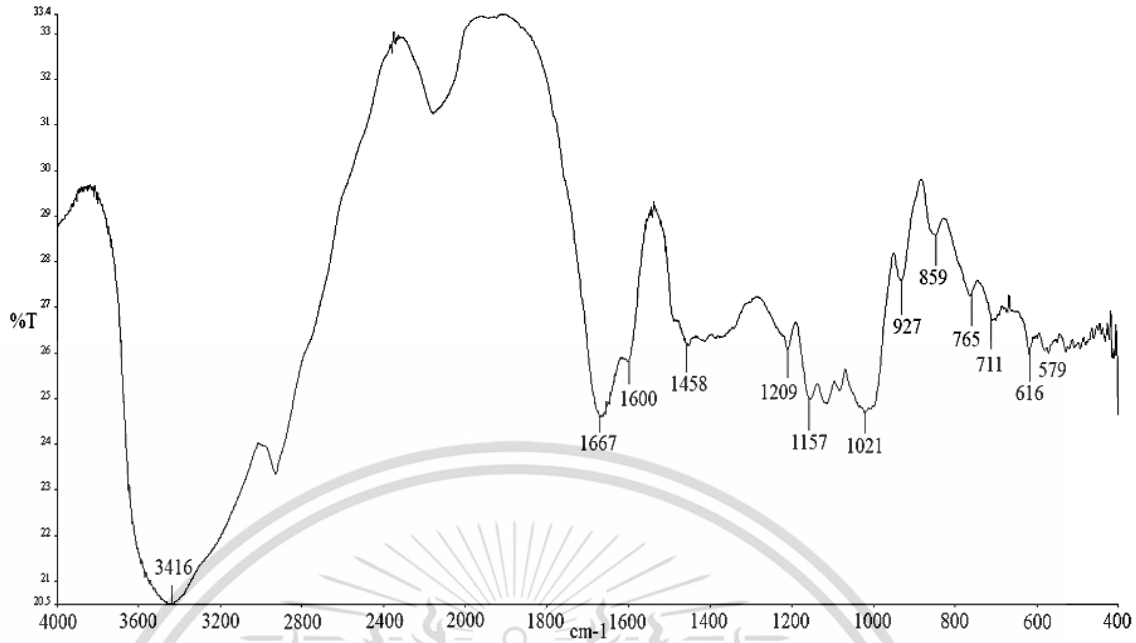

Figure A-17 FT-IR spectrum of TPGS-60MAM

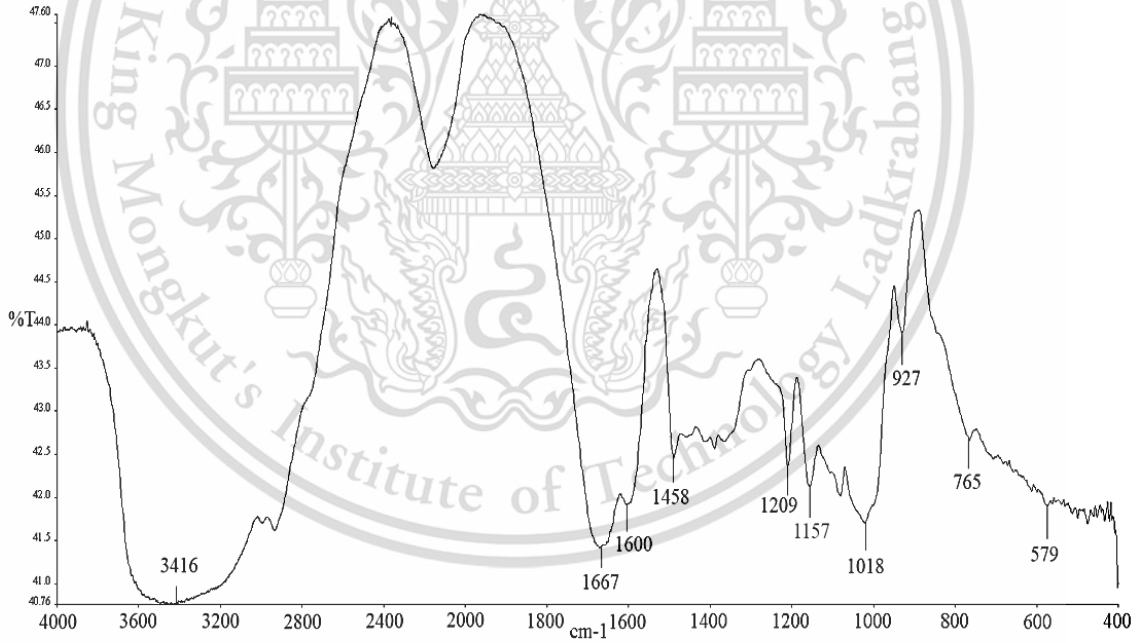

Figure A-18 FT-IR spectrum of TPGS-90MAM

This material is reserved for educational use only, not allowed for commercial use.
Forbidden to modify the content, and cite the document when use.

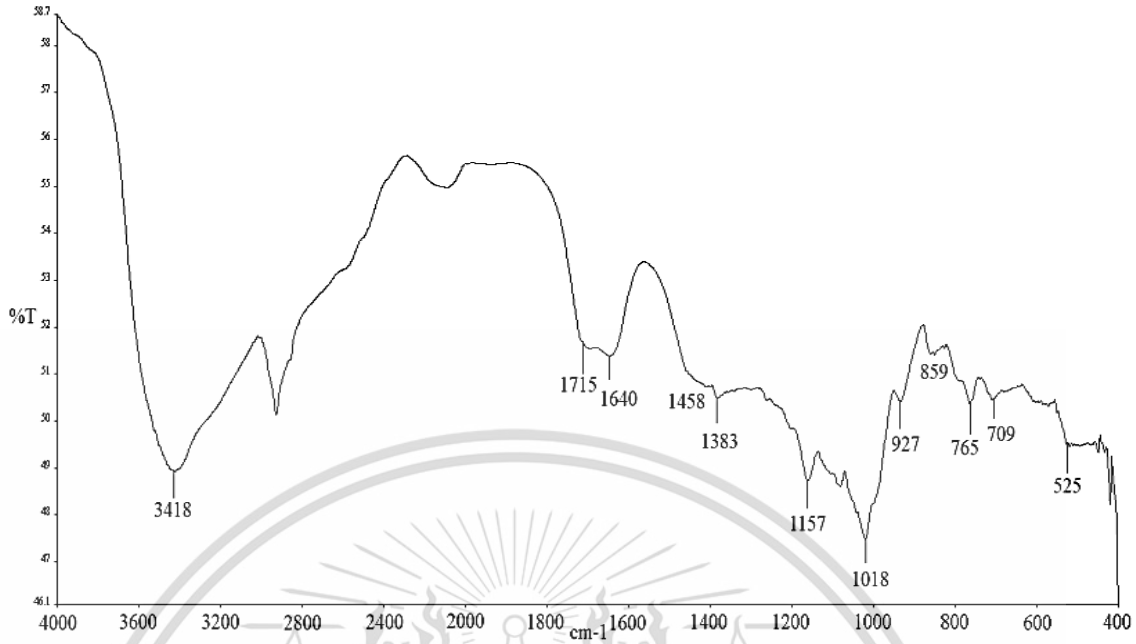

Figure A-19 FT-IR spectrum of TPGS-20MAA

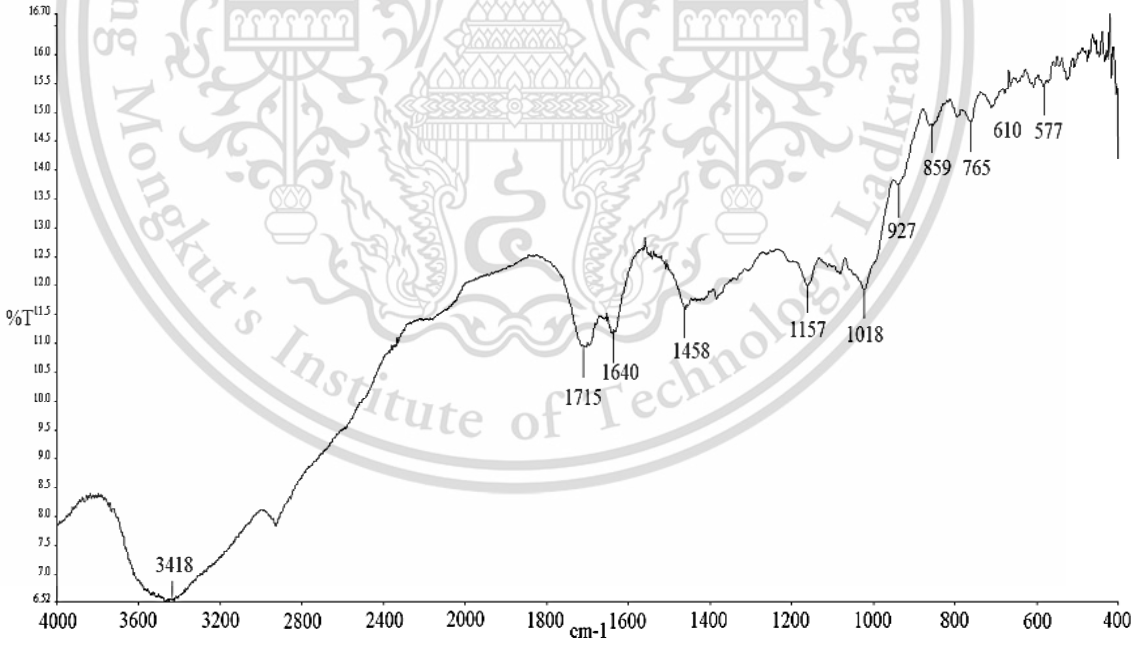

Figure A-20 FT-IR spectrum of TPGS-40MAA

This material is reserved for educational use only, not allowed for commercial use.
Forbidden to modify the content, and cite the document when use.

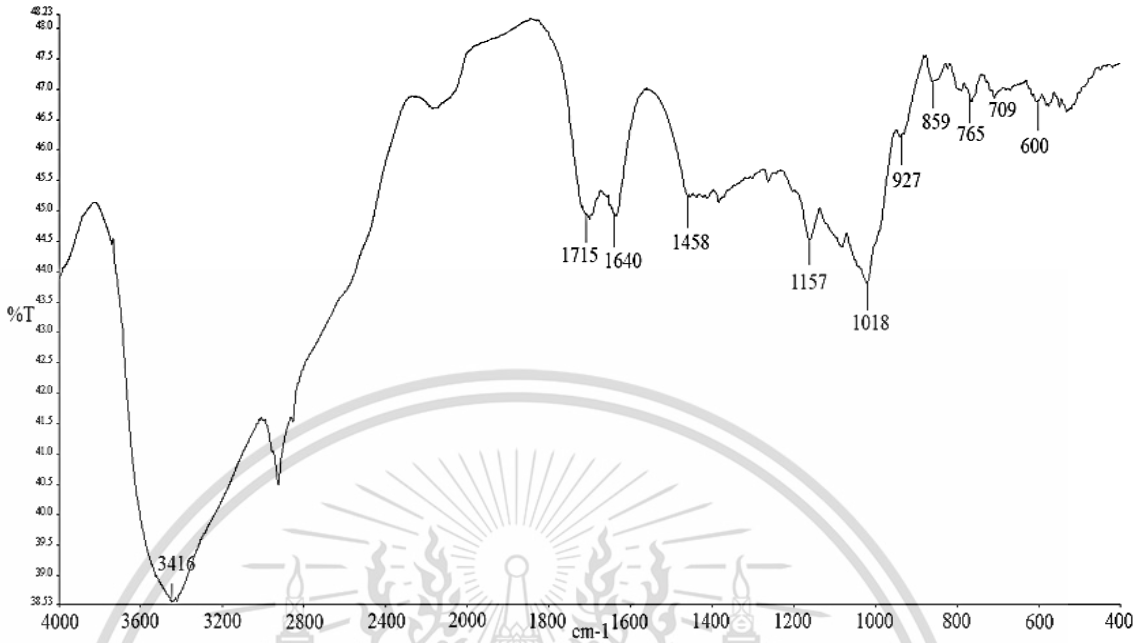

Figure A-21 FT-IR spectrum of TPGS-60MAA

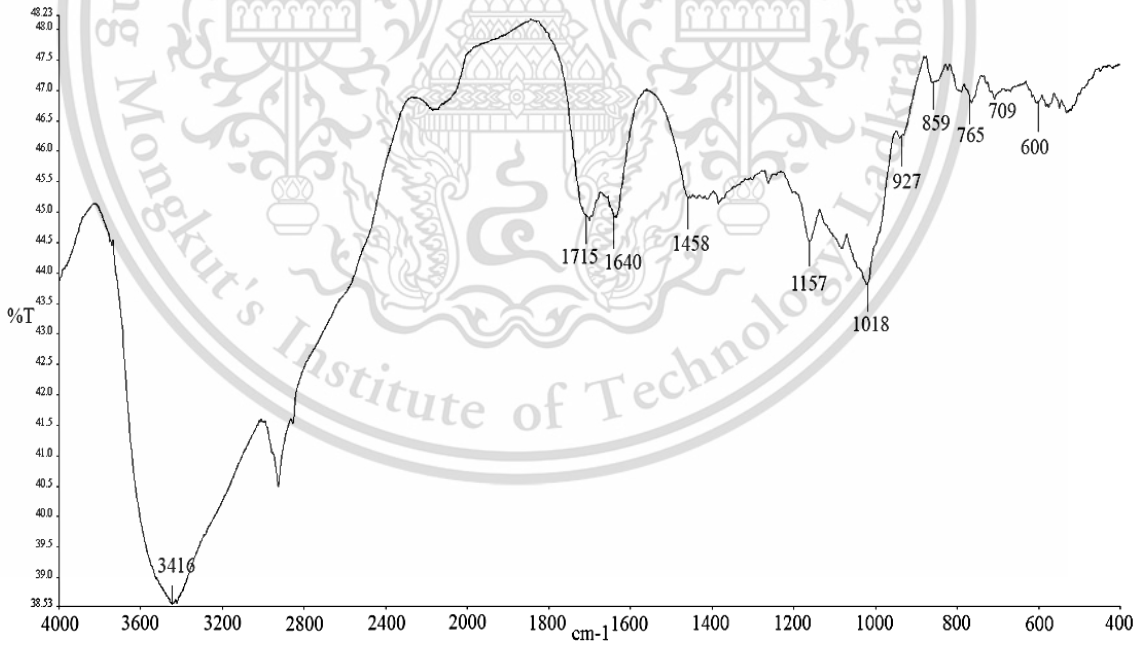

Figure A-22 FT-IR spectrum of TPGS-90MAA

This material is reserved for educational use only, not allowed for commercial use.
Forbidden to modify the content, and cite the document when use.

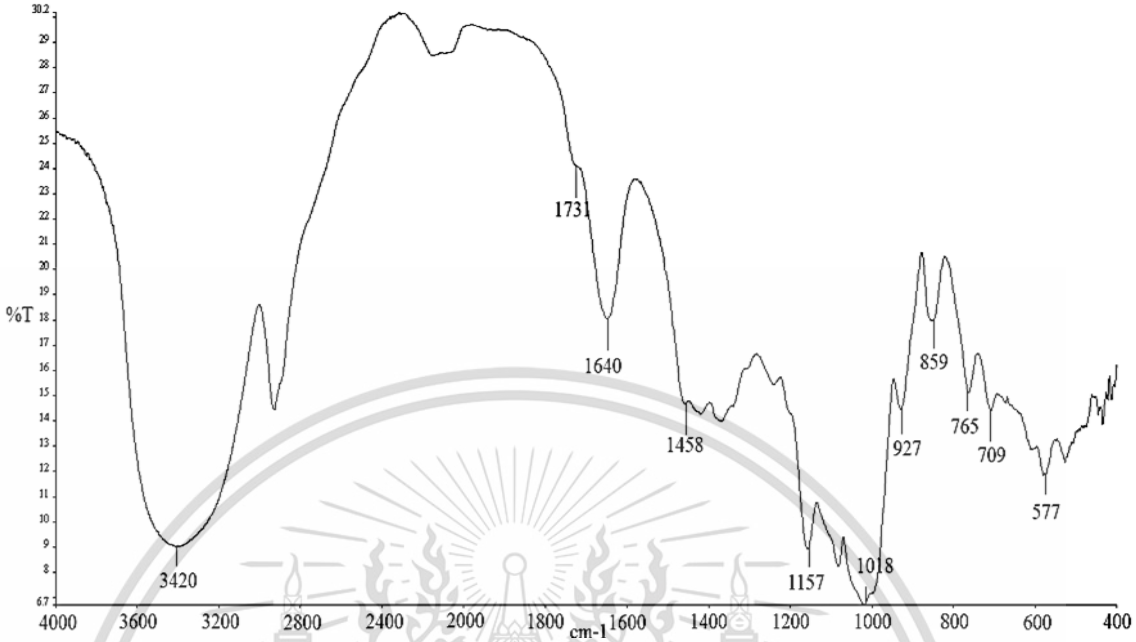

Figure A-23 FT-IR spectrum of TPGS-20MMA

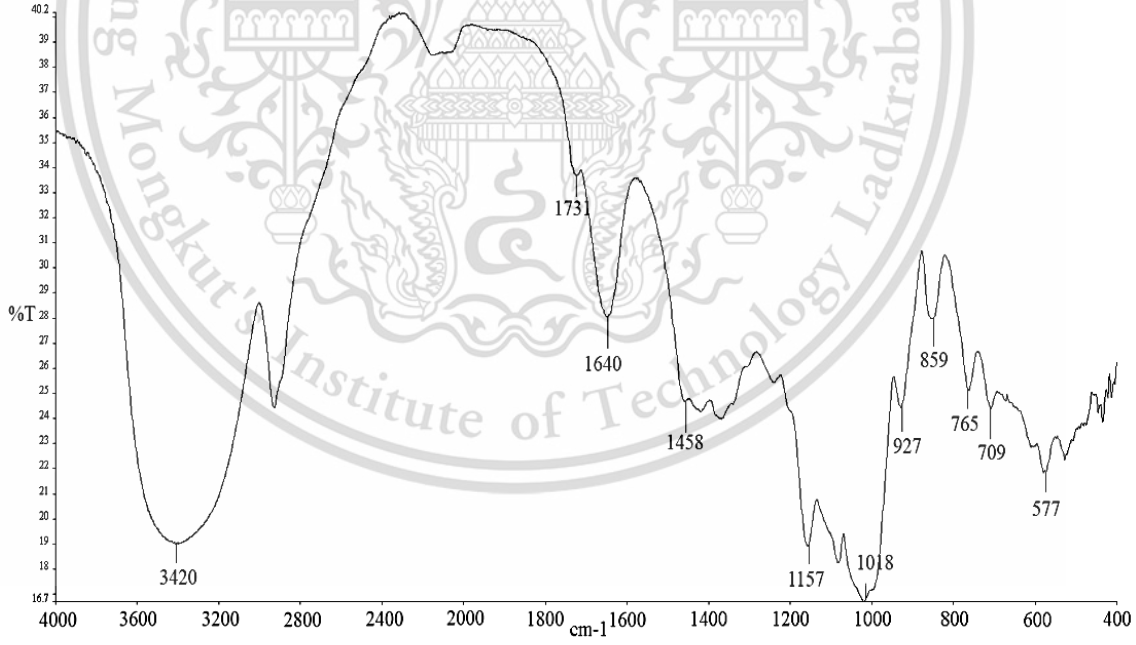

Figure A-24 FT-IR spectrum of TPGS-40MMA

This material is reserved for educational use only, not allowed for commercial use.
Forbidden to modify the content, and cite the document when use.

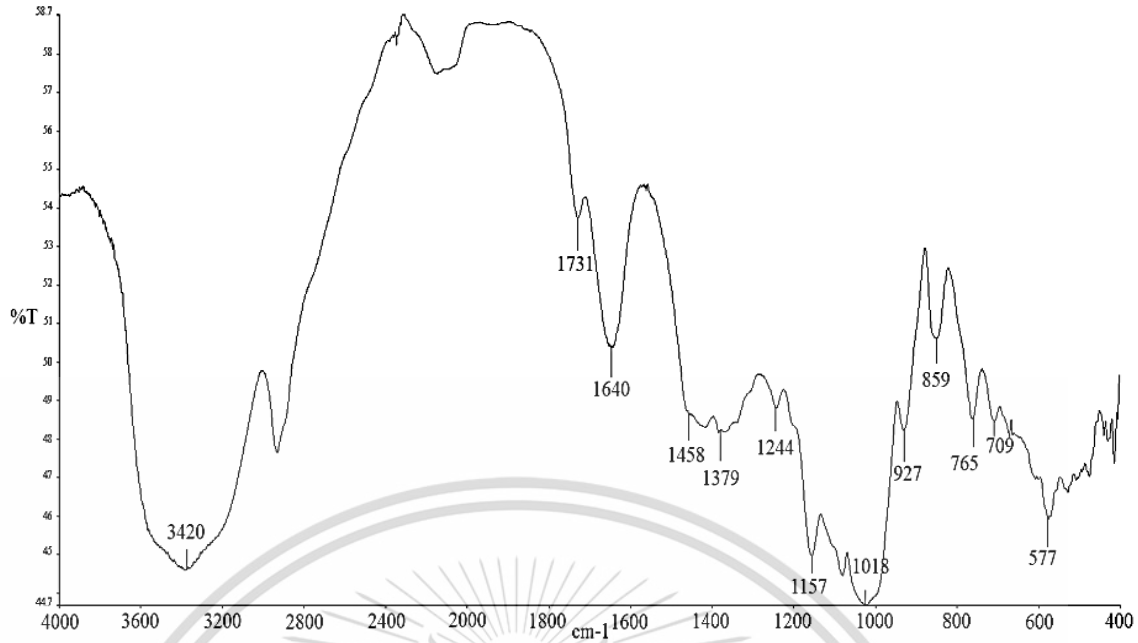

Figure A-25 FT-IR spectrum of TPGS-60MMA

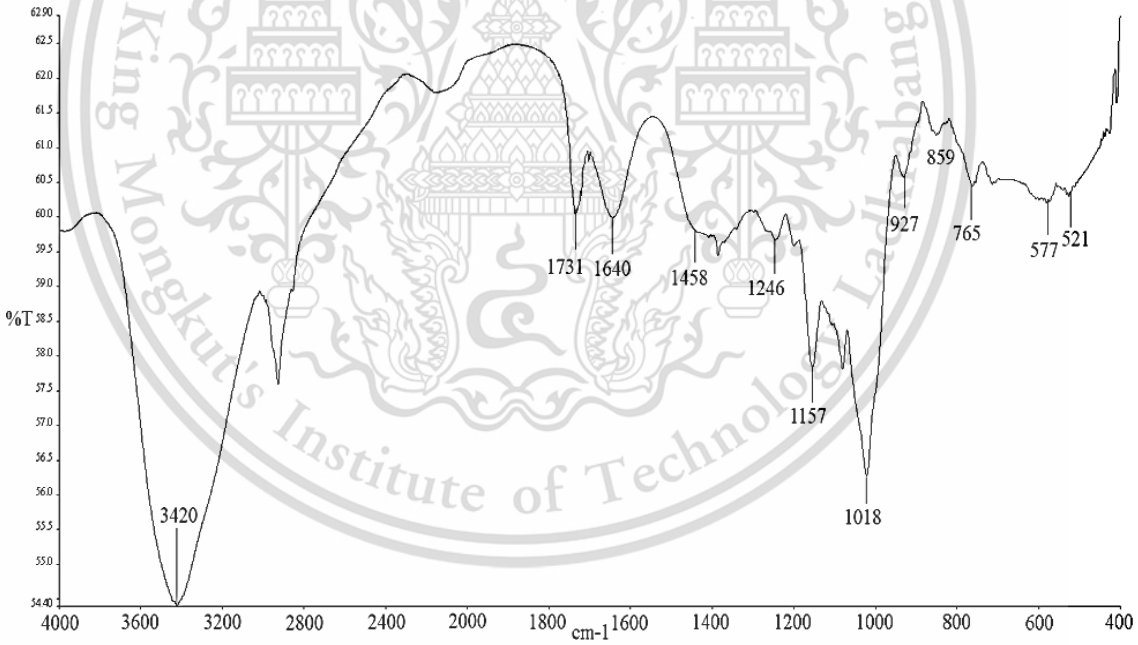

Figure A-26 FT-IR spectrum of TPGS-90MMA

This material is reserved for educational use only, not allowed for commercial use.
Forbidden to modify the content, and cite the document when use.

Appendix B

Thermal property by TGA technique

TGA thermograms of NS, various GS, TPNS film and TPGS films

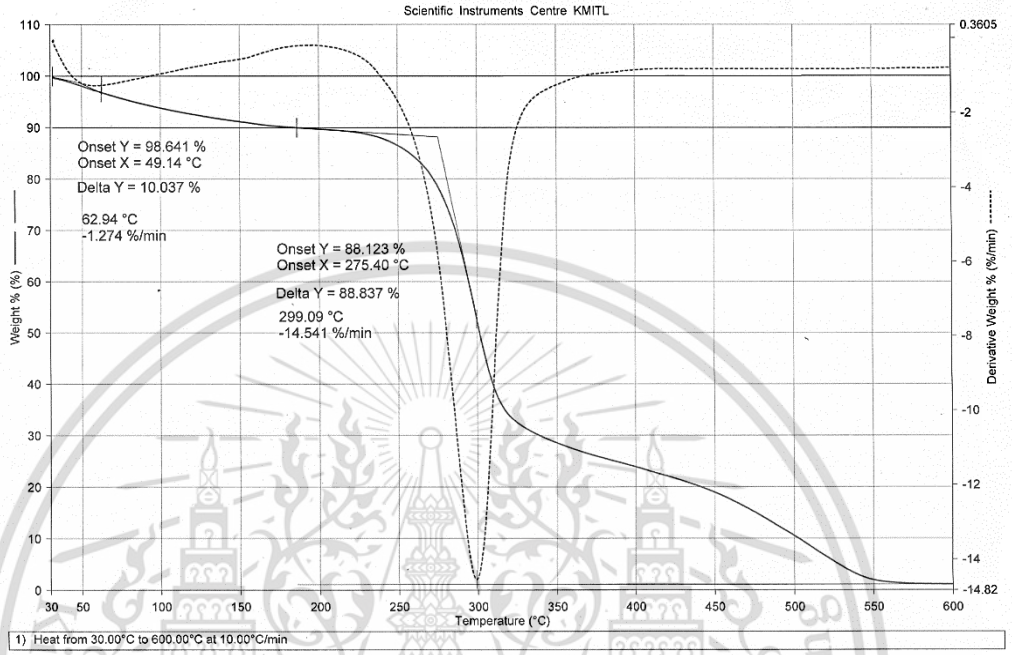

Figure B-1 TGA thermogram of NS

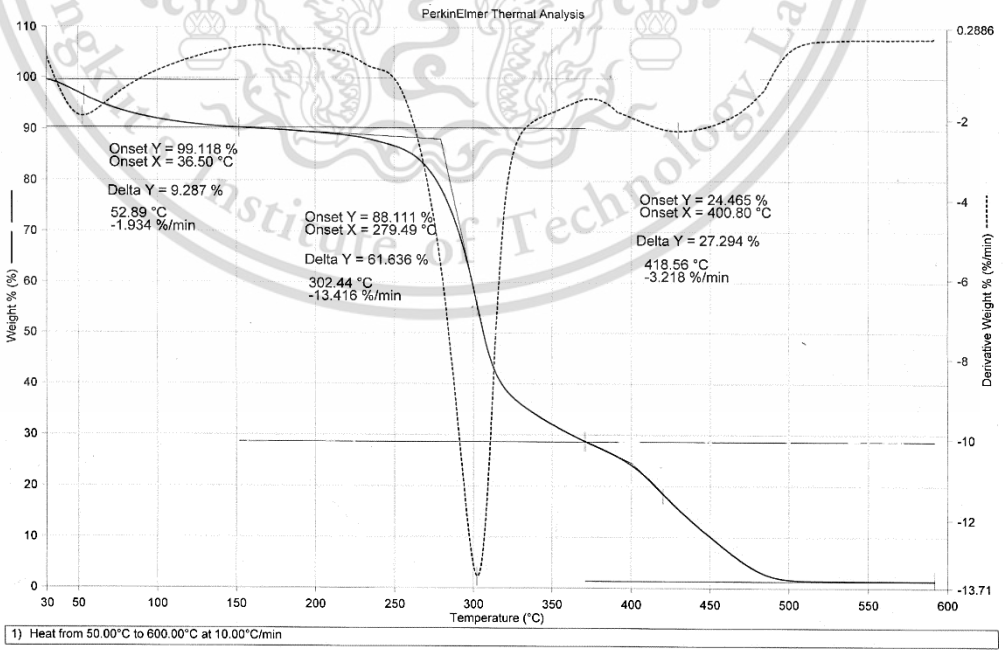

Figure B-2 TGA thermogram of GS-20MAM

This material is reserved for educational use only, not allowed for commercial use.
Forbidden to modify the content, and cite the document when use.

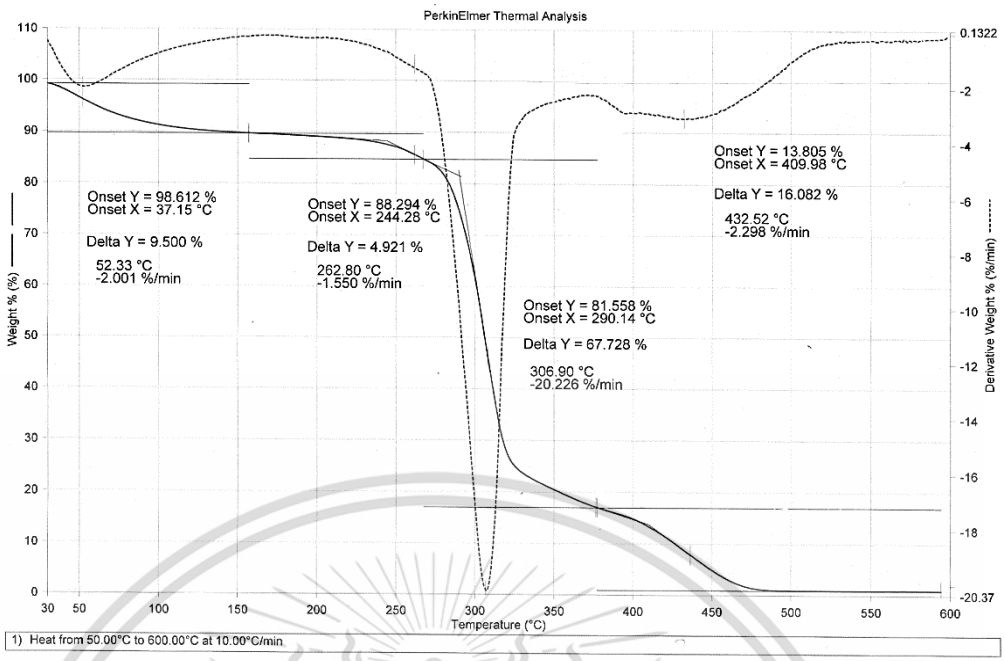

Figure B-3 TGA thermogram of GS-40MAM

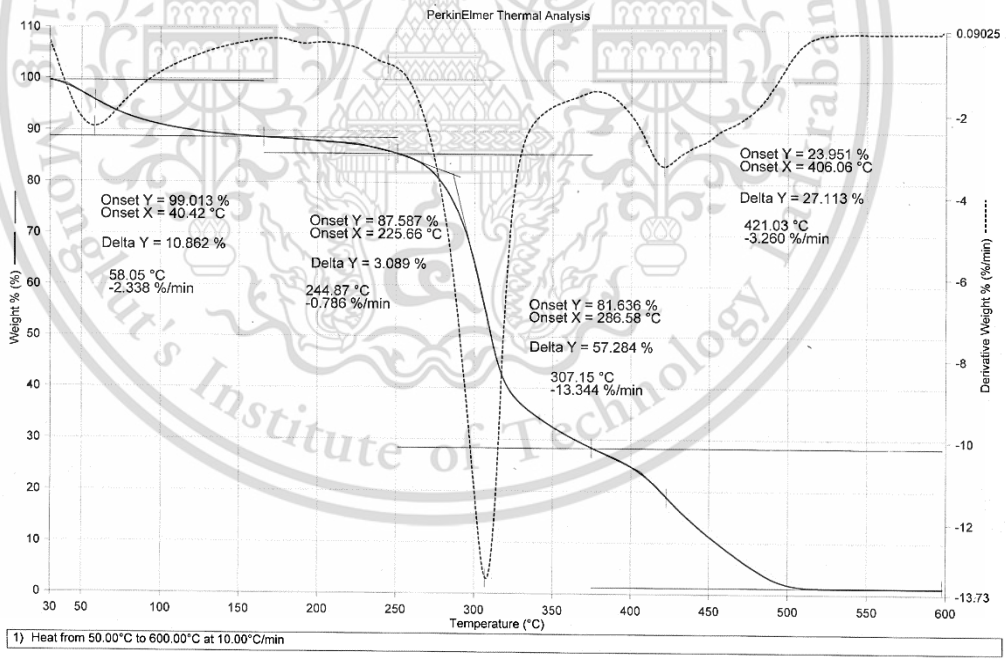

Figure B-4 TGA thermogram of GS-60MAM

This material is reserved for educational use only, not allowed for commercial use.
Forbidden to modify the content, and cite the document when use.

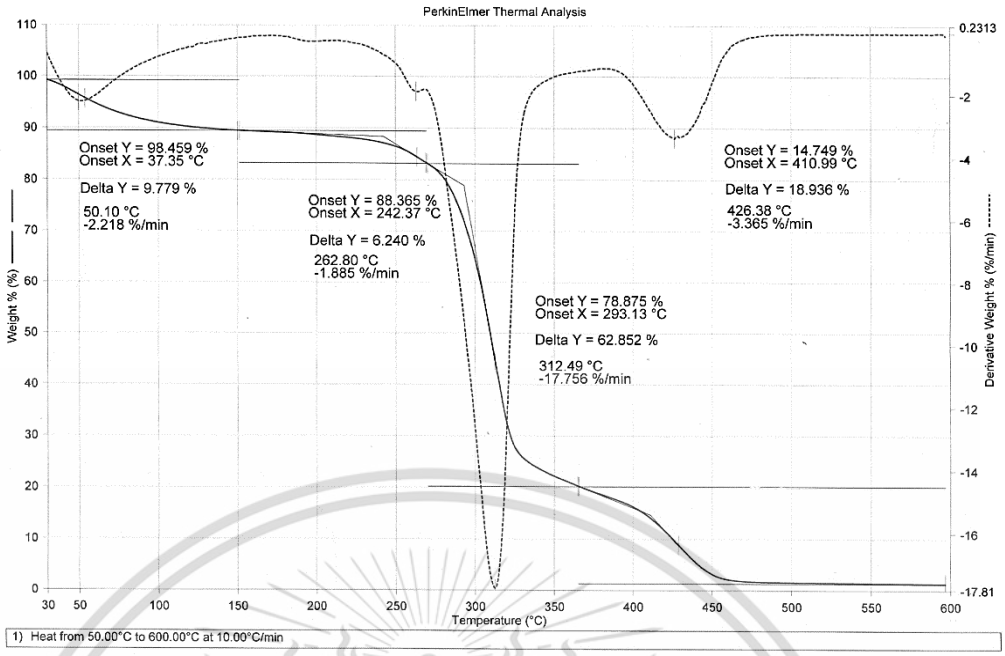

Figure B-5 TGA thermogram of GS-90MAM

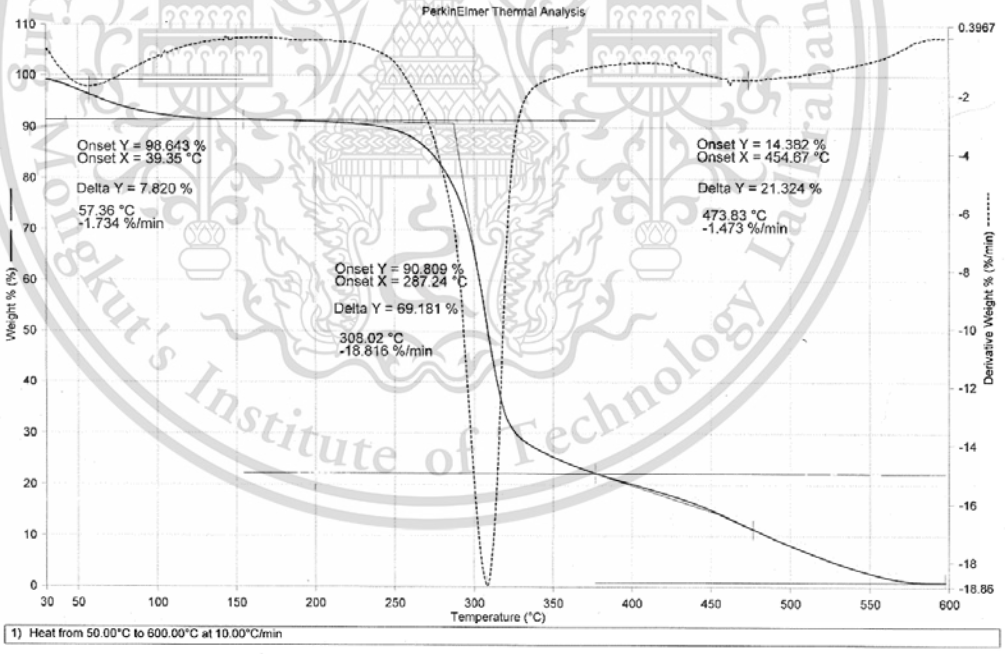

Figure B-6 TGA thermogram of GS-20MAA

This material is reserved for educational use only, not allowed for commercial use.
Forbidden to modify the content, and cite the document when use.

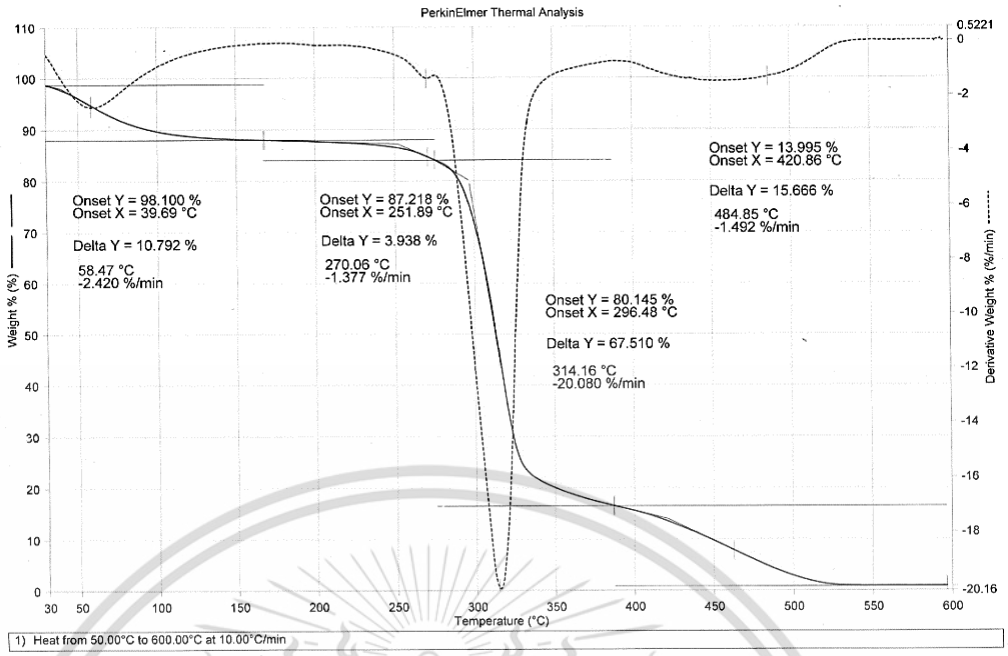

Figure B-7 TGA thermogram of GS-40MAA

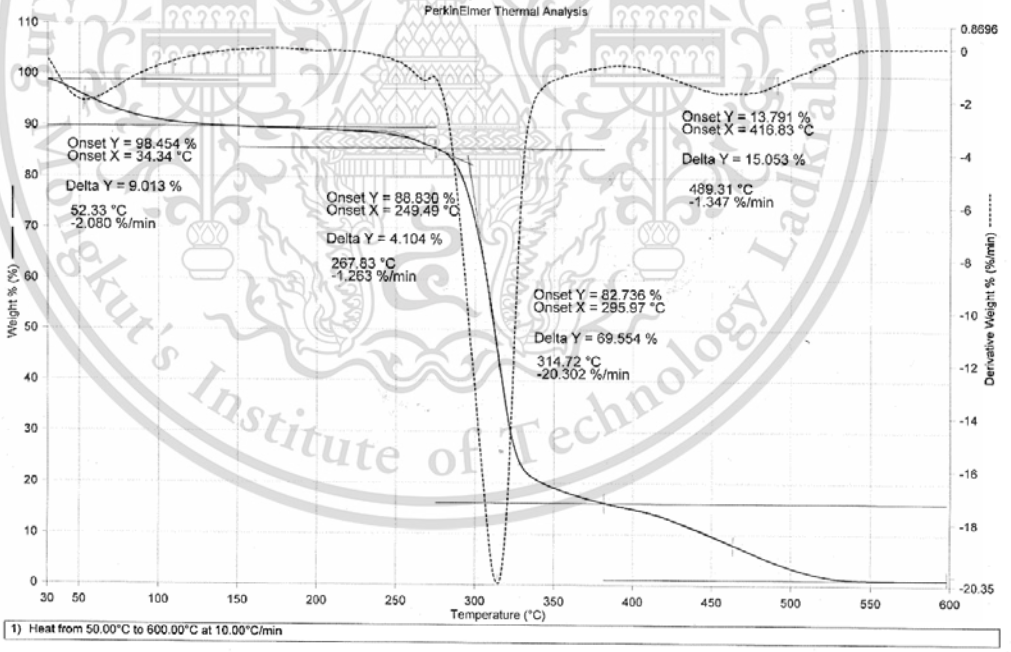

Figure B-8 TGA thermogram of GS-60MAA

This material is reserved for educational use only, not allowed for commercial use.
Forbidden to modify the content, and cite the document when use.

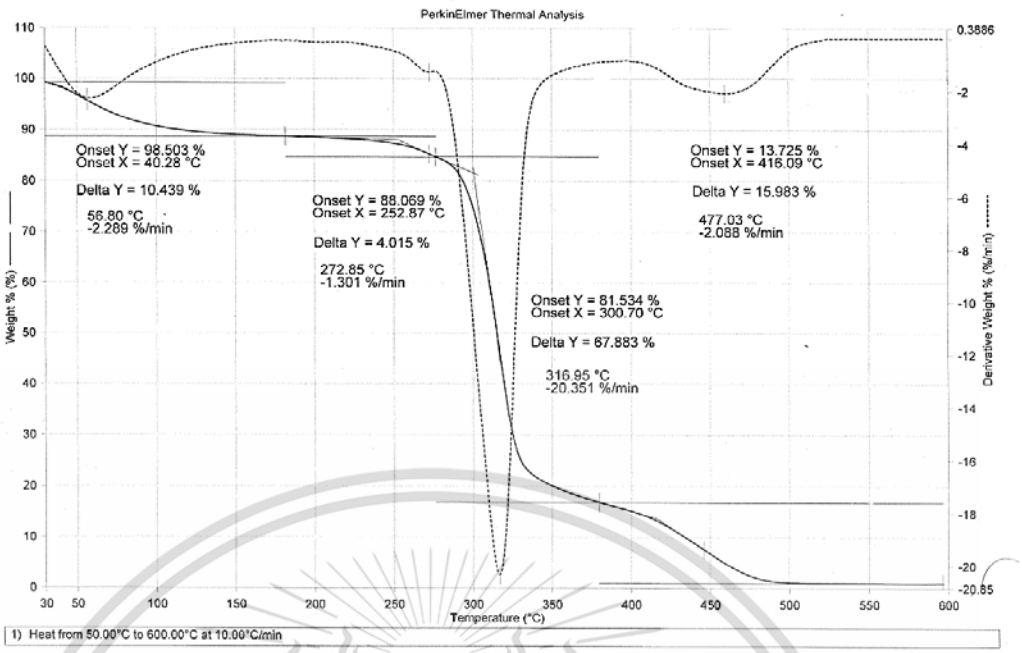

Figure B-9 TGA thermogram of GS-90MAA

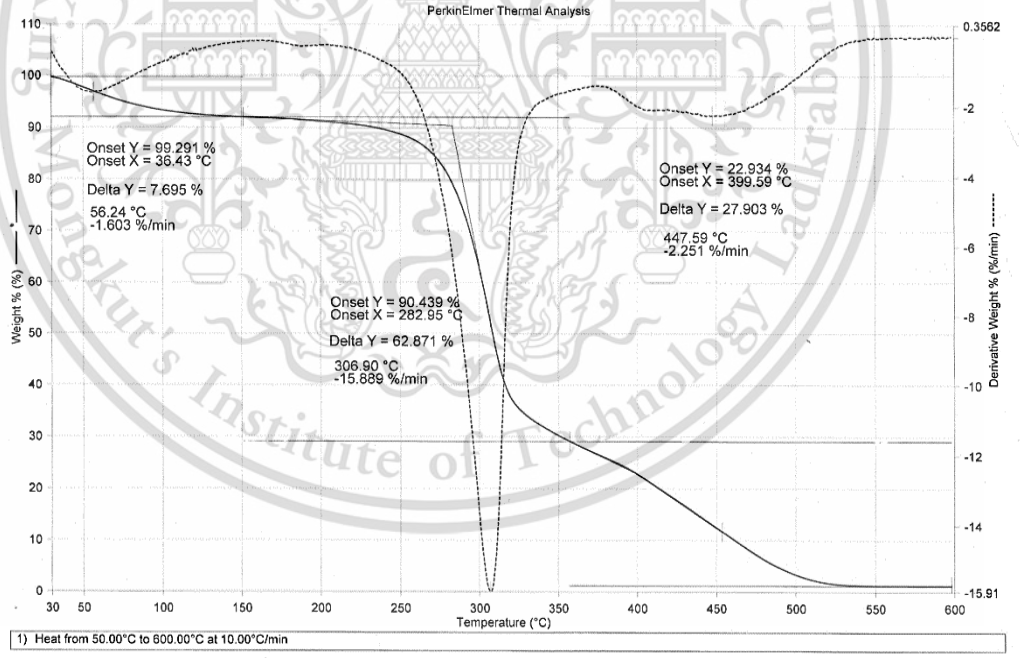

Figure B-10 TGA thermogram of GS-20MMA

This material is reserved for educational use only, not allowed for commercial use.
Forbidden to modify the content, and cite the document when use.

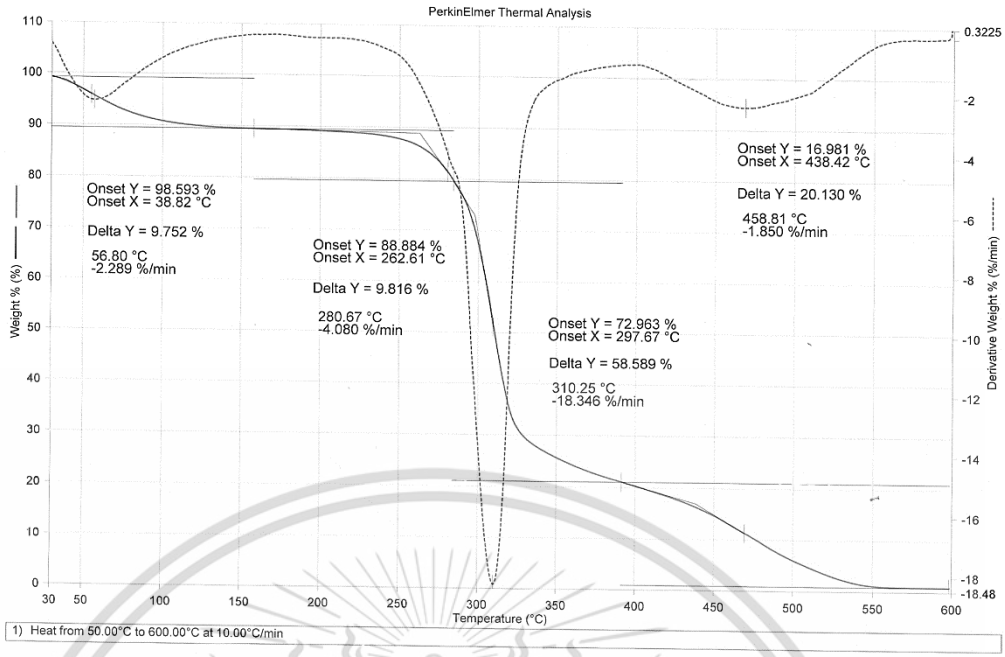

Figure B-11 TGA thermogram of GS-40MMA

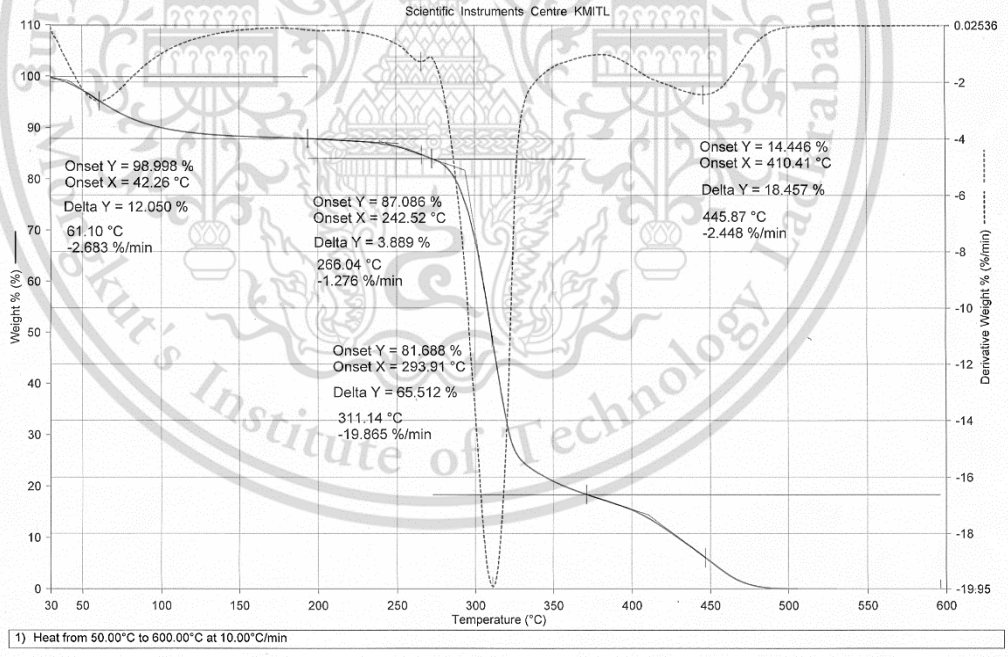

Figure B-12 TGA thermogram of GS-60MMA

This material is reserved for educational use only, not allowed for commercial use.
Forbidden to modify the content, and cite the document when use.

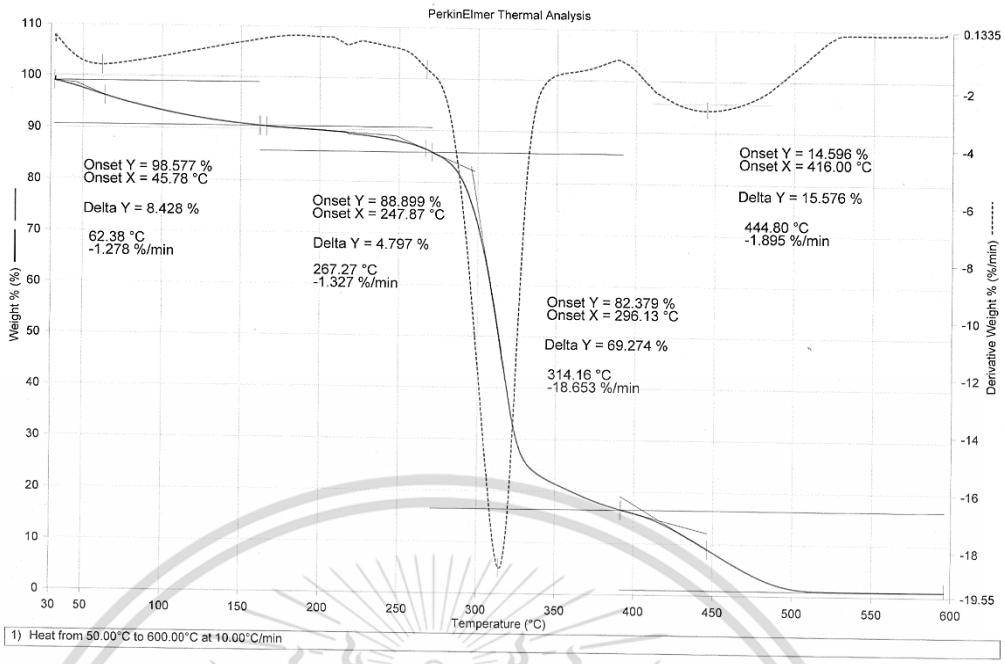

Figure B-13 TGA thermogram of GS-90MMA

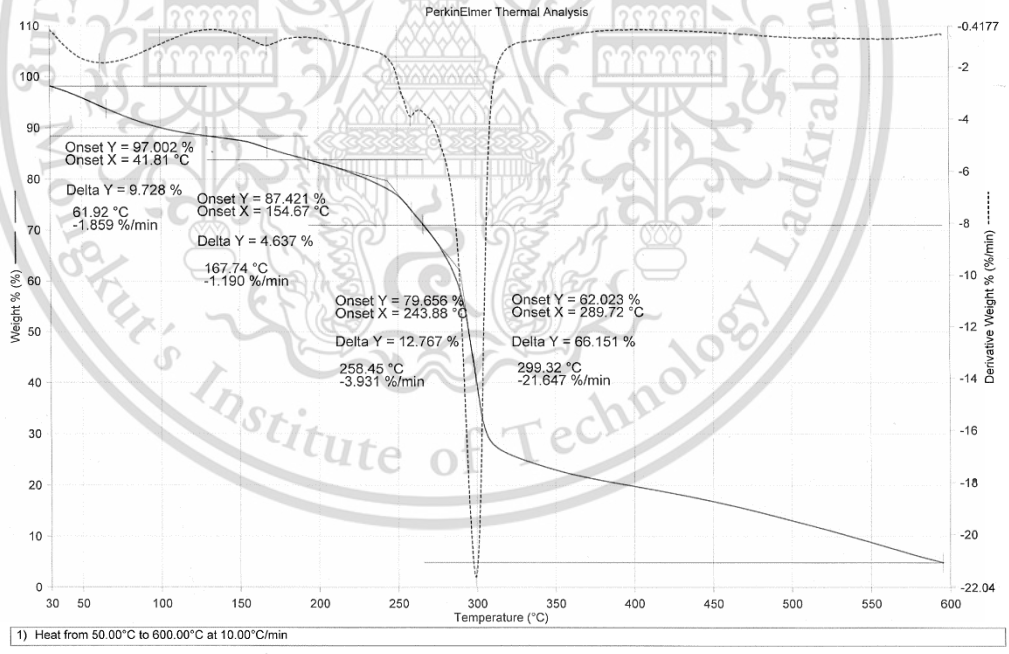

Figure B-14 TGA thermogram of TPNS

This material is reserved for educational use only, not allowed for commercial use.
Forbidden to modify the content, and cite the document when use.

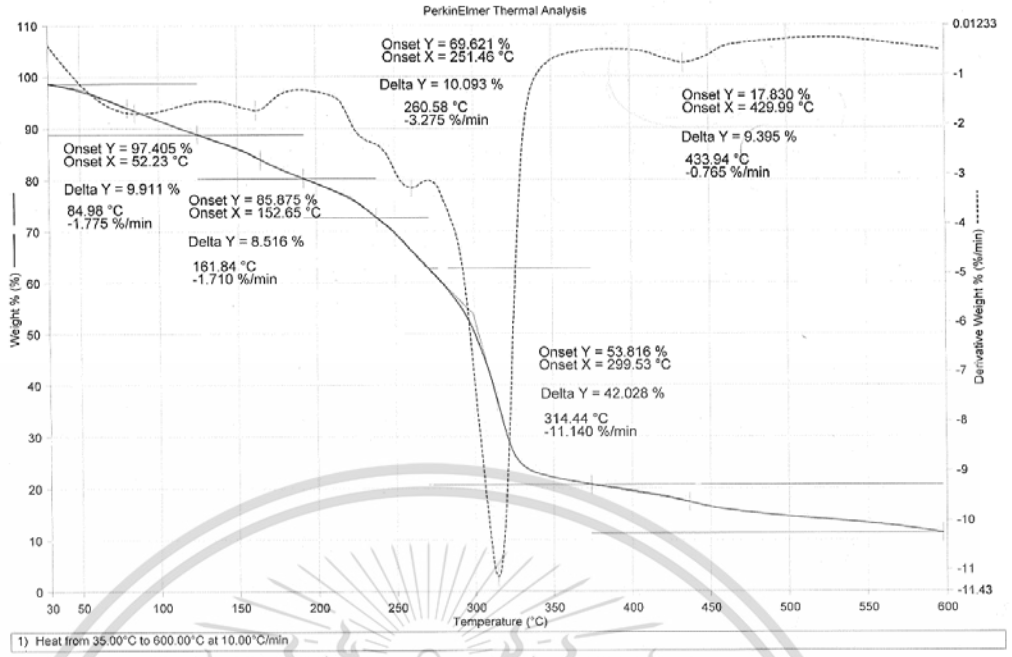

Figure B-15 TGA thermogram of TPGS-20MAM

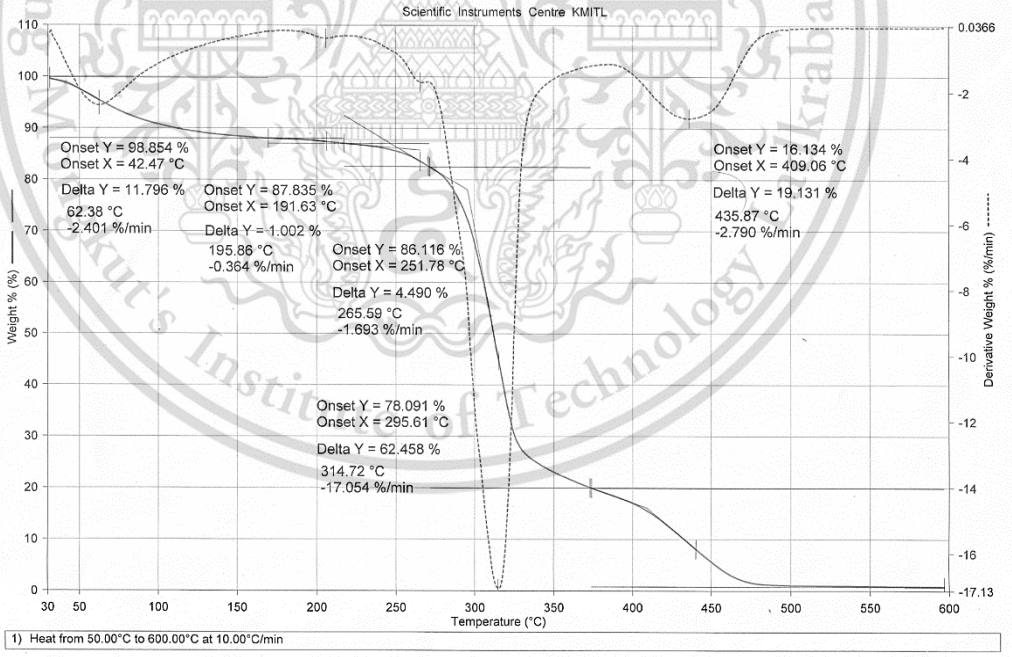

Figure B-16 TGA thermogram of TPGS-40MAM

This material is reserved for educational use only, not allowed for commercial use.
Forbidden to modify the content, and cite the document when use.

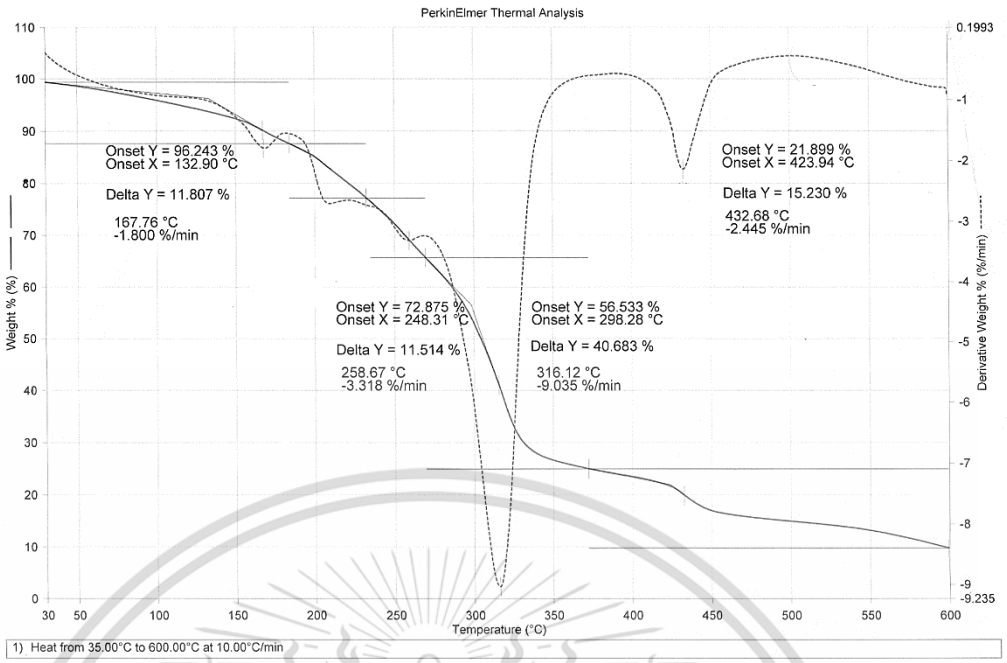

Figure B-17 TGA thermogram of TPGS-60MAM

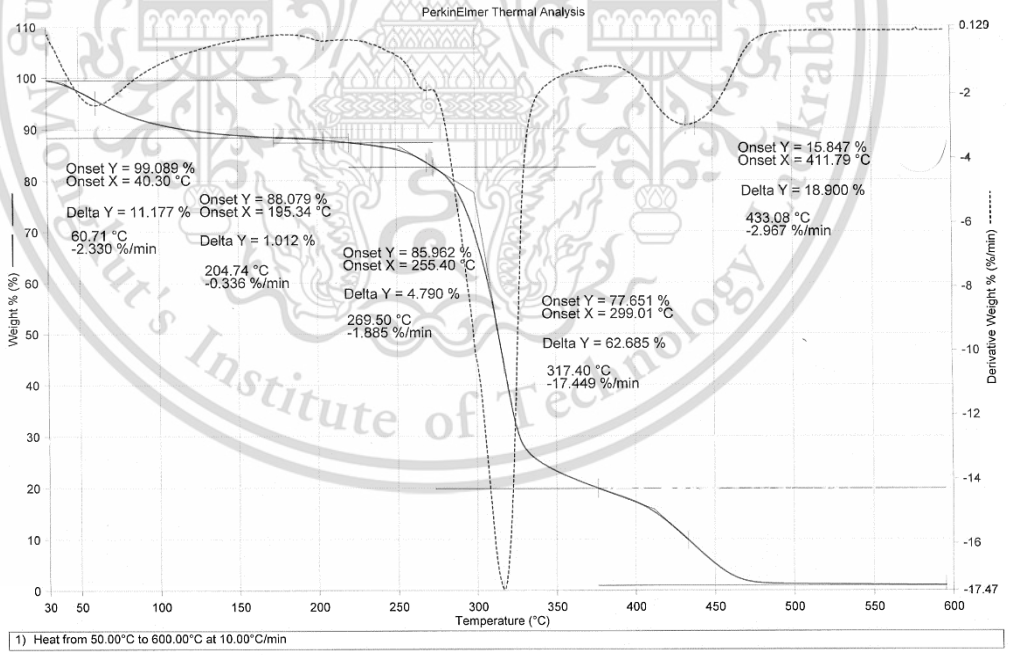

Figure B-18 TGA thermogram of TPGS-90MAM

This material is reserved for educational use only, not allowed for commercial use.
Forbidden to modify the content, and cite the document when use.

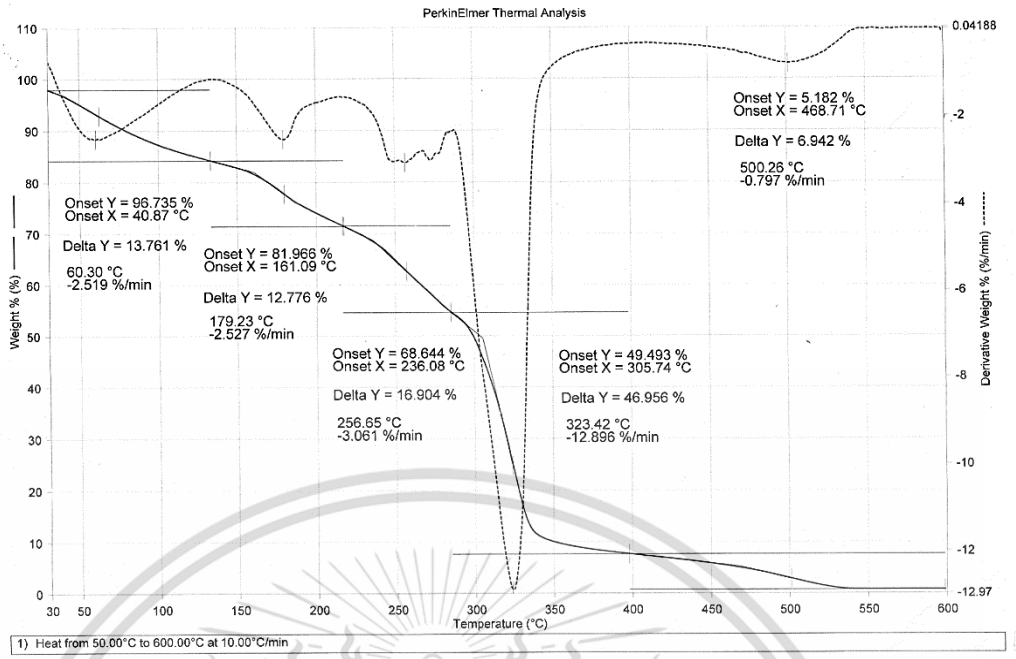

Figure B-19 TGA thermogram of TPGS-20MAA

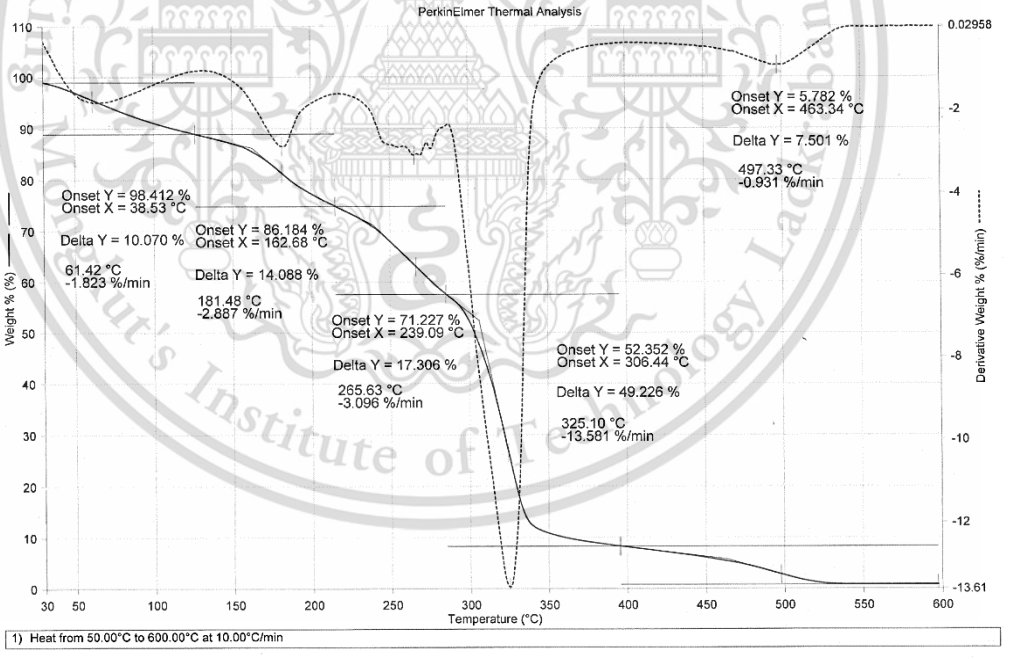

Figure B-20 TGA thermogram of TPGS-40MAA

This material is reserved for educational use only, not allowed for commercial use.
Forbidden to modify the content, and cite the document when use.

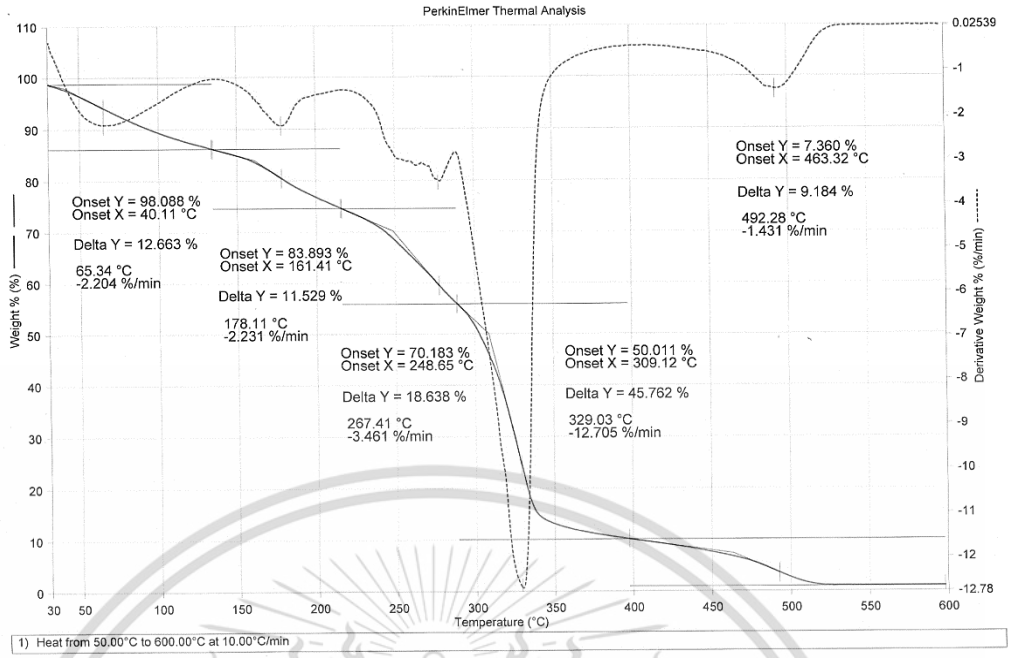

Figure A-21 TGA thermogram of TPGS-60MAA

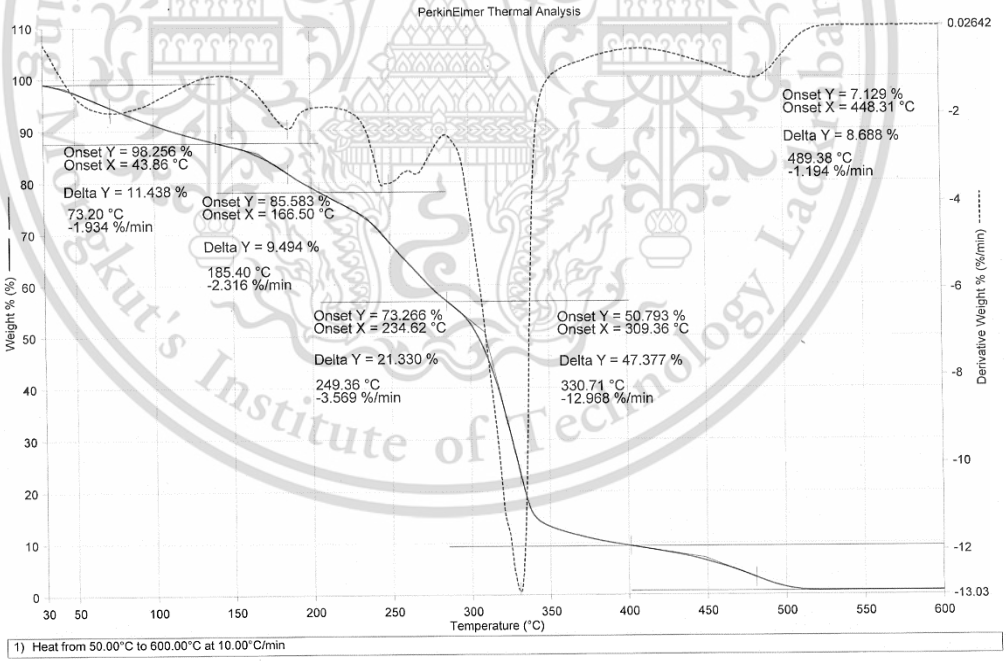

Figure A-22 TGA thermogram of TPGS-90MAA

This material is reserved for educational use only, not allowed for commercial use.
Forbidden to modify the content, and cite the document when use.

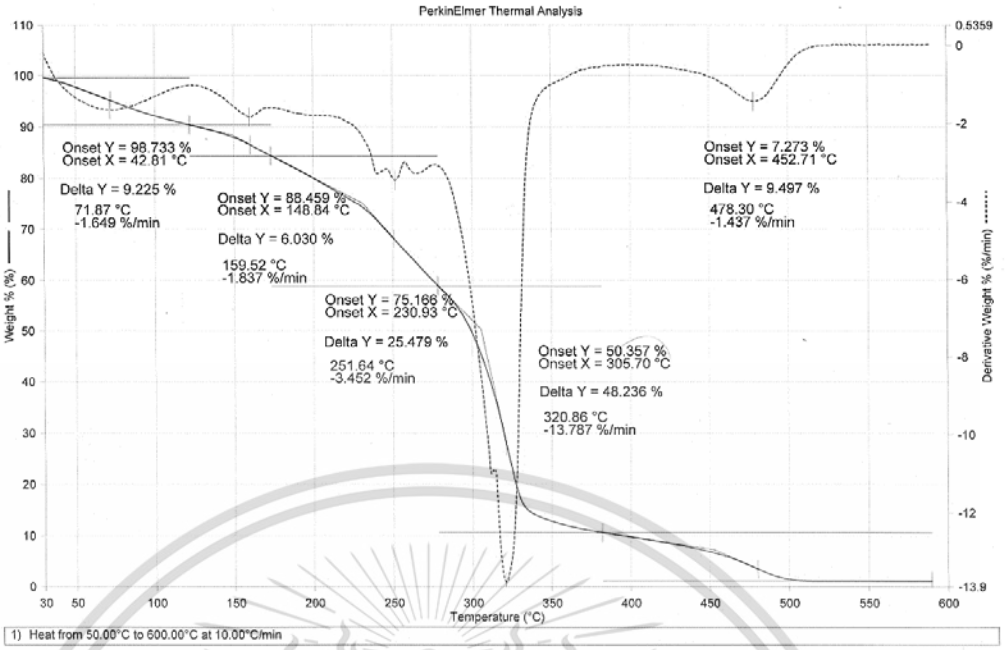

Figure A-23 TGA thermogram of TPGS-20MMA

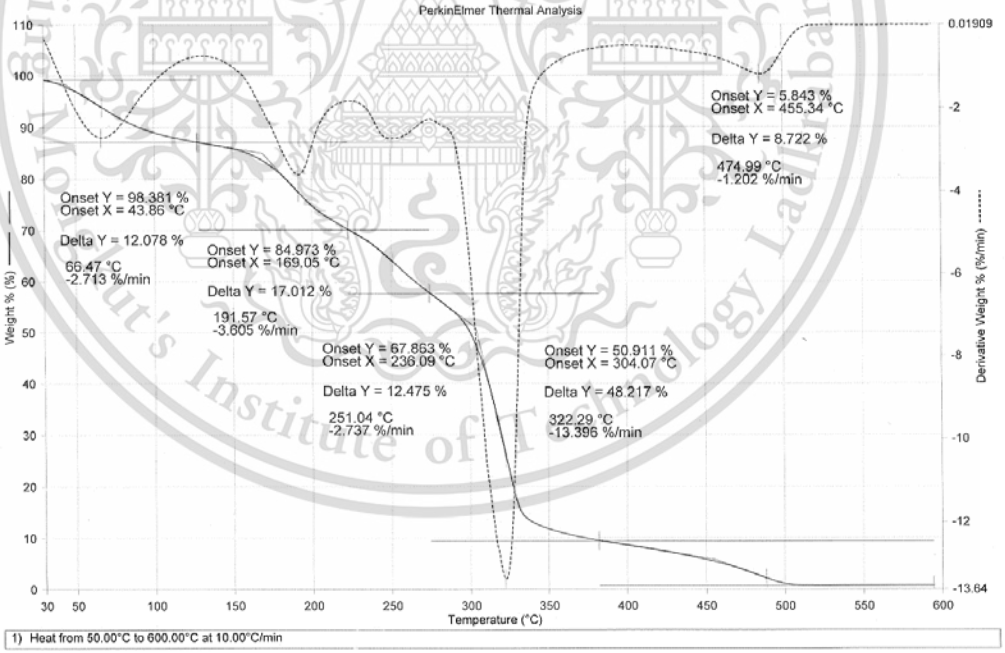

Figure A-24 TGA thermogram of TPGS-40MMA

This material is reserved for educational use only, not allowed for commercial use.
Forbidden to modify the content, and cite the document when use.

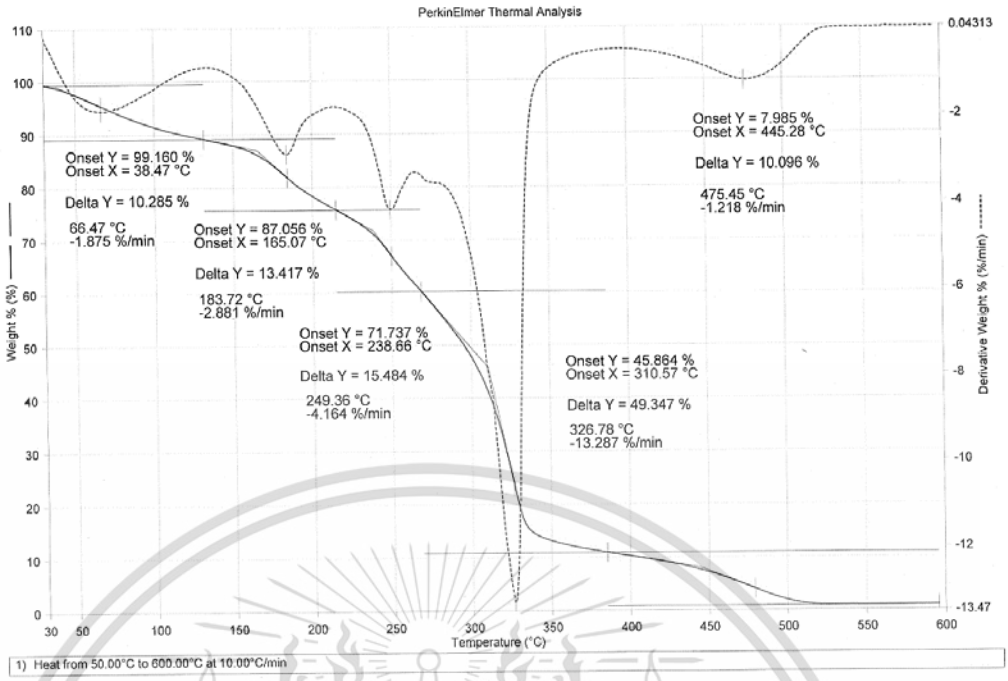

Figure A-25 TGA thermogram of TPGS-60MMA

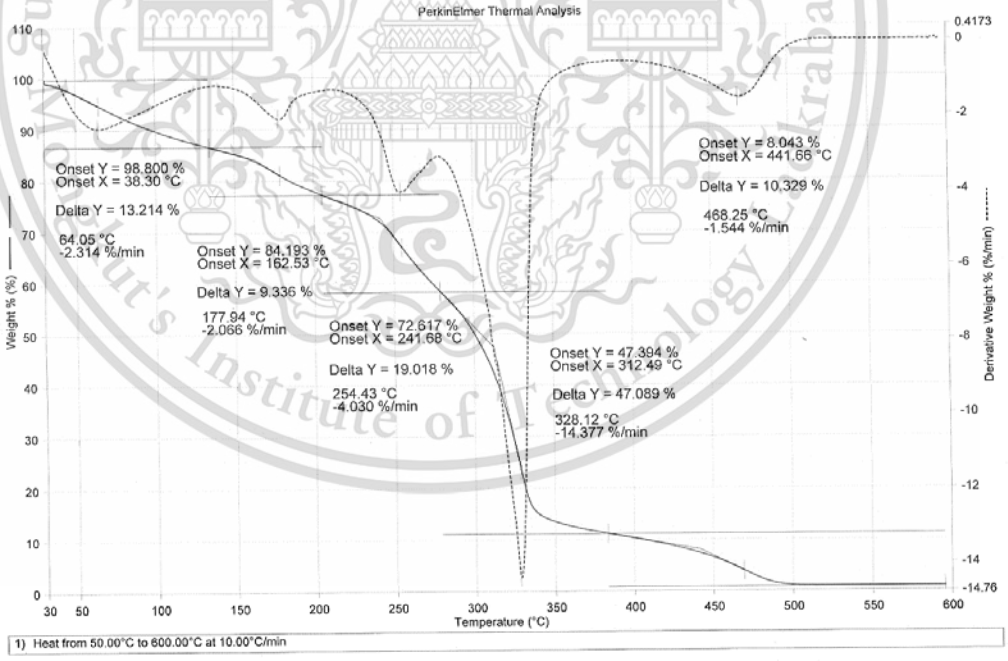

Figure A-26 TGA thermogram of TPGS-90MMA

This material is reserved for educational use only, not allowed for commercial use.
Forbidden to modify the content, and cite the document when use.

Appendix C

XRD study

X-ray diffraction of TPNS film and various TPGS films

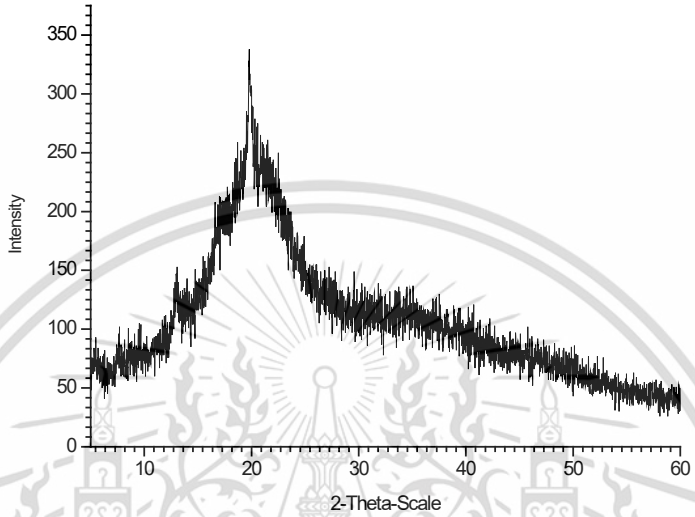

Figure C-1 X-ray diffractogram of TPNS

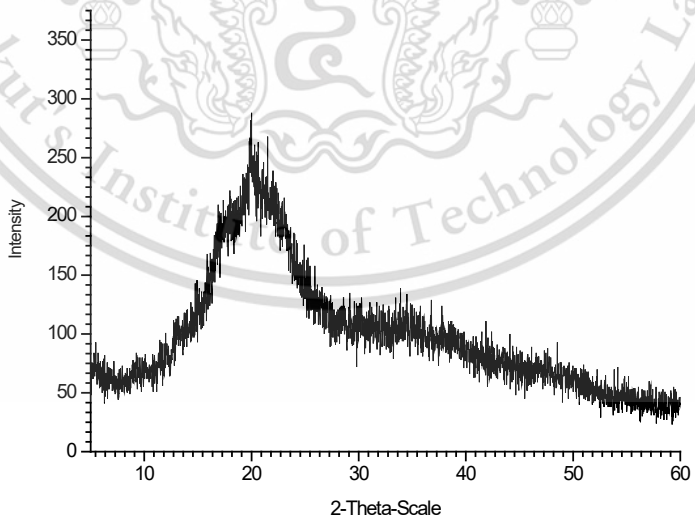

Figure C-2 X-ray diffractogram of TPGS-20MAM

This material is reserved for educational use only, not allowed for commercial use.
Forbidden to modify the content, and cite the document when use.

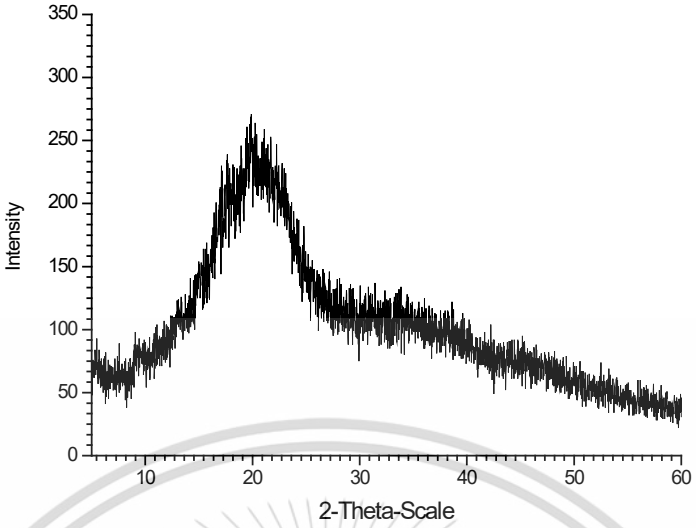

Figure C-3 X-ray diffractogram of TPGS-40MAM

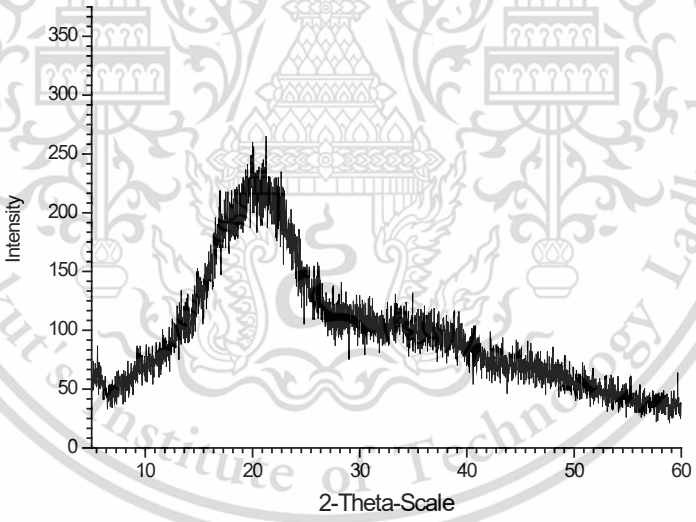

Figure C-4 X-ray diffractogram of TPGS-60MAM

This material is reserved for educational use only, not allowed for commercial use.
Forbidden to modify the content, and cite the document when use.

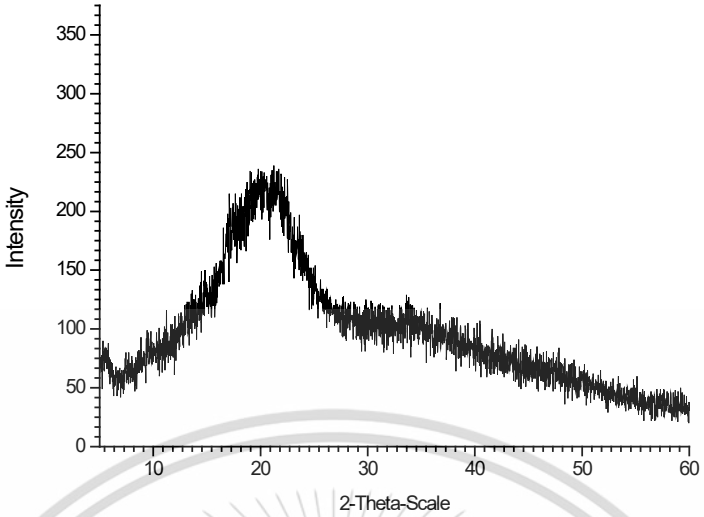

Figure C-5 X-ray diffractogram of TPGS-90MAM

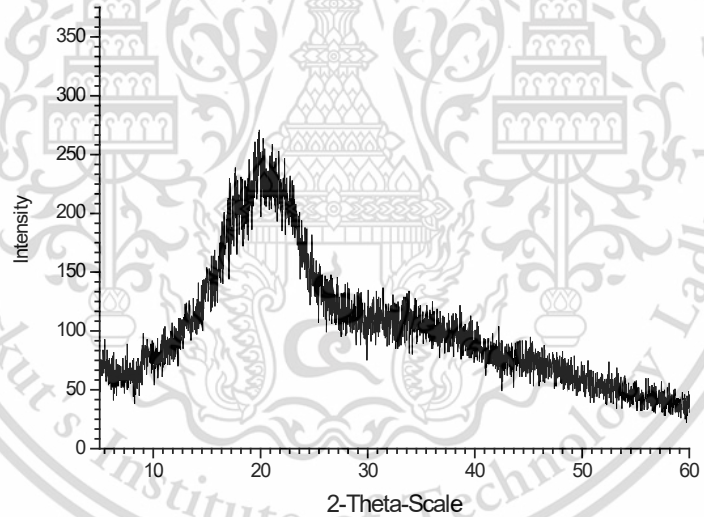

Figure C-6 X-ray diffractogram of TPGS-20MAA

This material is reserved for educational use only, not allowed for commercial use.
Forbidden to modify the content, and cite the document when use.

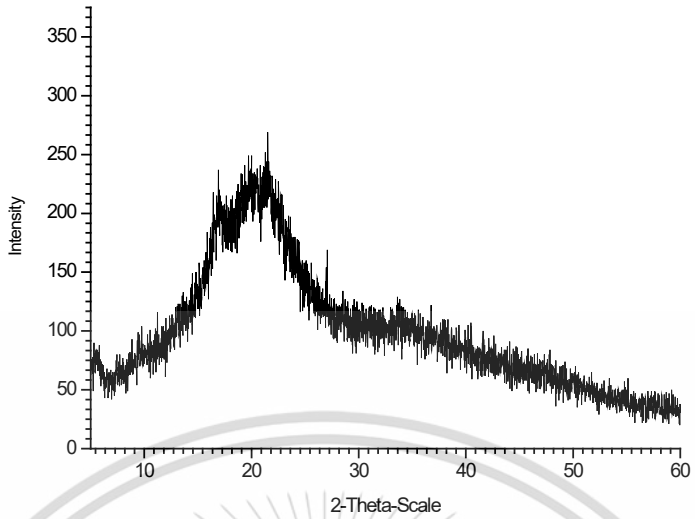

Figure C-7 X-ray diffractogram of TPGS-40MAA

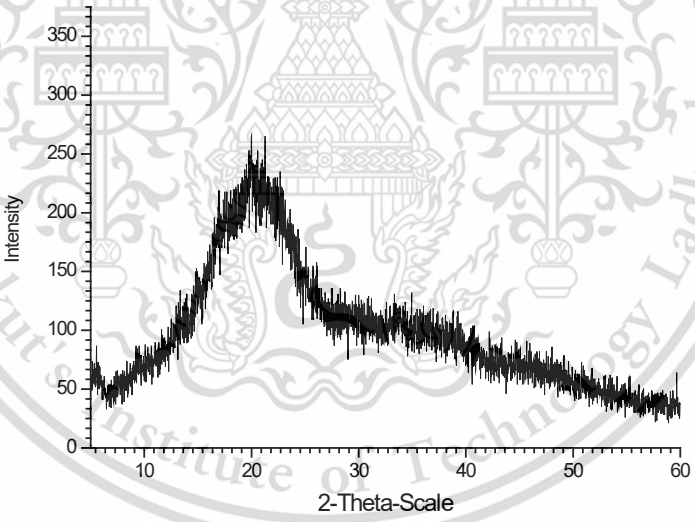

Figure C-8 X-ray diffractogram of TPGS-60MAA

This material is reserved for educational use only, not allowed for commercial use.
Forbidden to modify the content, and cite the document when use.

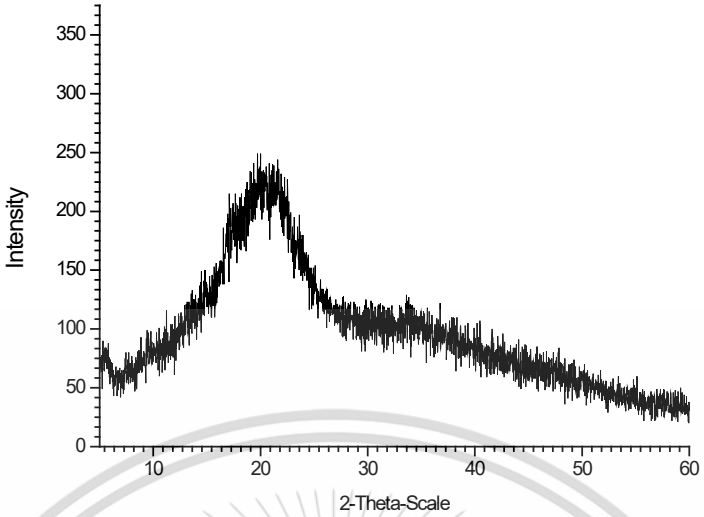

Figure C-9 X-ray diffractogram of TPGS-90MAA

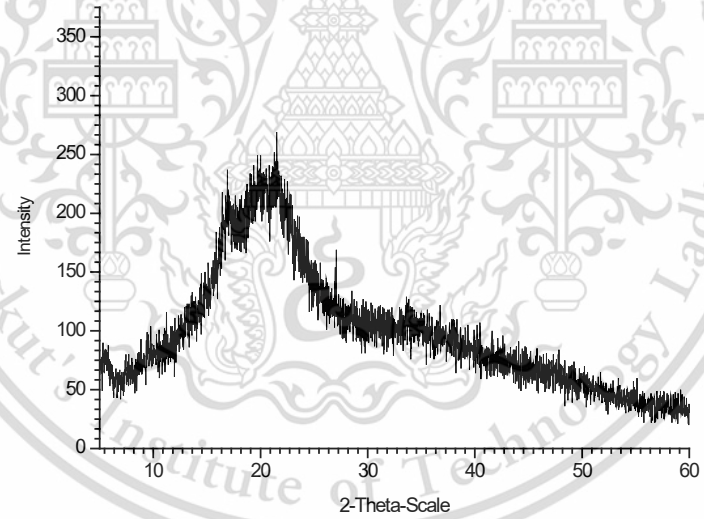

Figure C-10 X-ray diffractogram of TPGS-20MMA

This material is reserved for educational use only, not allowed for commercial use.
Forbidden to modify the content, and cite the document when use.

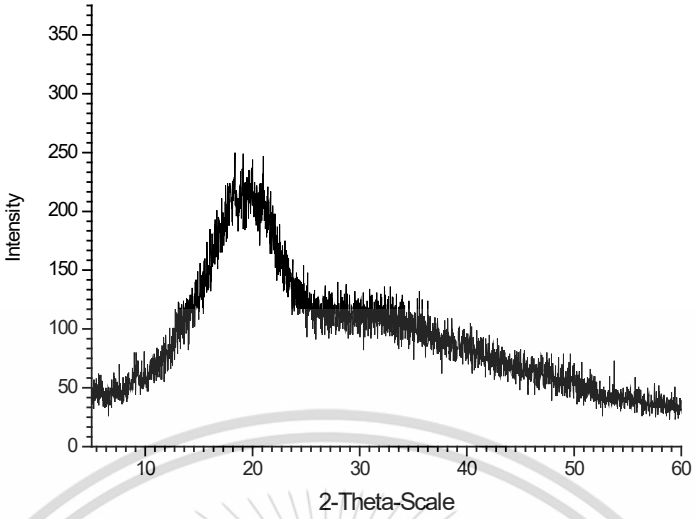

Figure C-11 X-ray diffractogram of TPGS-40MMA

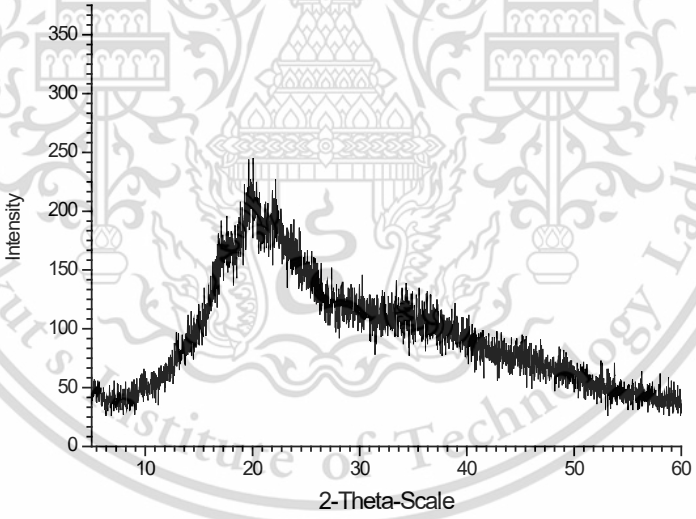

Figure C-12 X-ray diffractogram of TPGS-60MMA

This material is reserved for educational use only, not allowed for commercial use.
Forbidden to modify the content, and cite the document when use.

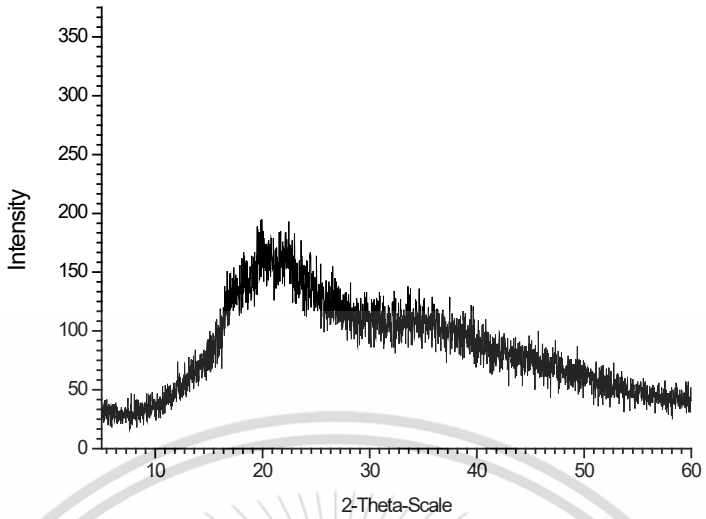

Figure C-13 X-ray diffractogram of TPGS-90MMA

This material is reserved for educational use only, not allowed for commercial use.
Forbidden to modify the content, and cite the document when use.

Appendix D

Swelling power

Table D-1 Degrees of swelling of TPNS film and various TPGS films with MAM for the immersion time of 1, 2, 3, 4, 5, 6 and 72 h

Time (h)	Degree of swelling (%)				
	TPNS	TPGS-20MAM	TPGS-40MAM	TPGS-60MAM	TPGS-90MAM
0	0	0	0	0	0
1	260.15±2.23	280.20±2.54	300.56±2.21	230.12±3.90	218.34±2.56
2	300.24±3.29	315.23±3.21	330.45±2.81	280.34±1.67	263.56±2.11
3	320.67±2.90	360.56±2.65	380.23±3.09	290.56±2.54	278.87±2.99
4	330.23±3.87	380.53±3.45	390.12±4.21	310.45±2.78	283.90±1.76
5	340.34±2.12	400.32±2.65	420.67±4.00	320.67±3.46	308.11±2.34
6	360.23±1.90	410.12±1.27	430.87±1.28	325.09±1.12	313.89±1.89
72	380.23±3.21	440.90±2.34	460.45±3.10	340.34±1.12	323.19±1.78

Table D-2 Degrees of swelling of various TPGS films with MAA for the immersion time of 1, 2, 3, 4, 5, 6 and 72 h

Time (h)	Degree of swelling (%)			
	TPGS-20MAA	TPGS-40MAA	TPGS-60MAA	TPGS-90MAA
0	0	0	0	0
1	300.23±3.23	340.54±1.76	245.89±1.35	230.98±2.00
2	330.45±2.62	370.98±0.45	290.45±2.00	273.90±0..65
3	380.67±1.07	400.56±1.35	300.25±1.23	285.67±0.12
4	400.98±2.23	420.23±0.67	320.88±1.45	302.31±0.89
5	420.12±1.67	440.09±0.12	330.98±1.21	317.89±2.21
6	440.98±0.21	460.20±0.45	350.89±2.67	322.90±0.45
72	455.21±1.87	474.98±1.56	370.76±1.56	345.11±2.32

This material is reserved for educational use only, not allowed for commercial use.
Forbidden to modify the content, and cite the document when use.

Table D-3 Degrees of swelling of various TPGS films with MMA for the immersion time of 1, 2, 3, 4, 5, 6 and 72 h

Time (h)	Degree of swelling (%)			
	TPGS-20MMA	TPGS-40MMA	TPGS-60MMA	TPGS-90MMA
0	0	0	0	0
1	230.09±2.32	210.87±0.65	195.54±0.78	180.56±0.12
2	270.65±0.76	250.77±0.34	240.98±2.21	220.98±1.34
3	300.23±3.12	270.76±0.87	250.76±0.87	230.98±2.21
4	310.87±2.56	280.66±1.23	270.98±1.45	250.76±0.78
5	320.45±3.76	300.45±0.67	290.45±0.11	270.98±0.56
6	345.87±2.34	310.98±0.86	300.55±0.98	280.98±2.21
72	350.76±0.29	320.45±1.08	310.98±1.98	296.87±2.34

King Mongkut's Institute of Technology Ladkrabang

This material is reserved for educational use only, not allowed for commercial use.
Forbidden to modify the content, and cite the document when use.

Appendix E

Moisture uptake

Table E-1 Percentages of moisture uptake of TPNS film and various TPGS films with MAM for the time of 0-15 days

Time (Day)	Moisture uptake (%)				
	TPNS	TPGS-20MAM	TPGS-40MAM	TPGS-60MAM	TPGS-90MAM
0	0	0	0	0	0
1	20.15±1.20	27.34±0.43	35.24±0.21	16.20±0.23	10.90±0.32
2	24.24±0.32	30.02±0.80	40.04±0.23	18.98±0.23	13.23±0.22
3	26.67±0.45	33.09±0.70	43.11±0.23	20.34±0.42	18.21±0.21
4	28.23±0.76	37.21±0.54	47.30±0.12	23.24±0.65	21.30±0.45
5	30.34±0.56	44.23±0.83	50.12±0.22	25.88±0.22	23.65±0.87
6	37.23±0.80	48.54±1.21	52.23±0.34	28.26±0.34	2.23±0.43
7	39.25±0.60	50.34±0.87	54.34±0.23	31.52±0.67	28.21±0.56
8	41.15±0.87	52.65±0.12	56.23±0.45	34.32±0.22	31.45±0.77
9	43.24±0.82	54.28±0.51	58.23±0.23	36.24±0.43	33.42±0.67
10	50.67±0.65	57.12±0.54	60.23±0.56	43.23±0.78	38.87±0.45
11	54.23±1.23	61.21±0.34	68.23±0.12	45.21±0.75	40.21±0.22
12	60.34±0.76	65.12±0.32	71.23±0.64	50.12±0.45	43.67±0.45
13	65.23±0.53	68.21±0.12	72.23±0.23	50.42±0.89	43.65±0.48
14	67.25±0.87	72.23±0.35	74.22±0.43	50.43±0.78	43.78±0.56
15	67.15±0.43	72.23±0.43	74.22±0.45	50.43±0.45	43.87±0.34

This material is reserved for educational use only, not allowed for commercial use.
Forbidden to modify the content, and cite the document when use.

Table E-2 Percentages of moisture uptake of various TPGS films with MAA for the time of 0-15 days

Time (Day)	Moisture uptake (%)			
	TPGS-20MAA	TPGS-40MAA	TPGS-60MAA	TPGS-90MAA
0	0	0	0	0
1	30.12±1.23	40.23±0.45	16.84±0.40	13.15±0.98
2	34.31±0.34	44.12±0.76	20.09±0.67	15.24±0.69
3	36.53±0.46	45.45±0.70	23.01±0.63	20.67±0.72
4	40.76±0.65	49.65±0.50	25.21±0.91	22.23±0.80
5	48.21±0.54	53.56±0.76	27.23±0.45	25.34±0.11
6	51.62±0.65	56.76±1.09	30.54±0.78	27.67±0.80
7	53.21±0.89	58.23±0.56	34.34±0.80	30.25±0.87
8	55.23±0.45	60.56±0.43	37.65±0.19	33.15±0.99
9	57.23±0.56	65.34±0.49	39.28±0.78	36.24±0.77
10	60.23±0.34	70.90±0.30	46.12±0.55	49.67±0.65
11	69.23±0.23	74.23±0.87	50.21±0.34	43.23±1.23
12	73.23±0.56	76.17±0.56	55.12±0.32	47.34±0.71
13	75.89±0.57	80.34±0.60	55.21±0.12	47.23±0.53
14	75.23±0.45	80.34±0.78	55.65±0.33	47.20±0.99
15	75.35±0.45	80.34±0.45	55.65±0.43	47.15±0.43

This material is reserved for educational use only, not allowed for commercial use.
Forbidden to modify the content, and cite the document when use.

Table E-3 Percentages of moisture uptake of various TPGS films with MMA for the time of 0-15 days

Time (Day)	Moisture uptake (%)			
	TPGS-20MMA	TPGS-40MMA	TPGS-60MMA	TPGS-90MMA
0	0	0	0	0
1	18.23±1.23	14.23±0.32	11.23±0.31	8.12±0.23
2	22.12±0.43	19.23±0.22	16.90±0.45	10.89±0.45
3	24.34±0.32	21.23±0.42	17.21±0.32	15.23±0.56
4	25.67±0.54	23.12±0.32	21.76±0.65	17.20±0.61
5	27.31±1.23	25.13±0.54	23.23±0.76	19.89±0.22
6	33.23±0.65	30.12±0.43	27.98±0.45	22.31±0.60
7	35.24±1.23	33.23±0.56	30.04±0.23	24.21±0.45
8	37.78±0.64	36.24±0.32	32.78±0.56	26.11±0.67
9	39.83±0.50	37.12±0.45	34.98±0.78	28.90±0.12
10	45.231.23	42.12±0.23	38.90±0.19	30.12±0.46
11	50.23±0.42	46.12±0.54	40.33±0.12	34.23±0.78
12	55.24±0.45	50.23±0.11	48.12±0.11	36.89±0.64
13	60.24±0.78	55.34±0.23	48.16±0.90	38.90±0.68
14	60.23±0.89	55.67±0.45	48.12±0.33	38.89±0.54
15	60.12±0.12	55.65±0.52	48.12±0.54	38.89±0.21

This material is reserved for educational use only, not allowed for commercial use.
Forbidden to modify the content, and cite the document when use.

Figure E-1 TPNS and various TPGS films before the test of moisture uptake property at 100% RH for 0 day

This material is reserved for educational use only, not allowed for commercial use.
Forbidden to modify the content, and cite the document when use.

Figure E-2 TPNS and various TPGS films after the test of moisture uptake property at 100% RH for 5 days

This material is reserved for educational use only, not allowed for commercial use.
Forbidden to modify the content, and cite the document when use.

Figure E-3 TPNS and various TPGS films after the test of moisture uptake property at 100% RH for 15 days

This material is reserved for educational use only, not allowed for commercial use.
Forbidden to modify the content, and cite the document when use.

Appendix F

Mechanical properties

Table F-1 Mechanical properties of TPNS film and various TPGS film

Sample	Mechanical properties		
	Stress at maximum load (MPa)	Young's modulus (MPa)	Strain at maximum load (%)
TPNS	3.02±0.01	105.23±1.23	75.21±1.22
TPGS-20MAM	2.62±0.03	95.03±1.65	85.23±1.23
TPGS-40MAM	2.33±0.03	85.21±1.34	90.45±1.29
TPGS-60MAM	2.03±0.04	75.56±2.12	98.56±1.34
TPGS-90MAM	1.66±0.23	65.21±1.29	110.12±1.56
TPGS-20MAA	2.82±0.45	98.43±1.21	79.34±0.87
TPGS-40MAA	2.54±0.32	90.21±0.56	85.31±1.31
TPGS-60MAA	2.22±0.52	80.03±2.12	93.42±1.21
TPGS-90MAA	1.76±0.03	70.12±0.21	100.21±1.45
TPGS-20MMA	2.38±0.01	87.34±1.56	93.23±1.56
TPGS-40MMA	2.01±0.07	80.03±1.72	100.87±1.76
TPGS-60MMA	1.85±0.02	70.21±0.89	125.34±1.88
TPGS-90MMA	1.47±0.01	62.43±0.45	135.11±1.34

This material is reserved for educational use only, not allowed for commercial use.
Forbidden to modify the content, and cite the document when use.

Appendix G

Biodegradable property by the soil burial test

Table G-1 Mechanical properties of TPNS film and various TPGS films after the soil burial test for 5 days

Sample	Mechanical properties after the soil burial test for 5 days		
	Stress at maximum load (MPa)	Young's modulus (MPa)	Strain at maximum load (%)
TPNS	2.07±0.01	80.23±1.54	45.67±0.82
TPGS-20MAM	0.92±0.03	57.45±1.34	55.34±0.56
TPGS-40MAM	0.87±0.08	46.65±0.55	45.67±1.28
TPGS-60MAM	1.50±0.12	64.54±1.42	80.34±0.45
TPGS-90MAM	1.20±0.01	55.23±0.52	89.34±1.34
TPGS-20MAA	1.21±0.03	60.67±0.54	50.23±1.23
TPGS-40MAA	1.00±0.03	50.56±1.65	48.34±1.77
TPGS-60MAA	1.82±0.13	70.23±1.34	88.76±0.45
TPGS-90MAA	1.30±0.03	54.23±1.23	90.12±1.32
TPGS-20MMA	1.52±0.03	70.12±0.58	70.24±1.43
TPGS-40MMA	1.43±0.03	65.23±1.20	80.05±1.21
TPGS-60MMA	1.35±0.02	60.03±1.08	110.65±0.45
TPGS-90MMA	1.20±0.05	52.54±0.75	120.55±1.21

This material is reserved for educational use only, not allowed for commercial use.
Forbidden to modify the content, and cite the document when use.

Table G-2 Mechanical properties of TPNS film and various TPGS films after the soil burial test for 10 days

Sample	Mechanical properties after the soil burial test for 10 days		
	Stress at maximum load (MPa)	Young's modulus (MPa)	Strain at maximum load (%)
TPNS	1.05±0.01	50.04±0.87	25.12±1.12
TPGS-20MAM	0.70±0.03	35.34±1.09	20.23±1.67
TPGS-40MAM	0.53±0.03	18.34±1.22	14.34±1.22
TPGS-60MAM	1.32±0.04	52.23±1.67	70.45±1.09
TPGS-90MAM	1.00±0.02	45.34±1.25	75.45±1.34
TPGS-20MAA	0.70±0.03	35.67±1.23	15.23±1.23
TPGS-40MAA	0.45±0.06	20.21±1.89	20.29±1.93
TPGS-60MAA	1.56±0.02	63.32±1.34	82.23±2.30
TPGS-90MAA	0.83±0.03	40.45±1.57	70.23±0.86
TPGS-20MMA	0.71±0.03	55.23±1.23	50.45±1.23
TPGS-40MMA	0.81±0.05	53.23±1.54	60.02±0.87
TPGS-60MMA	0.95±0.03	48.45±1.67	93.24±1.13
TPGS-90MMA	1.05±0.02	46.32±1.56	110.23±1.68

This material is reserved for educational use only, not allowed for commercial use.
Forbidden to modify the content, and cite the document when use.

TPNS TPGS-20MAM TPGS-40MAM TPGS-60MAM TPGS-90MAM

TPGS-20MAA TPGS-40MAA TPGS-60MAA TPGS-90MAA

This material is reserved for educational use only, not allowed for commercial use.
Forbidden to modify the content, and cite the document when use.

TPGS-20MMA TPGS-40MMA TPGS-60MMA TPGS-90MMA

Figure G-1 TPNS film and various TPGS film after the soil burial test for 10 days

This material is reserved for educational use only, not allowed for commercial use.
Forbidden to modify the content, and cite the document when use.

Preparation and properties of cassava starch grafted by methacrylamide (MAA)

Chayapa Weerapoprasit[1] and Jutarat Prachayawarakorn[1,2*]

[1]*Department of Chemistry, Faculty of Science,*

King Mongkut's Institute of Technology Ladkrabang (KMITL), Bangkok 10520, Thailand

[2]*Advanced Materials Research Unit, Faculty of Science,*

King Mongkut's Institute of Technology Ladkrabang, Ladkrabang, Bangkok 10520, Thailand

*e-mail: jutarat.si@kmitl.ac.th

Abstract:

One alternative to improve properties of native starch is achieved by graft copolymerization method. In this article, biodegradable polymers were synthesized by graft copolymerization of methacrylamide (MAA) monomer onto cassava starch using potassium persulphate (PPS) as a free radical initiator. The graft copolymerization reaction was carried out using the ratio of MAA monomer: starch of 1:1, the temperature of 80 °C and the PPS concentration of 2% wt of the dry starch. It was found that the graft yield increased with the reaction time and the optimum values for the reaction time was 5 hours. The grafted starch was characterized by FTIR, SEM and water uptake properties. FT-IR spectrum of the grafted starch showed the C=O stretching and N-H bending band became more intense with higher grafting percentage. SEM micrographs also showed that the granular structure of starch was not maintained after the graft copolymerization. Moreover, the water uptake values of the MAA-grafted starch were significantly decreased with higher grafting percentage.

1. Introduction

In recent years, research and development on biodegradable materials have been accelerated. Starch is one of the interesting materials due to its abundant, availability, low price and totally biodegradability.[1] However, it may need to be further modified for some special application because the native starch has several disadvantages such as low thermal stability, high water absorption and poor mechanical properties. One alternative to improve the properties of native starch is achieved by graft copolymerization method with vinyl monomers. Starch graft copolymers are becoming increasingly important because of their various applications related to agriculture, industry and medical applications.[2]

Many studies have focused their attention on grafted starch with vinyl monomer, mainly methyl methacrylate (MMA), acrylic acid (AA) and acrylamide (AM) monomer.[3] However, there has been a few studies on the preparation and characterization of cassava starch grafted with methacrylamide (MAA) monomer.

MAA is one of the most important vinyl monomers. It is highly water-soluble, relatively less toxic, polar and expensive than other vinyl monomer.[4] The purpose of this study was to study on the preparation and properties of the MAA-grafted starch.In addition, the grafted starch was compared with the native starch and gelatinized starch. Water uptake, morphology and function group analysis by FT-IR were also examined.

This material is reserved for educational use only, not allowed for commercial use.

Forbidden to modify the content, and cite the document when use.

2. Materials and Methods

2.1 Materials

Cassava starch was obtained from Chaopraya Phuchrai 2999 Co., Ltd. (Kamphaengphet, Thailand). MAA monomer was obtained from Italmar Co., Ltd. (Bangkok, Thailand). PPS and methanol were purchased from Lab System Co., Ltd. and Chemical Innovation, Co., Ltd. (Bangkok, Thailand), respectively.

2.2 Preparation of the MAA-grafted starch

The reaction was carried out by taking the mixture of 5 g of dried starch with 100 mL of water and stirring magnetically at the temperature of 80 °C for 30 min under nitrogen atmosphere in order to prepare a gelatinized starch. The starch was the treated with PPS for 10 min to facilitate free radical formation and, then, the MAA monomer was added at ratio of 1:1 (w/w) (MAA : starch). The solution was stirred for the different reaction times, i.e., 0.5, 2, 4, 5 and 6 hours. After the certain time, the solution was immediately precipitated with methanol. The residue was washed with warm water in order to remove homopolymer. The residue was, then, dried in a hot air-oven at the temperature of 50 °C for 24 hr.

2.3 Sample characterization

2.3.1 Grafting parameters

Percentage grafting efficiency (% GE) and percentage grafting (% G) were based on gravimetric estimation and were calculated as follows:

$$\% GE = 100 (W_2 - W_1) / W_3$$

$$\% G = 100 (W_2 - W_1) / W_1$$

where W_1, W_2 and W_3 are the weights of pure starch, the MAA-grafted starch and the MAA monomer, respectively.

2.3.2 FT-IR technique

A sample was characterized by FT-IR analysis on a Spectrum 2000 GX spectrometer (PerkinElmer, USA) using KBr disk technique with a resolution of 4 cm^{-1} using 16 scans per sample.

2.3.3 Scanning electron microscopy

Morphology of a sample was observed by Scanning Electron Microscope (LEO 1450 VP). The sample was sputter-coated with a thin layer of gold to prevent electrical charging during the observation.

2.3.4 Water uptake properties

A sample was dried at 105 °C for 2 h and, then, stored at 100% relative humidity at a temperature of 25 ± 2 °C prior to water absorption evaluation. The amount of water absorbed by the sample was determined until the constant weight was obtained. The percentage of water absorption was calculated as follows:

$$\text{Water absorption} = (W_2 - W_1)/W_1 \times 100$$

where W_2 and W_1 were the wet weight and the dried weight of the sample, respectively.

3. Results & Discussion

3.1 Effect of the reaction time on the grafted copolymerization

Table 1. Percentage of grafting and grafting efficiency

Reaction Time (hr)	%G	%GE
0.5	12.3±1.6	14.6±0.3
2	40.3±1.2	32.7±0.1
4	60.6±2.0	54.7±0.4
5	90.7±1.6	85.1±0.3
6	83.0±1.2	83.0±0.8

This material is reserved for educational use only, not allowed for commercial use.
Forbidden to modify the content, and cite the document when use.

Table 1 presents %G and %GE of the MAA-grafted starch according to different reaction times. The result showed that the %G and %GE increased with increasing reaction times from 0.5 to 5 hr and the maximum value of approximately 90.7 % was obtained at the reaction time of 5 hours. The results indicated that higher grafting copolymerization could be obtained with longer reaction times.

However, a decrease of the %G and %GE was obtained when the reaction time was 6 hr. The result related with basis of progressive consumption of the monomer and initiator with time. It might be attributed to the grafting reaction occurs at the surface of the starch particle. There were fixed numbers of grafting sites available on the starch particle surface.[5]

3.2 FT-IR spectroscopic study

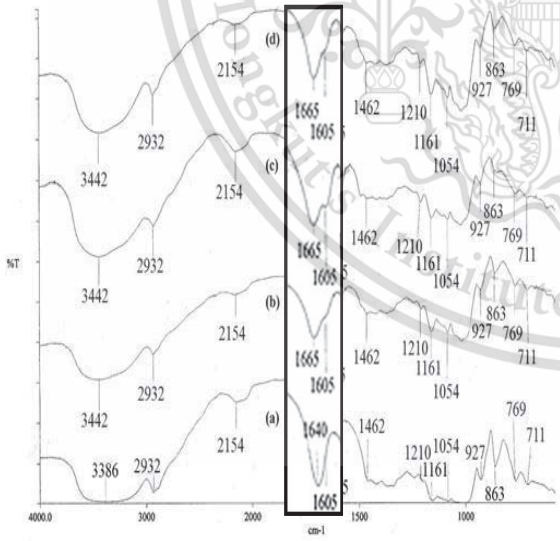

Figure 1 IR spectra of different grafting percentage of various MAA-grafted starch (a) 0% (b) 12.2% (c) 60.6% and (d) 90.7%.

FTIR spectra of different grafted starch are shown in Figure 1. The result showed a broad absorption band ranging from 3,500 to 3,200 cm^{-1}, which was attributed to O-H stretching and N-H bending. Another wavenumber at about 2,800-3,000 cm^{-1} were arisen from CH asymmetric stretching. The band at 1641-1,646 cm^{-1} corresponding to the vibration of bound water. The addition band in the range of 1,450-1,475 cm^{-1} was presented for $-CH_2-$ deformation. The peak at 1070-1,275 cm^{-1} and 1000-1,200 cm^{-1} were attributed to C-O-C stretching and C-O-H stretching.[4]

After the grafting reaction (Figures 1(b)-1(c)), there were new peaks at 1,665 and 1,605 cm^{-1}, attributed to C=O stretching vibrations and N-H bending vibrations in the amide,[5-7] obtained from the grafting reaction. In addition, the intensity of both peaks became more pronounced with the increasing reaction times. It indicates that the degree of grafting on starch backbone increased with the reaction time.

3.3 Morphology

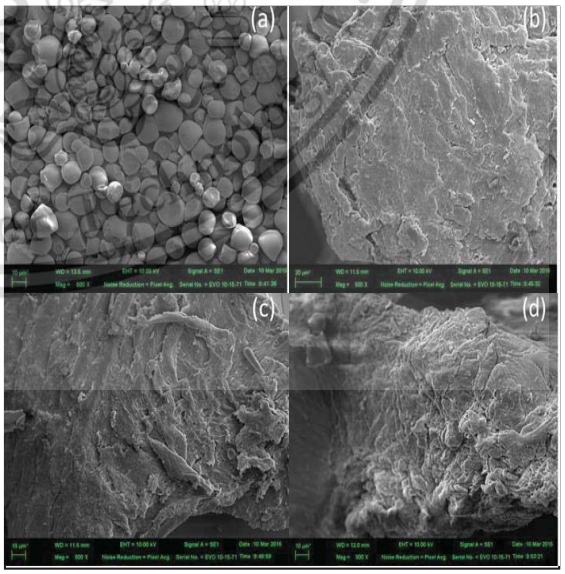

Figure 2 SEM micrographs of different percentage grafting of various MAA-grafted starch (a) 0% (b) 12.3% (c) 60.6% and (d) 90.7%.

This material is reserved for educational use only, not allowed for commercial use.
Forbidden to modify the content, and cite the document when use.

SEM micrographs of different types of starch were represented in Figure 2. The result showed that the native starch (Figure 2(a)) presented granular structures, while the grafted starch (Figures 2(b)-2(d)) showed different morphologies, compared with the native starch.

For the MAA-grafted starch (Figures 2(c) and 2(d)), the starch granules were disappeared. The granule surface was apparently covered with the MAA monomer. The change in the morphology of the native starch granular results related to the graft copolymerization with the MAA monomer.[6]

3.4 Water absorption properties

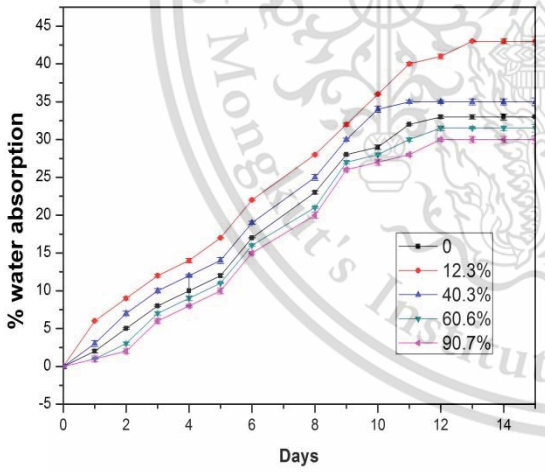

Figure 3 Water uptake of various MAAgrafted starch with different grafting percentage (a) 0% (b) 12.3 % (c) 40.3 % (d) 60.6 % and (e) 90.7 %

The result of water uptake percentage of different types of starch performed at the temperature of 30 ± 2 °C is shown in Figure 3. It was found that the MAA-grafted starch with 12.3% and 40.3% grafting presented higher percentage water uptake than the native starch. It could be due to the hydrophilic in nature of the MAA monomer and loose morphology of starch after the grafting reaction, leading to the higher water uptake when compared with native starch.

However, the MAA-grafted starch percentage with 60.6% and 90.7% grafting presented lower water uptake than the native starch. The results indicate that the high grafting process of the MAA could cause the reduction of voids and blocking water absorption of the starch backbone.[6] This behavior of the grafted sample could be explain that by grafting the active sites responsible for the moisture absorbance was blocked by MAA. Therefore, the affinity of grafted starch toward OH group of water decreases which results in decrease of hydrophilic character.[7]

4. Conclusion

The native cassava starch was successfully grafted by the MAA monomer. The optimum condition giving the maximum percentage of grafting (90.7%) was derived from the reaction time of 5 hours. IR spectroscopy was used to confirm the formation of the MAA-grafted starch. SEM micrographs presented direct evidence of the grafting of MAA monomers onto the cassava starch. Moreover, the lowest percentage water uptake was found for the MAA-grafted starch with 95.7% grafting.

Acknowledgements

The authors express their sincere appreciation to the KMITL Research Fund for supporting the study financially.

References

1. Ritz, P.; Krempf, M.; Cloarec, D.; Champ, M.; Charbonnel, B. *American Journal of Clinical Nutrition* **1991**, 855-859

This material is reserved for educational use only, not allowed for commercial use.

Forbidden to modify the content, and cite the document when use.

2.Athawale, V.D.; Rathi, S.C. *Reactive and Functional Polymer* **1997***,* 11-17.
3.Gao, J.; Tian, R.; Duan, M. *Journal of Applied Polymer Science* **1994,** 1091-1102.
4.Bower, D.I.; Maddams, W.F. The Vibrational Spectroscopy of Polymers2nd Edition; Cambridge University Press: Cambridge, U.K. **1996.**
5. Cao, Y.; Qing, X., Sun, J., Zhou, F.; Lin, S. *European Polymer Journal* **2002**, 1921-1924.
6. Celik, M. *Journal of Applied Polymer Science* **2006***,* 1519-1525.
7. Deepak, P.; Reena, S. Advanced Material Letter. 2012, 3(2), 136-142.

This material is reserved for educational use only, not allowed for commercial use.
Forbidden to modify the content, and cite the document when use.

BIOP-P7

Preparation and properties of cassava starch grafted by methyl methacrylate (MMA)

Chayapa Weerapoprasit[1] and Jutarat Prachayawarakorn[1,2*]

[1] Department of Chemistry, Faculty of Science, King Mongkut's Institute of Technology Ladkrabang (KMITL), Bangkok 10520, Thailand, *

[2] Advanced Materials Research Unit, Faculty of Science, King Mongkut's Institute of Technology Ladkrabang, Ladkrabang, Bangkok 10520, Thailand

E-mail: jutarat.si@kmitl.ac.th Tel : +668-3298400 ext 6235

Abstract

In the present work, native starch was modified by graft copolymerization. The biodegradable starch polymer was prepared by grafted with methyl methacrylate (MMA) monomer onto cassava starch via free radical polymerization using the potassium persulphate (PPS) as an initiator. The graft copolymerization reaction was synthesized using the monomer to starch ratio 1:1, reaction temperature of 80 °C and the PPS concentration of 2 % wt of the dry starch. It was found that the grafting percentage and grafting efficiency significantly increased with the reaction time and the highest grafting percentage of 90.1% was obtained. FT-IR results showed the presence of the MMA at the peak position of 1731 cm^{-1} and the peak position was more intense with higher grafting percentage. SEM micrographs presented the granular structure of starch attached with MMA monomer after the grafting reaction. Moreover, thermal stability of the MMA-grafted starch was significantly increased with the increasing of grafting percentage.

Keywords: grafted starch, methyl methacrylate, modified starch

1. Introduction

In recent years, research has been focused on biodegradable materials to replace petroleum based plastics in a cost effective manner. Starch is a biopolymer which is naturally available, biocompatible and biodegradable [1]. However, native starch does not meet functional properties required in some applications due to disadvantages of native starch such as low thermal properties, high water absorption and poor mechanical properties. Hence, it is still needed to be further modified.

Chemical modification of native starch via graft copolymerization can improve its properties such as absorbency, ion exchange capabilities, elasticity, thermal resistance . Starch graft copolymer is one of the interesting material and can widely use in many fields because of their various applications related to agriculture, industry and medical applications [2].

Many studies have focused their attention on grafted starch with different vinyl monomers, mainly acrylic acid (AA) and acrylamide (AM) monomer [3]. Currently, there is little information on the properties of chemically modified grafted starch with MMA that can be used to develop for further applications. MMA is one of the most important vinyl monomers. It has low watersoluble properties, low toxicity and good impact strength [4].

The purpose of this study was to study on the preparation and properties of the MMA-grafted starch. In addition, the grafted starch was compared with the native starch on the function group analysis by FT-IR morphology and thermal properties by TGA.2. Experimental methods

2.1 Materials

Cassava starch was purchased from Chaopraya Phuchrai 2999 Co.,Ltd. (Kamphaengphet, Thailand). MMA was purchased

This material is reserved for educational use only, not allowed for commercial use.
Forbidden to modify the content, and cite the document when use.

from Italmar Co., Ltd. (Bangkok, Thailand). PPS and methanol were obtained from Lab System Co., Ltd. and Chemical Innovation, Co., Ltd. (Bangkok, Thailand), respectively.

2.2 Preparation of the MMA-grafted starch

5 g of cassava starch was dissolved in 100 ml of distilled water in a 500 ml three round bottom flask. Simultaneously, the mixture was stirred using a magnetic stirrer under heating with the temperature of 80°C for 30 min under nitrogen atmosphere to form the homogeneous starch solution. The PPS initiator was added into the homogeneous solution and, then, the MMA monomer was added at the starch to monomer ratio 1:1.The solution was stirred for the different reaction times, i.e., 0.5, 2, 4 and 6 hours. After the certain time, the solution was poured into excess methanol to precipitate the graft copolymer. The copolymer was extracted thoroughly with acetone to remove the MMA homopolymer. Finally, the graft copolymer was then dried in an hot air-oven at the temperature of 50 °C for 24 hours and cooled to a room temperature until constant weight was obtained.

2.3 Sample characterization

2.3.1 Grafting parameters

Percentage grafting efficiency (% GE) and percentage grafting (% G) were based on gravimetric estimation and were calculated as follows:

$\%\ GE = 100\ (W_2 - W_1)\ /W_3\ \%\ G = 100\ (W_2 - W_1)\ /W_1$ where W_1, W_2 and W_3 were the weights of native starch, the MMA-grafted starch and the MMA monomer, respectively.

2.3.2 FT-IR spectroscopic study

A sample was characterized by FT-IR analysis on a Spectrum 2000 GX spectrometer (PerkinElmer, USA) using KBr disk technique with a resolution of 4 cm^{i1} using 16 scans per sample. Complete analysis was done at ambient temperature.

2.3.3 Scanning electron microscopy

Scanning Electron Microscope (FEI, quanta 250, USA) was used to observe morphology of a sample. The sample was sputter-coated with a thin layer of gold to prevent electrical charging during the observation. Sample surface was observed with a secondary electron detector using the accelerating voltage of 15 kV

2.3.4 Thermogravimetric analysis

Thermogravimatric analyser (Pyris I TGA HT, Perkin Elmer, USA) was operated under nitrogen atmosphere. A sample approximately 10-12 mg was heated from the temperature of 50 to 600 °C at the heating rate of 10 °C/min.

3. Results and discussions

3.1 Effect of the reaction time on the percentage of grafting and grafting efficiency of the grafted copolymers.

Table 1 Percentage of grafting and grafting efficiency

Reaction times (hr)	% G	% GE
0.5	8.1±0.3	6.6±0.3
2	40.3±0.2	35.1±0.1
4	60.9±0.3	54.0±0.2
6	90.1±0.1	82.1±0.2

*The grafting reactions were carried out at different time intervals between 0.5 hr to 6 hr.

Table 1 shows the effect of reaction times on the values of %G and %GE of the MMA-grafted starch. With the increase in reaction time from 0.5 to 4 hours, % G and % GE clearly increased and the maximum value of approximately 90.1 % was obtained at the reaction time of 6 hr. The results revealed that higher grafting process occurred with the longer reaction time. The increase in graft yield with time related to the increasing in the number of grafting sites on the starch chains in the initial stages of the polymerization.

However, a decrease of the %G and %GE was obtained with the reaction time of 6 hr. This was the because the reduction of both monomer and initiator concentration as well as the decreasing of the number of available active grafting sites onto starch backbone with the longer reaction times [5].

This material is reserved for educational use only, not allowed for commercial use.
Forbidden to modify the content, and cite the document when use.

3.2 FT-IR spectroscopic study

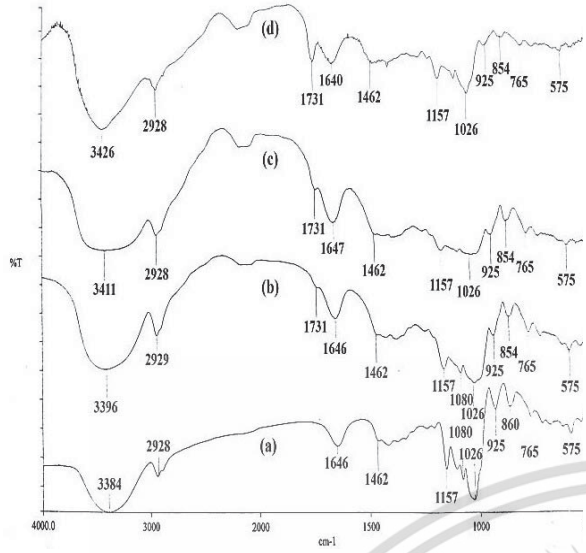

Figure 1 IR spectra of different percentage grafting of various MMA-grafted starches (a) 0% (b) 8.1(c) 40.3 % and (d) 90.1 %.

FTIR spectra of different grafted starch are shown in Figure 1. The result showed a broad absorption band ranging from 3500 to 3300 cm^{-1}, which was attributed to O-H stretching. Another wavenumber at about 2800-3000 cm^{-1} was ascribed to C–H asymmetric stretching. The absorption band at 1641-1646 cm^{-1} indicated the vibration of bound water. The addition band in the range of 14501475 cm^{-1} was presented for O-H bending. The peak at 1070-1275 cm^{-1} and 1000-1200 cm^{-1} were attributed to C– O–C stretching and C–O–H stretching [6].

After the grafting reaction (Figures 1(b)-1(c)), the grafted copolymer showed the extra peak position at 1730 cm^{-1} corresponding to C=O stretching vibrations in esters characteristic [2, 5]. The additional peak confirmed the grafting of the MMA onto cassava starch. In addition, the intensity of C=O stretching peaks increased with the increasing of grafting percentage.

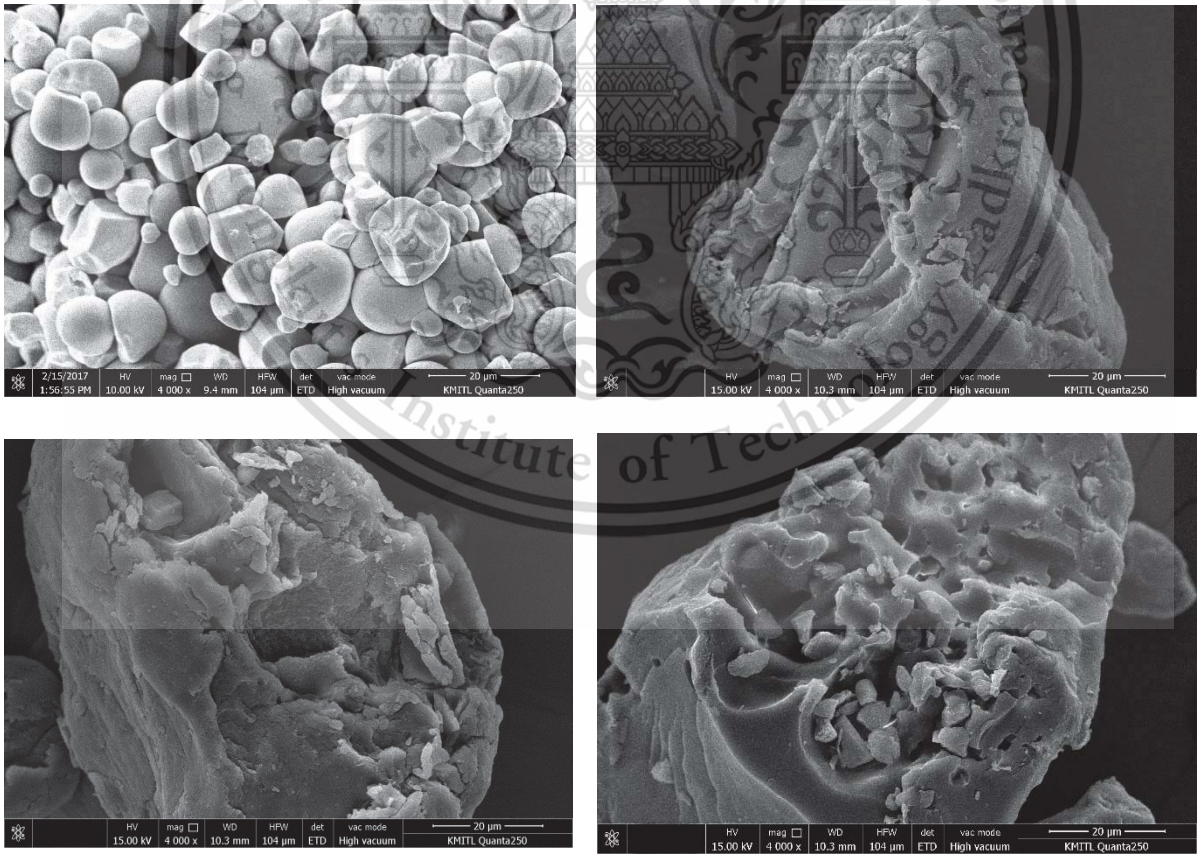

Figure 2 SEM micrographs of various MMA-grafted starches with different percentage grafting (a) 0% (b) 8.1 % (c) 40.3 % and (d) 90.1%

This material is reserved for educational use only, not allowed for commercial use.
Forbidden to modify the content, and cite the document when use.

SEM micrographs of native starch and different grafted starches were presented in Figure 2. The results in Figure 2(a) suggested that the native starch represented smooth granular structure; whereas, the MMA-grafted starch (Figures 2(b)-2(d)) showed different morphologies and the starch granules were disappeared. The granule surface was apparently attached with the MMA monomer. This observation could confirm that the cassava starch was successfully grafted with the MMA monomer [2, 5, 8]. 3.4 Thermal properties

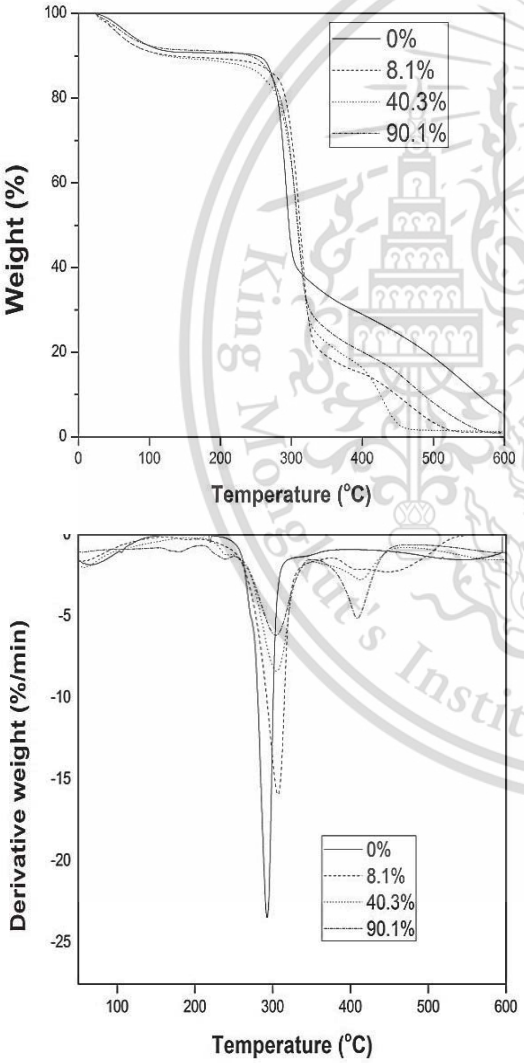

Figure 3 (a) TGA and (b) DTG thermograms of different of various MMA-grafted starches with different percentage grafting (a) 0% (b) 8.1 % (c) 40.3 % and (d) 90.1%

Table2. Thermal decomposition temperatures of different MMA-grafted starches

Samples	Degradation temperature (° C)
Native starch	299.0
MMA-Grafted starch (%G = 8.1%)	306.6
MMA-Grafted starch (%G = 40.3%)	310.2
MMA-Grafted starch (%G = 90.1%)	314.2

Thermal properties of different grafted starches are shown in Figure 3. It was found that the native starch and grafted starch exhibited a three-stage thermal decomposition process. The initial stage at around 100°C corresponded to the loss of adsorbed and bound water. The second stage from 280 to 320°C was attributed to the decomposition of the starch, and the third stage from 430-480 °C was attributed to the decomposition of the MMA grafted copolymer, respectively [8].

It should be noted that the appearance of third stages indicates the structure of starch chains was changed, which was due to the grafting of PMMA chains.

In addition, Table 2 presents the thermal decomposition temperatures of different grafted starches. The result showed that MMA-grafted starch presented higher degradation temperatures than that of the native starch. It implies that the grafting process can improve the thermal stability of the native starch.

4. Conclusions

The native cassava starch was successfully grafted by the MMA monomer. The highest grafted yield was obtained from the reaction time of 6 hours. FTIR spectra could confirm the successfully synthesized of the MMA-grafted starch. SEM micrographs also supported the direct evidence of the grafting of MMA monomers onto the cassava starch. Moreover, the MMA-grafted starch showed higher degradation temperature than the native starch.

Acknowledgements

The authors express their sincere appreciation to the KMITL Research Fund for supporting the study financially.

This material is reserved for educational use only, not allowed for commercial use.
Forbidden to modify the content, and cite the document when use.

References

[1] Ritz, P., Krempf, M., Cloarec, D., Champ, M. andCharbonnel, B., "Comparative continuous-indirect calorimetry study of two carbohydrates with different glycemic indices", *American Journal of Clinical Nutrition* : 855-859 (1991).

[2] Fanta, G. F. and Shogren, R. L., "Modification of Starch-poly (methyl acrylate) graft copolymers by steam jet cooking", *Journal of Applied Polymer Science* : 1021-
1029 (1997),

[3] Kiatkamjornwong, S., Mongkolsawat, K. and Sonsuk, M., "Synthesis and property characterization of cassava starch grafted poly [acrylamide-co-(maleic acid)] superabsorbent via J-irradiation", *Polymer* : 3915-3924 (2002).

[4] Timothy, K., Jensen, J. and Mary, E. "Cardiovascular Effects of Poly(methyl methacrylate) Use in Percutaneous Vertebroplasty", *American Journal of Neuroradiology*. :2601–6044. (2002)

[5] Pimpan, V. and Thothong, P." Synthesis of cassava starch-g-poly(methyl methacrylate) copolymers with benzoyl peroxide as an initiator", *Journal of Applied Polymer Science* : 4083-3089 (2006).

[6] Lagos, A. and Reyes, J. "Grafting onto chitosan. I. Graft copolymerization of methyl methacrylate onto chitosan with Fenton's reagent (Fe^{2+}iH$_2$O$_2$) as a redox initiator", *Polymer Chemistry* : 985-991 (1988).

[7] Çankaya, N. "Synthesis of graft copolymers onto starch and its semiconducting properties", *Results in Physics* :538-542 (2016).

[8]. Celik, M. and Sacak, M. "Synthesis and Characterization of Starch-Poly(methylmethacrylate) Graft Copolymers", *Journal of Appied Polymer Science* :53–57 (2002).

This material is reserved for educational use only, not allowed for commercial use.
Forbidden to modify the content, and cite the document when use.

International Journal of Biological Macromolecules 123 (2019) 657–663

Contents lists available at ScienceDirect

International Journal of Biological Macromolecules

journal homepage: http://www.elsevier.com/locate/ijbiomac

Characterization and properties of biodegradable thermoplastic grafted starch films by different contents of methacrylic acid

Chayapa Weerapoprasit [a], Jutarat Prachayawarakorn [a,b,*]

[a] Department of Chemistry, Faculty of Science, King Mongkut's Institute of Technology Ladkrabang (KMITL), Bangkok 10520, Thailand
[b] Advanced Materials Research Unit, Faculty of Science, King Mongkut's Institute of Technology Ladkrabang (KMITL), Bangkok 10520, Thailand

ARTICLE INFO

Article history:
Received 21 September 2018
Received in revised form 19 October 2018
Accepted 12 November 2018
Available online 13 November 2018

Keywords:
Biopolymer
Grafting
Modified starch
Thermoplastic starch

ABSTRACT

Due to poor mechanical and thermal properties of native starch (NS) film; in the present work; NS was modified by graft copolymerization. Thermoplastic starch (TPS) grafted by methacrylic acid (MAA) with different percentage of grafting, i.e., 0%, 18.3%, 36.3%, 52.1% and 89.7% were prepared and tested. The result demonstrated that the intensity of IR peak of acrylic group increased with the increasing percentage of grafting. The higher graft copolymerization with MAA also significantly reduced degree of crystallinity. The strain at maximum load of TPS film grafted by MAA increased with the increasing percentage of grafting. However, water uptake of TPS film grafted by MAA reduced with high percentage of grafting (52.1% and 89.7%). In addition, different TPS films grafted by MAA were also examined for morphology, water vapor permeability, thermal property and biodegradable property by soil buried test.

© 2018 Elsevier B.V. All rights reserved.

1. Introduction

Among natural materials, starch is one of the well-known biodegradable polymers and the main source of carbohydrate. However, native starch (NS) shows certain disadvantages, e.g., high water absorption, low thermal stability, high viscosity and difficulty in controlling processing. These characteristics of NS are undesirable for biodegradable film application. One of the important techniques for modifying physical and chemical properties of NS is chemical modification [1].

Chemical modifications such as acid hydrolysis, acetylation and crosslinking have been successfully used to modify properties of NS [2,3]. Graft copolymerization can also be used as an alternative way for improving several properties of NS film by generating structural alternation and producing new function groups. Grafted starch (GS) is commonly prepared by graft copolymerization with various monomers such as styrene (S), acrylonitrile (AN), acrylamide (AM), acrylic acid (AA), methyl methacrylate (MMA) and methacrylic acid (MAA) [4,5]. All these monomers affected variety of functional groups, which altered physicochemical properties and modified structures of GS. MAA is an interesting monomer due to its high water solubility and thermal stability. It has been used in commercial applications because it shows low toxicity but high hydrophilicity and polarity [6]. Therefore, many researchers have studied on the preparation and properties of GS with MAA monomer. V. Nikolic et al. reported on the synthesis of the grafted starch by MAA with high percentage of grafting by various amine activators. The resulted showed the new IR peak position at 1730 cm^{-1}, corresponding to MAA monomer characteristic from function group analysis. The best activator in this study was 4 (2 hidroxyethyl) morpholine [7]. Furthermore, percentage of grafting, grafting efficiency, percentage homopolymer and apparent viscosity of the grafting with MAA onto hydrolysed maize starch depended on initiator, monomer contents, and temperatures [8]. D. Pathania and R. Sharma reported that morphology of MAA-grafted potato starch granules showed different morphology. NS granules were clearly destroyed after graft copolymerization. Grafting NS with MAA monomer led to the improvement of thermal stability and properties observed by TGA studies [9]. Additionally, solubility and swelling properties of maize and potato starch grafted with MAA significantly reduced with high percentage of grafting [9–11]. Grafted corn starch could completely degraded by natural microorganism after 21 days and biodegradation of MAA-grafted corn starch was more obvious with time [12].

In recent years, thermoplastic starch (TPS) has been commonly regarded as a biodegradable plastic. Traditionally, TPS is performed by the mixing of starch with plasticizer under high pressure, temperature and shear rate. Nevertheless, TPS has several drawbacks such as high water absorption and low mechanical properties (i.e., low strength, low elongation and brittleness). Interestingly, TPS prepared by GS is a new progressive material of their potential uses in industry. Z. Shi et al. mentioned that the compressed TPS sheet grafted by hexamethylacrylate (HMA) exhibited the improvement of flexibility, caused by the stearic hindrance from monomer with long side chains

* Corresponding author at: Department of Chemistry, Faculty of Science, King Mongkut's Institute of Technology Ladkrabang (KMITL), Bangkok 10520, Thailand.
E-mail address: jutarat.si@kmitl.ac.th (J. Prachayawarakorn).

https://doi.org/10.1016/j.ijbiomac.2018.11.083
0141-8130/© 2018 Elsevier B.V. All rights reserved.

This work is reserved for educational use only, not allowed for commercial use.

Forbidden to modify the content, and cite the document when use.

[13]. Furthermore, improvement of thermal stability and biodegradation of casted TPS films with MMA have also been reported [14]. Besides, the compressed TPS sheet grafted by caprolactone (PCL) showed lower tensile strength but higher flexibility as compared to compressed TPS sheet from NS. The compressed TPS sample based on NS was completely biodegraded; while, TPS sheet by GS with PCL was partially biodegraded after enzymatic degradation [15]. To best of our knowledge, the effect of different percentage of grafting on physiochemical properties of different TPS films grafted by MAA has never been reported.

Consequently, the main purposes in this article were to evaluate and compare physiochemical and mechanical properties of various TPS films grafted by MAA with different percentage of grafting (%G), i.e., 0%, 18.3 ± 0.02%, 36.3 ± 0.03%, 52.1 ± 0.01% and 89.7 ± 0.02%. Different TPS films grafted by MAA were compounded by internal mixer and; then, processed by compression molding machine. The characterization and properties of the samples were investigated by function group analysis, X-ray diffraction, morphology, water uptake, water permeability, mechanical properties, biodegradable properties and also thermal property.

2. Materials and methods

2.1. Materials

Cassava starch was obtained from Chaopraya 1999 Co., Ltd. (Kamphaengphet Thailand), containing approximately 16.4 wt% amylose and 83.6 wt% amylopectin. MAA monomers were supplied from Sigma-Aldrich (St. Louis, U.S.A.). Potassium persulphate and methanol were provided from Merck (Darmstadt, Germany). Glycerol was purchased from Lab System Co., Ltd. (Bangkok, Thailand).

2.2. Experimental

2.2.1. Preparation of GS with MAA

Dried cassava starch (5 g) was dispersed in 100 mL of distilled water and poured into a three-neck bottom flask and kept at a constant temperature of 80 °C for 30 min under nitrogen atmosphere. Potassium persulphate was added to the starch slurry and allowed to react for 10 min; followed by the addition of MAA under steady stirring for different time intervals, i.e. 1, 2, 3 and 5 h. After the required reaction time, the reaction mixture was poured into excess methanol to precipitate the graft copolymer and; then, filtered. MAA homopolymer was thoroughly removed by washing with warm water. GS with MAA was dried in a hot air-oven (Memmert, Germany) at the temperature of 50 °C for 24 h. After that, GS was cooled to a room temperature and weighed. By using different reaction times, i.e. 1, 2, 3 and 5 h, MAA-grafted starch showed various percentage of grafting (%G) of 18.3 ± 0.02%, 36.3 ± 0.03%, 52.1 ± 0.01% and 89.7 ± 0.02% respectively. Chemical structure of GS with MAA is presented in Fig. 1. Moreover, percentage of grafting was determined by the following equation:

$$\text{Percentage of grafting} = \frac{W_s}{W_i} \times 100 \quad (1)$$

where W_s and W_i were weight of GS and initial starch, respectively [5].

2.2.2. Preparation of TPS films grafted by MAA

Different TPS films grafted by MAA were prepared by mixing with glycerol as a plasticizer in a polyethylene bag. The weight ratio of starch and glycerol was fixed at 65:35. Blending was compounded to obtain a homogeneous material using an internal mixer (PL 2000/PL 2001, C. Melchers, Thailand) at the temperature of 150 °C and the rotor speed of 40 rpm for 5 min. The sample was compression molded to form 0.3 mm film using a compression molding machine (MGLP 20 AT, Match Group, Thailand), operated at 150 °C and at a pressure of 1700 psi.

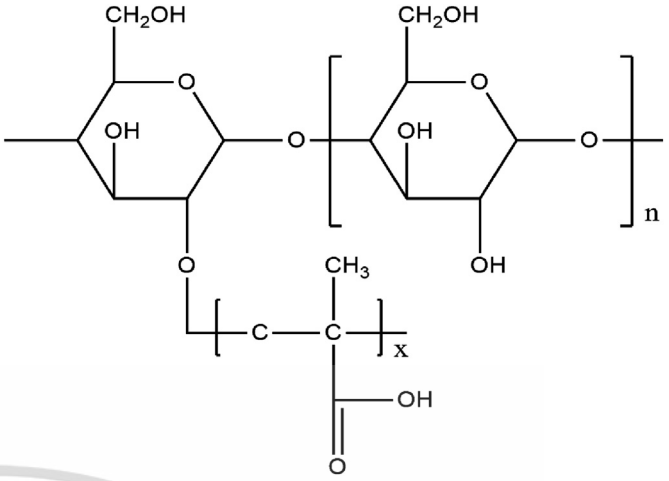

Fig. 1. Chemical structure of GS grafted by MAA.

2.3. Characterization and testing of TPS films grafted by MAA

2.3.1. Function group analysis

FT-IR spectrum of a sample was carried out using Spectrum 2000 GX spectrometer (PerkinElmer, U.S.A.) on an attenuated total transmission mode using KBr disk technique. A sample was scanned for 10 times from 4000 to 400 cm^{-1} at a resolution of 4 cm^{-1}.

2.3.2. X-ray diffraction (XRD)

XRD studies were carried out on D8 Advance X-ray diffractometer (Bruker, Madison, U.S.A.) using CuKα radiation (wavelength 0.1542 nm) operating at 40 kV and 35 mA. A sample was scanned from 5° to 60° with a step size of 0.02° and a sampling interval of 10 s. Percentage crystallinity of each sample was determined by Eq. (2):

$$\text{Crystallinity}(\%) = \frac{A_c}{A_c + A_a} \times 100 \quad (2)$$

where A_c and A_a were the area of crystallinity region and the area of amorphous region of a sample determined from a diffractogram, respectively.

2.3.3. Morphology

Morphology of a sample was observed by Scanning Electron Microscope (FEI, quanta 250, U.S.A.). In order to prevent electric charge before observation, a tested sample was sputter coated with a thin layer of gold.

2.3.4. Water uptake

Percentage of water uptake was performed according to ASTM D-570 standard method. Firstly, a sample was dried at 105 °C for 2 h and; then, kept in a closed container in distilled water at 100% RH at room temperature. The amount of water absorbed for 5 and 10 days was measured. Three samples were measured for each of testing. Percentage of water uptake was calculated as follows:

$$\text{Water uptake}(\%) = \frac{W_2 - W_1}{W_1} \times 100 \quad (3)$$

where W_2 and W_1 were the wet and the dried weights of a sample, respectively.

2.3.5. Water vapor permeability (WVP)

WVP was determined by a gravimetric method according to ASTM E96. A sample of known weight was placed in the humidity chamber maintained at a 75 ± 5% humidity level with sodium chloride saturated

This material is reserved for educational u
Forbidden to modify the content, and cite the document when use.

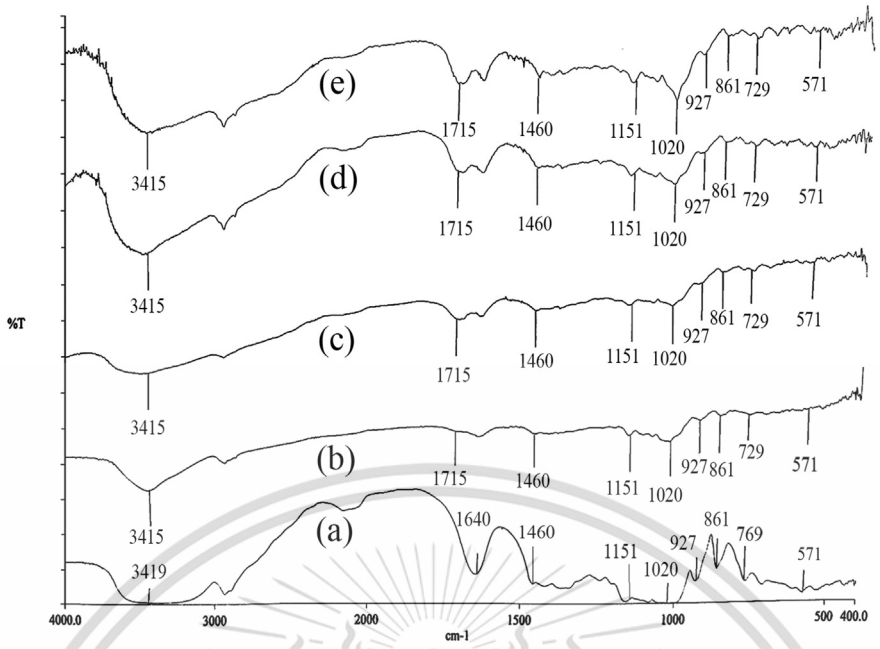

Fig. 2. FT-IR spectra of various TPS films grafted by MAA with different % grafting (a) 0% (b) 18.3% (c) 36.3% (d) 52.1% and (e) 89.7%.

solution for 24 h at the temperature of 30 ± 2 °C. The weight of the sample was recorded every 24 h for the test durations of 7 days and three samples were measured to obtain averaged values. WVP was calculated according with the following formula:

$$\mathrm{WVP} = \frac{W \times X}{t \times A \times \Delta P} \quad (4)$$

where W/t was the slope of system weight gain vs. time (g/day), X was the film thickness (mm), A was the area of the exposed surface of the film (32.15 cm^2) and ΔP = vapor pressure difference (kPa).

2.3.6. Mechanical properties

Mechanical property measurements of a sample were tested, according to ASTM D-638 at a temperature of 23 ± 1 °C and 60 ± 5%RH. A sample was obtained from keeping in the standard condition for 24 h prior to the test. Ten dumbbell-shaped specimens were tested to obtain averaged mechanical property results using a Universal Testing Machine (LR 5K Lloyd, West Sussex, UK) with a 1 kN load cell and the crosshead speed of 40 mm/min.

2.3.7. Biodegradability

A sample was buried at approximately 10 cm under soil surface. Water content of soil was maintained in the range of 5–10%. Temperature and pH of soil were controlled at 30 ± 2 °C and 7 ± 1, respectively. Mechanical properties of a specimen after 5 and 10 days of testing were examined.

2.3.8. Thermal property

In order to determine thermal decomposition temperature, a sample of approximately 10–12 mg was tested on a Thermogravimetric analyser (Pyris I TGA HT PerkinElmer, U.S.A.) in the temperature range of 50 to 600 °C at the heating rate of 10 °C/min under nitrogen atmosphere.

3. Results and discussion

3.1. Function group analysis

Influence of graft copolymerization by MAA monomer with different percentage of grafting on function group analysis is shown in Fig. 2. FT-IR spectra in Fig. 2 showed the same characteristic peaks for different TPS films grafted by MAA at 3200–3400 cm^{-1}, originated from O—H stretching. The bands appeared at 2800–3000 $cm^{-1}$and 1640–1670 cm^{-1} were attributed to C—H stretching and bending vibration of bound water, respectively. The peak characteristic for C—H bending of —CH_2— at 1460 cm^{-1} was observed. Other peak positions located at 1200–1300 cm^{-1} and 1000–1200 cm^{-1}, were assigned to C—O—C stretching and C—O—H bending, respectively [16,17].

The most important peak of FT-IR spectrum of TPS films grafted by MAA was a new absorption peak at 1715 cm^{-1}, attributed to C═O stretching formation of methacrylic group of TPS film grafted by MAA [18,19]. This investigation could confirm the success of the graft copolymerization with MAA monomer onto starch chain. In addition, higher intensity of 1715 cm^{-1} characteristic peak of TPS film grafted by MAA was observed with the increasing of percentage of grafting, indicating the increment of the formation MAA-graft chain.

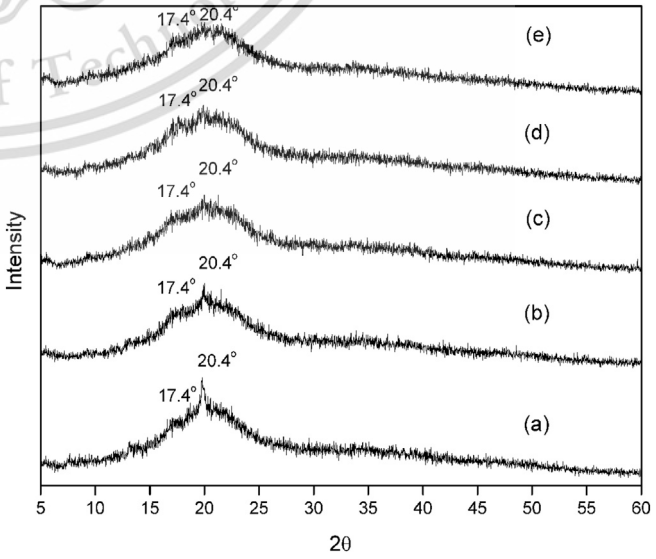

Fig. 3. X-ray diffractograms of various TPS films grafted by MAA with different % grafting (a) 0% (b) 18.3% (c) 36.3% (d) 52.1% and (e) 89.7%.

This document is licensed for personal use only. Commercial use.
Forbidden to modify the content, and cite the document when use.

Table 1
Degree of crystallinity and WVP of various TPS films grafted by MAA with different percentage of grafting.

Grafting (%)	Degree of crystallinity (%)	WVP ($g \cdot mm/m^2 \cdot day \cdot kPa$)
0	49.87 ± 0.02	20.12 ± 0.02
18.3	45.21 ± 0.03	25.73 ± 0.03
36.3	44.21 ± 0.02	26.51 ± 0.03
52.1	43.57 ± 0.04	19.21 ± 0.03
89.7	42.11 ± 0.10	17.32 ± 0.15

3.2. X-ray diffraction

Fig. 3 presents XRD diffractograms of different TPS films grafted by various contents of MAA. X-ray diffraction pattern of all TPS films showed similar V_h-type crystallization, which presented the diffraction peak (2θ) at 17.4° and 20.4° [20]. In addition, different TPS films grafted by MAA demonstrated the decrease of degree of crystallinity compared with TPS film with NS (Fig. 3 and Table 1), which indicated that a change in crystallinity after graft copolymerization by MAA. This was because graft copolymerization disturbed hydrogen bonding formation between hydroxyl groups of starch molecules due to the formation of grafted chain and reduction of crystalline phase. The result obviously confirmed that MAA monomer was firmly grafted into starch chains [9,10].

With the increasing of percentage of grafting, the degree of crystallinity was apparently decreased. This might be due to the increase in the length of the alkyl chain of methacrylic group. Similar results for the drop of degree of crystallinity with the increasing of percentage of grafting were reported for MAA and PCL-grafted starch [19,21].

3.3. Morphology

In this investigation, Fig. 4 depicts SEM micrographs of different TPS films grafted by MAA. The SEM micrograph of TPS film with NS in Fig. 4 (a) showed a rough fractured surface. It should be noted that there was a change in morphology of TPS film, before and after grafted polymerization with MAA monomer. This evidence could also confirm the disruption of starch granules and the successful grafting with MAA into starch structure.

With the increasing of grafting percentage of TPS film grafted by MAA, the morphology of TPS film grafted by MAA showed more surface roughness. Similar results in the recent literatures were reported for GS with MAA monomer [7,9].

3.4. Water uptake

The result of percentage water uptake of different TPS films grafted by MAA at 100% RH is shown in Fig. 5. The increase in water uptake of different TPS films grafted by MAA was observed when the water absorption time increased. It was observed that water uptake of TPS films grafted by MAA with 18.3% and 36.3% determined at days 5 and

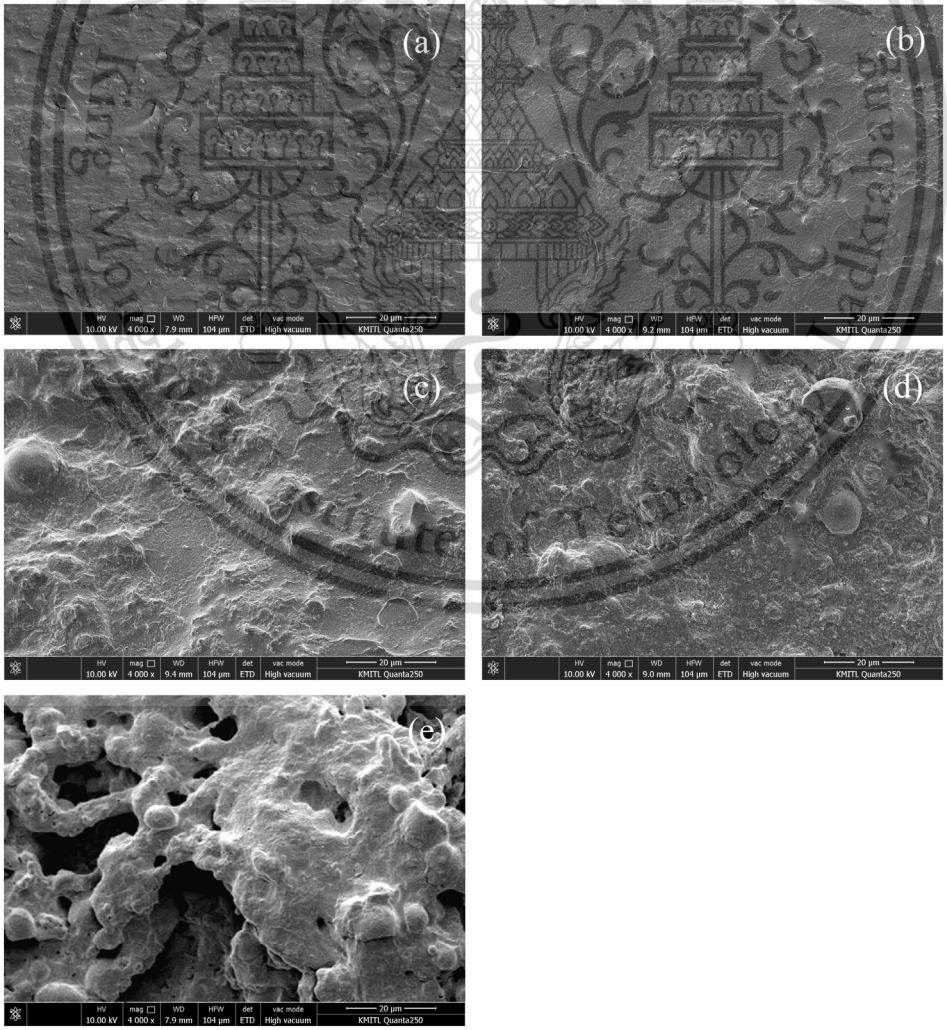

Fig. 4. SEM micrographs of various TPS films grafted by MAA with different % grafting (a) 0% (b) 18.3% (c) 36.3% (d) 52.1% and (e) 89.7%.

This material is for educational purpose only. Forbidden to modify the content, and cite the document when use.

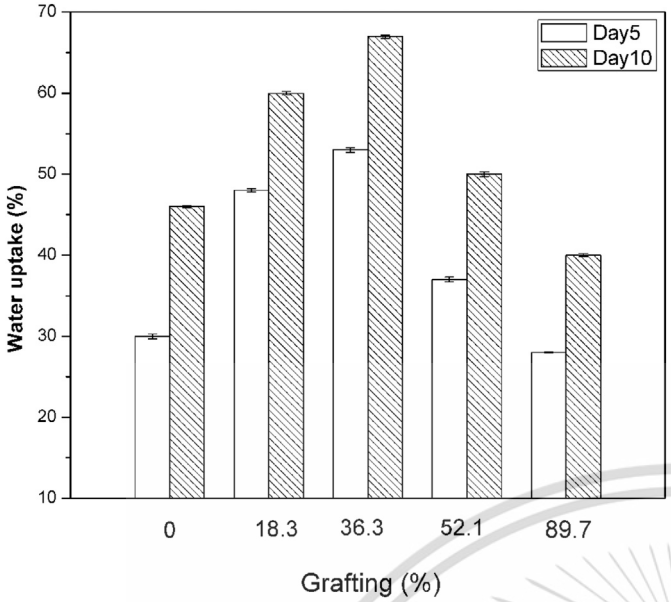

Fig. 5. Water uptake at 100% RH of various TPS films grafted by MAA with different percentage of grafting.

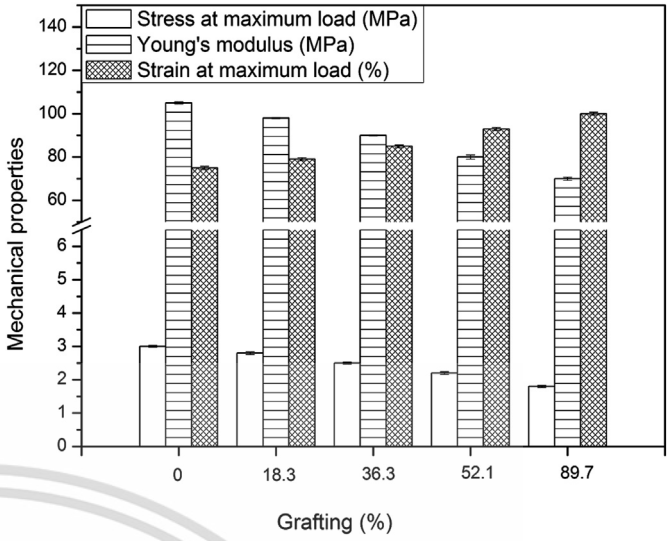

Fig. 6. Mechanical properties of various TPS films grafted by MAA with different percentage of grafting.

10 was higher than that of TPS film with NS because of high hydrophilic characteristics of MAA monomer.

With increasing percentage of grafting (52.1 and 89.7%), water uptake of TPS film grafted by MAA; however, decreased. This was because high degree of grafting of MAA monomer not only reduced hydroxyl groups of starch backbone significantly but also generated hydrogen bonding between two methacrylic groups, leading to the drop in water absorption affinity [11]. The results were consistent with the previous report for the literature of GS with MAA monomer [9,10]. In this study, TPS film grafted by MAA with 36.3% presented the highest percentage of water uptake of 68.2%. On the contrary, the lowest percentage of water uptake of 40.2% was obtained from TPS grafted by MAA with 89.7%.

3.5. Water vapor permeability

WVP test was performed by the gravimetric method at the temperature of 30 ± 2 °C and 75% RH. Table 1 shows the WVP result of different TPS films grafted by MAA. It was observed that the WVP values of TPS films grafted by MAA with 18.3% and 36.3% were higher than that of TPS film with NS. This possibly caused by the fact that MAA side chains presented more hydrophilic characteristic in nature. Nevertheless, WVP values of TPS films grafted by MAA with 52.1% and 89.7% were found to decrease approximately 4.73% and 16.16%. The decrease in WVP values probably because higher degree of grafting with MAA created the hydrogen bonding formation between two methacrylic groups and the amount of hydroxyl groups of starch chain was declined by grafting with MAA monomer [11]. It could reduce and block water vapor absorption of the starch backbone. The decrease of WVP values of different TPS films grafted by MAA also related to results from the water uptake (Fig. 5). In addition, the finding agreed with D. Pathania and R. Sharma who reported that the grafting of MAA onto starch (at 28% percentage of grafting) negatively affected the solubility properties of starch [9].

3.6. Mechanical properties

Mechanical properties of various TPS films grafted by MAA are presented in Fig. 6. The results indicated that stress at maximum load and Young's modulus were decreased as compared to TPS film by NS. Conversely, the incorporation of MAA onto grafted starch caused the increase in strain at maximum load. The tensile property results were also related to degree of crystallinity from XRD result (Table 1). The grafted copolymerization led to the disruption in crystalline phase of starch, which increased the mobility of the starch chains and led to flexible chain polymer. Similar finding related to the study of the compressed TPS sheet grafted by PCL [15].

A significant increase in the strain at maximum load together with the decrease of stress at maximum load and Young's modulus was observed when percentage of grafting increased from 0 to 89.7%. It might be because higher degree of grafting participated in increasing mobility of the starch molecules and flexibility of side chain [15,22,23]. These results related to the degree of crystallinity (Table 1). Based on these results, the highest stiffness, observed by stress at maximum load and Young's modulus, was obtained from TPS film with NS. In addition, the highest of strain at maximum load or flexibility was found in TPS film grafted by MAA with 89.7% (at 110.5% strain). On the contrary, TPS film with NS exhibited the lowest of strain at maximum load (at 78.2% strain).

3.7. Biodegradability

The effect of grafted copolymerization on mechanical properties of different TPS films grafted by MAA before and after soil burial test is shown in Fig. 7. It can be seen that stress at maximum load, Young's modulus and strain at maximum load of different TPS films grafted by MAA were clearly dropped. The decrease in the strength and elasticity was due to not only water absorption from soil but also degradation by micro-organisms existed in soil [12,23,24]. Additionally, the biodegradable property result was also consistent with WVP result in Table 1 and water absorption result in Fig. 5. The result of the reduction of tensile properties claimed biodegradability of TPS grafted by MAA with low and high percentage of grafting. Similar results were reported for TPS grafted by MMA and PCL monomers. The result was found that casted film and TPGS sheet from GS with MMA and PCL was partially biodegraded after biodegradation in soil, fungus and enzymatic degradation [14,15,23].

3.8. Thermal property

TGA technique was carried out in order to examine thermal property of TPS films grafted by MAA with different percentage of grafting. TG

This article is protected by copyright. Forbidden to modify the content, and cite the document when use.

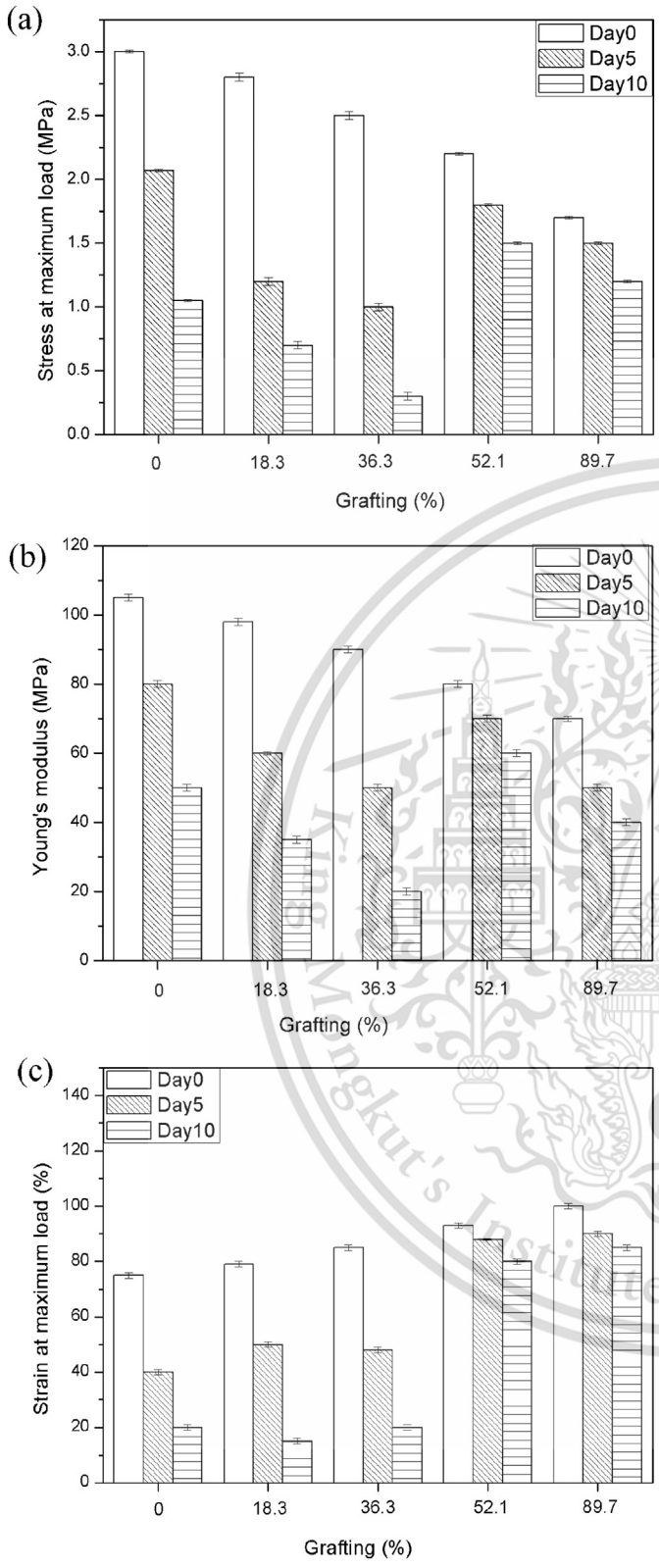

Fig. 7. Mechanical properties before and after soil burial test of various TPS films grafted by MAA with different percentage of grafting.

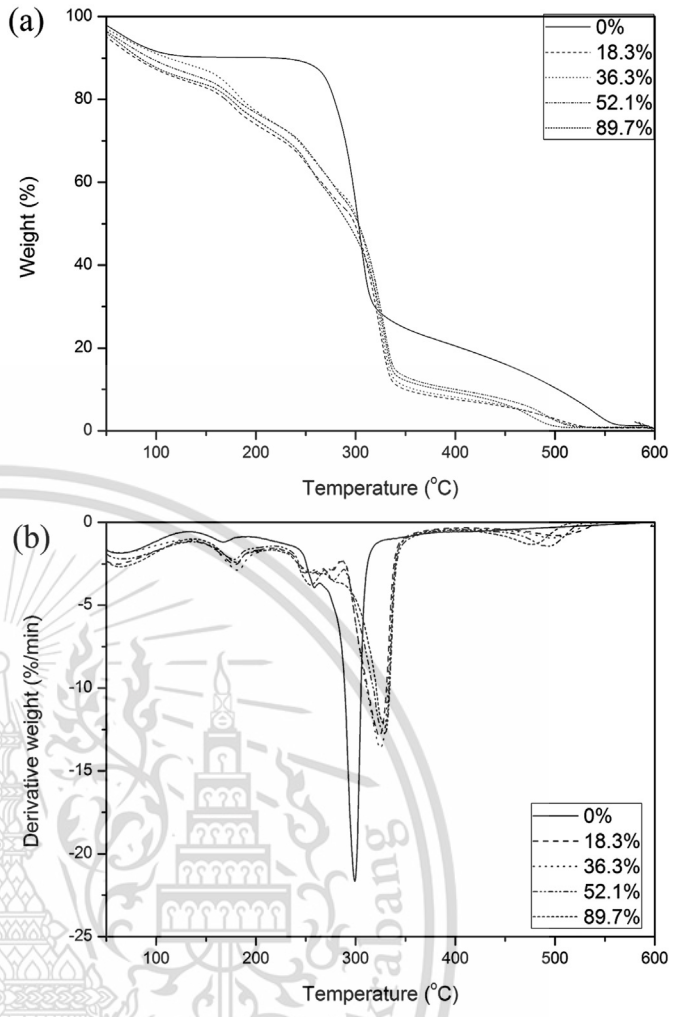

Fig. 8. (a) TGA and (b) DTG thermograms of various TPS films grafted by MAA with different percentage of grafting.

and DTG thermograms were detected from temperature 50 to 600 °C. It was found from Fig. 8 and Table 2 that 3 degradation steps in the thermograms were found for TPS film with NS. However, the thermal transition of different TPS films grafted by MAA showed 4 transitions of thermal degradation. The first maximum degradation temperature of different TPS films grafted by MAA was found from 170 to 180 °C due to the decomposition temperature of glycerol [25,26]. The second decomposition temperature was found in the range of 245–268 °C, probably corresponding with the degradation of starch molecules occurred during the preparation. The main degradation step exhibited a thermal transition from 300 to 330 °C, arisen from the decomposition temperature of starch [23,27]. Besides, the new degradation transition of different TPS films grafted by MAA in the range of 490–501 °C was also noticed, related to the decomposition temperature of MAA-grafted copolymer [9,10]. This result also confirmed the successful graft copolymerization.

As shown in Fig. 8 and Table 2, the results demonstrated that the thermal degradation temperatures of TPS films grafted by MAA were apparently higher than that of TPS with NS, representing the improvement of thermal stability caused by the graft copolymerization with

Table 2
Thermal decomposition temperatures of various TPS films grafted by MAA with different percentage of grafting.

Grafting (%)	Degradation temperature (°C)			
	Step 1	Step 2	Step 3	Step 4
0	171.8	245.0	300.2	–
18.3	179.2	256.6	323.4	501.2
36.3	181.4	265.6	325.1	497.3
52.1	178.1	267.4	329.0	492.1
89.7	180.5	254.7	330.2	490.8

Forbidden to modify the content, and cite the document when use.

MAA [9,10]. Furthermore, thermal degradation temperature of starch was significantly raised when percentage of grafting was increased. This finding indicated that the increase in thermal degradation temperatures caused by an increase in amount of MAA-grafted chain onto starch backbone, leading to the improvement of thermal property.

4. Conclusion

In this work, the synthesis of GS grafted by MAA was successfully carried out. This result could confirm by the presence of new IR peak position, arising from C═O stretching of GS with MAA and rough morphology. As a result of X-ray diffraction, degree of crystallinity decreased by grafting reaction with MAA monomer. The graft copolymerization with MAA noticeably improved strain at maximum load of TPS films. Different TPS films grafted by MAA also demonstrated biodegradability by soil burial test. Additionally, TPS films grafted by MAA at high percentage of grafting exhibited the improvement of extendibility, WVP, water uptake and thermal degradation temperature when compared with TPS film with NS and TPS films grafted by MAA at low percentage of grafting.

Acknowledgments

The authors express their sincere appreciation to KREF 046108 Research Fund for financially support.

References

[1] B.L. Scallet, E.A. Sowell, in: R.L. Whistler, E.F. Paschall (Eds.), Starch Chemistry and Technology Vol. II, Academic Press, New York 1967, pp. 237–251.
[2] X. Wang, Z. Gu, H. Qin, L. Li, X. Yang, X. Yu, Crosslinking effect of dialdehyde starch (DAS) on decellularized porcine aortas for tissue engineering, Int. J. Biol. Macromol. 79 (2015) 813–821, https://doi.org/10.1016/j.ijbiomac.2015.05.044.
[3] M. Wu, J. Wang, Y.L. Xiong, Q. Ge, H. Yu, Rheology and microstructure of myofibrillar protein–starch composite gels: comparison of native and modified starches, Int. J. Biol. Macromol. 118 (2018) 988–996, https://doi.org/10.1016/j.ijbiomac.2018.06.173.
[4] D. Trimnell, E.I. Stout, W.M. Doane, C.R. Russell, Graft copolymers from thiolated starch and vinyl monomers, J. Appl. Polym. Sci. 21 (1977) 655–663, https://doi.org/10.1002/app.1977.070210307.
[5] M. Celik, M. Sacak, Synthesis and characterization of starch-poly(methyl methacrylate) graft copolymers, J. Appl. Polym. Sci. 86 (2002) 53–57, https://doi.org/10.1002/app.10902.
[6] W. Bauer, Methacrylic acid and derivatives, Ullmann's Encyclopedia of Industrial Chemistry, Wiley-VCH, Weinheim, 2011.
[7] V. Nikolic, S. Velickovic, A. Popovic, Amine activators influence on grafting reaction between methacrylic acid and starch, Carbohydr. Polym. 88 (2012) 1407–1413, https://doi.org/10.1016/j.carbpol.2012.02.027.
[8] M.K. Zahran, E.M. Ahmed, M.H. El-Rafie, Synthesis and characterization of hydrolysed starch g poly(methacrylic acid) composite, Int. J. Biol. Macromol. 87 (2016) 473–480, https://doi.org/10.1016/j.ijbiomac.2016.02.068.
[9] D. Pathania, R. Sharma, Synthesis and characterization of graft copolymers of methacrylic acid onto gelatinized potato starch using chromic acid initiator in presence of air, Adv. Mater. Lett. 3 (2012) 136–142, https://doi.org/10.5185/amlett.2011.8297.
[10] V.D. Athawale, S.C. Rathi, Syntheses and characterization of starch–poly (methacrylic acid) graft copolymers, J. Appl. Polym. Sci. 66 (1997) 1399–1403, https://doi.org/10.1002/(SICI)1097-4628(19971114)66:7<1399::AID-APP18>3.0.CO;2-Y.
[11] Kh.M. Mostafa, Graft polymerization of methacrylic acid on starch and hydrolyzed starches, Polym. Degrad. Stab. 50 (1995) 189–194, https://doi.org/10.1016/0141-3910(95)00147-6.
[12] V. Nikolic, S. Velickovic, D. Antonovic, A. Popovic, Biodegradation of starch–graft–polystyrene and starch–graft–poly(methacrylic acid) copolymers in model river water, J. Serb. Chem. Soc. 78 (2013) 1425–1441, https://doi.org/10.2298/JSC121216051N.
[13] Z. Shi, N. Reddy, L. Shen, X. Hou, Y. Yang, Effects of monomers and homopolymer contents on the dry and wet tensile properties of starch films grafted with various methacrylates, J. Agric. Food Chem. 62 (2014) 4668–4676, https://doi.org/10.1021/jf5013709.
[14] M.C. Li, J.K. Lee, U.R. Cho, Synthesis, characterization, and enzymatic degradation of starch-grafted poly(methyl methacrylate) copolymer films, J. Appl. Polym. Sci. 125 (2012) 405–414, https://doi.org/10.1002/app.35620.
[15] Z.B. Cuevas-Carballo, S. Duarte-Aranda, G. Canché-Escamilla, Properties and biodegradability of thermoplastic starch obtained from granular starches grafted with polycaprolactone, Int. J. Polym. Sci (2017), 3975692. https://doi.org/10.1155/2017/3975692.
[16] S. Pal, D. Mal, R.P. Singh, Cationic starch: an effective flocculating agent, Carbohydr. Polym. 59 (2005) 417–423, https://doi.org/10.1016/j.carbpol.2004.06.047.
[17] J. Prachayawarakorn, L. Hommanee, D. Phosee, P. Chairapaksatien, Property improvement of thermoplastic mung bean starch using cotton fiber and low-density polyethylene, Starch-Starke 62 (2010) 435–443, https://doi.org/10.1002/star.201000002.
[18] R.C. Mundargi, S.A. Agnihotri, S.A. Patil, T.M. Aminabhav, Graft copolymerization of methacrylic acid onto guar gum, using potassium persulfate as an initiator, J. Appl. Polym. Sci. 101 (2006) 618–623, https://doi.org/10.1002/app.23325.
[19] M.A. Güler, M.K. Gök, A.K. Figen, S. Özgümüs, Swelling, mechanical and mucoadhesion properties of Mt/starch-g-PMAA nanocomposite hydrogels, Appl. Clay Sci. 112-113 (2015) 44–52, https://doi.org/10.1016/j.clay.2015.04.019.
[20] A.M. Stephen, G.O. Phillips, P.A. Williams (Eds.), Food Polysaccharides and Their Applications, second ed.Taylor and Francis, CRC Press, Boca Raton, New York, 2006.
[21] L. Najemi, T. Jeanmaire, A. Zerroukhi, M. Raihane, Organic catalyst for ring opening polymerization of ε-caprolactone in bulk. Route to starch-graft-polycaprolactone, Starch-Starke 62 (2010) 147–154, https://doi.org/10.1002/star.200900198.
[22] M.M. Fares, A.S. El-Faqeeh, M.E. Osman, Graft copolymerization onto starch–I. Synthesis and optimization of starch grafted with N tert butylacrylamide copolymer and its hydrogels, J. Polym. Res. 10 (2003) 119–125, https://doi.org/10.1023/A:1024928722345.
[23] A.R. Hernandez, A. Aparicio-Saguilan, J.L. Mata-Mata, G. Gonzalez-Garcı, H. Hernandez-Mendoza, E. Baez-Garcıa, C. Conde-Acevedo, Clusters of starch-g-PCL and its effect on the physicochemical properties of films, Starch-Starke 70 (2018) 1700135, https://doi.org/10.1002/star.201700135.
[24] C.S. Tena-Salcido, F.J. Rodríguez-González, M.L. Méndez-Hernández, J.C. Contreras-Esquivel, Effect of morphology on the biodegradation of thermoplastic starch in LDPE/TPS blends, Polym. Bull. 60 (2008) 677–688, https://doi.org/10.1007/s00289-008-0903-0.
[25] C. Weerapoprasit, J. Prachayawarakon, Properties of biodegradable thermoplastic cassava starch/sodium alginate composites prepared from injection molding, Polym. Compos. 37 (2016) 3365–3372, https://doi.org/10.1002/pc.23534.
[26] X.F. Ma, J. Yu, J.F. Kennedy, Studies on the properties of natural fibers reinforced thermoplastic starch composites, Carbohydr. Polym. 62 (2005) 19–24, https://doi.org/10.1016/j.carbpol.2005.07.015.
[27] V.D. Athawale, V. Lele, Thermal studies on granular maize starch and its graft copolymers with vinyl monomers, Starch-Starke 52 (2000) 205–213, https://doi.org/10.1002/1521-379X(200007)52:6/7<205::AID-STAR205>3.0.CO;2-3.

This material is reserved for educational use only, not allowed for commercial use.
Forbidden to modify the content, and cite the document when use.

Author Biography

Name	Miss. Chayapa Weerapoprasit
Date of Birth	22 December 1988
Address	443/19 Moo.5 Nongpaikaew, Banbung, Chonburi 20220
Education	(2010) Bachelor of science in industrial chemistry (King Mongkut's Institute of Technology Ladkrabang) (2013) Master of science in polymer technology (King Mongkut's Institute of Technology Ladkrabang)
Scholarship	Scholarship for Master Degree of Science Scholarship for Doctor Degree of Science

Academic Publications

1. C.Weerapoprasit and J.Prachayawarakorn. 2013. "Effect of Sodium Alginate on Properties of Biodegradable Polymer Blends from Thermoplastic Cassava Starch and Low-density Polyethylene Blends using Injection Molding Technique."349-353. in The 39th Congress on Science and Technology of Thailand (STT-39), Bangkok
2. C.Weerapoprasit and J.Prachayawarakorn, 2016. "Properties of Biodegradable Thermoplastic Cassava Starch/Sodium Alginate Composites Prepared From Injection Molding" *Polymer Composites*. 37(12) : 3365-3372.
3. C.Weerapoprasit and J.Prachayawarakorn. 2017. "Preparation and Properties of Cassava Starch Grafted by Methacrylamide (MAM)."1456-1460. in Pure and Applied Chemistry international conference 2017 (PACCON 2017), Bangkok.
4. C.Weerapoprasit and J.Prachayawarakorn. 2017. "Preparation and Properties of Cassava Starch Grafted by Methyl Methacrylate (MMA)" 54-58. in International Polymer Conference of Thailand 2017 (PCT-7). Bangkok.
5. C.Weerapoprasit and J.Prachayawarakorn, 2019, "Characterization and Properties of Biodegradable Thermoplastic Grafted Starch Films by Different Contents of Methacrylic Acid." *International Journal of Biological Macromolecules*. 123: 657-663.
6. C.Weerapoprasit and J.Prachayawarakorn. "Effects of methacrylamide content on mechanical property and

This material is reserved for educational use only, not allowed for commercial use.
Forbidden to modify the content, and cite the document when use.

hydrophilicity of thermoplastic grafted starch film" *Starch/Starke* Submitted for publication

This material is reserved for educational use only, not allowed for commercial use.
Forbidden to modify the content, and cite the document when use.